ROLE OF CD8+ T CELLS IN ADULT AND PAEDIATRIC HIV INFECTION

This thesis is submitted in partial fulfillment of the requirements for the degree of Doctor of Philosophy in Paediatrics
University of Oxford, Hilary Term 2016

Ellen M. Leitman
St. Hugh's College, Department of Paediatrics

Supervised by:

Professor Philip J. R. Goulder
Department of Paediatrics

Dr. Philippa C. Matthews
Department of Infectious Diseases and Microbiology

ABSTRACT

Infection with HIV is a continuing global health problem. Antiretroviral therapy effectively suppresses viraemia, but the viral reservoir in latently infected CD4+ T-cells persists for decades and is the main obstacle to HIV eradication. The central role of CD8+ T-cell-mediated immune control of natural adult HIV infection has long been established and recent studies suggest that CD8+ T-cells are likely to be crucial in eliminating reactivated reservoirs. However, the questions of what constitutes an effective anti-HIV CD8+ T-cell response and how to induce it therapeutically are outstanding. Moreover, even less is known about the antiviral function of CD8+ T-cells in paediatric HIV infection. Although outnumbered by adult infections, paediatric infection may offer opportunities to achieve HIV cure that could be more widely applicable to cure strategies in adults.

Here, I explore the specific aspects of the interplay between host and virus in order to gain a better understanding of the optimal CD8+ T-cell-mediated immune responses. I demonstrate that in contrast to the Gag-specific response that mediates viral control in the context of HLA-B*57, among HLA-B*14-restricted responses, Env-specific cells are more potent than those targeting Gag. This is associated with higher antigen sensitivity and stronger selection pressure in the Env-specific population. I define two broadly distinct phenotypes of HIV non-progression in children. These are characterised by differential protein specificity of the antiviral CD8+ T-cell response but children of both phenotypes demonstrate strong selection pressure exerted on the virus by CD8+ T-cells in the first weeks of life. Next, in the context of the HIV vaccine tested in the Phambili trial, I report an HLA-specific effect of vaccine on disease progression, as a result of altering the natural CD8+ T-cell immunodominance hierarchy. Finally, I demonstrate a new method which allows to selectively deplete human HIV-specific CD8+ T-cell *in vitro*, and thereby to evaluate the contribution and efficacy of particular CD8+ T-cell specificities to viral inhibition – a critical question to HIV vaccine design and reservoir eradication studies.

The work described here adds important insights to our understanding of the HIV-specific CD8+ T-cell responses that are generated from birth through childhood and into adulthood and is relevant to the future studies directed at harnessing the most effective CD8+ T-cell response to achieve HIV cure.

CONTRIBUTIONS TO THIS THESIS

First of all, none of this work would have been possible without the willingness of the study participants and the excellence of the nurses and doctors at all the sites in South Africa, the UK and the USA.

I am very grateful to the following individuals who have contributed their expertise to the work presented in this thesis:

Chapter 3:

- **Chris Willberg** performed cell sorting and guided in the antibody panel set up;
- **Hendrik Streeck** provided ELISPOT data for the 1999 'Berlin patient;'
- **Huabiao Chen** and **Victor Appay** shared cloning protocols;
- **Mary Carrington** and **Ying Qi** had access to large multicentre cohorts and analysed the associations between HLA expression and HIV control;
- **Ming-Han Tsai** performed viral fitness assays;
- **Steve Deeks** contributed to the HLA-B*14 samples

Chapter 4:

- **Astrid Gall and Paul Kellam** performed deep sequencing and genome assemblies;
- **Azim Ansari** determined epitope haplotypes.
- **Christina Thobakgale** provided the ELISPOT data of the PEHSS cohort for analysis;

Chapter 5:

- **Jake Hurst** constructed mixed effects models;
- **Jonathan Carlson** analysed the associations between HLA expression and CD8+ T-cell responses to HIV;
- **Masa Mori** provided continuing guidance and expertise in data analysis.

Chapter 6:

- **Anette Stryhn** and **Soren Buus** generated tetramers;
- **Becky Payne** and **Stuart Sims** made MHC monomers;
- **Marcus Altfeld** and **Christine Palmer** provided AC198 samples;
- **Paul Hess** continually provided his expertise and guidance in the use of the cytotoxic tetramers.

Separately, I would like to acknowledge **Asier Saez-Cirion** and **Pierre Versmisse** who kindly hosted me at the Pasteur Institute and shared their expertise in performing viral inhibition assays. They provided continuing guidance, feedback and discussions thereafter. This work would not have been possible without their support.

Many thanks to **Max Muenchhoff** and **Julia Roider** for the excellent management of the cohorts in Durban and to **Henrik Kloverpris** for informative scientific discussions.

This D.Phil. was funded by the 3-year Clarendon Fund Scholarship provided by the University of Oxford. The last 6 months were funded by the Department of Paediatrics, University of Oxford.

ACKNOWLEDGEMENTS

First of all, I would like to thank my supervisors, Philip and Philippa, for these unforgettable and unlike anything else 3.5 years in Oxford and for guiding me to become the scientist I am today. Thank you, Philip, for letting me join your group and believing in me, for making the world seem an orderly and conquerable place so often, for always challenging me to reach a new best and tackle the 'untackable,' for guiding through the difficulties and encouraging to go on, for teaching, for inspiring, for patiently answering millions of emails, many of them in the middle of the night, for sharing your thoughts and listening to me; thank you for being my mentor. Philippa, from the first day of the D.Phil. you have been my inspiration and my role model of a scientist, a physician and a person that one day I hope to become. Thank you for seeing the best in any situation and helping find a solution; thank you for your warm support and enthusiasm; and thank you for always encouraging me 'to go for it.'

I would like to also thank Marcus Altfeld for introducing the world of HIV immunology to me and letting me spend some time in the Durban lab – it was that firsthand experience that inspired me to pursue this D.Phil.

I am hugely indebted to my undergraduate mentors: Carmen – thank you for letting me set a foot into your new lab in my very first year of college when I knew nothing and for instilling love and passion for research into me; and Roger – thank you for always bringing me 'back to earth,' saying what needs to be said, teaching me that having fun once in a while is OK and continuing to guide me through life.

I would like to thank my med school mentor, Dr. Anthony D'Amico, for always being there for me even across the ocean, for guiding me and giving me the skills to get through the toughest events of the past year and to accept the unchangeable. I am so looking forward to being back in med school under your mentorship.

Masa, I cannot thank you enough. You have become my best friend and my rock in any situation. Thank you for supporting me through the worst and the best, for your kindness and readiness to help at any minute of day and night. I am looking forward to our cross-Pacific clinical discussions.

I would also like to thank Jodi, Jacqui, Matt P, Matt J, Jake, Gen, Morgane, Emily H, Alba, Leo and JT – your love, kindness and support have literally carried me through all my D.Phil. years and in particular through the lowest of the lows of the past year. Kate Southey, thank you for your wisdom, advice and warm love. Lyle, the office has never been the same without you. Jo, Ayako and Leo, thank you for helping me get through the first LSRII crisis a few years ago, showing me your passion for science in all subsequent years and being examples for me. Anna, thank you for helping with anything and everything. And thanks to everyone in the Medawar for being such a big part of my everyday D.Phil life.

Finally, I would not have been able to achieve anything without the unconditional support and love of my family. Mom, sis and Bill – I am the luckiest person to have you. It is your standing behind me 100% that gives me strength to strive for the best. Thank you for dealing with me – probably not always the easiest job!

For my dad.

You will always be with me.

ABBREVIATIONS

ºC – degree Celsius
aa – amino acid
Ad5 – adenovirus serotype 5
AIDS – acquired immunodeficiency syndrome
APC – allophycocyanin or antigen presenting cell
Arg – arginine
ART – antiretroviral therapy
BCG – Bacillus Calmette-Guerin
bp – base pair
CD – cluster of differentiation
CDK – cyclin dependent kinase
CI – confidence interval
CMV – cytomegalovirus
CTL – cytotoxic T lymphocyte
Cy5/Cy5.5/Cy7 – cyanine dye 5, 5.5 or 7
DC – dendritic cell
DMSO – dimethyl sulfoxide
DNA – deoxyribonucleic acid
dNTP – deoxynucleotide triphosphate
EBV – Epstein-Barr virus
ELISA – enzyme-linked immunosorbent assay
ELISPOT – enzyme-linked immunospot
FACS – fluorescence-activated cell sorting
FCS – foetal calf serum
FITC – fluorescein isothiocyanate
FRESH study – Females Rising through Education, Support and Health study
GFP – green fluorescent protein
GWAS – genome-wide association study
HCV – hepatitis C virus
HDAC – histone deacetylase
HIV – human immunodeficiency virus
HLA – human leukocyte antigen
HPLC – high performance liquid chromatography
HR – hazard ratio
HSV-2 – herpes simplex virus type 2
HVTN – HIV Vaccine Trials Network
IFN – interferon
IL – interleukin (e.g. interleukin-2, 4, 5, etc.)
IQR – interquartile range
IU – international unit
KIR – killer-cell immunoglobulin receptor
LCMV – lymphocytic choriomeningitis
LILRB – leukocyte immunoglobulin-like receptor subfamily B
LTR – long terminal repeat
MHC – major histocompatibility coplex
µg – microgram
µl – microlitre

ml – millilitre
mm^3 – cubic millimetre
MRK – Merck
MTCT – mother-to-child transmission
NFAT – nuclear factor of activated T-cells
NFkB – nuclear factor kappa-light-chain-enhancer of activated B-cells
OLP – overlapping peptide
OR – odds ratio
PBMC – peripheral blood mononuclear cells
PBS – phosphate buffered saline
PCR – polymerase chain reaction
PE – phycoerythrin
PEHSS – Paediatric Early HAART and Strategic Treatment Interruption Study
PerCP – peridinin chlorophyll protein
PHA – phytohaemmagglutinin
PKC – protein kinase C
PSP – paediatric slow progressor
PTC – post-treatment control
P-TEFb – positive transcription elongation factor
RNA – ribonucleic acid
Rpm – revolutions per minute
RPMI medium – Roswell Park Memorial Institute medium
SAP – saporin
SEB – Staphylococcal enterotoxin B
s.e.m – standard error of mean
SFC – spot-forming cell
SM – sooty mangabey
SNP – single nucleotide polymorphism
START trial – Strategic Timing of Antiretroviral Therapy trial
TCR – T-cell receptor
Tet - tetramer
Tet-APC – tetramer- allophycocyanin
Tet-PE – tetramer-phycoerythrin
Tet-SAP – tetramer-saporin
T_{FH} – T follicular helper cell
TGF – transforming growth factor
TLR – Toll-like receptor
TNF – tumor necrosis factor
T_{REG} – regulatory T-cell
Trp – tryptophan
Tx – treatment
U – unit
UNAIDS – Joint United Nations Programme on HIV/AIDS
VC – viraemic controller
VRC – viral replicative capacity
WHO – World Health Organisation

D. Phil. Publications

- **Leitman, E.M**, Hurst, J., Mori, M., Kublin, J., Ndung'u, T., Walker, B.D., Carlson, J., Gray, G.E., Matthews, P.C., Frahm, N., Goulder, P.J.R. **2016**. Lower Viral Loads and Slower CD4 Decline in MRKAd5 HIV-1 Vaccinees Expressing Disease-Susceptible HLA-B*58:02. *J. Infect. Dis.* Pii: jiw093. Epub ahead of print.

- Goulder, P.J., Lewin S.R. & **Leitman, E.M. 2016 Mar 14**. Paediatric HIV infection: the potential for cure. *Nature Reviews Immunology*. 10. 1038/nri.2016.19. Epub ahead of print.

- **Leitman, E.M.**, Willberg, C.B., De Burgh-Thomas, A., Streeck, H., Goulder, P. J. R., Matthews, P. C. A. **2016.** Subdominant Gag-specific anti-HIV efficacy in an HLA-B*57-positive elite controller. *AIDS* 30(6): p. 972-974.

Contributing Author Publications

- Brener, J., Gall, A., Batrosky, R., Riddell, L., Buus, S., **Leitman, E.**, Kellam, P., Allen, T., Goulder, P., Matthews, PC. **2015**. Disease progression despite protective HLA expression in an HIV-infected transmission pair. *Retrovirology* 12:55.

- Juarez-Molina, C.I., Payne, R., Soto-Nava, M., Avial-Rios, S., Valenzuela-Lonce, H., Adland, E., **Leitman, E.**, Brener, J., Muenchoff, M., Branch, S., Landis, C., Reyes-Teran, G., Goulder, P. **2014**. Impact of HLA-associated pressure on HIV fitness at a population level. *J. Virol.* 88:18 10392-10398.

- Payne, R., Branch, S., Kloverpris, H.N., Matthews, P.C., Koofhethile, C.K., Strong, T., Adland, E., **Leitman, E.**, Frater, J.A., Ndung'u, T., Hunter, E., Haubrich, R., Mothe, B., Edwards, A., Riddell, L., Chen, F., Harrigan, R., Brumme, Z.L., Mallal, S., John, M., Jooste, P., Shapiro, R.L., Deeks, S.G., Walker, B.D., Brander, C., Landis, C., Carlson, J.M., Prado, J., Goulder, P. **2014**. Differential escape patterns within the dominant HLA-B*57:03-restricted HIV Gag epitope reflect distinct clade-specific functional constraints. *J. Virol*. 88(9):4668-78.

TABLE OF CONTENTS

Chapter 1. Introduction 21

1.1 Overview of CD8+ T-cell development and function 21

1.1.1 CD8+ T-cell lineage 21

1.1.2 CD8+ T-cell response to infection 21

1.1.3 CD8+ T-cells in HIV infection 26

1.2 Origin, spread and basic biology of HIV 27

1.2.1 The origin of HIV epidemic 27

1.2.2 The scale and impact of the current HIV epidemic 30

1.2.3 Coreceptor usage by HIV 30

1.2.4 Viral life cycle 34

1.2.5 Phenotypes of HIV infection in adults and children 37

1.3 CD8+ T-cells and HLA class I in non-progressing adult infection 40

1.3.1 Hyperacute CD8+ T-cell response determines disease progression 40

1.3.2 What constitutes an effective CD8+ T-cell response? 41

1.3.3 HLA class I molecules and disease outcome in adult infection 42

1.4 CD8+ T-cells and HLA class I in non-progressing paediatric infection 45

1.4.1 Immunological tolerance in early life 46

1.4.2 CD8+ T-cells and HLA class I in paediatric HIV 47

1.5 ART and non-progressing HIV infection 49

1.5.1 Reservoir and ART 49

1.5.2 Reservoir and CD8+ T-cells 50

1.5.3 Post-treatment control 51

1.6 Strategies to achieve durable HIV remission: potential for CD8+ T-cells 52

1.7 Aims and hypotheses of this thesis 54

Chapter 2. Materials and methods 56

2.1 Study subjects 56

2.2 Blood processing 59

2.2.1 Separation of plasma and isolation of PBMCs 59

2.2.2 Cryopreservation of cells 60
2.2.3 DNA extraction 60
2.2.4 RNA extraction 61
2.3 HLA typing, viral load measurements and CD4+ T-cell counts 61
2.4 IFN-γ ELISPOT assay 61
2.4.1 ELISPOT method 61
2.4.2 Screening for HIV-specific CD8+ T-cell responses 62
2.4.3 Measurement of functional avidity 63
2.5 Flow cytometry 64
2.5.1 Antibody staining 64
2.5.2 Data acquisition and compensation 65
2.5.3 Tetramer generation 66
2.5.4 Tetramer staining 66
2.6 CD8+ T-cell lines and clones 66
2.6.1 Generation of epitope-specific CD8+ T-cell lines 66
2.6.2 Generation of CD8+ T-cell clones 67
2.7 Immortalised cell lines 67
2.8 Viral inhibition assay 69
2.8.1 Method 1 69
2.8.2 Method 2 70
2.9 HIV sequencing 73
2.9.1 Sanger sequencing of full-length proviral genome 73
2.9.2 Sanger sequencing of proviral Gag and Env 76
2.9.3 Amplification of full-length viral RNA for ultra-deep sequencing 78
2.9.4 Ultra-deep sequencing and de novo assembly of genomes 80
2.9.5 Determination of haplotypes 80
2.10 Viral fitness assays 81
2.10.1 Site-directed mutagenesis of NL4-3 81
2.10.2 Virus production and replication kinetics 81
2.11 Media composition 82
2.12 Statistical analysis 82

Chapter 3. Antiviral efficacy of Gag- and non-Gag-specific CD8+ T-cells in the immune control of adult HIV infection 84

3.1 Preface 84

3.2 Part I: Subdominant Gag-specific anti-HIV efficacy in an HLA-B*57-positive elite controller 84

3.3 Part II: HLA-B*14:02-restricted Env-specific CD8+ T-cell activity has highly potent anti-viral efficacy that is associated with immune control of HIV infection 89

3.3.1 Introduction 89

3.3.2 Chapter-specific materials and methods 91

3.3.2.1 Additional cohorts used for analysis 91

3.3.2.2 Statistical analysis of HLA association and HIV immune control 92

3.3.3 Results 92

*3.3.3.1 Higher antiviral potency of HLA-B*14:02-Env-EL9 versus –Gag-DA9 CD8+ T-cell response 92*

3.3.3.2 Higher functional avidity, antigen recognition and magnitude of EL9 versus DA9 98

*3.3.3.3 Differential Env-EL9 and Gag-DA9 selection pressure in HLA-B*14:01 versus HLA-B*14:02 ..... 101*

3.3.3.4 Impact of Gag-DA9 and Env-EL9 escape mutants on viral fitness and HIV outcome 103

*3.3.3.5 Stronger association of HLA-B*14:02 than HLA-B*14:01 with HIV immune control 106*

3.3.4 Discussion 109

Chapter 4. Contrasting CTL impact in distinct phenotypes of non-progressing paediatric HIV 114

4.1 Introduction 114

4.2 Chapter-specific materials and methods 117

4.2.1 Confirmatory analysis of deep sequenced genomes 117

4.2.2 Escape in HLA-relevant and HLA-irrelevant CD8+ T-cell epitopes in PSPs ... 117

4.3 Results 118

4.3.1 Paediatric slow progressors categorized into high- and low-viraemic groups . 118

4.3.2 SM-like PSPs have greater non-Gag-specific CD8+ T-cell responses early in life 123
4.3.3 Development of CD8+ T-cell-mediated selection pressure with age among PSPs 127
4.3.4 Contrasting selection pressure in VC-like and SM-like children targeting Gag-TL9 133
4.4 Discussion 145

Chapter 5. Lower viral loads and slower CD4 decline in MrkAd5 HIV vaccinees expressing disease-susceptible HLA-B*58:02 152

5.1 Introduction 152
5.2 Chapter-specific materials and methods 154
5.2.1 Study design 154
5.2.2 Interferon-γ ELISPOT assays 159
5.2.3 Statistical analysis 160
5.3 Results 162
5.3.1 HLA-independent vaccine effects 162
5.3.2 HLA-specific vaccine effects on viral load and CD4+ T-cell counts: Protective HLA alleles 164
5.3.3 HLA-specific vaccine effects on viral load and CD4+ T-cell counts: Disease-susceptible HLA alleles 167
5.3.4 HLA-specific vaccine effects on viral load and CD4+ T-cell counts: Neither protective nor disease-susceptible HLA alleles 170
5.3.5 HLA-specific vaccine effects on anti-HIV CD8+ T-cell responses 173
5.4 Discussion 181

Chapter 6. Saporin-conjugated tetramers identify efficacious anti-HIV CD8+ T-cell specificities 186

6.1 Introduction 186
6.2 Chapter-specific materials and methods 187
6.2.1 Tetramer generation 187

6.2.2 Tetramer staining 189
6.2.3 Tetramer internalisation experiments 189
6.2.4 Timecourse of cell-depletion mediated by tetramer-SAP 189
6.3 Results and Discussion 190
6.3.1 Recognition and internalisation of conventional and cytotoxic tetramers 190
6.3.2 Tet-SAP effectively and specifically depletes cognate CD8+ T-cells 193
6.3.3 Contribution of KK10 to immune control of HIV development by tet-SAP 195
6.3.4 Definition of antiviral efficacy of different CD8+ T-cell responses using tet-SAP 198
6.3.5 Discussion 204

Chapter 7. Conclusions 205

Appendix 209

References 216

LIST OF TABLES

Table 2.1. Antibodies used for flow cytometry 65
Table 2.2. HIV-permissive cell lines used for *in vitro* studies 68
Table 2.3. PCR mastermix reaction 73
Table 2.4. PCR amplification primers (Henn et al., 2012) 74
Table 2.5. PCR cycling conditions to amplify full genome (Henn et al., 2012) 74
Table 2.6. Full genome sequencing primers 75
Table 2.7. Composition of the PCR mastermix to amplify HIV *gag* and partial *env* 76
Table 2.8. *Gag* and *env* amplification primers 77
Table 2.9. PCR cycling conditions to amplify HIV *gag* and partial *env* 77
Table 2.10. Sequencing primers for *gag* and partial *env* 78
Table 2.11. RT-PCR mastermix composition 79
Table 2.12. RT-PCR primer sequences (Gall et al., 2012) 79
Table 2.13. RT-PCR cycling conditions 80

Table 3.1. Frequency of HLA-B*14:01 versus HLA-B*14:02 among viraemic controllers and non-controllers 107
Table 3.2. HLA-B*14:02 is significantly enriched among viraemic controllers 108

Table 4.1. Characteristics of the PSPs 119
Table 4.2. Virological and CD4= T-cell profile in VC-like PSPs, SM-like PSPs and healthy HIV-uninfected children 122
Table 4.3. Additional HLA-associated escape mutations that developed in VC-like 133-C within the first years of life 138
Table 4.4. Early escape in SM-like child 517-C develops in non-Gag epitopes 140
Table 4.5. Additional HLA-associated escape mutations that developed in SM-like child 517-C 142
Table 4.6. Sequence evolution in the SM-like child 021-C 144

Table 5.1. Baseline characteristics of the 60 infected Phambili participants studied in this report 158

Table 5.2. Characteristics of the unvaccinated ART-naïve HLA-B*58:02-positive C-clade infected subjects outside of the trial (n=66) 159
Table 5.3. Demographic table stratified by HLA groups 166
Table 5.4. Univariate Cox regression model comparing time to reach CD4+ T-cell count of <350 cells/mm^3 in vaccinees versus placebo-recipients expressing protective HLA-B*57/58:01/81:01 169
Table 5.5. Univariate Cox regression model comparing time to reach CD4+ T-cell count of <350 cells/mm^3 in vaccinees versus placebo-recipients expressing disease-susceptible HLA-B*58:02 171

Table 8.1. Epitopes restricted by HLA-A alleles used in the analysis of paediatric deep sequence data (Chapter 4) 209
Table 8.2 Epitopes restricted by HLA-B alleles used in the analysis of paediatric deep sequence data (Chapter 4) 211
Table 8.3. Epitopes restricted by HLA-C alleles used in the analysis of paediatric deep sequence data (Chapter 4) 214

LIST OF FIGURES

Figure 1.1. T-cell development in the thymus 22
Figure 1.2. Schematic representation of TCR-HLA class I binding 23
Figure 1.3. CD8+ T-cell response in acute and chronic infection 25
Figure 1.4. Geographical distribution of HIV-1 subtypes in 2004-2007 29
Figure 1.5. HIV prevalence and number of HIV-infected people receiving ART worldwide 31
Figure 1.6. Schematic structure and genomic organisation of HIV 33
Figure 1.7. HIV life cycle 35
Figure 1.8. Changes in viral load following HIV infection in paediatric and adult cases 39

Figure 2.1. Example of megamatrix setup 63
Figure 2.2. Representative example confirming absence of HLA-B*27:05 in untransfected H9 cells and HLA-B*27:05 expression in the transfected H9 cells 68
Figure 2.3. Schematic of viral inhibition assay, Method 1 70
Figure 2.4. Schematic of viral inhibition assay, Method 2 71
Figure 2.5. Timecourse to compare CD4+ T-cell activation using PHA/IL2 or CD3/CD28/IL2/IL7 72

Figure 3.1. Clinical profile and anti-HIV suppressive activity of the 1991 Jamaica patient 87
Figure 3.2. Higher antiviral potency of B*14:02-EL9 versus -DA9 CD8 T-cell response 93
Figure 3.3. Maximum-likelihood phylogenetic tree of Env sequences in HLA-B*14 subjects 94
Figure 3.4. Suppressive capacity of epitope-specific Env and Gag CTL lines and clones 97
Figure 3.5. Higher functional avidity, antigen recognition, and magnitude of EL9 versus DA9 99
Figure 3.6. Differential Env-EL9 and Gag-DA9 selection pressure in HLA-B*14:01 versus B*14:02 102

Figure 3.7. Impact of Gag-DA9 and Env-EL9 escape mutants on viral fitness and HIV outcome 104
Figure 3.8. CD4+ T-cell counts in HLA-B*14-positive subjects with either wild type or mutated autologous sequences in Env-EL9 and Gag-DA9 epitopes 105

Figure 4.1. PSPs can be separated into two groups based on their virological profile – SM-like and VC-like 121
Figure 4.2. SM-like PSPs have larger non-Gag-specific CD8+ T-cell responses early in life 124
Figure 4.3. Longitudinal breadth of CD8+ T-cell responses in the PSPs 125
Figure 4.4. SM-like PSPs have greater non-Gag-specific CD8+ T-cell responses early in life 126
Figure 4.5. Maximum likelihood phylogenetic tree from 43 full-genome sequences of the 11 PSP and their mothers 128
Figure 4.6. Development of CD8 T-cell-mediated selection pressure with age among PSPs 129
Figure 4.7. Differences in accumulation of HLA-associated polymorphisms in VC-like versus SM-like children 130
Figure 4.8. Difference in accumulation of polymorphisms in HLA-relevant versus in HLA-irrelevant CD8+ T-cell epitopes in the VC-like PSPs and SM-like PSPs 132
Figure 4.9. Differential CD8+ T-cell targeting and selection pressure in VC-like child 133-C and SM-like children 517-C and 021-C 134
Figure 4.10. HLA-associated Gag-specific escape develops within the first 3 months of life in the VC-like child 133-C 136

Figure 5.1. Phambili ancillary study profile 156
Figure 5.2. Longitudinal viraemia, CD4+ T-cell counts, and CD8+ T-cell responses in the 60 infected vaccinees and placebo-recipients, irrespective of HLA 163
Figure 5.3. Chronic viral setpoint and CD4+ T-cell counts in the infected Phambili subjects expressing protective HLA-B*57/58:01/81:01 or disease-susceptible HLA-B*58:02 allele 168
Figure 5.4. Chronic viral setpoint and CD4+ T-cell counts in the infected 172

Phambili subjects expressing neither protective nor disease-susceptible HLA alleles
Figure 5.5. CD8+ T-cell responses in the infected Phambili subjects expressing disease-susceptible HLA-B*58:02 or those expressing neither protective nor disease-susceptible alleles 174
Figure 5.6. Correlations of Gag- and Nef-specific breadth and magnitude with viral load or CD4 counts in all subjects irrespective of HLA expression and subjects expressing disease-susceptible HLA 176
Figure 5.7. Correlations of Gag- and Nef-specific breadth and magnitude with viral load or CD4 counts in subjects expressing protective HLA and neither protective nor disease-susceptible HLA 177
Figure 5.8. HLA-dependent differential immunodominance hierarchy of CD8+ T-cell responses in chronically C-clade infected, ART-naïve, South African adults 180

Figure 6.1. Example of tetramer validation 188
Figure 6.2. Similar levels of CD8+ T-cell responses are detected with both conventional tet-PE and tet-SAP 190
Figure 6.3. Recognition and internalisation of conventional and cytotoxic tetramers 192
Figure 6.4. Tet-SAP effectively and specifically depletes cognate CD8+ T cells 194
Figure 6.5. Contribution of KK10 to immune control of HIV determined by tet-SAP 197
Figure 6.6. Workflow of the method to assess anti-HIV efficacy of different CD8+ T-cell specificities in human cells using tet-SAP 199
Figure 6.7. Definition of antiviral efficacy of different CD8+ T-cell responses using tet-SAP 201
Figure 6.8. Examples of HIV-infected HLA-B*27:05-positive individuals with low viral loads in whom control of viral replication was dependent on Gag-KK10 response 203

CHAPTER 1. INTRODUCTION

1.1 Overview of CD8+ T-cell development and function

1.1.1 CD8+ T-cell lineage

CD8+ T-cells are major mediators of the immune antiviral response. They originate from committed lymphoid progenitors, which arise in the bone marrow from the pluripotent haematopoietic precursor and migrate to the thymus [reviewed in (Bosselut, 2004; Germain, 2002)]. In the thymus, the lymphoid progenitors (thymocytes) receive signals from the thymic stroma to turn on or off specific genes, such as *Notch*, and to express certain cell-surface molecules, such as CD4 and CD8 co-receptors, and thus become committed to the T-cell lineage and undergo successive developmental stages (**Figure 1.1**). First, the early thymocytes rearrange the TCR genes and assemble the receptor; then they start expressing both CD4 and CD8 (double positive precursors) and their TCR can interact with self-peptide:HLA complexes on thymic epithelial cells. Very weak or very strong interactions of the T-cell precursors lead to cell death of the thymocytes (death by neglect and negative selection, respectively), whereas intermediate level of TCR interaction results in positive selection of the precursors to survive and mature into CD8+ T-cells (those with HLA class I-restricted TCR) or CD4+ T-cells (those with HLA class II-restricted TCR). The mature T-cells then emigrate from the thymus into the bloodstream.

1.1.2 CD8+ T-cell response to infection

The newly formed CD8+ T lymphocytes continuously recirculate between blood and peripheral lymphoid tissues via lymphatics and are known as naïve T-cells until antigen encounter [reviewed in (van Lier, ten Berge, and Gamadia, 2003; Zhang and Bevan, 2011)]. To mount an adaptive immune response during an acute infection, for example, a

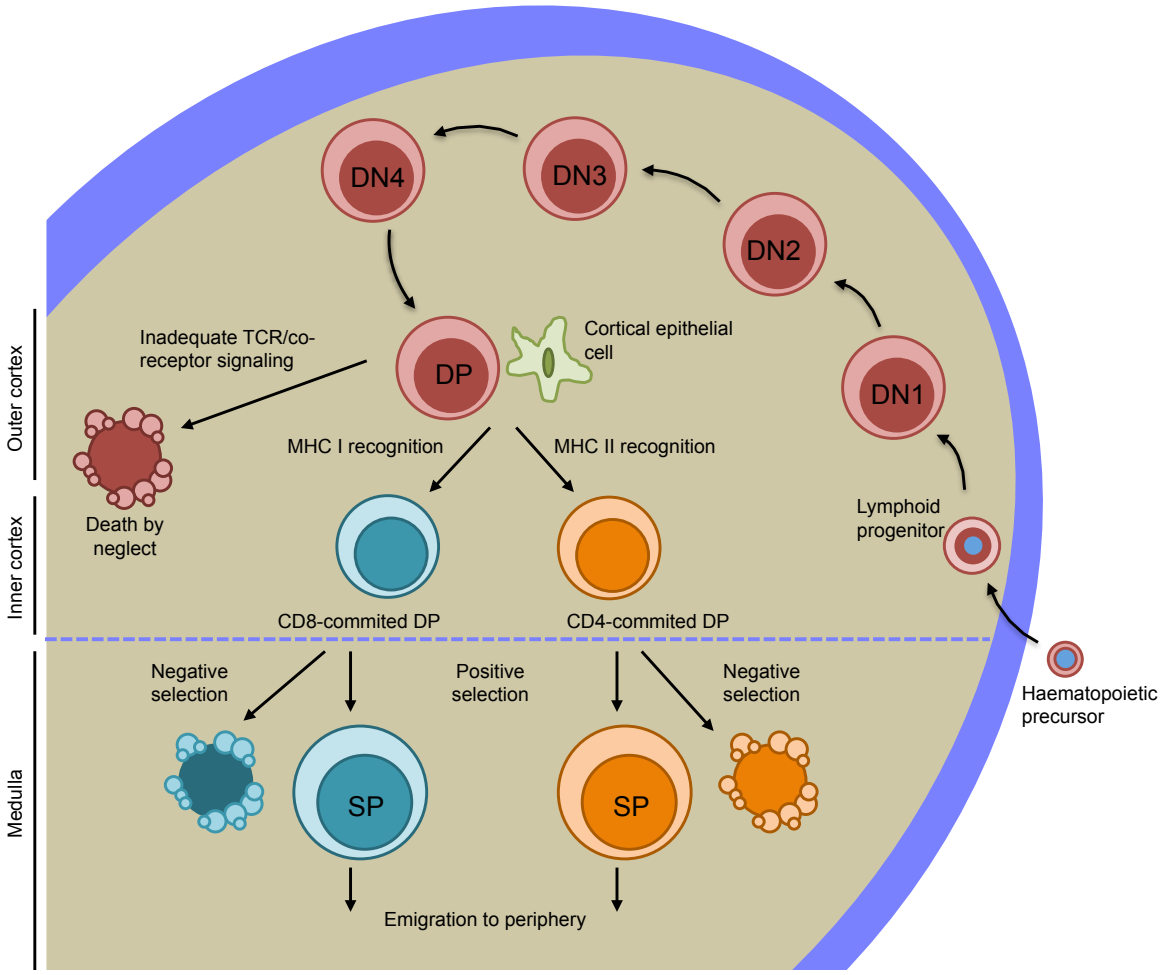


Figure 1.1. T-cell development in the thymus. Early T-cell precursors lack expression of TCR, CD4 and CD8 – double-negative thymocytes (DN, CD4-CD8-). DN thymocytes go through four consecutive differentiation stages defined by expression of CD44 and CD25 (DN1: CD44+CD25-; DN2: CD44+CD25+; DN3: CD44-CD25+; DN4: CD44-CD25-). The thymocytes express pre-TCR (pre-TCR α-chain and rearranged TCR β-chain) at DN2-DN4; at the transition to double positive stage (DP, CD4+CD8+), TCR α-chain is rearranged and a complete αβ-TCR is expressed. TCR on DP thymocytes interact with HLA I or II on epithelial cells presenting self-peptides. Too much or too little interaction leads to apoptosis (negative selection and death by neglect, respectively); intermediate interaction results in positive selection. HLA I-binding thymocytes become single-positive (CD8+) T cells, and HLA II-binding thymocytes become single-positive (CD4+) T cells; both types then migrate to periphery as naïve T cells. Adapted from Germain, R. N. *Nature Rev. Immunol.* 2002.

naïve CD8+ T-cell must recognise its specific foreign antigen. CD8+ T-cells can only recognise pathogen-derived antigens that have been processed intracellularly and are presented by HLA class I molecules (**Figure 1.2**) (Zinkernagel and Doherty, 1974); this requirement allows CD8+ T-cells to act only against intracellular pathogens, such as viruses or intracellular bacteria. Antigen recognition by a naïve CD8+ T-cell will trigger robust clonal expansion and differentiation of naïve antigen-specific T-cells into specialised effector cells – primary immune response that will last for 1-2 weeks (**Figure 1.3A**). It is at this stage that cytotoxic CD8+ T-cells are generated; these are capable of producing cytotoxic molecules (e.g. perforin, granzymes) and cytokines (e.g. IFN-γ and TNF-α) and directly killing infected target T-cells.

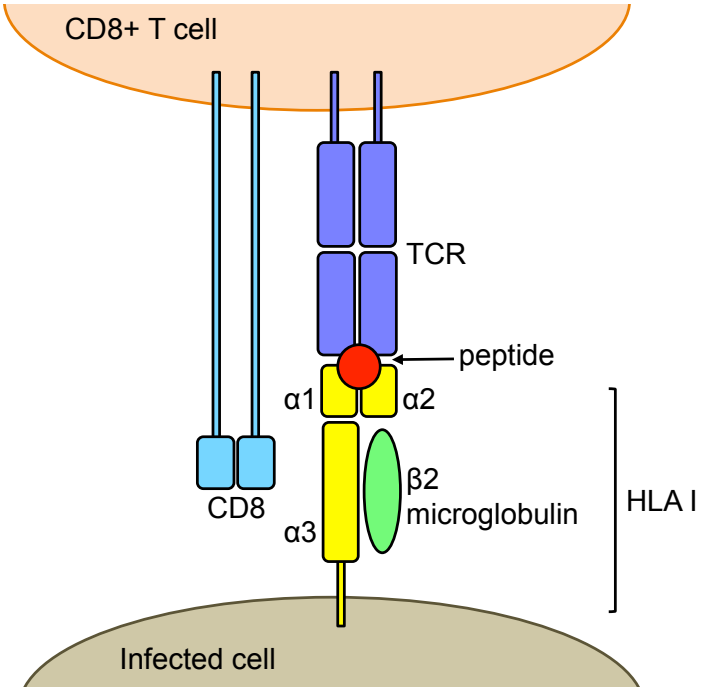


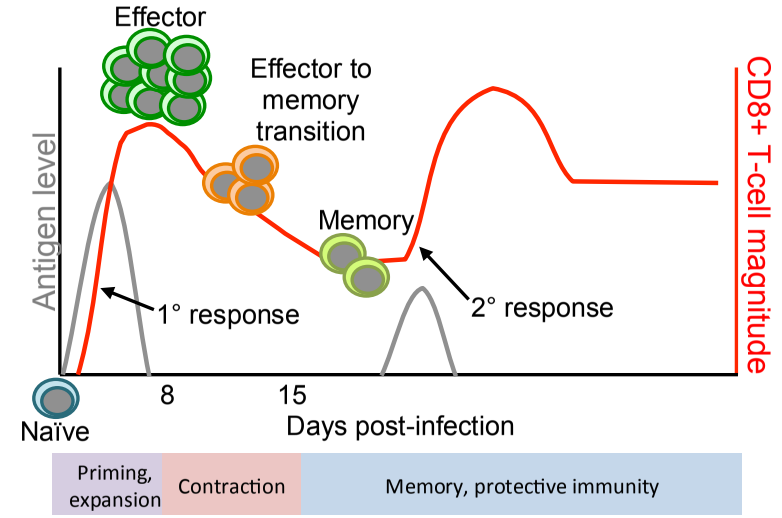
Figure 1.2. Schematic representation of TCR-HLA class I binding. An antigen-derived peptide within the HLA class I binding groove on the surface of an infected cell is presented to the cognate CD8+ T-cell for TCR recognition. Binding of the CD8 co-receptor makes an additional contact with the HLA molecule stabilising the TCR-HLA interaction. Coreceptor binding is required for a CD8+ T-

cell to make an effective response to an antigen. Adapted from Murphy, K. Chapter 6. Antigen presentation to T lymphocytes. In: Murphy, K. *Janeway's Immunobiology*, 8th ed. New York, NY: Garland Science; 2012: 201-237.

Typically, an acute infection can be resolved within days and over the following weeks the majority (>90%) of effector CD8+ T-cells will die – the contraction phase of the immune response. The surviving T-cells will gradually develop into memory T-cells, first effector memory and then central memory. Memory CD8+ T-cells can proliferate and persist for a long time in the absence of antigen supported by IL-7 and IL-15 [reviewed in (Surh and Sprent, 2008)]; and upon restimulation (e.g. reinfection) they can rapidly reactivate effector functions (secondary response), conferring protective immunity. At each stage of differentiation, from naïve to central memory, CD8+ T-cells express different phenotypes that reflects T-cell homing potential and interactions with other cells (**Figure 1.3B**). It is also important to note that CD4+ T-cell help is essential in order for CD8+ T-cells to generate an efficient primary response (with an exception of some infections; reviewed in (Laidlaw, Craft, and Kaech, 2016)) and provide protective memory.

Despite the robustness of the CD8+ T-cell antiviral response, some viruses are not fully eliminated, resulting in chronic infection. In this setting, excessive and continuous antigenic stimulation drives CD8+ T-cell exhaustion, whereby CD8+ T-cell effector and memory function become progressively impaired and antigen-specific cells eventually undergo apoptosis (**Figure 1.3C**).

A

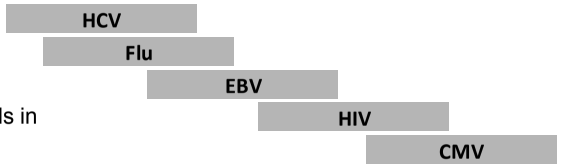


B

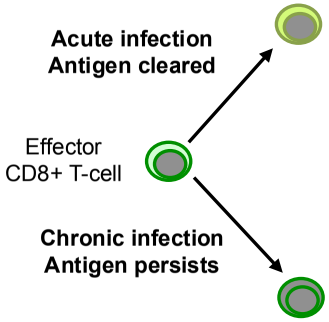
Differentiation of CD8+ T-cell subsets

Naive	Antigen experienced			
CCR7+	CCR7+	CCR7-	CCR7-	CCR7-
CD45RA+	CD45RA-	CD45RA-	CD45RA+/-	CD45RA+/-
CD27+	CD27+	CD27+	CD27+	CD27-
CD28+	CD28+	CD28+	CD28-	CD28-

Patterns of antigen-specific CD8+ T-cells in different infections



C



Highly polyfunctional memory CD8+ T-cell

IFN-γ	TNF	Cytotoxic potential	IL-2	Proliferative potential	Apoptosis
+++	+++	+++	+	+++	-

Activity: +++ (High) → - (Low)

Hierarchical exhaustion of CD8+ T-cell

+++	++	++/-	+/-	++	-
++	+	+	-	+	-
+/-	+/-	+/-	-	+/-	+/-
+/-	-	-	-	-	++
					+++



Figure 1.3. CD8+ T-cell response in acute and chronic infection. A. Three phases of the CD8+ T-cell response in acute infection. Upon antigen encounter, cognate naïve CD8+ T-cells undergo clonal expansion differentiating into short-lived effector T cells. Upon antigen clearance, effector CD8+ T-cell-response contracts and effector cells differentiate into memory cells that are able to rapidly re-expand upon secondary exposure to the antigen and clear it more rapidly than during the primary response. Adapted from Pauken, K. E. & Wherry, J. E. *Trends in Immunology* 2015. **B.** Phenotype of CD8+ T-cells during differentiation from naïve to central memory cells based on expression of CD45RA (T-cell activation/co-stimulation), CCR7 (lymphoid homing), CD27 (T-cell co-stimulation) and CD28 (T-cell co-stimulation). Distribution of different virus-specific CD8+ T-cell phenotypes in several viral infections (upon clearance of antigen (Flu) or latent stage (HCV, EBV, HIV, CMV) is shown. Adapted from Appay, V. *et al. Cytometry* 2008. **C.** Memory formation in acute and chronic infections. When antigen is cleared, effector CD8+ T-cells differentiate into highly functional memory cells that can produce cytokines, kill infected cells and proliferate. In chronic infection, antigen persistence causes T-cell dysfunction, hierarchical loss of effector functions, increased expression of inhibitory receptors (PD-1, Lag-3, Tim-3, etc.) and eventual death. Adapted from Wherry, E. J. *Nature Immunology* 2011.

1.1.3 CD8+ T-cells in HIV infection

A case in point of a chronic infection is HIV. Many lessons have been learned from studies of natural HIV-specific CD8+ T-cell response:

- Early in HIV research, virus-specific HLA-restricted CD8+ T-cells capable of killing infected cells were identified (Walker et al., 1988; Walker et al., 1987);
- Then sequencing of proviral DNA revealed accumulation of mutations within CD8+ T-cell epitopes suggesting that these cells exert selection pressure on the virus forcing it to escape (Phillips et al., 1991);
- In a few more years, the temporal association between the acute phase viral load decline and appearance of an HIV-specific CD8+ T-cell response in the absence of an antibody response was established (Borrow et al., 1994; Koup et al., 1994), and this was also shown to coincide with early selection of escape mutations (Goonetilleke et al., 2009);

- Soon the first genetic study showed that expression of HLA class I molecules most strongly influences HIV disease progression, thus underscoring the role of HLA-restricted CD8+ T-cells (Kaslow et al., 1996); this was confirmed in later GWAS (Fellay et al., 2007; Pereyra et al., 2010);
- Additionally, CD8+ T-cell depletion experiments in SIV-infected macaques demonstrated the requirement for CD8+ T-cell-mediated suppression of viral replication *in vivo* (Jin et al., 1999; Schmitz et al., 1999);
- Finally, a rare group of 'elite controllers,' individuals who remain disease-free without therapy for decades, was identified (Deeks and Walker, 2007; Migueles and Connors, 2010); in these individuals, HLA-restricted CD8+ T-cell response plays the central role in their successful control of infection (Goulder and Walker, 2012).

However, many questions remain outstanding. What makes their immune system, in particular their CD8+ T-cells, capable of this extraordinary control? Can these cellular qualities be therapeutically induced in other infected people? What is the gold standard of a CD8+ T-cell response that needs to be elicited? And finally, are there similar patterns in paediatric infection?

1.2 Origin, spread and basic biology of HIV

1.2.1 The origin of HIV epidemic

Infection with HIV typically results in persistent viraemia and progressive disease culminating in increasingly profound loss of immunocompetence known as AIDS. The current HIV pandemic began when in 1981 the first five AIDS cases in the United States were reported (Gottlieb et al., 1981) and two years later HIV was isolated and discovered

to be the etiologic agent of AIDS (Barre-Sinoussi et al., 1983; Gallo et al., 1983). Phylogenetically, there are two types of the virus, HIV-1 and HIV-2 (Clavel et al., 1986; Guyader et al., 1987). HIV-1 is further subdivided into 4 groups based on genetic variation: M (major, that further diversifies into 9 subtypes A-D, F-H and multiple recombinant forms; **Figure 1.4**), O (outlier), N (non-M, non-O) and recently discovered P (continuing through the alphabet according to the guidelines) (Hemelaar et al., 2011; Plantier et al., 2011; Robertson et al., 2000; Vallari et al., 2011). It is HIV-1 group M that is the most virulent and pathogenic with subtype C accounting for nearly 50% of the infections worldwide and subtype B being the most geographically dispersed (Hemelaar et al., 2011). Progenitor virus of the pandemic HIV-1 lineage group M is most closely related to the SIV from *Pan troglodytes troglodytes* apes in southern Cameroon that was passed from chimpanzees to humans, possibly through bushmeat hunting (Keele et al., 2006).

The first documented case of HIV-1 (further referred to as HIV) infection in humans was retrospectively identified from a plasma sample obtained in 1959 from a male with sickle-cell trait living in what is now Kinshasa, the Democratic Republic of Congo (Nahmias et al., 1986; Zhu et al., 1998). However, only recently evolutionary analyses revealed that the HIV epidemic originated in the early 1920s in Kinshasa from a single cross-species transmission event to humans (Faria et al., 2014). From Kinshasa, the infections, transmitted in human adults by contact with body fluids, increasingly dispersed geographically as a result of a compilation of political and socio-economic factors: the busy transportation network that connected largest cities in sub-Saharan Africa, urban growth, gain of independence by Congo followed by changes in the behaviour of sex workers (e.g. exposure to contaminated injections and higher rate of partner exchange) and even

iatrogenic interventions (e.g. unsterilised injections in sexually transmitted disease clinics) (Faria et al., 2014).

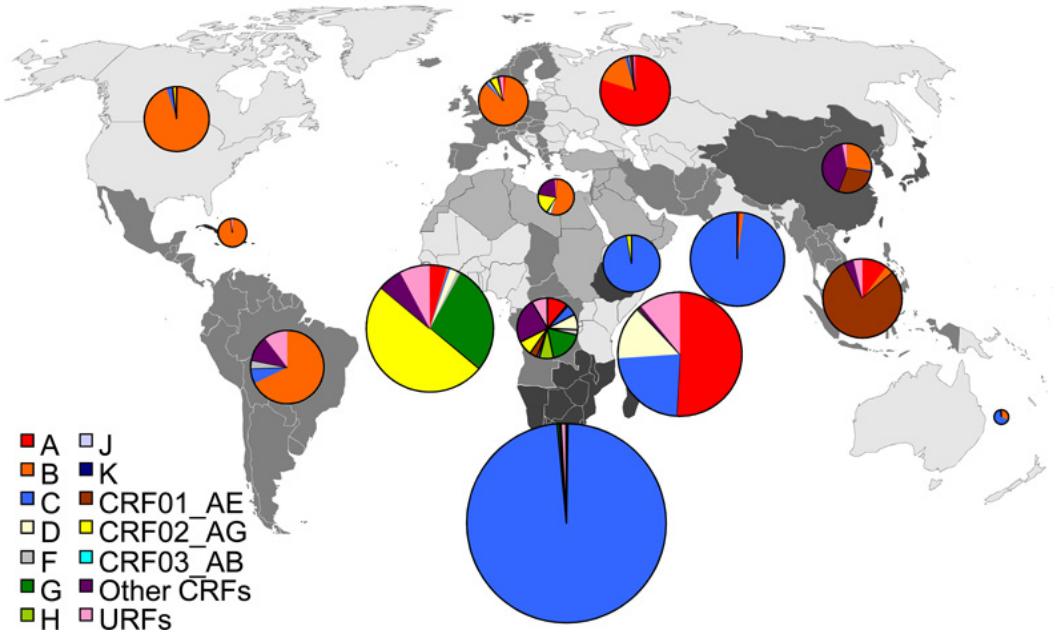


Figure 1.4. Geographical distribution of HIV-1 subtypes in 2004-2007. The surface areas of the pie-charts (representing the 15 regions of the world based on UNAIDS classification) correspond to the relative numbers of HIV-infected people in the regions. Adapted from Hemelaar, J. *et al. AIDS* 2011.

1.2.2 The scale and impact of the current HIV epidemic

Since the isolation of HIV, >34 million people have died of it and as of 2014, nearly 37 million are living with HIV, of whom almost 10% are children (**Figure 1.5A**) (AVERT, 2016). ART has saved millions of lives and prevented millions of transmissions; an estimated 15.8 million people are receiving ART today and the number is continuously growing (**Figure 1.5B**) (WHO, 2015a), but the problems of the associated stigma, expense and adherence, particularly among adolescents (Bobat, Archary, and Lawler, 2015), remain very pertinent. Moreover, there is now a striking shift in the burden of co-morbidities away from AIDS-defining illness and towards cancer, cardiovascular disease and liver disease; and while the prevalence of non-AIDS mortality reaches 53% among HIV-infected ART-treated people in high-income countries, in sub-Saharan Africa non-AIDS complications contribute to 18.5% of deaths but this number is increasing now as ART is being widely rolled out (Farahani et al., 2016).

1.2.3 Coreceptor usage by HIV

HIV is an enveloped retrovirus (**Figure 1.6**) of the *Lentivirus* genus, able to integrate into host T-cell genome and persist for many years causing slowly evolving disease [reviewed in (Pollard and Malim, 1998)]. To gain cell entry, viral gp120 binds to a CD4 molecule and a coreceptor, typically a chemokine receptor CCR5 (Choe et al., 1996; Deng et al., 1996) or CXCR4 (Bleul et al., 1996; Oberlin et al., 1996), followed by gp41-mediated fusion of the viral envelope with cell membrane and release of the viral genome into the cytoplasm (**Figure 1.7A**). Most frequently transmitted HIV strains use CCR5 coreceptors (R5 viruses) and strains that use CXCR4 coreceptors (X4 viruses) tend to emerge later in the disease and are associated with more rapid progression (Connor et al., 1997).

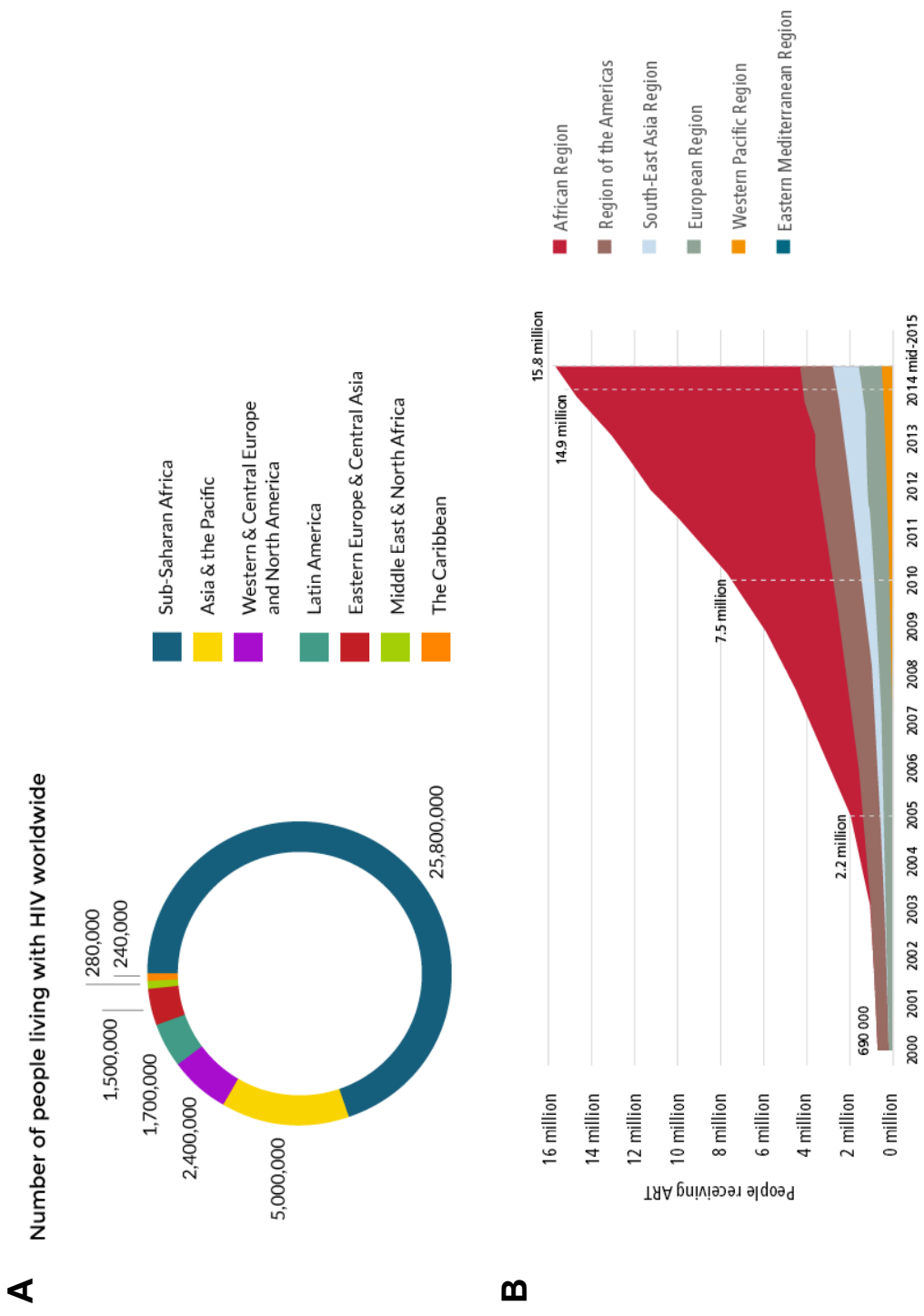
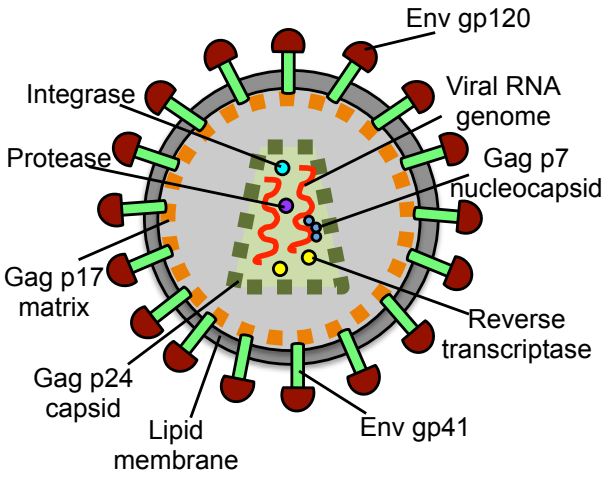
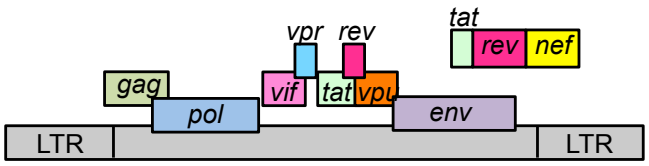

A
Number of people living with HIV worldwide
Sub-Saharan Africa
Asia & the Pacific
Western & Central Europe and North America
Latin America
Eastern Europe & Central Asia
Middle East & North Africa
The Caribbean
25,800,000
5,000,000
2,400,000
1,700,000
1,500,000
280,000
240,000
B
African Region
Region of the Americas
South-East Asia Region
European Region
Western Pacific Region
Eastern Mediterranean Region
People receiving ART
0 million
2 million
4 million
6 million
8 million
10 million
12 million
14 million
16 million
690 000
2.2 million
7.5 million
14.9 million
15.8 million
2000
2001
2002
2003
2004
2005
2006
2007
2008
2009
2010
2011
2012
2013
2014 mid-2015

Figure 1.5. HIV prevalence and number of HIV-infected people receiving ART worldwide. A. Number of HIV-infected people worldwide based on the 2014 data. Source: AVERT, http://www.avert.org/professionals/hiv-around-world/global-statistics#footnote2_e2c543m. **B.** Estimated number of people receiving ART globally and by WHO region, 2000-2015. Source: Global AIDS Response Progress Reporting (UNAIDS/UNICEF/WHO) and UNAIDS/WHO estimates; http://www.who.int/hiv/data/art_2003_2015.png?ua=1.

In addition to the coreceptors that are required for viral entry, there are other factors that may promote HIV infection. For example, a subset of CD4+ T_H17 cells enriched in the gut exhibit higher levels of HIV infection than other CD4+ T-cell subsets; this enhanced susceptibility is due to higher expression level of the integrin α4β7, a gp120 binding receptor that promotes HIV binding to target T-cells prior to infection, and due to the almost complete inability of the CD4+ T_H17 cells to secrete MIP-1α and MIP-1β – CCR5 ligands that are produced by some CD4+ T-cells and that can prevent infection by R5 HIV strains (Alvarez et al., 2013; Gosselin et al., 2010; Monteiro et al., 2011).

The importance of the coreceptor usage by HIV comes from the studies showing that homozygosity for a 32bp deletion in the *CCR5* allele (*CCR5*Δ32) renders T-cells markedly resistant to HIV infection (Dean et al., 1996; Huang et al., 1996; Liu et al., 1996) and heterozygosity for CCR5Δ32 significantly delays disease progression and AIDS onset (Feeney et al., 2006; Michael et al., 1997; Misrahi et al., 1998; Smith et al., 1997). This is further substantiated by the report of the 'Berlin patient', an HIV-infected individual who underwent a stem-cell transplantation to treat acute myeloid leukemia, using a transplant from a donor homozygous for *CCR5*Δ32; the 'Berlin patient' has been in HIV remission since the first report by Hutter and colleagues (Hutter et al., 2009; Yukl et al., 2013). These findings led to the first human trial in a cohort of 12 chronically infected ART-treated participants in which the *CCR5* gene in patients' autologous CD4+ T-cells was made





Gene		Gene product/function
gag	Group-specific antigen	Core and matrix proteins
pol	Polymerase	Reverse transcriptase, protease and integrase enzymes
env	Envelope	Transmembrane glycoproteins; gp120 binds to CD4 and CCR5/CXCR4; gp41 is required for viral fusion
tat	Transactivator	Positive regulator of transcription
rev	Regulator of viral expression	Allows export of mRNA transcripts from nucleus
vif	Viral infectivity factor	Affects particle infectivity
vpr	Viral protein R	Transport of preintegration complex to nucleus; augments virion production; cell growth arrest
vpu	Viral protein U	Promotes intracellular CD4 degradation; enhances release of virus from cell membrane
nef	Negative-regulation factor	Augments viral replication; decreases CD4, HLA I and II expression

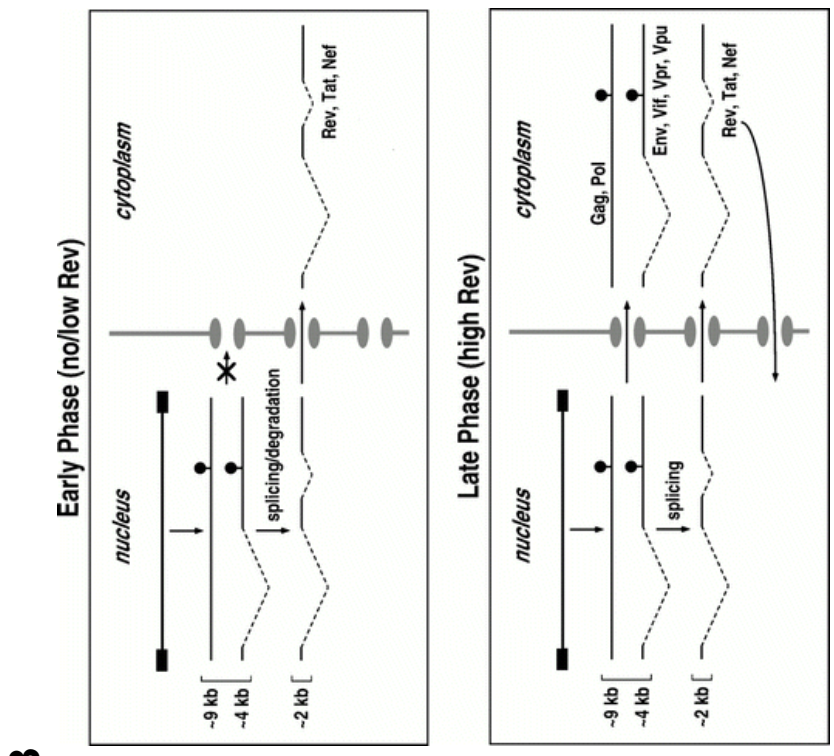
Figure 1.6. Schematic structure and genomic organisation of HIV. Like all retroviruses, HIV RNA genome contains 5' and 3' long terminal repeats (LTR) that are important for viral integration and transcription. The genome can be translated in three frames; genes, their products and functions are listed. Adapted from Murphy, K. Chapter 13. Acquired immune deficiency syndrome. In: Murphy, K. *Janeway's Immunobiology*, 8th ed. New York, NY: Garland Science; 2012: 509-570.

dysfunctional *ex vivo* with zinc-finger nucleases and the modified cells were then reinfused back (Tebas et al., 2014). The trial demonstrated safety of the procedure, engraftment and persistence of the modified cells, and one participant had a long delay of viral rebound upon treatment interruption which then reached undetectable levels prior to treatment restart. This individual was found to be heterozygous for the *CCR5*Δ32 mutation prior to the trial and results in his case underscored the likely need for biallelic *CCR5* knockout,

should this approach be successful. In an animal study, expression of a fusion molecule of CD4-Ig with CCR5-mimetic peptide that binds HIV Env, protected four macaques from consecutive SIV challenges (Gardner et al., 2015). Overall, the CCR5 approach is an area of active research.

1.2.4 Viral life cycle

Once the virus has entered the cell and released its RNA genome into the cytoplasm, viral RNA is reverse-transcribed into linear double-stranded cDNA by the viral enzyme reverse transcriptase; the cDNA has terminal duplications (long terminal repeats, LTR) that are not present in the RNA form (**Figure 1.7A**) [reviewed in (Pollard and Malim, 1998)]. At this point, the cDNA is incorporated into the preintegration complex, enters the nucleus in association with the viral Vpr and is integrated into the cellular genome by the viral enzyme integrase. The integrated form of HIV is known as the provirus, which remains indefinitely in the host genome and serves as a template for viral transcription - establishing the state of latency.


B
Early Phase (no/low Rev)
nucleus
cytoplasm
~9 kb
~4 kb
~2 kb
splicing/degradation
Rev, Tat, Nef
Late Phase (high Rev)
nucleus
cytoplasm
~9 kb
~4 kb
~2 kb
splicing
Gag, Pol
Env, Vif, Vpr, Vpu
Rev, Tat, Nef

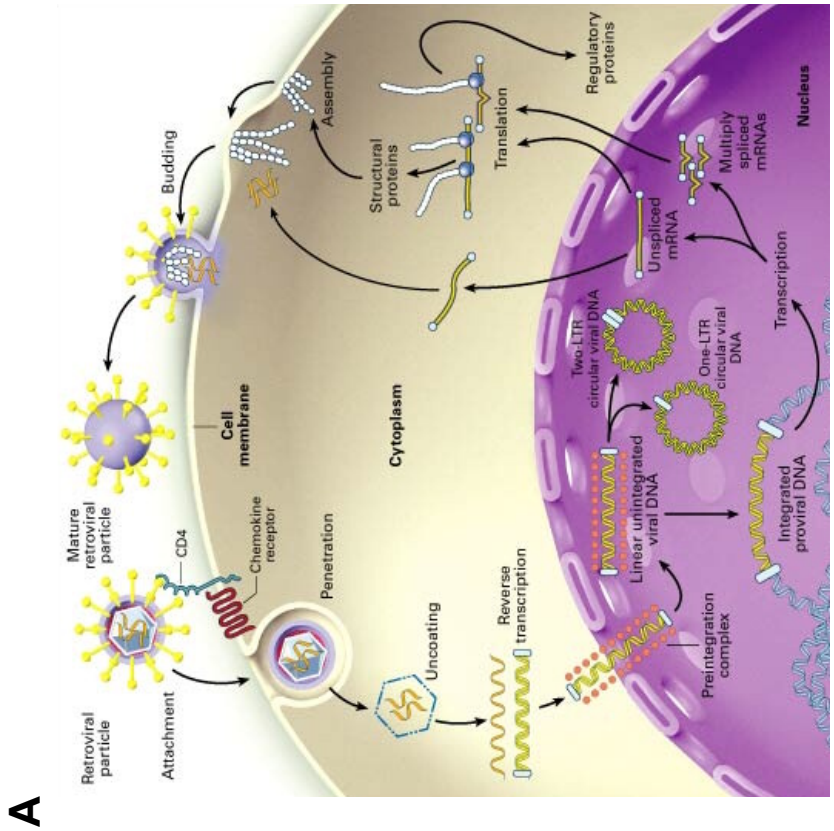

A
Retroviral particle
Attachment
Mature retroviral particle
CD4
Chemokine receptor
Penetration
Cell membrane
Uncoating
Reverse transcription
Preintegration complex
Linear unintegrated viral DNA
Two-LTR circular viral DNA
One-LTR circular viral DNA
Integrated proviral DNA
Cytoplasm
Nucleus
Transcription
Unspliced mRNA
Multiply spliced mRNAs
Regulatory proteins
Translation
Structural proteins
Assembly
Budding

Figure 1.7. HIV life cycle. A. Main steps in viral life cycle, starting from virion attachment to CD4 and a chemokine coreceptor, fusion with cell membrane, entry into the cell, reverse transcription of the viral genome into linear double stranded cDNA, transport to the nucleus and integration into host cell DNA (provirus formation). Unintegrated circular forms of viral cDNA are by-products of the integration. Upon cellular activation, low level transcription of the proviral DNA ensues, generating mostly multiply spliced transcripts, encoding regulatory proteins Tat and Rev and accessory Nef. Activation of transcription by Tat leads to increase in the levels of Rev and a shift to predominantly unspliced viral transcripts, encoding structural proteins Gag and Pol, and incompletely spliced transcripts, encoding Env, Vif, Vpr and Vpu. These are exported from the nucleus, translated and packaged into immature virions, which are the released from the cell. Maturation of the viral particles is completed with the protease-mediated cleavage of the products of *gag* and *pol* genes into their final forms. Furtado, M. R. *et al. NEJM* 1999. **B.** Bi-phasic HIV-gene expression. In the early phase, Rev is low or absent and unspliced or incompletely spliced transcripts cannot be exported from the nucleus. Multiply spliced transcripts are constitutively exported into the cytoplasm and viral proteins Tat and Rev are produced. When levels of Rev are sufficiently high, unspliced and incompletely spliced transcripts are exported to the cytoplasm. Adopted from Pollard, V. W. & Malim, M. H. *Ann. Rev. Microbiol*. 1998.

HIV transcription and production of infectious virions occurs only in activated CD4+ T-cells [reviewed in (Siliciano and Greene, 2011)]. Cellular activation leads to the expression of transcription factors NFkB and NFAT, which bind to the proviral LTR and initiate transcription. Transcription of the proviral DNA and alternative mRNA splicing generate different mRNA species: ~2kb multiply spliced mRNAs, encoding Tat, Rev or Nef; ~4kb incompletely spliced mRNAs, encoding Env Vpu, Vif or Vpr; and ~9kb unspliced mRNAs encoding structural proteins Gag and Pol. HIV gene expression is biphasic (**Figure 1.7B**) [reviewed in (Pollard and Malim, 1998)]. In the early Rev-independent phase, ~2kb mRNAs are constitutively exported from the nucleus into the cytoplasm, irrespective of the levels of Rev, and produce Tat, Rev and Nef. Tat enhances viral transcription by forming a complex with P-TEFb (the cellular cyclin T1 and cyclin-dependent kinase 9 (CDK9)), binding to the transcriptional activation region in the 5' LTR of the provirus and

phosphorylating RNA polymerase to promote viral elongation. At this stage, however, ~4kb and ~9kb transcripts are confined strictly to the nucleus and are either spliced or degraded until sufficiently high levels of Rev accumulate in the nucleus. Rev is absolutely required for the nuclear export of the incompletely spliced and unspliced transcripts and is therefore essential for the expression of viral structural proteins. Once the concentration of Rev is sufficiently high, Rev exports the ~4kb and ~9kb transcripts into the cytoplasm (late phase), where they are translated to produce all the other viral proteins. Structural proteins and two copies of viral unspliced transcipts (future viral genome) then assemble into immature virions and become enveloped into membrane, Env, as they bud from the cell. The final step, when the viral enzyme protease cleaves the structural proteins to their fully functional forms, completes maturation of the new viral particle, which can now infect other cells.

It is important to note that viral transcription can only take place in activated cells, the reason being that in resting cells, the transcriptional environment prevents active transcription [reviewed in (Siliciano and Greene, 2011)]. For example, transcription factor NFkB and NFAT are not present in the nucleus in resting cells (Nabel and Baltimore, 1987; Shaw et al., 1995); the activity of the positive elongation factor P-TEFb is inhibited in resting cells (Contreras et al., 2007); and epigenetic modifications of the chromatin in resting cells, such as hypermethylation of the proviral 5' LTR (Blazkova et al., 2009), repress HIV transcription.

1.2.5 Phenotypes of HIV infection in adults and children

[This section is part of the published review by Goulder, P.J., Lewin S.R. & **Leitman, E.M. 2016 Mar 14**. Paediatric HIV infection: the potential for cure. *Nature Reviews Immunology*. 10. 1038/nri.2016.19. Epub ahead of print.]

In a typical progressing ART-naïve HIV infection in adults, a viral setpoint of ~30,000 HIV RNA copies/ml is reached by ~6 weeks post-infection and median times to AIDS and death are 10 and 11 years, respectively (Babiker et al., 2000) (**Figure 1.8**). In contrast, in a typical paediatric untreated perinatal HIV infection, viral setpoint is reached by 5 years, median time to AIDS is 1 year (>70% progress to AIDS within 6 months of age) (Mphatswe et al., 2007) and >50% children will have died by the age of 2 years (Newell et al., 2004).

In the small subset of ART-naïve individuals infected with HIV who maintain normal CD4+ T-cell counts and immune function and therefore do not progress to disease, the mechanisms operating in children and adults are markedly different. Non-progressing adult infection, in elite controllers, is typically characterised by a strong HIV-specific CD8+ T-cell response restricted by 'protective' HLA class I molecules such as HLA-B*27 and HLA-B*57 (Kaslow et al., 1996; Kiepiela et al., 2007; Pereyra et al., 2010), such that high CD4+ T-cell counts are maintained as a consequence of successful suppression of viraemia beneath the levels of detection (normally <50 HIV RNA copies/ml). By contrast, non-progressing HIV infected children (defined as healthy ART-naïve children >5 years old who maintain absolute CD4+ T-cell counts in the normal range for age-matched uninfected children, i.e. >750 cells/mm^3) (Shearer et al., 2003) maintain normal CD4+ T-cell counts despite median viral loads of ~30,000 copies/ml plasma (Adland et al., 2014), and here the HLA-B alleles that strongly influence disease outcome in adult infection do not play a significant role (Adland et al., 2015). It is important to note the distinction between non-progressing infection, defined above by the maintenance of normal CD4 counts in the absence of ART, and long-term survivors who typically have low CD4 counts and high immune activation (Adland et al., 2014) but may be asymptomatic, presenting late, and in the case of children

are usually stunted (Ferrand et al., 2007; Judd et al., 2009). Non-progressing adult and paediatric infection is characterised by low levels of immune activation but through distinct

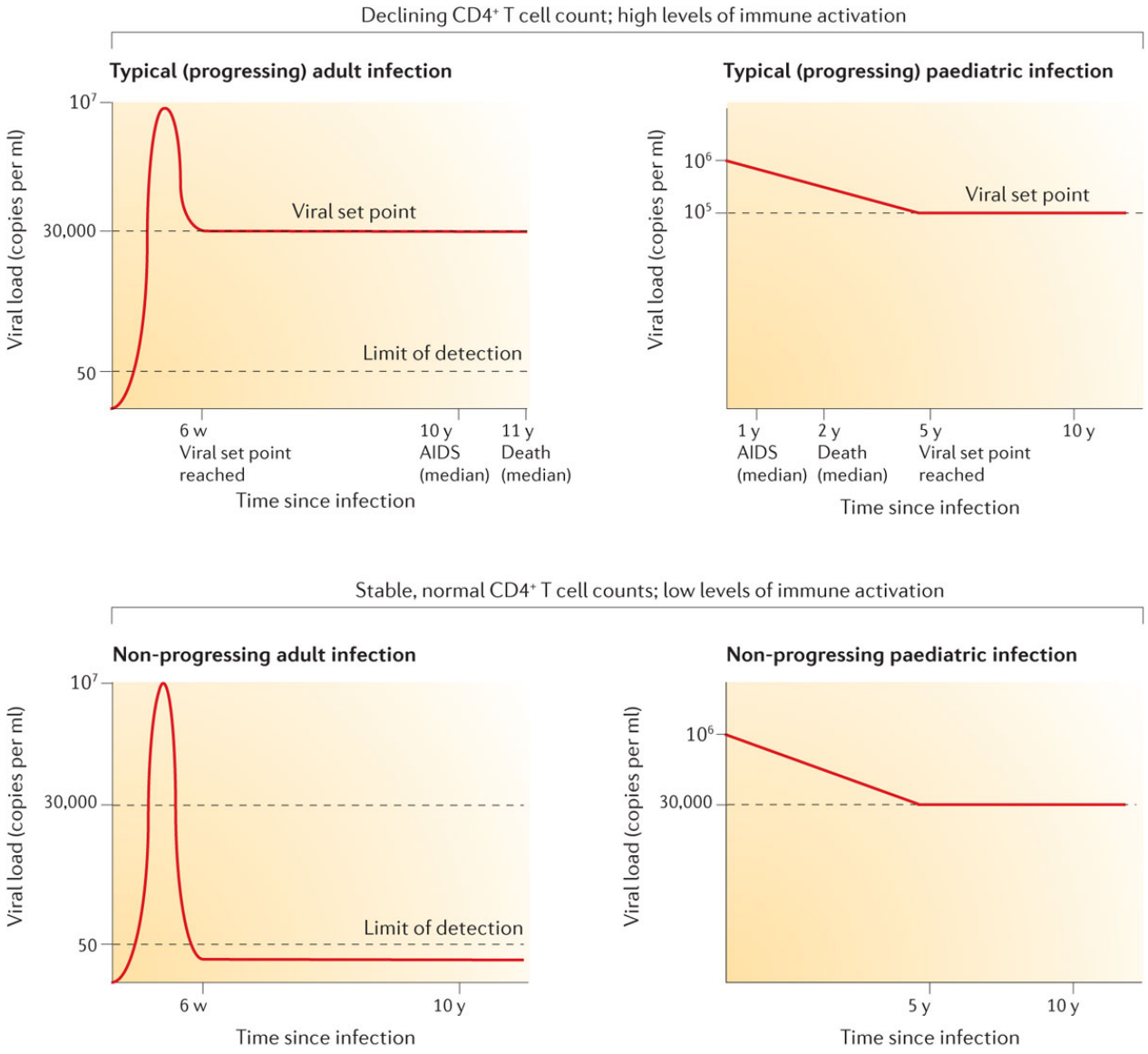


Figure 1.8. Changes in viral load following HIV infection in paediatric and adult cases. Typical, progressing adult and paediatric infection (upper panels), and non-progressing adult and paediatric infection (lower panels) (Adland et al., 2014; Adland et al., 2015; Babiker et al., 2000; Mori et al., 2015). Typically, in HIV infection of ART-naïve adults, a viral setpoint is reached after 6 weeks, and the median time to AIDS is 10 years. In typical, ART-naïve paediatric infection with HIV, a viral setpoint is reached after 5 years, and the median time to AIDS is 1 year. Non-progressing adult infection is characterised by low or undetectable viral loads and low levels of immune

activation. The prevalence of non-progressing paediatric infection is 5-10% and of adult elite controllers is ~0.3%. Non-progressing paediatric infection also features low levels of immune activation but in the setting of high viral loads (~30,000 copies/ml). This figure is adapted from the review by Goulder, P.J., Lewin S.R. & **Leitman, E.M.** in *Nature. Rev. Immunol.* 2016.

mechanisms. In non-progressing adult infection this is achieved through HLA-mediated suppression of viral replication. In non-progressing paediatric infection, the mechanism by which immune activation remains low in some patients despite persistent high levels of viraemia (Adland et al., 2014) is unknown. The phenotype of normal CD4+ T-cell count and low immune activation despite high viral loads is reminiscent of the natural hosts of SIV infection, such as sooty mangabey and African green monkey, who live normal life spans with normal CD4+ T-cell counts and low levels of immune activation, with median viral loads of ~10^5 SIV copies/ml (Silvestri et al., 2003).

1.3 CD8+ T-cells and HLA class I in non-progressing adult infection

1.3.1 Hyperacute CD8+ T-cell response determines disease progression

As describe above (see Section 1.1.3), CD8+ T-cells play the central role in the control of adult HIV infection. However, why are CD8+ T-cells unable to clear the infection fully even in the elite controllers, despite CD8+ T-cell robust and effective antiviral response? An important insight emerged from the recent FRESH study that enrolled HIV-seronegative young women in South Africa and monitored their HIV status twice weekly, so that in cases of infection, they could 'catch' the earliest events occurring in the first ~20 days of transmission, prior to the peak viraemia (Ndhlovu et al., 2015a). Examination of CD8+ T-cell responses in the women who acquired infection showed, for the first time, that even in this hyperacute phase CD8+ T-cells mounted a massive HIV-specific response; the faster

the virus-specific cells reached maximum activation and the higher the activation was, the lower the viral setpoint was. This is important because viral setpoint is predictive of disease progression (Lyles et al., 2000). However, the early effective HIV-specific CD8+ T-cells underwent rapid apoptosis, unless treatment was initiated (Walker, 2016). These findings for the first time showed the crucial role of CD8+ T-cells during the earliest events in infection that largely determine the subsequent course of disease progression.

1.3.2 What constitutes an effective CD8+ T-cell response?

Several studies suggest a number of CD8+ T-cell functional characteristics that distinguish elite controllers from progressors. Although no consensus exists and the explanation is likely to be multifactorial, CD8+ T-cells from elite controllers have been shown to exhibit the following qualities:

- A peculiar pattern of activation markers that is different from progressors or individuals on ART (Saez-Cirion et al., 2007);
- High proliferation potential and polyfunctionality in response to antigenic stimulation (Betts et al., 2006; Horton et al., 2006; Migueles et al., 2002);
- High functional avidity (Almeida et al., 2007; Almeida et al., 2009);
- Effective acquisition of effector-cell phenotype and elimination of infected cells (Chen et al., 2012; Hersperger et al., 2010; Migueles et al., 2008; Migueles et al., 2000; Saez-Cirion et al., 2007);
- Particular TCRs capable to cross-recognise viral mutants (Chen et al., 2012; Ladell et al., 2013); and
- Targeting of specific viral epitopes. Population-level studies showed that Gag-specific CD8+ T-cell responses, particularly their breadth, are associated with lower viral loads and slower disease progression (Kiepiela et al., 2007), in large part due

to the fitness cost imposed on the virus by selection of escape mutations (Crawford et al., 2009; Crawford et al., 2007; Martinez-Picado et al., 2006; Miura et al., 2009; Schneidewind et al., 2007). By contrast, Env-specific targeting is associated with higher viral loads and rapid disease progression and is frequently restricted by disease-susceptible HLA alleles (Kiepiela et al., 2007; Masemola et al., 2004; Ngumbela et al., 2008). Gag-specific CD8+ T-cell responses also correlate with antiviral suppressive capacity of CD8+ T-cells in elite controllers (Saez-Cirion et al., 2009).

However, despite this extensive knowledge of the features of effective antiviral CD8+ T-cells, we still do not know which functions are necessary to induce by vaccine or another intervention, what level of function would be sufficient, and how to achieve this.

1.3.3 HLA class I molecules and disease outcome in adult infection

HLA class I allele expression strongly influences disease outcome in adult HIV infection (Fellay et al., 2007; Kaslow et al., 1996). The recent GWAS by Pereyra and colleagues also demonstrated that SNPs significantly associated with a differential HIV disease outcome are located exclusively within the HLA loci (Pereyra et al., 2010). Particularly, HLA-B alleles have the strongest influence (Kiepiela et al., 2004). Most extreme examples include 'protective' HLA alleles, such as HLA-B*57:01/27:05 in Caucasians or HLA-B*57/58:01/81:01 in Africans, associated with slow disease progression and low viral loads (Kiepiela et al., 2007; Leslie et al., 2010; Pereyra et al., 2010) and enriched among elite controllers (Migueles and Connors, 2010; Pereyra et al., 2008). There are many other alleles that are less well studied but may in some instances be associated with elite control, such as HLA-B*14 (Pereyra et al., 2010), which is the subject of my studies reported in Chapter 3. On the other hand, 'disease-susceptible' alleles such as HLA-

B*35:01 in Caucasians or HLA-B*58:02/18:01 in Africans are associated with rapid disease progression and higher viral loads (Carlson, 2012; Kiepiela et al., 2007; Leslie et al., 2010; Pereyra et al., 2010). Additionally, heterozygosity at the HLA loci is associated with delayed HIV disease progression, while homozygosity has the opposite effect (Carrington et al., 1999).

Several potential mechanisms have been proposed to explain the HLA impact on disease progression:

- ***Specific epitope targeting.*** For instance, protective HLA-B*57 targets an array of dominant Gag-specific epitopes (Goulder et al., 1996) while disease-susceptible HLA-B*58:02 targets a dominant epitope in Env (Ngumbela et al., 2008). As described above, Gag-specific CD8+ T-cell responses are associated with a more potent viral suppression and selection of mutations that significantly attenuate viral fitness because they are located in highly conserved regions (Crawford et al., 2009; Martinez-Picado et al., 2006; Schneidewind et al., 2007). Additionally Gag is abundant in the incoming virions (Zhu et al., 2003), thus it does not have to be generated *de novo* and Gag-specific epitopes can be processed and presented for CD8+ T-cell recognition as early as 2 hours post-infection (Sacha et al., 2007a). By contrast, Env- and other non-Gag-specific responses exert minimal selection pressure on the virus with insignificant impact on viral fitness (Troyer et al., 2009), tend to be less effective at inhibiting viral replication and are not generated until at least 12 hours post-infection (Kloverpris et al., 2013a; Payne et al., 2010; Sacha et al., 2007a; Sacha et al., 2007b). However, not all Gag-specific responses are equal in antiviral potency (Honeyborne et al., 2006) and some human (Adland et al., 2013) and macaque (Maness et al., 2008; Valentine et al., 2009) studies have

demonstrated effective Vif- and Nef-specific responses;

- ***HLA-B peptide binding groove.*** A recent GWAS showed that the specific amino acids within the HLA-B peptide-binding groove are associated with differential disease outcome (Pereyra et al., 2010). The strongest association was found with amino acid at position 97, which is located in the C pocket, is involved in binding viral peptides and can be represented by 1 of 6 variants. Interestingly all HLA-B alleles associated with protection, HLA-B*57:01/27:05/14:01, had a unique residue at position 97 (Val, Asn, and Trp, respectively), whereas all other alleles carried the other three variants, and Arg97 was the most common among them, including disease-susceptible HLA-B*35:01. In addition, position 97 is also implicated in HLA cell surface expression and protein folding (Blanco-Gelaz et al., 2006);
- ***T-cell selection in the thymus.*** A computational study suggested that immature CD8+ T-cells restricted by the protective HLA-B*57/27 recognise fewer self-peptides during thymic selection than disease-susceptible HLA-B*35:01. Thus a larger number of HLA-B*57/27-restricted cells would survive negative selection, bind viral peptides and could be expected to be more cross-reactive to self peptides (Kosmrlj et al., 2010);
- ***Peptide-binding motifs.*** Protective HLA molecules show preference for unique peptide-binding motifs, particularly at the anchor positions in the B (peptide position 2) and F (peptide carboxy-terminus) pockets of HLA binding groove (Goulder and Walker, 2012). For example, HLA-B*57 has a strong preference for Trp at the carboxy-terminus of the peptide, an amino acid that is difficult to substitute without selecting stop codons or interfering with protein function. Similarly, HLA-B*27 requires Arg at the anchor position 2, a positively charged amino acid that provides the most tight binding of the peptide and the most stability to the HLA-peptide complex (Madden et al., 1992);

- ***Interactions with NK cells.*** HLA class I molecules can be divided into Bw4 and Bw6 groups based on their epitopes spanning residues 79-83 in the alpha 1 helix of HLA that are ligands for KIR receptors on NK cells. Most protective alleles express Bw4 motif, while most disease-susceptible alleles express Bw6 motif, although exceptions exist (Flores-Villanueva et al., 2001). Moreover, Bw4-expressing HLA alleles with an isoleucine at position 80 in combination with NK-cell receptors KIR3DS1 and KIR3DL1 are associated with delayed disease progression, possibly through modulation of antiviral NK-cell activity (Martin et al., 2002; Martin et al., 2007); and
- ***Interactions with DCs.*** The strength of HLA class I interaction with inhibitory leukocyte immunoglobulin-like receptors on DCs affects DC function, such that weak binding, observed among protective HLA alleles, leads to preservation of antigen-presenting properties by DCs, while strong binding, observed among disease-susceptible alleles, leads to DC inhibition (Bashirova et al., 2014).

1.4 CD8+ T-cells and HLA class I in non-progressing paediatric infection

In the context of perinatal infection, HIV enters an immunological environment that is markedly different from that found in adults, due to the constantly evolving patterns of immune development from fetal life into childhood, adolescence and adulthood. Longitudinal detailed studies following this natural immune ontogeny in paediatric infection from birth are difficult to conduct, but they can aid in our understanding of the largely unknown immunology of non-progressing paediatric HIV infection and point to potential therapeutic and cure strategies.

1.4.1 Immunological tolerance in early life

[This section is part of the published review by Goulder, P.J., Lewin S.R. & **Leitman, E.M. 2016 Mar 14**. Paediatric HIV infection: the potential for cure. *Nature Reviews Immunology*. 10. 1038/nri.2016.19. Epub ahead of print.]

The immune system *in utero* and in early life is exquisitely adapted to meet the particular challenges of that phase of life. *In utero*, the need to avoid making inflammatory anti-maternal responses during the frequent exposure to non-inherited maternal antigens is facilitated by the high levels of TGF-β in the fetus that direct peripheral differentiation of naïve T-cells, in the presence of the cognate antigen, into 'adaptive' regulatory T-cells (T_{Reg} cells) (Mold et al., 2008). These memory T_{Reg} cells are long-lived and can be found in children up to the age of 7-17 years (Mold et al., 2008). T_{Reg} cells make up 15% of peripheral T-cells in fetal blood, compared with ~5% in adult blood (Takahata et al., 2004). Also, innate immune cells at birth, compared with adulthood, respond to a panel of TLR agonists by secreting higher levels of IL-6, IL-1β and IL-23, which supports T_H17 cell differentiation and lower levels of pro-inflammatory cytokines such as type I interferons, and hence lower levels of IFN-γ, TNF and IL-12, which support T_H1 differentiation (Kollmann et al., 2009; Upham et al., 2002). The higher levels in neonates of immunoregulatory and anti-inflammatory cytokines (such as IL-10 and TGF-β) and of T_H2 cell supporting cytokines (IL-4, IL-5, IL-9 and IL-13) (Elyaman et al., 2009; Nowak et al., 2009) further function to dampen down T_H1 cell responses. Finally, plasma levels of adenosine are higher in neonates than in adults and may contribute to the T_H17 cell bias and low levels of immune activation in early life via increased IL-6 synthesis and decreased TNF production (Levy et al., 2006). The immune response *in utero* and in early life therefore establishes a tolerogenic environment that is broadly anti-inflammatory and that promotes T_H17 cell-mediated host defence against extracellular bacterial and fungal

pathogens, at the expense of a strong T_H1 cell-driven response which, by contrast, is a feature of antiviral cell-mediated immunity in adults.

In the setting of HIV infection in early life, one effect of these immune adaptations is to eliminate the possibility of HLA class I-restricted CD8+ T-cell-mediated suppression of viraemia that is observed in adult elite controllers. However, the tolerogenic environment in early life favours low levels of immune activation, which could interfere with the vicious cycle of immune activation, increased bystander cell death via apoptosis and pyroptosis (Doitsh et al., 2014; Munoz-Arias et al., 2015), increased susceptibility of activated CD4+ T-cells to further infection, and increased virus production that normally occurs during adult infection. However, there are also opposing factors that act to increase immune activation, and thus viral replication and pathogenicity in early life; these include microbial translocation, particularly in premature (born <37 weeks gestation) infants (Kourtis et al., 2013; Papasavvas et al., 2011), changing composition of the intestinal microbiota (Kourtis et al., 2013; Wallet et al., 2010), mixed feeding (Coovadia et al., 2007; Iliff et al., 2005), side effects of certain vaccinations (e.g. BCG) resulting in increased immune activation (Tchakoute et al., 2015) and co-infections, such as CMV that is highly prevalent particularly in sub-Saharan Africa (nearly two-thirds of children have become infected with CMV by the age of 3 months) (Miles et al., 2007). All of these factors that function to increase immune activation in early life may oppose the benefits in terms of HIV infection and disease progression that would be expected to result from the tolerogenic immune environment described above.

1.4.2 CD8+ T-cells and HLA class I in paediatric HIV

The role of CD8+ T-cell activity in paediatric non-progressing disease is poorly characterised. Given the persistently high viraemia observed in non-progressing children

and the Th2 bias in early life, it would be reasonable to hypothesise that CD8+ T-cells do not play an instrumental role in non-progression. However in HIV infection, virus-specific CD8+ T-cell responses are detected in infected children even in the first days of life; and although these responses are dominated by Env- and Nef- specific targeting, suggestive of their lack of potency based on studies in adults, some children generate Gag responses very early in life, which could potentially be of significance in terms of their impact on the virus (Brander et al., 1999; Luzuriaga et al., 1995; Thobakgale et al., 2007). Moreover, infant CD8+ T-cells have been shown to suppress HIV replication in association with longer survival (Pollack et al., 1997), as well as drive selection of escape mutations (Feeney et al., 2005). Additionally, in other infections, e.g. malaria, T-cell vaccine approach using prime-boost regimens of chimpanzee adenovirus and modified vaccinia virus Ankara in adults showed 58% efficacy of the vaccine, and highly immunogenic vaccine-induced CD8+ T-cell responses that correlated with protection (Ewer et al., 2013). The same vaccine was assessed in phase I and II trials in infants and children in the Gambia and Burkina Faso and showed high vaccine-induced CD8+ T-cell immunogenicity, similar to the levels observed in adults (Ewer, 2014). This is a promising result, although the efficacy of this vaccine and CD8+ T-cell role in children are yet to be determined.

On the other hand, as described above, the HLA-B alleles that have a substantial impact in adult infection, do not significantly influence paediatric disease outcome as measured by viral loads and CD4+ T-cell counts (Adland et al., 2015). In fact, *in utero* HIV-infected children as a group are enriched for HLA alleles associated with rapid disease progression. This is explained by the fact that MTCT is strongly related to maternal viral load (Dickover et al., 1996; Sperling et al., 1996), thus transmitting mothers are more likely to express HLA alleles associated with high viral setpoints (Goulder and Walker, 2012) and at least half of maternal alleles will be inherited by the child. Some HLA-related benefit

to the child was reported in cases when the mother expressed an HLA allele that was not shared with the child, thus transmitting a pre-adapted virus with lower replicative capacity (Prado et al., 2010; Thobakgale et al., 2009). However, because the child shares at least half of maternal HLA alleles, perinatally transmitted virus may already be pre-adapted to the key CD8+ T-cell epitopes restricted by the shared alleles, compromising the child's potential to generate effective responses (Goulder et al., 2001b).

The role of CD8+ T-cell selection pressure, effector function, phenotype in paediatric non-progressing infection and its evolution with age remain to be investigated in longitudinal studies.

1.5 ART and non-progressing HIV infection

Regularly taken ART effectively suppresses viral load and maintains it at undetectable levels. Criteria for ART initiation change every several years, but are based either on absolute CD4+ T-cell count (or CD4% in children <5 years of age) or clinical stage of disease. In July 2015, the investigators of the START trial reported that people who start ART while their CD4+ T-cell count is still high (>500 cells/mm^3 in the trial participants) have significantly lower risk of serious AIDS- or non-AIDS-related events or death than individuals who wait until their CD4+ T-cell count drops to <350 cells/mm^3 (Lundgren et al., 2015). Based on this finding, WHO is now recommending the initiation of ART in all HIV-infected persons, adults and children, at any CD4+ T-cell count (WHO, 2015b).

1.5.1 Reservoir and ART

Despite its high efficacy in viral suppression, ART does not cure HIV infection due to persistence of reservoir – a pool of long-lived latently infected resting memory CD4+ T-cells that are transcriptionally silent, harbour replication-competent virus and can start viral

production upon reactivation (Eisele and Siliciano, 2012). Reservoir is seeded as early as 3 days post-infection (Whitney et al., 2014); its size can (most commonly) be measured by PCR-based techniques, Quantitative Viral Outgrowth Assay from resting CD4+ T-cells and now the new *Tat*/*rev* Induced Limiting Dilution Assay (Eriksson et al., 2013; Procopio et al., 2015).

The earlier ART is initiated, the smaller the reservoir is in both adults (Chun et al., 2010; Hocqueloux et al., 2013; Schmid et al., 2010; Zhang et al., 1999) and children (Ananworanich et al., 2014; Bitnun et al., 2014; Luzuriaga et al., 2014; Martinez-Bonet et al., 2015; van Zyl et al., 2015). However, its decline in size is very slow with a half-life of 44m in adults if ART is initiated in chronic infection (Crooks et al., 2015; Finzi et al., 1999; Siliciano et al., 2003). If treatment in adults is initiated during acute infection, frequency of latently infected cells is 10-100 fold lower when measured in terms of either HIV DNA or replication competent virus (Chun et al., 2010; Hocqueloux et al., 2013; Zhang et al., 1999). In infants who were initiated on ART at 8 weeks old, the half-life of latently infected resting CD4+ T-cells was 11 months (Persaud et al., 2012). Interestingly, whereas in adult infection reservoir size seems to plateau after ~4 years (Besson et al., 2014), in children it continues to decay (Luzuriaga et al., 2014).

It is because of the reservoir, that upon treatment interruption, viraemia typically rebounds within days or weeks (Davey et al., 1999). Even undetectable (or borderline detectable by modern assay) levels of HIV reservoir do not guarantee its inability to rebound (Henrich et al., 2014; Luzuriaga et al., 2015).

1.5.2 Reservoir and CD8+ T-cells

Reservoir location in resting cells renders these cells 'invisible' for CD8+ T-cell recognition as very little viral protein is produced. Additionally, a lot of latently infected cells compartmentalise in immunological sanctuaries, such as B-cell follicles in lymph nodes, which are inaccessible to CD8+ T-cells (Fukazawa et al., 2015). However, new data suggest that even on ART, when CD8+ T-cell response is largely contracted in the absence of antigen, virus-specific CD8+ T-cells still play an important role: SIV-infected macaques continuously remaining on ART experience a rapid increase in viraemia when CD8+ T-cells are depleted (Cartwright et al., 2016).

1.5.3 Post-treatment control

The concept of PTC was recently introduced in the VISCONTI study, that reported 14 adult individuals who received ART in primary infection within a median of 3 months after HIV acquisition, discontinued treatment after a median of 3 years and have been aviraemic since then for up to 10 years (Saez-Cirion et al., 2013). Post-treatment controllers had several distinctive characteristics: enrichment with disease-susceptible HLA alleles, weak HIV-specific CD8+ T-cell responses, less potent viral suppression and lower CD8+ T-cell activation than most elite controllers, and low reservoir size.

In paediatric infection, most infants started on therapy in the first days of life experience viraemic relapse within days of ART cessation (Bitnun et al., 2014; Butler et al., 2015; Giacomet et al., 2014; Vigano et al., 2006). One case that received a lot of attention was that of the 'Mississippi child' – an *in utero* infected child who was put on ART at 30 hours of age and continued for the next 18 months. Upon treatment interruption the child remained aviraemic for 28 months, raising hopes that the virus had been eliminated; however, she subsequently relapsed (Luzuriaga et al., 2015; Persaud et al., 2013). So far,

only one reported paediatric case of durable PTC exists – the French teenager who has remained aviraemic for 12 years since treatment interruption (Frange et al., 2016).

The mechanism of PTC is unclear, but the fact that there are only anecdotal cases of PTC, especially among children, highlight the fact that ART alone is not sufficient either to eradicate HIV entirely or to achieve long-term remission.

1.6 Strategies to achieve durable HIV remission: potential for CD8+ T-cells

Armed with today's technological advances, the scientific community is seeking viable strategies to achieve HIV remission and it is most likely that a successful strategy will involve a multifaceted approach. One of the leading candidates is the 'shock and kill' strategy (Deeks, 2012), in which latently infected cells are reactivated with a latency-reversing agent (e.g. HDAC inhibitor, PKC agonists, TCR activators) to make them 'visible' to immune cells for killing [reviewed in (Spivak et al., 2015)]. Harnessing a potent CD8+ T-cell effector function here is crucial to success.

However, several obstacles that require further investigation and understanding exist, some of which are as follows:

- It is currently largely unknown what level of CD8+ T-cell functionality would be sufficient to eliminate reactivated reservoir cells to the point of no return for the virus. This is exemplified by the most recent trial result in which study participants were first immunised with therapeutic HIV p24 vaccine and then treated with an HDAC inhibitor romidepsin (Leth et al., 2016). The result showed that despite a significant decrease in reservoir size, all 17 participants had a viral rebound at a

median of 14 days upon treatment interruption. CD8+ T-cell vaccines, that could induce strong cellular antiviral activity, have been largely unsuccessful to date (Buchbinder et al., 2008; Gray et al., 2011; Hammer et al., 2013).

- Large T-cell vaccine trials (e.g. Step and Phambili) were terminated not only due to lack of efficacy, but also because of vaccine-associated increase in HIV acquisition (Buchbinder et al., 2008; Gray et al., 2011; Gray et al., 2014) (see Introduction in Chapter 5). The success of a recently described HIV vaccine in animal studies, which has the potential to induce a very strong CD8+ T-cell response, unconventionally restricted by MHC-E or MHC II (Hansen et al., 2011; Hansen et al., 2013; Hansen et al., 2016), requires substantial further investigation in humans.
- Unless therapy is initiated very early in infection, which is impossible for anyone with established infection, more than 98% of latent viruses contain escape mutations in the dominant CD8+ T-cell epitopes (Deng et al., 2015). This means that upon reservoir reactivation, CD8+ T-cells will not be able to recognise the escaped variants; to be able to do so CD8+ T-cell function will need to be appropriately enhanced (Deng et al., 2015; Shan et al., 2012) – and the optimal mechanism remains to be determined.
- An additional complication is T-cell exhaustion, i.e. persistent expression and upregulation of inhibitory receptors such as PD1, Lag 3, Tim 3 and others, which leads to T-cell anergy and dysfunction (Wherry and Kurachi, 2015). Recent findings suggest that the level of T-cell exhaustion prior to initiation of therapy may predict time to viraemic rebound after therapy cessation (Hurst et al., 2015), highlighting the importance of this aspect of CD8+ T-cell phenotype in 'cure' approaches. The potential for a successful solution to this problem is drawn from the cancer field where blockers of such inhibitory receptors are now being used in patients to enhance CD8+ T-cell anti-tumour activity (Brahmer et al., 2012; Rizvi et al., 2015;

Topalian et al., 2012; Tumeh et al., 2014). Evaluation of such blockade is already happening in HIV and SIV (Eron et al., 2016; Mylvaganam et al., 2016).

All in all, these observations re-emphasise the need for an effective CD8+ T-cell response to achieve durable HIV control.

1.7 Aims and hypotheses of this thesis

Studies that dissect the function and activity of the CD8+ T-cell response in naturally controlled HIV infection provide crucial insights into what constitutes a successful antiviral CD8+ T-cell response – the factors (molecular, immunological, genetic) on which it depends, how it can be manipulated *in vitro* and possibly *in vivo* and how this knowledge can be taken further into therapeutic and preventive approaches.

In this thesis, I set out to explore specific aspects of the interplay between host and virus in order to further our understanding of the optimum CD8+ T-cell-mediated immune responses. I have called upon a variety of strategies, from examination of the results of a large vaccine trial, to deep sequencing of the virus, to developing new *in vitro* assays that tease out the contribution of individual CD8+ T-cell populations, applying these methods to both adult and paediatric infection with a particular focus on some of the world's most vulnerable populations in sub-Saharan Africa. The aims and hypotheses are as follows:

(i) ***Hypothesis:*** Gag-specific responses are the most effective and mediate viral control in adult HIV infection.

Aim: To identify the CD8+ T-cell specificities that mediate immune control in adult infection under 'classic' HLA-B*57 restriction and 'non-classic' HLA-B*14 restriction.

(ii) ***Hypothesis:*** HLA-restricted CD8+ T-cells play minimal role in paediatric non-progression and selection pressure does not emerge until late childhood.

Aim: To examine the role of HLA-mediated CD8+ T-cell responses in paediatric non-progressing HIV infection and follow the evolution of the antiviral response from birth through childhood.

(iii) ***Hypothesis:*** MRKAd5 HIV-1 Gag/Pol/Nef vaccine, tested in the Phambili trial, induced Gag-specific responses in individuals who do not target this protein in natural infection, improving their disease outcome.

Aim: To investigate the ability of an HIV vaccine to redirect HLA-restricted CD8+ T-cell responses and improve immune control of the infection.

(iv) ***Hypothesis:*** Depleting antigen-specific CD8+ T-cell populations, using HLA class I tetramers, could be a technique for exploring in detail the contribution of individual CD8+ T-cell specificities to viral suppression.

Aim: To develop and refine a novel *in vitro* method to selectively remove particular HIV-specific CD8+ T-cells to evaluate the contribution of that antiviral specificity to viral inhibition.

CHAPTER 2. MATERIALS AND METHODS

Chapter-specific methods are presented in the Methods sections of the relevant chapters. Components of media are listed in section 2.11. Contributions are explicitly stated where relevant.

2.1 Study subjects

Subjects from the following cohorts were studied:

(i) **Acute HIV Infection cohort** (Altfeld et al., 2001; Streeck et al., 2014): acutely HIV-infected adults were recruited at the Massachusetts General Hospital, Brigham and Women's Hospital and the Fenway Institute of the Beth Israel Deaconess Medical Center, Boston, MA, USA. Primary infection was classified using Fiebig staging, as previously described (Fiebig et al., 2003). Subject AC198 from this cohort was studied in Chapter 6. He is an adult Caucasian male, enrolled in 2005 during early acute infection (estimated 10-15 days post-infection, Fiebig II (Fiebig et al., 2003)) and received six months of ART that was ceased as part of randomly assigned treatment interruption. This study was approved by the Massachusetts General Hospital Institutional Review Board and all subjects provided written informed consent for participation in the study.

(ii) **Gateway cohort** (Payne et al., 2014): chronically HIV-infected women were recruited in Durban, South Africa. Thirty eight women were ART-naïve antenatal mothers and 226 were postnatal mothers, who were attending a baby immunisation clinic and had had zidovudine therapy from the date of enrolment during pregnancy to delivery and a single dose of nevirapine during labour following the national guidelines in South Africa (NDOH, 2010) and no therapy

thereafter. ELISPOT, HLA and viral load data from this cohort (and the Sinikithemba cohort) were used to identify associations between HLA expression and recognition of HIV-specific peptides (Chapters 4, 5); additionally samples from 17 subjects from the Gateway cohort were used for the HLA-B*14 studies (Chapter 3). Ethics approval was given by the University of KwaZulu-Natal Review Board and Oxford Research Ethics Committee. Written informed consent was obtained from all subjects.

(iii) **Paediatric Early HAART and Strategic Treatment Interruption Study (PEHSS) cohort** (Mphatswe et al., 2007; Prendergast, 2008): this feasibility study enrolled 75 HIV-infected infants born to HIV-positive mothers at St. Mary's and Prince Mshiyeni Hospitals in KwaZulu-Natal, South Africa, in 2003-2005. Antenatal mothers were recruited in the third trimester of pregnancy; mothers and infants received a single dose of nevirapine at delivery (the only available treatment for prevention of mother-to-child transmission at the time; infant treatment was not available at government hospitals). Infants were randomised to deferred treatment, immediate uninterrupted treatment for 12 months or immediate 18-month treatment with structured interruptions. Eleven children from this cohort did not meet ART criteria by the age of 5 years (CD4>350 cells/mm^3). These were termed 'paediatric slow progressors' and studied in Chapter 4. The study was approved by the Biomedical Research Ethics Committee of the University of KwaZulu-Natal and the Institutional Review Boards of the Massachusetts General Hospital and the University of Oxford. The mothers gave written informed consent for participation of their children.

(iv) **Phambili Ancillary Study cohort** (Gray et al., 2011; Gray et al., 2014): adult subjects enrolled in the Phambili/HVTN503 trial who subsequently acquired HIV infection (n=100) (see Chapter 5, Methods for details). This study was approved by the Institutional Review Board of the University of Oxford and Ethics Committee at each clinical site; all subjects provided written informed consent for participation in the study.

(v) **Sinikithemba cohort** (Kiepiela et al., 2004; Kiepiela et al., 2007): chronically HIV-infected ART-naïve adults were enrolled from antenatal and follow-up clinics in Durban, South Africa. ELISPOT, HLA and viral load data from this cohort (and the Gateway cohort) were used to identify associations between HLA expression and recognition of HIV-specific peptides (Chapters 4, 5). This study was approved by the Institutional Review Boards at the University of KwaZulu-Natal, Massachusetts General Hospital and the University of Oxford and written informed consent was obtained from all participants.

(vi) **The Study of the Consequences of Protease Inhibitor Era (SCOPE) cohort** (Hunt et al., 2003): chronically HIV-infected ART-naïve adults recruited at the University of California, San Francisco, USA. Samples from 3 subjects from this cohort were used in Chapters 3 and 6. This study was approved by the Institutional Review Board of the University of California, San Francisco and all subjects gave written informed consent.

(vii) **Thames Valley cohort** (Payne et al., 2010): chronically HIV-infected ART-naïve adults were recruited from the Royal Berkshire Hospital, Reading, UK; Northampton General Hospital, Northampton, UK; Churchill Hospital, Oxford, UK;

and Wycombe Hospital, High Wycombe, UK. Samples from subjects in this cohort were used in the HLA-B*57 and HLA-B*14 studies (Chapter 3), in the studies with cytotoxic tetramers (Chapter 6) and for optimisation of the viral inhibition assay (Chapters 3, 6). This study was approved by the Institutional Review Board of the University of Oxford and all subjects provided written informed consent for participation in the study.

Additionally, Leukocyte Reduction System cones from HIV-negative donors (Cook et al., 2003) were obtained from the John Radcliffe Hospital, Oxford University Hospitals, Headington, UK. These cells were used as feeder cells for cloning (Chapter 3) and optimisation of antibody panels (Chapters 3, 6). Samples from HIV-negative healthy adult individuals from the Peter Medawar Building for Pathogen Research, University of Oxford, were used in the assays with cytotoxic tetramers (Chapter 6) and for optimisation of the viral inhibition assay (Chapters 3, 6). All subjects provided an informed consent under the ethics approval of the Institutional Review Board of the University of Oxford.

2.2 Blood processing

2.2.1 Separation of plasma and isolation of PBMCs

Fresh blood samples were processed within 6 hours of collection. Whole blood was spun for 10 minutes at 2000rpm to separate plasma. Plasma was frozen in 1.5-ml aliquots at -80°C. Blood was then diluted with PBS, layered onto Lymphoprep (Stemcell Technologies) at 1:1:1 ratio and spun for 25 minutes at 2000rpm without brakes. Buffy coat layer containing PBMC was transferred to a new 50-ml Falcon tube with a Pasteur pipette, washed three times with RPMI-1640 (Sigma) and resuspended in R10 medium for further use.

2.2.2 Cryopreservation of cells

Cells were pelleted for 5 minutes at 2000rpm, resuspended in a drop-wise manner in cold FCS containing 10% DMSO (Sigma), transferred to pre-chilled cryovials and placed into a pre-chilled 'Mr. Frosty' freezing container (Nalgene) that allows constant rate of cooling at 1°C/minute. The container was immediately placed at -80°C overnight; cryovials were then transferred to liquid nitrogen for long-term storage. To thaw, a cryovial was placed in a 37°C water bath, quickly transferred to pre-warmed R10, pelleted at 2000rpm for 5 minutes and washed twice with pre-warmed R10.

2.2.3 DNA extraction

Genomic DNA was extracted from fresh whole blood using QIAamp DNA Blood reagents (QIAGEN). To extract DNA, 3ml whole blood was incubated with 9ml red cell lysis for 10 minutes at room temperature and periodically inverted. It was then pelleted at 2000rpm for 10 minutes, resuspended in 3ml white cell lysis and incubated at room temperature. After ≥48 hours, 1ml protein precipitation solution was added and the mixture was pulse-vortexed for 20 second, pelleted as before, transferred into 3ml isopropanol, inverted 50 times, pelleted, washed with 3ml 70% ethanol, pelleted for 3 minutes and left to dry overnight. DNA was resuspended in 250µl DNase/RNase free water (HyClone). Concentration and purity were determined on Thermo Scientific NanoDrop 1000 spectrophotometer (NanoDrop Products). DNA was kept at -20°C for long-term storage or 4°C for immediate use.

For samples where no fresh blood was available (AC198, Chapter 6), PBMCs used in ELISPOT were collected after the 14-16-hour incubation, washed with PBS and DNA was extracted using QIAamp DNA Mini Kit (QIAGEN) following manufacturer's protocol.

2.2.4 RNA extraction

One-ml plasma aliquots were thawed in 37°C water bath and centrifuged for 1.5 hours at 15,000rpm; 860 µl supernatant was removed and viral RNA was isolated from the remaining 140 µl using QIAmp Viral RNA Mini Kit (QIAGEN) following manufacturer's instructions. Samples with a viral load <2,000 copies/ml were concentrated by putting 2-3 aliquots of plasma (if available) through the same QIAmp column.

2.3 HLA typing, viral load measurements and CD4+ T-cell counts

HLA typing was performed using a locus specific PCR amplification strategy and a heterozygous DNA sequencing methodology for exon 2 and 3 of the class I PCR amplicon (Cano et al., 2007). HIV plasma viral load was measured by the Roche Amplicor version 1.5 assay with with COBAS AmpliPrep or TaqMan 48 for the Acute HIV Infection cohort or with COBAS Amplicor for the other cohorts. CD4+ T-cell counts were determined by flow cytometry using standard clinical protocol. CD4+ T-cell counts and viral loads were measured on clinical grounds and the data were supplied by the Centre of Recruitment.

2.4 IFN-ɣ ELISPOT assay

2.4.1 ELISPOT method

ELISPOT assays were performed in sterile 96-well plates with a Polyvinylidene Fluoride membrane (Millipore). Plates were pre-coated with anti-human IFN-ɣ monoclonal antibody (Mabtech, Sweden) in PBS at 1:2000 and incubated at 4°C overnight. Prior to use, plates were washed with blocking buffer (1% heat-inactivated FCS in PBS) six times and 50 µl/well R10 was added after the final wash. Peptides were added to a final concentration of 1.25-2.5 µg/ml. Each plate contained two positive controls with 250 µg/ml PHA (Roche)

and four negative controls with no peptide or PHA. PMBCs were added to each well (0.5-1x10^5 cells in a final volume of 160 µl).

Following 14-16-hour incubation at 37°C with 5%CO_2, plates were developed as follows:

1. Wash 6 times with PBS;
2. Incubate with biotinylated anti-IFN-*γ* antibody (Mabtech, Sweden) at 1:2000 in PBS at room temperature for 90 minutes in the dark;
3. Wash 6 times with PBS;
4. Incubate with streptavidin-alkaline phosphatase conjugate (Mabtech, Sweden) in PBS at 1:2000 for 45 minutes at room temperature in the dark;
5. Wash 6 times with PBS;
6. Develop with substrate colour solution (Bio-Rad Laboratories);
7. Air-dry overnight.

Spots were counted on an automated ELISPOT reader (AID ELISPOT v.4.0, Autoimmun Diagnostika, Germany) and manually checked. Background (mean of the 4 negative controls + 3 x standard deviation) was subtracted from values of all wells, and the final result was expressed as number of SFC per 10^6 PBMCs. Positive responses were considered >50 SFC/10^6 PBMCs after background subtraction.

2.4.2 Screening for HIV-specific CD8+ T-cell responses

A panel of 410 overlapping 18mer peptides (OLPs), spanning the entire HIV-1 proteome, was synthesised based on 2001 B- and C-clade consensus sequences (Massachusetts General Hospital Peptide Core Facility, Boston, MA, USA) (Kiepiela et al., 2004; Kiepiela et al., 2007). These were mixed in 72 pools with 9-12 OLPs/pool with each peptide present in two different pools. Therefore, a given peptide could be identified by positive responses

in the two corresponding pools. An example is shown in **Figure 2.1**. OLPs identified by the megamatrix approach were then tested individually by ELISPOT assay. To screen HLA-restricted HIV-specific CD8+ T-cell responses to optimal epitopes, a panel of well-characterised epitopes was used (LLano A, 2013) (www.hiv.lanl.gov). All peptides used were >80% purity, as shown by HPLC profile.

A

A1	A2	A3	A4	A5	A6	A7	A8	A9	A10	A11	A12
B1	B2	B3	B4	B5	B6	B7	B8	B9	B10	B11	B12
C1	C2	C3	C4	C5	C6	C7	C8	C9	C10	C11	C12
D1	D2	D3	D4	D5	D6	D7	D8	D9	D10	D11	D12
E1	E2	E3	E4	E5	E6	E7	E8	E9	E10	E11	E12
F1	F2	F3	F4	F5	F6	F7	F8	F9	F10	F11	F12
						-	-	-	-	+	+

B

	Pool B1	**Pool B2**	Pool B3	Pool B4	Pool B5	**Pool B6**	Pool B7	Pool B8	Pool B9	Pool B10	Pool B11	Pool B12
Pool A1	1	**2**	3	4	5	**6**	7	8	9	10	11	-
Pool A2	13	**14**	15	16	17	**18**	19	20	21	22	-	12
Pool A3	**25**	**26**	**27**	**28**	**29**	**30**	**31**	**32**	**33**	**-**	**23**	**24**
Pool A4	37	**38**	39	40	41	**42**	43	44	-	34	35	36

Figure 2.1. **Example of megamatrix setup. (A)** ELISPOT plate layout with 72 HIV-specific peptide pools shown as A1-A12, B1-B12, C1-C12, etc. "+" indicates positive control (PHA) wells, "-" indicates negative control with no peptides or PHA. Purple shading shows positive responses (pools A3, B2 and B6). **(B)** Identification numbers of peptides that constitute pools A1-A4 and B1-B12 are shown (only four peptides for pools B1-B12 are shown for convenience). Purple shading indicates the three positive responses in (A). Responses to pools A3/B2 and A3/B6 point to reactivity to OLP 26 and 30, respectively. OLP 26 and 30 would be used individually in a confirmatory ELISPOT.

2.4.3 Measurement of functional avidity

Functional avidity, or antigen sensitivity, was defined as the concentration of an exogenous peptide required to elicit half-maximum cellular response (Almeida et al., 2007). Functional avidity of CD8+ T-cells within PBMCs was assessed in *ex vivo* IFN-γ ELISPOT assays by incubating $1x10^5$ PBMC per well with serial peptide dilutions over a

range of seven $\log_{10}$ units in triplicate and determining the peptide concentration required to induce half-maximum cellular response. ELISPOT assays were performed as described above.

2.5 Flow cytometry

2.5.1 Antibody staining

For surface staining, cells were washed with PBS and incubated with fluorescently-conjugated antibodies (**Table 2.1**) for 15-20 minutes at room temperature in the dark. Cells were then washed and fixed in 2% formaldehyde. For intracellular staining, cells were first stained for surface markers (including the viability marker, **Table 2.1**) as above, washed, fixed and permeabilised with BD Cytofix/Cytoperm kit (BD Biosciences), incubated with antibodies against intracellular markers for 15-20 minutes at room temperature in the dark, washed and kept at 4°C protected from light until data acquisition by FACS.

Table 2.1. Antibodies used for flow cytometry.

Marker	Fluorochrome	Clone	Manufacturer	Dilution
CD107a	PE-Cy5	H4A3	BD Pharmingen	1:15
CD25	PE	BC96	BioLegend	1:50
CD3	Brilliant Violet 421	UCHT1	BioLegend	1:150
	Pacific Orange	UCHT1	Invitrogen	1:25
CD4	APC	OKT4	BioLegend	1:50
	FITC	OKT4	BioLegend	1:50
	APC	SK3	BD Biosciences	1:100
CD69	PerCP-Cy5.5	FN50	BD Pharmingen	1:40
CD8α	PerCP-Cy5.5	RPA-T8	BioLegend	1:100
	PE-Cy7	RPA-T8	BioLegend	1:100
	V450	RPA-T8	BD Biosciences	1:200
HLA-A,B,C	APC	G46-2.6	BD Pharmingen	1:50
HLA-B*27	FITC	HLA-ABC-m3	Abcam	1:50
IFN-ɣ	PE-Cy7	4S.B3	BD-Pharmingen	1:100
Ki67	FITC	B56	BD Biosciences	1:50
Live/Dead	Near IR	n/a	Invitrogen	1:50 (of 1:130 stock)
p24	PE	Kc-57	Beckman Coulter	1:200
Saporin	Alexa Fluor 488	n/a	Advanced Targeting Systems	1:50

2.5.2 Data acquisition and compensation

Samples were acquired on LSRII (BD Biosciences) or MACSQuant analyser (Miltenyi Biotec) within 6 hours of staining and analysed in FlowJo v9.7.6 (Tree Star, Inc.). To compensate (to correct for fluorescence spill-over from one channel into another), anti-mouse Ig κ beads and negative control beads (no binding capacity) (BD Biosciences) were mixed in equal proportions and singly-stained with antibodies used in a given experiment. For the Live/Dead marker, ArC amine reactive beads (Life Technologies) were used. Compensation matrix was created in FlowJo v9.7.6 (Tree Star, Inc.) and applied to samples. Compensation was done every time before acquiring samples.

2.5.3 Tetramer generation

Peptide-MHC class I tetramers were generated using streptavidin-PE, streptavidin-APC or streptavidin-saporin (Advanced Targeting Systems) in the laboratory of Prof. Soren Buus (University of Copenhagen, Copenhagen, Denmark) according to their published approach (Leisner et al., 2008). Additional tetramers used in Chapter 6 are described in the chapter-specific Methods (section 6.2.1).

2.5.4 Tetramer staining

For staining with fluorescently-conjugated tetramers, 0.5-1x10^6 cells per stain were washed with PBS, incubated with relevant tetramers for 30 minutes at room temperature, washed, further incubated with fluorochrome-conjugated antibodies for 15-20 minutes at room temperature in the dark and fixed in 2% formaldehyde solution at 4°C. Controls included cells incubated with no tetramer and with HLA-mismatched tetramers; these were used to set up negative gates during analysis. Samples were hierarchically gated on singlets, lymphocytes, live cells and CD3+ cells and gated around tetramer-specific CD8+ cell populations.

2.6 CD8+ T-cell lines and clones

2.6.1 Generation of epitope-specific CD8+ T-cell lines

Epitope-specific CD8+ T-cells were generated as previously described (Payne et al., 2010) with modifications. Briefly, fresh PBMCs were peptide-pulsed (2-3x10^6 PBMC/peptide at 200 µg/ml final concentration) for 1 hour and fed with fresh R10/50 every 2-3 days for 14-21 days. Specificity was tested by tetramer or intracellular IFN-γ staining. Before IFN-γ staining, CD8+ T-cells were stimulated with HLA-matched peptide-pulsed B-cells (final peptide concentration 50 µg/ml, 1 hour, 37°C) in the presence of Brefeldin A (10µg/ml;

Sigma), Golgi Stop (4µl/ml; BD Biosciences) and CD107a (**Table 2.3**) for 6 hours at 37°C and then stained for surface and intracellular markers as described above. Positive control was SEB (final concentration 1 µg/ml; Sigma), negative – B-cells with no peptide.

To remove non-specific cells, tetramer-positive cells were sorted by Dr. Christian Willberg (University of Oxford, Oxford, UK) on MoFlo XDP (Beckman Coulter) and further expanded in R10/50 supplemented with monoclonal OKT3 antibody (eBioscience) at 0.1 µg/ml. At the time of the initial set-up and every 10-14 days after, peptide-pulsed irradiated HLA-matched B-cells and irradiated feeder PBMCs from three HIV-negative donors were added to the sorted cells at a 1:1:1 ratio. Specificity and purity of expanded CD8+ T-cells was confirmed by tetramer staining immediately before using them as effector cells in viral inhibition assays.

2.6.2 Generation of CD8+ T-cell clones

Epitope-specific clones were generated as previously described (Chen et al., 2012). Briefly, PBMCs were stained with fluorescently labeled tetramers. Tetramer-specific were sorted on MoFlo XDP (Beckman Coulter) by Dr. Christian Willberg (University of Oxford, Oxford, UK) directly into U-bottom 96-well plates (single cell/well) in R10/50 containing anti-CD3 antibody (OKT3, 0.1 µg/ml; eBioscience) and irradiated feeders from three healthy donors (0.2-0.5x10^6 PBMC/well). Twice a week half of the media was replaced with fresh R10/50. After 2-3 weeks, cells were tested for specificity by tetramer staining. Epitope-specific clones were subsequently transferred to 48- and 24-well plates; at the time of transfer and/or every 14-21 days, clones were restimulated with the anti-CD3 antibody, peptide-pulsed irradiated HLA-matched B-cells and irradiated feeder PBMCs.

2.7 Immortalised cell lines

HIV-permissive cell lines H9, T1 and MT-4 (**Table 2.2**) were grown in suspension in R10 and split every 2-3 days and 24 hours prior to infection. Additionally, H9 cells transfected with *HLA-B*27:05* and *HLA-B*57:01* genes and T1 cells transfected with *HLA-B*14:02* gene (gift from Prof. Otto Yang, Geffen School of Medicine at the University of California, Los Angeles, USA) were used in viral inhibition assays as target cells. Protein expression of the transfected genes was confirmed by flow cytometry (**Figure 2.2**).

Table 2.2. HIV-permissive cell lines used for *in vitro* studies

Cell line	Description	Antigen expression	Reference
MT-4	T-cell line established from cord blood lymphocytes cocultured with leukemic cells from patients with adult T-cell leukemia.	OKT4, IL2 receptor	(Harada, Koyanagi, and Yamamoto, 1985)
H9	Clonal derivative of HUT-78 cell line originating from an adult with lymphoid leukemia; also designated as HT (human T) cell line.	CD4; HLA-A*01, B*62, C*03, DR4, DQ3	(Mann et al., 1989; Popovic et al., 1984; Weiss et al., 1985)
T1	Hybrid between CEM^{R}.3 (8-azaguanine and ouabain-resistant variant of CEM – T lymphoblastic cell line derived from a child with acute leukemia) and 721.174 (variant of B lymphoblastoid cell line 721).	HLA-A*02, B*05, Bw4, Bw6, DR7; CD7	(Foley et al., 1965; Salter, Howell, and Cresswell, 1985)

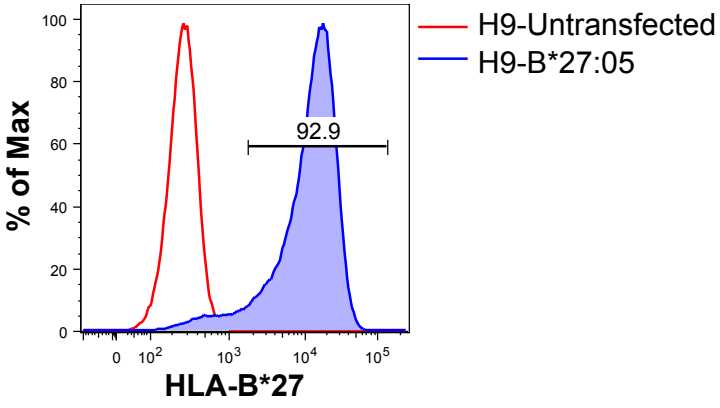


Figure 2.2. Representative example confirming absence of HLA-B*27:05 in untransfected H9 cells and HLA-B*27:05 expression in the transfected H9 cells. Gated on live CD4+ cells.

2.8 Viral inhibition assay

To evaluate antiviral efficacy of CD8+ T-cell responses, viral inhibition assays were performed based on a previously described method (Saez-Cirion et al., 2010). The originally described assay by Saez-Cirion and colleagues involves purification of target CD4+ and effector CD8+ T-cell populations from fresh PBMCs, activation of CD4+ T-cells, superinfection of the activated CD4+ T-cells by spinoculation with HIV, followed by culture of CD4+ T-cells with or without CD8+ T-cells and assessment of viral replication for the subsequent 10-14 days. Following modifications were as below:

2.8.1 Method 1 (Figure 2.3)

This method allows to assess HIV-suppressive capacity by CD8+ T-cells when autologous CD4+ T-cells are unavailable or insufficient; it was used in Chapters 3 and 6. HIV-permissive cell lines (**Table 2.2**) untransfected or transfected with an HLA gene of interest (HLA-B*27:05/57:03/14:02) were used as target cells. Cells were split 24 hours before the assay. Effector cells were:

(i) Bulk CD8+ T-cells: PBMCs were treated with a bi-specific monoclonal CD3.4 antibody (the NIH AIDS Reagent Program) to eliminate CD4+ T-cells and expand CD8+ T-cells (Chen et al., 2009; Jones et al., 2003; Wong and Colvin, 1987) and cultured for 10-20 days in R10/50 to achieve sufficient cell numbers.

(ii) CD8+ T-cells depleted of an antigen specificity: 24-48 hours prior to the inhibition assay, expanded (as in [i]) CD8+ T-cells were treated with tetramer-SAP or a control (untreated, HLA-mismatched tetramer-SAP, tetramer-PE, free SAP) (see Chapter 6, section 6.2.4). When cell numbers allowed, cell-depletion was confirmed by tetramer staining. Alternatively, antigen-specific cells were removed using anti-PE magnetic beads.

(iii) Epitope-specific cell lines (see section 2.6.1).

(iv) CD8+ T-cell clones (see section 2.6.2).

For the initial setup, target cells were infected with NL4-3-GFP by spinoculation for 1 hour, incubated at 37°C for 1 hour, repeatedly washed and further cultured with or without effector cells in duplicate or triplicate. Every 2-3 days, cultures were fed and stained to assess live GFP+ cells. Background (%GFP+ uninfected target cells) was subtracted from all values. HIV-suppressive capacity was calculated at the time of the peak of viral growth: suppressive capacity = $\log_{10}$(%GFP+ infected target cells without effector cells / %GFP+ target cells with effector cells) (Saez-Cirion et al., 2010).

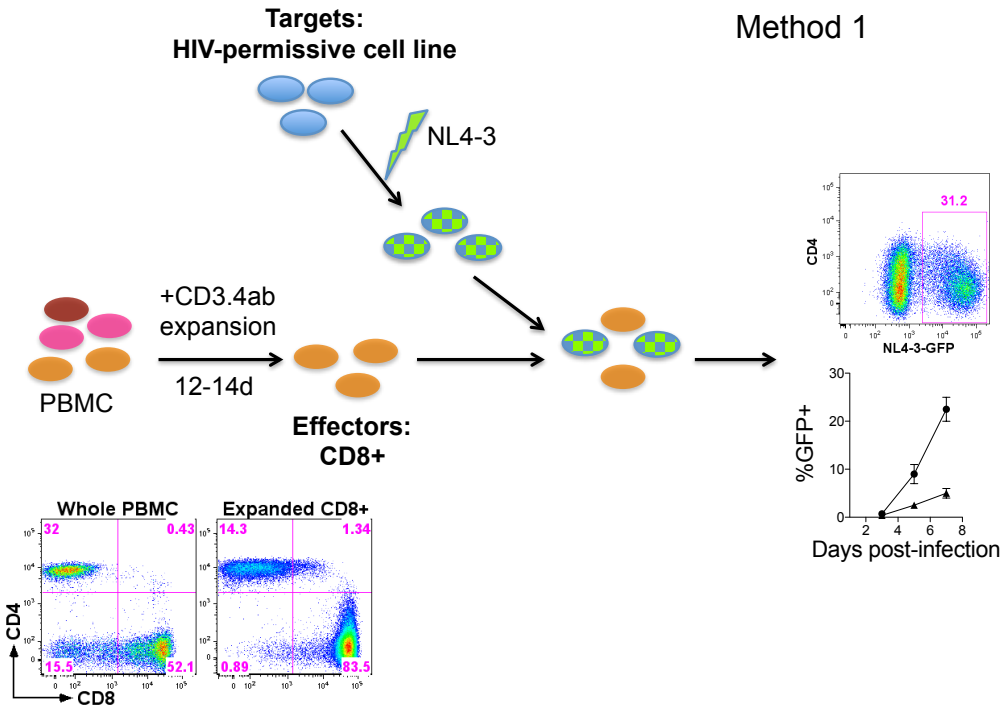


Figure 2.3. Schematic of viral inhibition assay, Method 1.

2.8.2 Method 2 (Figure 2.4)

This method was developed to evaluate *ex vivo* capacity of CD8+ T-cells to suppress autologous virus replication in viraemic subjects. First, CD4+ T-cells were isolated from PBMCs by positive selection (EasySep, Stemcell Technologies); CD8+ T-cells were then enriched (negative selection) from the remaining CD4-depleted fraction and left in R10 to rest for 3 days. CD4+ T-cells were treated for 3 days with IL2 (100IU/ml), IL7 (10ng/ml; premium grade, Miltenyi Biotec), anti-CD3 (1µg/ml) and anti-CD28 (1µg/ml; pure, Miltenyi Biotec) antibodies (Saez-Cirion et al., 2013) to reactivate autologous virus. (This cocktail was selected based on the comparison with PHA (2µg/ml; Sigma) and IL2 (100IU/ml) activation, **Figure 2.5**). After 3 days of activation, 'CD4 alone' and 'CD4:CD8 co-cultures' were set up for 14 days. On days 3, 7, 10 and 14 cells were fed with fresh R10/100. HIV p24 protein in the collected supernatant was measured by ELISA (ZeptoMetrix). Suppressive capacity was calculated as above.

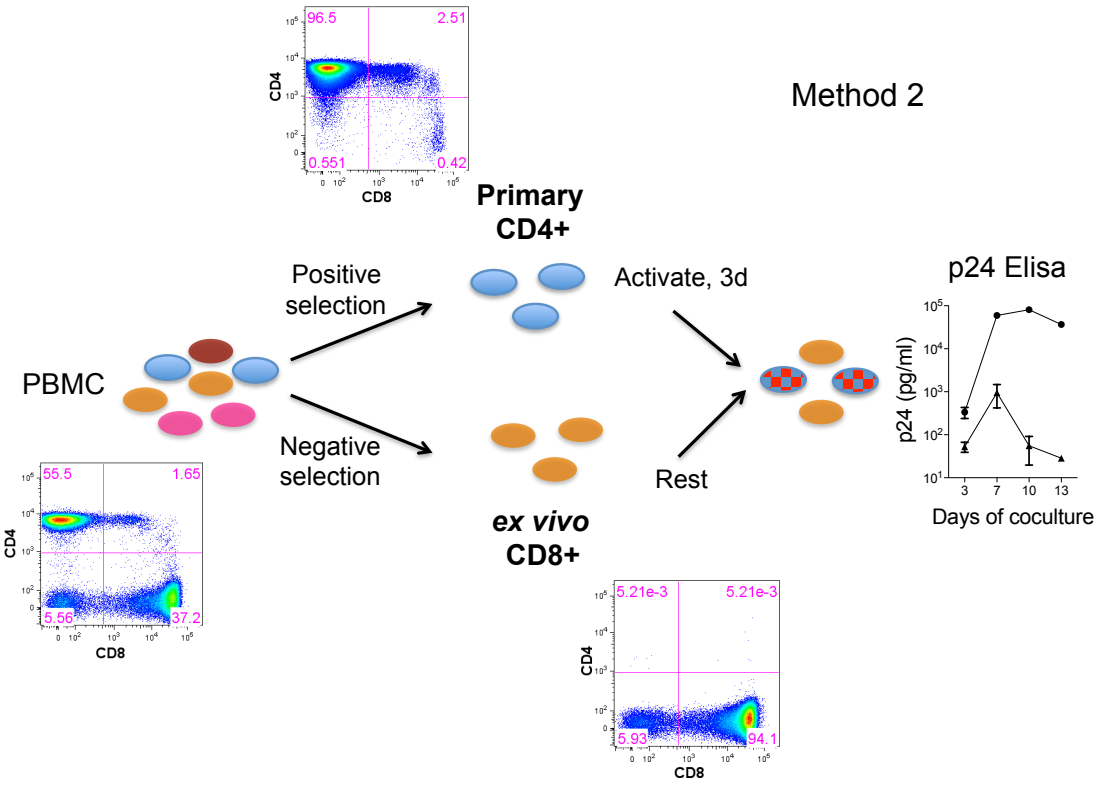


Figure 2.4. Schematic of viral inhibition assay, Method 2.

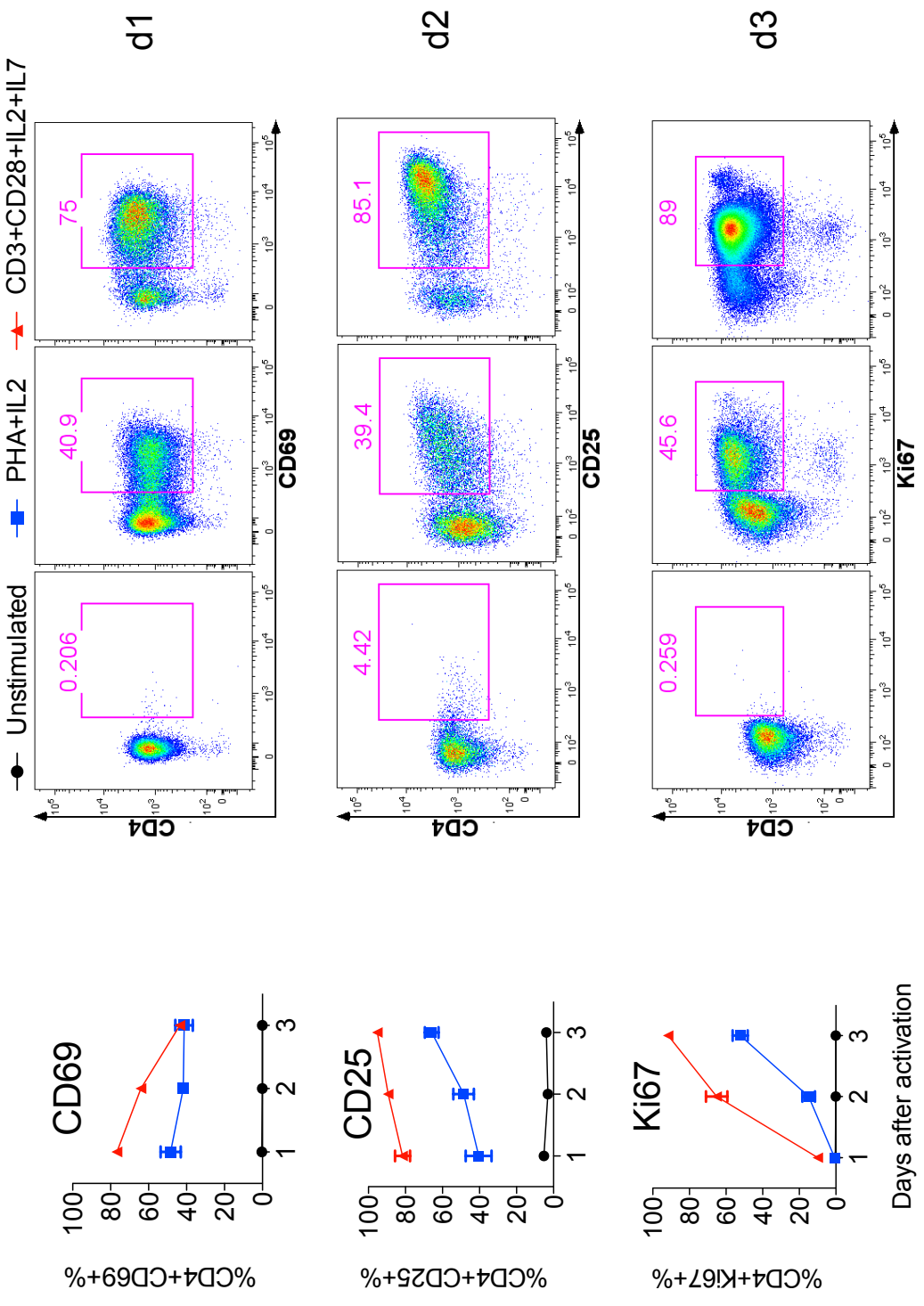

Unstimulated
PHA+IL2
CD3+CD28+IL2+IL7
d1
d2
d3
CD4
CD69
CD25
Ki67
0.206
40.9
75
4.42
39.4
85.1
0.259
45.6
89
%CD4+CD69+%
%CD4+CD25+%
%CD4+Ki67+%
Days after activation

Figure 2.5. Timecourse to compare CD4+ T-cell activation using PHA/IL2 or CD3/CD28/IL2/IL7. Markers measured were CD69, CD25 and Ki67. Representative dot plots are shown.

2.9 HIV sequencing

2.9.1 Sanger sequencing of full-length proviral genome

For the studies in Chapter 6, full-length HIV proviral genome was sequenced, using a published method (Henn et al., 2012). Briefly, during amplification a 9kb product was generated in the first round; second round PCR generated 5' (4.5kb) and 3' (4.6kb) amplicons. Platinum Taq DNA Polymerase High Fidelity (Invitrogen) and PCR grade 10mM dNTP mix (Invitrogen) were used; mastermix reaction composition, amplification primers and PCR cycling conditions are shown in **Tables 2.3-2.5**. One negative control (water instead of template DNA) was run for each PCR reaction. Following amplification, 5 µl PCR product was run on 1% agarose (Sigma) gel in TBE (Tris-borate-EDTA, Promega) containing ethidium bromide (5 µl/250 ml gel) at 180V for 65 minutes. Hyperladder I (Bioline) was run along side to determine the size of amplicons. Bands were visualised under UV light. Amplified products were kept at 4°C for immediate use or stored at -20°C long-term. Primers were synthesised by Eurofins Genomics.

Table 2.3. PCR mastermix reaction.

Component	Volume (µl)	Final Concentration
10x High Fidelity PCR Buffer	5	1x
50 mM $MgSO_4$	2	2 mM
10mM dNTP mix	1	0.2 mM each dNTP
Forward primer	1	0.2 mM
Reverse primer	1	0.2 mM
Platinum Taq DNA polymerase High Fidelity	0.2	1 Unit
Template DNA	4-10	Not applicable
Water	Up to 50	Not applicable

Table 2.4. PCR amplification primers (Henn et al., 2012).

Region of genome	Primer	Sequence (5'→3')	HXB2 coordinates
Round 1: 9kb	R1For1	AAATCTCTAGCAGTGGCGCCCGAACAG	623→649
	R1Rev1	ACGTGCCCTCAAGGCAAGCTTTATTGAGGC	9607←9632
Round 2.1: 5' half, 4.5kb Gag, Pol	R2For1	CAGGACTCGGCTTGCTGAAGC	692→712
	R2Rev1	CCCTAGTGGGATGTGTACTTCTGAAC	5195←5220
Round 2.2: 3' half, 4.6kb, Vif, Vpr, Vpu, Env, Tat, Rev, Nef	R2For2	TCTGGAAAGGTGAAGGGGCAGTAG	4954→4977
	R2Rev2	GGTCTAACCAGAGAGACCCAGTACAG	9532←9557

Table 2.5. PCR cycling conditions to amplify full genome (Henn et al., 2012).

Step	Temperature (°C)	Time (round 1)	Time (round 2)
1 - Denature	94	1 minute	1 min
2 - Anneal	65	20 sec	20 sec
3 - Extend	68	10 min	4.5 min
4 - Denature	94	15 sec	15 sec
5 - Anneal	65	20 sec	20 sec
6 - Extend	68	10 min	4.5 min
7 - Go to step 4, 13 more times (i.e. 14 cycles total)			
8 - Denature	94	15 sec	15 sec
9 - Anneal	65	20 sec	20 sec
10 - Extend	68	10 min + 20 sec/each additional cycle	4.5 min + 5 sec/each additional cycle
11 - Go to step 8, 19 more times (i.e. 20 cycles total)			
12 - Extend	68	20 min	20 min
13 - Hold	4	Forever	Forever

Amplified PCR products of the correct size were purified using ExoSAP-IT (USB, USA) or QIAquick PCR Purification Kit (QIAGEN) to remove leftover dNTP and primers. Sequencing primers (designed by Dr. Joris Hemelaar, University of Oxford; **Table 2.6**) were used to generate bidirectional overlapping fragments for the full-length genome. Sequencing was done using BigDye Terminator v3.1 Ready Reaction mix (Applied Biosystems) in a thermocycler (30 cycles of: 10 seconds at 96°C, 5 seconds at 50°C, 4 minutes at 60°C). Reaction product was precipitated using sodium acetate, spun at 4°C at 3500rpm for 2 hours, washed with ice-cold 70% ethanol and dried in the thermocycler for 1

minute at 94°C. Sequences were read by the Department of Zoology (University of Oxford), then manually edited for mixed bases using Sequencher 5.0 (Gene Codes corp.), translated in Geneious 6.1.3 and aligned in Clustal Omega.

Table 2.6. Full genome sequencing primers.

Primer	Sequence (5'→3')	HXB2 coordinates
HIV1-1F1	GAAGGAGAGAGATGGGTGC	779-797
HIV1-1F2	CATCAAGCAGCCATGCAAATG	1369-1389
HIV1-1F3	GGCACATAGCCAGAAATTGC	1985-2004
HIV1-1F4	GTCCCATTGAAACTGTACCAG	2557-2577
HIV1-1F5/2F2	GGGATTTACCACACCAGACAAG	3185-3206
HIV1-1R1	TCCCACTCAGGAATCCAGG	3775-3793
HIV1-1R2/2R5	GTTTCTTGTCTGGTGTGGTAAATCC	3186-3210
HIV1-1R3	CTGGTACAGTTTCAATGGGAC	2557-2577
HIV1-1R4	CCTGCAATTTCTGGCTATGTGC	1986-2007
HIV1-1R5	CATTTGCATGGCTGCTTGATG	1369-1389
HIV1-2F1	ACAATGGCCATTGACAGAAG	2615-2634
HIV1-2F3	CCTGGATTCCTGAGTGGGAG	3775-3794
HIV1-2F4	GACTGTAGTCCAGGGATATGGC	4392-4413
HIV1-2F5/3F2	GTGACATAAAGGTAGTACCAAGGAGG	4993-5018
HIV1-2R1	TGGTCTTCTGGGGCTTGTTC	5562-5581
HIV1-2R2/3R6	CCTCCTTGGTACTACCTTTATGTC	4995-5018
HIV1-2R3	GCCATATCCCTGGACTACAGTCTAC	4389-4413
HIV1-2R4	CTCCCACTCAGGAATCCAGG	3775-3794
HIV1-3F1	TGTAGTCCAGGAATATGGCA	4395-4414
HIV1-3F3	CTCAAGCAGGAAGCTGTCAGAC	5634-5655
HIV1-3F4	GCAGAAGACAGTGGCAATGAG	6209-6229
HIV1-3F5/4F2	CAACCATAACACAAGCCTGTCC	6820-6841
HIV1-3F6/4F3	GTGGAGGAGAATTTTTCTATTGC	7357-7379
HIV1-3R1	GGTGCAGATGAGTTTTCCAG	8020-8039
HIV1-3R2/4R5	TGCAATAGAAAAATTCTCCTCCAC	7357-7380
HIV1-3R3/4R6	GGACAGGCTTGTGTTATGGTTG	6820-6841
HIV1-3R4	CTCATTGCCACTGTCTTCTGC	6209-6229
HIV1-3R5	GTCTGACAGCTTCCTGCTTGAG	5634-5655
HIV1-4F1	GCAGAAGACAGTGGCAATGAG	6209-6229
HIV1-4F4	GCTGAGGGCTATAGAGGCG	7889-7907
HIV1-4F5	GTGGAGAGCAAGACAGAGACAG	8434-8455
HIV1-4F6	GCTTTCCAGTCAGACCTCAG	8996-9015
HIV1-4R1	CCTAGAGAGACCCAGTACAG	9532-9550
HIV1-4R2	CTGAGGTCTGACTGGAAAGC	8996-9015
HIV1-4R3	GTGCTAAGAATCCGCTCACTAATC	8464-8487
HIV1-4R4	CGCCTCTATAGCCCTCAGC	7889-7907

2.9.2 Sanger sequencing of proviral Gag and Env

For the HLA-B*14 studies (Chapter 3), Gag and partial Env (containing HLA-B*14-Env-EL9 ^{584}ERYLKDQQL^{592} epitope) segments were amplified by nested PCR, as previously described (Leslie et al., 2005; Leslie et al., 2004), using Bioline reagents. Mastermix reaction composition, amplification primers (Eurofins Genomics) and PCR cycling conditions are shown in **Tables 2.7-2.9**. PCR products were purified using QIAquick PCR Purification Kit (QIAGEN) and sequenced as above (section 2.9.1) using primers listed in **Table 2.10**. Maximum-likelihood trees of all sequences were generated using Mega6.06-mac software and FigTree v1.4.2, to exclude the possibility of contamination with laboratory viral strains. HIV subtypes were further confirmed with NCBI (website) and REGA (website) HIV genotyping tools.

Table 2.7. Composition of the PCR mastermix to amplify HIV *gag* and partial *env.*

Component	Volume (µl)
Buffer	5
MgCl2	3
5' primer	1
3' primer	1
dNTP	0.5
BioTaq	0.5
Template DNA	2
Water	Up to 50

Table 2.8. *Gag* and *env* amplification primers.

Region of genome	Clade	Primer	Sequence (5'→3')	HXB2 coordinates	Temperature 1 (°C)*	Temperature 2 (°C)*
Gag	B	F1_5'OP	AAATCTCTAGCAGTGGCGCC	623-642	64	61
		F1_3'OP	TGTTGGCTCTGGTCTGCTCT	2138-2157		
		F1_5'IP	ACTAGCGGAGGCTAGAA	765-781	60	57
		F1_3'IP	GCCACAATTGAAACACTT	1960-1977		
	C	F1_5'OP	CTCTAGCAGTGGCGCCCGAA	627-646	60	57
		F1_3'OP	TCCTTTCCACATTTCCAACAGCC	2023-2045		
		F1_5'IP	ACTCGGCTTGCTGAAGTGC	696-714	57	54
		F1_3'IP	CAATTTCTGGCTATGTGCCC	1984-2003		
Env	B	F7_5'OP	GGAGATATAAGACAAGCACATTG	7194-7216	60	57
		F7_3'OP	CCCTGTCTTATTCTTCTAGGT	8753-8773		
		F7_5'IP	GTGGAGGAGAATTTTTCTATTG	7357-7378	61	58
		F7_3'IP	CTATCTGTTCCTTCAGCTACTGC	8685-8707		
	C	F7_5'OP	GTATAAGGATAGGACCAGGACA	7147-7169	60	57
		F7_3'OP	CCCTGTCTTATTCTTCTAGGT	8753-8773		
		F7_5'IP	AGCAATGTATGCCCCTCCCAT	7520-7540	63	60
		F7_3'IP	CTATCTGTTCCTTCAGCTACTGC	8685-8707		

*Annealing temperatures during PCR (see Table 2.9).

Table 2.9. PCR cycling conditions to amplify HIV *gag* and partial *env*.

Step number	Temperature (°C)	Time
1	94	2 minutes
2	94	15 seconds
3	Temperature 1*	30 seconds
4	72	1 minute
5	*go to step 2, 19 times*	
6	94	15 seconds
7	Temperature 2*	30 seconds
8	72	1 minute
9	*go to step 6, 19 times*	
10	72	7 minutes
11	4	forever

*Temperatures 1 and 2 are shown in Table 2.8.

Table 2.10. Sequencing primers for *gag* and partial *env*.

Region of genome	Clade	Primer	Sequence (5'→3')	HXB2 coordinates
Gag	B	F1_5'IP	ACTAGCGGAGGCTAGAA	765-781
		F1_2	CCTGGAGGTTCTGCAC	1192-1207
		F1_3	GACACCAAGGAAGCTTTAG	1075-1093
		F1_4	ATCCCAGGATTATCCATC	1580-1597
		F1_5	CCAAGGGAAGTGACAT	1480-1496
		F1_3'IP	GCCACAATTGAAACACTT	1960-1977
	C	F1_5'IP	ACTCGGCTTGCTGAAGTGC	696-714
		F1_2	CTGCAGAATGGGATAGTTACAT	1415-1437
		F1_3	GACACCAAGGAAGCCTTAG	1075-1093
		F1_4	CTCCCACTGGAAtAGGTG	1550-1567
		F1_5	GGAACAAATAGCATGGATGAC	1521-1541
		F1_3'IP	CAATTTCTGGCTATGTGCCC	1984-2003
Env	B	F7_5'IP	GTGGAGGAGAATTTTTCTATTG	7357-7378
		F7_2	GTACCGTCAGCGTTATTG	7825-7842
		F7_3	TCCTTGGGTTCTTGGGAGC	7780-7798
		F7_4	ACCAATTCCACAGATTTTCC	8222-8241
		F7_5	TGGGATAAAGAAATTAGTAATTA	8115-8137
		F7_6	TCTTTTTTAGTTCCAGACCCCAA	8630-8652
		F7_3'IP	CTATCTGTTCCTTCAGCTACTGC	8685-8707
	C	F7_5'IP	AGCAATGTATGCCCCTCCCAT	7520-7540
		F7_2	GTACCGTCAGCGTTATTG	7825-7842
		F7_3	TCCTTGGGTTCTTGGGAGC	7780-7798
		F7_4	ACCAATTCCACAGATTTTCC	8222-8241
		F7_5	TGGGATAAAGAAATTAGTAATTA	8115-8137
		F7_6	TCTTTTTTAGTTCCAGACCCCAA	8630-8652
		F7_3'IP	CTATCTGTTCCTTCAGCTACTGC	8685-8707

2.9.3 Amplification of full-length viral RNA for ultra-deep sequencing

Deep sequencing of viral RNA was used in the paediatric studies in Chapter 4. Amplification of the full HIV genome in four fragments was performed using SuperScript III One-Step RT-PCR System with Platinum Taq High Fidelity (Invitrogen), as previously described (Gall et al., 2012). Mastermix composition and primers (Eurofins Genomics) are detailed in **Tables 2.11 and 2.12**. Mastermix (20 µl/well) was aliquoted into a 96-well Low Profile PCR plate; 5 µl/well RNA template (negative control – water, positive control –

known HIV-1 RNA) was added and PCR was run in a thermocycler (**Table 2.13**). To confirm amplification, PCR products were run on 1% agarose gel with 240V, 300mA for 1.5 hours and bands were visualised under UV light. Amplicons were then combined into one pool (5 µl amplicon 1 and 10 µl each amplicons 2, 3 and 4) and ultra-deep sequenced at the Wellcome Trust Sanger Institute (Cambridge, UK) in collaboration with Dr. Astrid Gall and Prof. Paul Kellam.

Table 2.11. RT-PCR mastermix composition.

Component	Volume (µl)
Nuclease-free water	4.5
2xReaction Mix	12.5
Pan-HIV-1-Mix 1,2,3, or 4*	2
SSIII RT/Platinum Taq High Fidelity Mix	1
Total volume	20

*Pan-HIV-1 primer mixes for each of the 4 amplicons were prepared by mixing forward and reverse primers in T0.1E buffer (Sigma) at a final concentration 10pmol/µl (Gall et al., 2012).

Table 2.12. RT-PCR primer sequences (Gall et al., 2012).

Primer	Sequence	HXB2 location
Pan-HIV-1_1F	AGC CYG GGA GCT CTC TG	480-496
Pan-HIV-1_1R	CCT CCA ATT CCY CCT ATC ATT TT	2385-2407
Pan-HIV-1_2F	GGG AAG TGA YAT AGC WGG AAC	1485-1505
Pan-HIV-1_2R	CTG CCA TCT GTT TTC CAT ART C	5037-5058
Pan-HIV-1_3F	TTA AAA GAA AAG GGG GGA TTG GG	4783-4805
Pan-HIV-1_3R	TGG CYT GTA CCG TCA GCG	7831-7848
Pan-HIV-1_4F	CCT ATG GCA GGA AGA AGC G	5967-5985
Pan-HIV-1_4R	CTT WTA TGC AGC WTC TGA GGG	9496-9517

Table 2.13. RT-PCR cycling conditions.

Step	Temperature (°C)	Time
1 - Reverse transcription	50°C	30 minutes
2 - Inactivation RT/ activation Taq	94°C	2 minutes
3 - Denaturation	94°C	15 seconds
4 - Annealing	58°C	30 seconds
5 - Extension	68°C	4.5 minutes
6 - Go to step 3, repeat 3-5 39 more times (40 cycles total)		
7 - Final extension	68°C	10 minutes
8 - End	10°C	hold

2.9.4 Ultra-deep sequencing and de novo assembly of genomes

Each pool of amplicons was given a unique bar code for Illumina library preparation and sequenced using MiSeq 300-bp paired-end technology. Consensus sequences were generated by *de novo* assembly, i.e. without a reference sequence, using Iterative Virus Assembler (Hunt et al., 2015). This was performed at the Sanger Institute by Dr. Astrid Gall.

2.9.5 Determination of haplotypes

Bioinformatical determination of minority calls for the HLA-associated epitopes (section 2.9.7) was performed by Dr. Azim Ansari (University of Oxford, UK) using V-Phaser 2 to call variants (Yang et al., 2013) and V-Profiler to call haplotypes (Henn et al., 2012). To find epitope locations within each subject's viral sequence, *de novo* assembled sequences were aligned to a reference subtype C genome that had been annotated with the epitopes of interest. This alignment was then used to obtain epitope location on the assembled sequences. Gaps in partial genomes were "filled" with maternal or reference sequence

before application of the above strategy. Only minority variants of >1% frequency were included in the analysis (see Chapter 4, Chapter-specific methods).

2.10. Viral fitness assays

(These assays were performed by Ming-Han Tsai, Goulder group, University of Oxford in the HLA-B*14 studies, Chapter 3.)

2.10.1. Site-directed mutagenesis of NL4-3

Y301F, K302R, and Y301F/K302R mutations of HIV-1 Gag sequence as well as K588Q and K588R mutations in Env sequence were introduced respectively into the HIV-1 subtype B NL4-3 plasmid by using QuikChange Lightning site-directed mutagenesis kit (Agilent technologies) along with custom-designed mutagenesis forward and reverse primers. The primers are shown as follows (mutated codons shown in bold): 5'-C CTG GCT GTG GAA AGA TAC CTA **CAG** GAT CAA CAG CT-3' (Env K588Q); 5'-GAC TAT GTA GAC CGA TTC **TTT** AAA ACT CTA AGA GCC GAG-3' (Gag Y301F); 5'-T AGA GAC TAT GTA GAC CGA TTC TAT **AGA** ACT CTA AGA GCC G-3' (Gag K302R); 5'-A GAC TAT GTA GAC CGA TTC **TTT AGA** ACT CTA AGA GCC GAG CAA G-3' (Gag Y301F/K302R). All mutations were confirmed by sequencing.

2.10.2. Virus production and replication kinetics

All plasmids were maxipreped according to manufacturer's instruction (HiSpeed® plasmid Maxi Kit, Qiagen, Hilden, Germany). To generate mutant viruses, the mutated NL4-3 Gag-Pro amplified purified PCR products with the BstE II (New England Biolabs, Ipswich, MA) linearized pNL4-3Δgag-protease were transfected into GFP reporter GXR cells via electroporation in a BioRad GenePulsar II using 0.4 cm cuvettes at 300 Volts, 500μF, and

infinite resistance (Miura et al., 2009). Virus propagation was then monitored by flow cytometry (LSRII, BD Biosciences) to detect GFP-expressing infected cells for two weeks in culture with GXR cells. Virus culture supernatants were harvested when 30% cells were GFP-positive. Viruses were aliquoted and stored at -80°C until use. All mutations were confirmed again by extracting viral RNA from the harvested supernatant and sequencing. Nucleotide similarity has reached 99.99%. Along with WT as positive controls and two negative controls without viruses, NL4-3 mutant viruses were incubated with GXR cells in a 24-well plate for determination of viral titres, as previously described (Brockman et al., 2007). A low MOI (0.01%) was set as the lowest threshold for determining the amount of virus required for inoculation. The GFP+ expression was measured by flow cytometry from day 2 to 7 before it reached the saturated 30-40%. The viral replication capacity was defined by the semi-log calculation of the mean slope of exponential growth in Excel. This was further calibrated to the normalised value relative to the wild type NL4-3 respectively. All assays were done at least in triplicate.

2.11. Media composition

- ***R10:*** RPMI-1640, 10% heat-inactivated FCS (Sigma), 1% L-glutamine (Sigma) and 1% penicillin-streptomycin (Sigma);
- ***R10/50:*** R10 supplemented with 50 U/ml human premium grade IL2 (Miltenyi Biotec);
- ***R10/100:*** R10 supplemented with 100IU/ml human premium grade IL2 (Miltenyi Biotec).

2.12. Statistical analysis

All analyses were performed in Prism (v5.0c, GraphPad) unless stated otherwise. Data were first confirmed to have parametric or nonparametric distribution (D'Agostino and Pearson omnibus normality test). For two-group analyses t-test (parametric) or Mann-Whitney U test (nonparametric) was performed; for ≥3-group analyses ANOVA (parametric) or Kruskal-Wallis (nonparametric) followed by post-hoc test was performed. Nominal data categorised in two distinct ways were compared by Fisher's Exact test. Strength of association between two variables was analysed by Pearson (nonparametric) or Spearman (parametric) correlation. Functional avidity was calculated using a dose-response function. P values <0.05 were considered significant. Other statistical analyses performed are specified in relevant chapters.

CHAPTER 3. ANTIVIRAL EFFICACY OF GAG- AND NON-GAG-SPECIFIC CD8+ T-CELLS IN THE IMMUNE CONTROL OF ADULT HIV INFECTION

3.1 Preface

The central role of HLA-mediated CD8+ T-cell activity in non-progressing adult HIV infection has long been established. However, not all HIV-specific CD8+ T-cell responses are equal in their antiviral efficacy, even among those that target Gag – viral most vulnerable component. Furthermore, whilst most studies have concentrated on investigating CD8+ T-cell-mediated control in the context of the typical protective HLA class I molecules HLA-B*57 or HLA-B*27, other alleles associated with protection in natural infection, such as HLA-B*14, have been largely neglected. In this Chapter, I set out to explore the antiviral efficacy of Gag and non-Gag specificities, first those restricted by the 'classic' HLA-B*57, then those restricted by 'non-classic' HLA-B*14, and discover the unexpected antiviral potential of a subdominant response in the first instance and of an Env-specific response in the second instance.

[HLA-B*57-related work (section 3.2) has been published in **Leitman, E.M.**, Willberg, C.B., De Burgh-Thomas, A., Streeck, H., Goulder, P. J. R., Matthews, P. C. A. **2016.** Subdominant Gag-specific anti-HIV efficacy in an HLA-B*57-positive elite controller. *AIDS* 30(6): p. 972-974.]

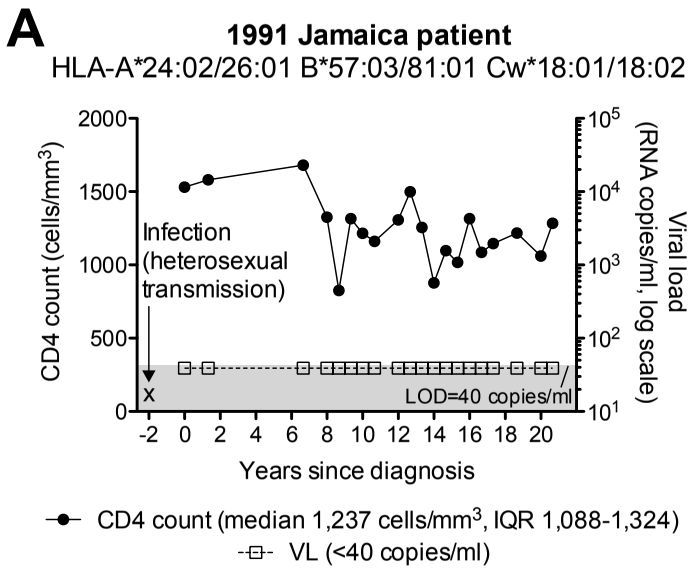
3.2. Part I: Subdominant Gag-specific anti-HIV efficacy in an HLA-B*57-positive elite controller

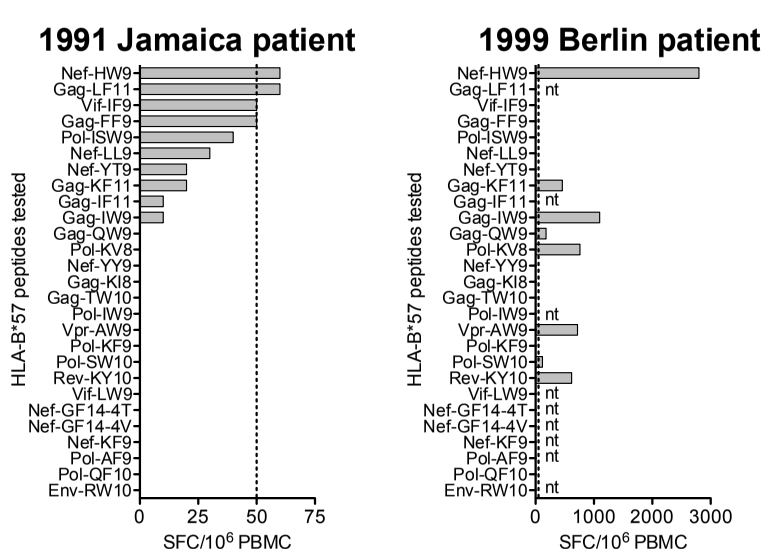
Despite HIV discovery over three decades ago, the 2008 'Berlin patient' is the only case of sustained HIV remission. Other cases of apparent 'cure' eventually relapsed (Henrich et al., 2014) and although early antiretroviral therapy (ART) has recently gained traction as a factor contributing to remission (Frange et al., 2016; Saez-Cirion et al., 2013), most cases are likely to relapse (Luzuriaga et al., 2015). In contrast, relapse in 'elite controllers' of HIV infection is less common. These are ART-naïve individuals who spontaneously suppress viraemia to undetectable levels. Approximately 40% of elite controllers express HLA-B*57 (Pereyra et al., 2008), an example being the original 1999 'Berlin patient', in whom virologic control has been maintained for >15 years to date (Jessen, Allen, and Streeck, 2014).

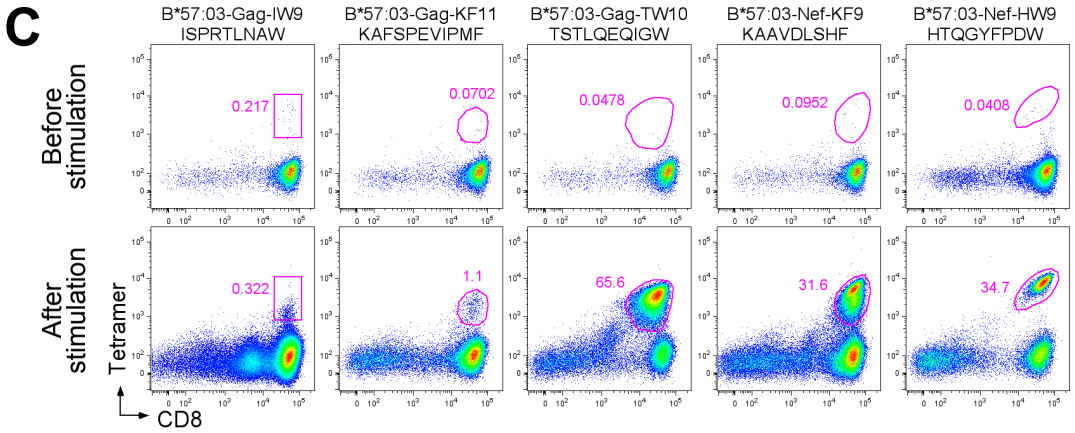
Mechanisms proposed to explain HLA-B*57-mediated immune control include immunodominant CD8+ T-cell-targeting of multiple conserved Gag epitopes from which mutational escape is detrimental to viral fitness, characteristics of the T-cell receptor on HLA-B*57-restricted CD8+ T cells, HLA-B*57-peptide binding affinity, and HLA-B*57 cross-talk with innate immune cells (Goulder and Walker, 2012). However, some HLA-B*57-positive elite controllers have no detectable Gag-specific responses without *ex vivo* expansion (Ndhlovu et al., 2012; Ndhlovu et al., 2015b). Here we studied one such elite controller, to determine whether the immunodominant CD8+ T-cell response in such cases mediates the most potent antiviral efficacy, since Gag-specific CD8+ T-cell responses typically have greater capacity to inhibit viral replication than non-Gag specificities (Chen et al., 2012; Payne et al., 2010).

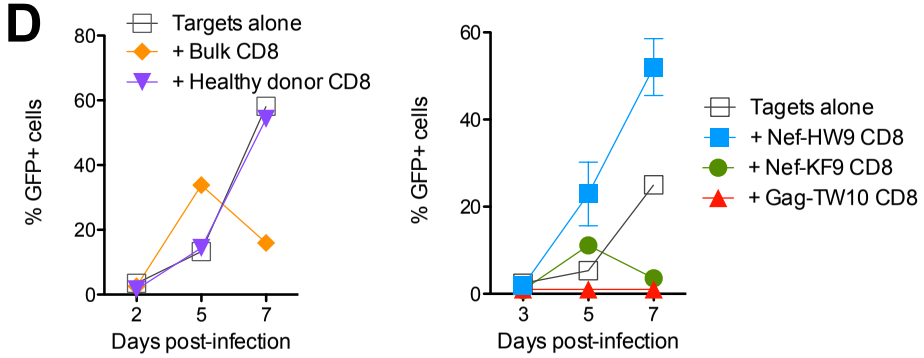
An African-Caribbean female was recruited in the UK at 52 years of age in 2013. She had been diagnosed with HIV in 1991, an estimated two years after heterosexual transmission in Jamaica (hence is referred to here as the '1991 Jamaica patient').

For >24 years she has remained ART-naïve and aviraemic with healthy CD4+ T-cell count (median 1,237 cells/mm^3) (**Figure 3.1A**). Despite being HLA-B*57:03-positive, she demonstrated only two HIV-specific CD8+ T-cell responses detectable by ELISPOT assay, neither greater than 60 SFC/million PBMCs and none detectable by tetramer staining (**Figures 3.1B,C**). This is in contrast to the '1999 Berlin patient', who had a dominant HLA-B*57-restricted Nef-HW9 response of 3,000 SFC/million PBMCs (Jessen et al., 2014) (**Figure 3.1B**). One of the two significant ELISPOT responses in the 1991 Jamaica patient was also against this same Nef-HW9 epitope (**Figure 3.1B**). However, via peptide stimulation of memory T-cell responses (Ndhlovu et al., 2012), we identified five HLA-B*57-restricted responses (**Figure 3.1C**), three of which we tested for their ability to inhibit HIV replication. Bulk CD8+ T cells demonstrated weak *ex vivo* ability to suppress viral replication (**Figures 3.1D,E**), fitting the profile of a subset of HLA-B*57-positive elite controllers (Lecuroux et al., 2014). Of the three expanded HLA-B*57-restricted CD8+ T-cell specificities tested, Gag-TW10-specific CD8+ T cells were significantly the most potent in suppressing HIV replication, followed by Nef-KF9 and then Nef-HW9 (**Figures 3.1D,E**).


A
1991 Jamaica patient
HLA-A*24:02/26:01 B*57:03/81:01 Cw*18:01/18:02
CD4 count (cells/mm3)
Viral load (RNA copies/ml, log scale)
Infection (heterosexual transmission)
LOD=40 copies/ml
Years since diagnosis
CD4 count (median 1,237 cells/mm3, IQR 1,088-1,324)
VL (<40 copies/ml)


B
1991 Jamaica patient
1999 Berlin patient
HLA-B*57 peptides tested
SFC/10^6 PBMC
Nef-HW9
Gag-LF11
Vif-IF9
Gag-FF9
Pol-ISW9
Nef-LL9
Nef-YT9
Gag-KF11
Gag-IF11
Gag-IW9
Gag-QW9
Pol-KV8
Nef-YY9
Gag-KI8
Gag-TW10
Pol-IW9
Vpr-AW9
Pol-KF9
Pol-SW10
Rev-KY10
Vif-LW9
Nef-GF14-4T
Nef-GF14-4V
Nef-KF9
Pol-AF9
Pol-QF10
Env-RW10
nt


C
B*57:03-Gag-IW9 ISPRTLNAW
B*57:03-Gag-KF11 KAFSPEVIPMF
B*57:03-Gag-TW10 TSTLQEQIGW
B*57:03-Nef-KF9 KAAVDLSHF
B*57:03-Nef-HW9 HTQGYFPDW
Before stimulation
After stimulation
Tetramer
CD8
0.217
0.0702
0.0478
0.0952
0.0408
0.322
1.1
65.6
31.6
34.7


D
Targets alone
+ Bulk CD8
+ Healthy donor CD8
% GFP+ cells
Days post-infection
Tagets alone
+ Nef-HW9 CD8
+ Nef-KF9 CD8
+ Gag-TW10 CD8

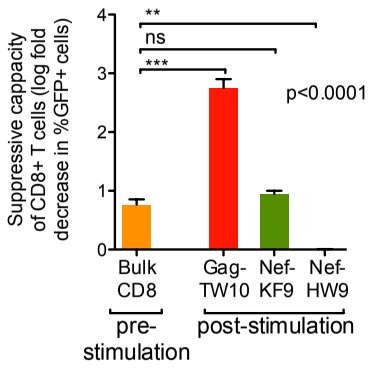

E
Suppressive cappacity of CD8+ T cells (log fold decrease in %GFP+ cells)
**
ns
***
p<0.0001
Bulk CD8
Gag-TW10
Nef-KF9
Nef-HW9
pre-stimulation
post-stimulation

Figure 3.1. Clinical profile and anti-HIV suppressive activity of the 1991 Jamaica patient. A. CD4+ T-cell count and HIV RNA viral load measurements. '0' is time of diagnosis. Limit of detection (LOD) for viral load is 40 copies/ml (gray area) and measurements are shown at 40 copies/ml for convenience. Although sequencing was unsuccessful due to lack of circulating virus, the 1991 Jamaica patient was likely infected with subtype-B HIV predominant in Jamaica. **B.** ELISPOT CD8+ T-cell responses in unstimulated PBMCs in the 1991 Jamaica patient (22 years post-diagnosis) to subtype-B consensus HLA-B*57-restricted defined optimal epitopes. Responses were considered positive if they were at least three times the mean number of SFC in the four negative control wells and had to be >50 SFC/10^6 PBMC (dotted line). CD8+ T-cell responses for the 1999 Berlin patient are shown to highlight the different patterns of responses (not for direct comparisons as the assays were done in different laboratories at different times). Nt=not tested. **C.** PBMCs (23 years post-diagnosis) were stimulated with a panel of 30 HLA-B*57/81:01-restricted optimal peptides. Five previously undetectable HLA-B*57-restricted responses were discovered post-stimulation, but no HLA-B*81:01-restricted responses. Three of these five responses were successfully expanded and tested in D. Gated on live CD3+CD4- cells around CD8+tetramer+ population; numbers indicate % tetramer+CD8+ cells (of CD3+CD4-). **D.** Viral replication in HLA-B*57:03-expressing H9 cells infected with NL4-3-GFP and cultured alone ('targets alone'), with unstimulated bulk CD8+ T cells (left panel) or stimulated epitope-specific CD8+ T cells (right panel) of the 1991 Jamaica patient (23 years post-diagnosis). Each symbol represents the mean of three replicates, error bars represent s.e.m. **E.** Suppressive capacity (log_{10} fold decrease in % of infected GFP+ cells) of bulk unstimulated CD8+ T cells or stimulated epitope-specific CD8+ T cells of the 1991 Jamaica patient. Results were compared to 'bulk CD8' (ANOVA with Dunnett's Multiple Comparison post-test). *p<0.05, **p<0.01, ***p<0.001, ns=not significant (p≥0.05).

The study of this HLA-B*57-positive individual confirms that in spite of HIV-specific responses being low frequency or undetectable by tetramer staining or ELISPOT assay, strong responses could be 'recalled' from memory, as previously reported (Ndhlovu et al., 2012). Among these, Gag-TW10-specific CD8+ T cells were more potent at inhibiting viral replication than Nef-KF9-specific cells, despite the latter being a stronger response in ELISPOT assays. These data support previous findings in subjects chronically infected with HIV (Frahm et al., 2006) indicating that subdominant responses may be more efficacious in terms of control of viraemia. The findings here are extended also to the case

of an HLA-B*57-positive elite controller. Although, like the 1999 Berlin patient, this is a single case report, the data are consistent with the hypothesis that HLA-B*57-mediated Gag-specific targeting by CD8+ T cells confers benefit to the host in HIV infection (Goulder and Walker, 2012; Kiepiela et al., 2007) and that vaccine induction of broad Gag-specific CD8+ T-cell responses would tend to increase immune control in HIV infection (Janes et al., 2013).

3.3. Part II: HLA-B*14:02-restricted Env-specific CD8+ T-cell activity has highly potent anti-viral efficacy that is assoclated with immune control of HIV infection

3.3.1 Introduction

Spontaneous durable control of HIV is observed in a rare subgroup (<0.3%) of infected individuals known as ‘elite controllers’ (Migueles and Connors, 2010). Classically, this non-progressive disease phenotype in HIV infection is associated with expression of certain HLA class I molecules (Kaslow et al., 1996; Pereyra et al., 2010), namely HLA-B*57 and HLA-B*27 alleles (Lambotte et al., 2005; Migueles and Connors, 2010; Migueles et al., 2000). An important mechanism underlying the HLA associations with HIV disease outcome is related to the particular HIV-specific epitopes presented by different HLA class I molecules. In particular, ‘protective’ HLA molecules typically present broad Gag-specific CD8+ T-cell responses, whereas disease-susceptible alleles such as HLA-B*35:01 and HLA-B*58:02 present Nef- and Env-specific epitopes, respectively, responses that are typically associated with poor immune control of HIV (Goulder and Walker, 2012; Kiepiela et al., 2007; Masemola et al., 2004; Matthews et al., 2012; Ngumbela et al., 2008).

Factors contributing to improved immune control in association with broad Gag and not Nef or Env responses include the sequence conservation especially of the capsid protein, because the cost to viral replicative capacity of Gag escape mutants is often significant (Crawford et al., 2009; Martinez-Picado et al., 2006; Miura et al., 2009; Schneidewind et al., 2007). In contrast, Env escape mutants, for example, are typically tolerated by the virus without significant impact on viral replicative capacity (Troyer et al., 2009). In addition, it appears that Gag capsid proteins are much more abundant than Env trimers in mature virions (1,000-1,500 per virion versus 10-20, respectively) (Zhu et al., 2003) and Gag epitopes can be presented within 2 hours of HIV gaining entry into the target cell, prior to *de novo* HIV protein synthesis. Hence, HIV-infected cells can be killed by Gag-specific CD8+ T-cells substantially before new virion production (Payne et al., 2010; Sacha et al., 2007a). In contrast, Nef- and Env-specific CD8+ T-cell responses kill virus-infected target cells only after *de novo* synthesis of viral proteins (Kloverpris et al., 2013a; Payne et al., 2010; Sacha et al., 2007a; Sacha et al., 2007b) and therefore following Nef-mediated HLA class I downregulation (Collins et al., 1998; Yang et al., 2002). Nonetheless, Gag-specific CD8+ T-cell responses are not equally efficacious (Honeyborne et al., 2007; Kiepiela et al., 2007; Kloverpris et al., 2012a), and there is evidence from the SIV/macaque model that certain non-Gag epitopes, for example within Nef and Vif, are important for immune control (Mudd et al., 2012).

To investigate further the possibility that effective CD8+ T-cell responses might exist outside of Gag, in proteins such as Env, we focused here on HLA-B*14, where the dominant HIV-specific CD8+ T-cell response is in Env (Johnson et al., 1992; Kalams et al., 1994). The association between HLA-B*14 and immune control of HIV has not been well-studied to date, since most studies of elite controllers have focused on those expressing HLA-B*27 or B*57 (Almeida et al., 2007; Chen et al., 2012; Horton et al., 2006; Migueles et

al., 2003; Migueles et al., 2002; Migueles et al., 2008; Migueles et al., 2009; Saez-Cirion et al., 2007). Although HLA-B*14 is not as strongly associated as HLA-B*27 or HLA-B*57 with HIV disease progression, nonetheless large studies have consistently shown a significant protective effect (Hendel et al., 1999; Kiepiela et al., 2004; Leslie et al., 2010; Pereyra et al., 2010). In addition to the dominant Env-specific CD8+ T-cell response, HLA-B*14-positive individuals also make a subdominant Gag-specific CD8+ T-cell response (Harrer et al., 1996). We set out to investigate the role of these two specificities in HLA-B*14-mediated suppression of HIV and to understand the mechanisms underlying differential antiviral activity among HLA-B*14-restricted CD8+ T-cell specificities.

3.3.2 Chapter-specific materials and methods

3.3.2.1 Additional cohorts used for analysis

To analyse the associations between the expression of HLA-B*14:01 and HLA-B*14:02 with immune control of HIV, viral load and HLA data of the ART-naïve chronically HIV-infected subjects (n=5,004; Caucasians: n=3,259; African Americans: n=1,745) were used. These subjects were from the cohorts from the following studies:

- AIDS Clinical Trial Group (ACTG) Study (https://actgnetwork.org);
- International HIV Controllers Study (Pereyra et al., 2010) (http://www.hivcontrollers.org);
- Multicenter AIDS Cohort Study (MACS) (Phair et al., 1992) (https://statepi.jhsph.edu/macs/macs.html);
- Multicenter Hemophilia Cohort Study (MHCS) (Goedert et al., 1989) (https://biolincc.nhibi.hih.gov/studies/mhcs);
- The Study of the Consequences of Protease Inhibitor Era (SCOPE) (Hunt et al., 2003) (https://hiv.ucsf.edu/research/scope.html);

- Swiss HIV Cohort Study (Schoeni-Affolter et al., 2010) (www.shcs.ch).

3.3.2.2 Statistical analysis of HLA association and HIV immune control

These analyses was performed by Prof. Mary Carrington and Dr. Yin Qi (National Cancer Institute, NIH, USA). SAS 9.2 (SAS Institute) was used for statistical analyses. Genotype frequencies on individual HLA-B alleles were computed using PROC FREQ. To calculate OR and 95% CI for controllers versus non-controllers with adjusting by HLA-B*27 and HLA-B*57 PROC LOGISTIC was used; OR<1 indicates protection. Presence versus absence of all individual HLA-B alleles that have a frequency equal to or greater than HLA-B*14:01 were included in the models with stepwise selection.

3.3.3 Results

*3.3.3.1 Higher antiviral potency of HLA-B*14:02-Env-EL9 versus -Gag-DA9 CD8+ T-cell response*

The starting point for this study was 'elite controller' subject, N119, who first tested HIV-positive in UK in 2011, having previously had two negative tests in 2005 and 2008 (**Figure 3.2A**). Since the positive HIV test, N119 maintained an undetectable viral load (<40 copies/ml) and healthy and stable CD4+ T-cell counts (median 1,555 cells/mm^3, IQR 1,345-1,788). Viral sequencing revealed that she was infected with subtype B virus (**Figure 3.3** and genotyping tools (see Chapter 2, section 2.9.2)). HLA genotyping showed that she was HLA-B*14:02/HLA-C*08:02 homozygous and also expressed HLA-A*74:01, associated with slow disease progression (Matthews et al., 2011).

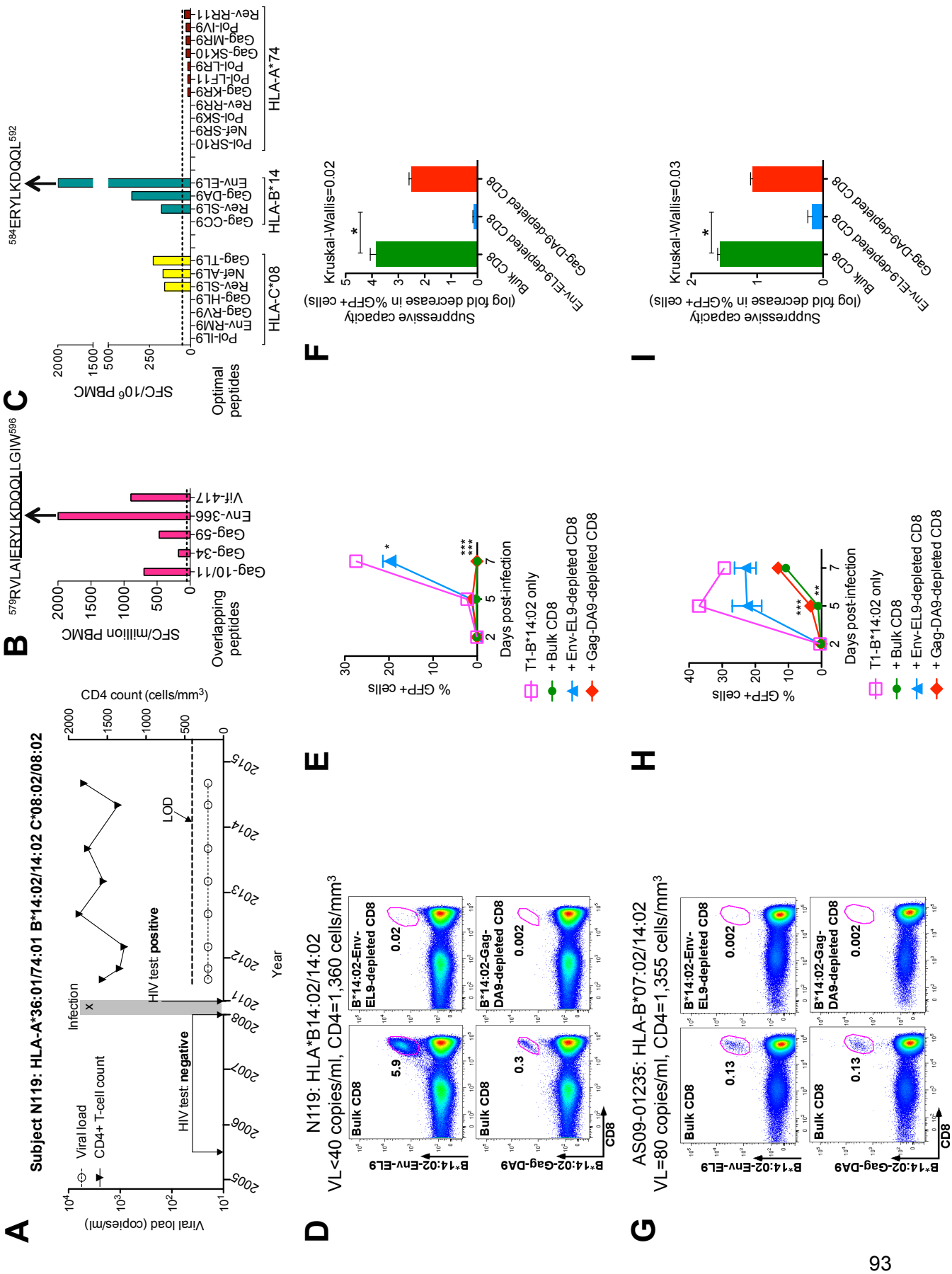

A
Subject N119: HLA-A*36:01/74:01 B*14:02/14:02 C*08:02/08:02
Viral load (copies/ml)
CD4 count (cells/mm3)
Viral load
CD4+ T-cell count
Infection
HIV test: positive
HIV test: negative
LOD
Year
B
579RVLAIERYLKDQQLLGIW596
SFC/million PBMC
Overlapping peptides
Gag-10/11
Gag-34
Gag-59
Env-366
Vif-417
C
584ERYLKDQQL592
SFC/10^6 PBMC
Optimal peptides
HLA-C*08
HLA-B*14
HLA-A*74
D
N119: HLA*B14:02/14:02
VL<40 copies/ml, CD4=1,360 cells/mm3
Bulk CD8
5.9
0.3
B*14:02-Env-EL9
B*14:02-Gag-DA9
B*14:02-Env-EL9-depleted CD8
0.02
B*14:02-Gag-DA9-depleted CD8
0.002
CD8
E
% GFP+ cells
Days post-infection
T1-B*14:02 only
+ Bulk CD8
+ Env-EL9-depleted CD8
+ Gag-DA9-depleted CD8
F
Kruskal-Wallis=0.02
Suppressive capacity
(log fold decrease in %GFP+ cells)
Bulk CD8
Env-EL9-depleted CD8
Gag-DA9-depleted CD8
G
AS09-01235: HLA-B*07:02/14:02
VL=80 copies/ml, CD4=1,355 cells/mm3
Bulk CD8
0.13
0.13
B*14:02-Env-EL9
B*14:02-Gag-DA9
B*14:02-Env-EL9-depleted CD8
0.002
B*14:02-Gag-DA9-depleted CD8
0.002
CD8
H
% GFP+ cells
Days post-infection
T1-B*14:02 only
+ Bulk CD8
+ Env-EL9-depleted CD8
+ Gag-DA9-depleted CD8
I
Kruskal-Wallis=0.03
Suppressive capacity
(log fold decrease in %GFP+ cells)
Bulk CD8
Env-EL9-depleted CD8
Gag-DA9-depleted CD8

Figure 3.2. Higher antiviral potency of B*14:02-EL9 versus -DA9 CD8 T-cell response. A. HIV-related clinical profile of subject N119; gray area shows time period during which infection occurred. All viral load measurements were undetectable (<40 copies/ml) and are shown below the limit of detection (LOD) of 40 copies/ml for convenience. Subject's full HLA type is shown. **B.** CD8+ T-cell IFN-γ ELISPOT responses to overlapping peptides spanning the entire HIV proteome in N119. Dotted line shows the cutoff magnitude (50 SFC/10^6 PBMC). **C.** CD8+ T-cell IFN-γ ELISPOT responses to epitopes restricted by N119's HLA class I alleles. HLA-A*36:01-restricted responses are not shown as these are not defined. Dotted line shows the cutoff magnitude (50 SFC/10^6 PBMC). **D-F.** Data for subject N119; **G-J.** Data for subject AS09-1235. **D,G.** Tetramer stainings confirming HLA-B*14:02-Env-EL9 (top panels) and HLA-B*14:02-Gag-DA9 (bottom panels) CD8+ T-cell responses in bulk (left panels) and tetramer-depleted cultures (right panels). Gated on live CD3+CD4- lymphocytes around CD8+ tetramer+ cells; numbers indicate % of CD8+ cells. **E,H.** Viral replication (%GFP+ cells) time course in infected T1-HLA-B*14:02-positive target cells with or without effector CD8+ T-cells. Results were compared to T1-HLA-B*14:02 target cells only at the peak of viral replication using paired t-tests. **F,I.** Suppressive capacity of 'Bulk,' 'Env-EL9-depleted' or 'Gag-DA9-depleted' effector cells calculated as described in the Methods. Kruskal-Wallis with Dunn's multiple comparison test. E,F,H,I, Error bars represent s.e.m. *p<0.05, **p<0.01, ***p<0.001. Only significant differences are shown.

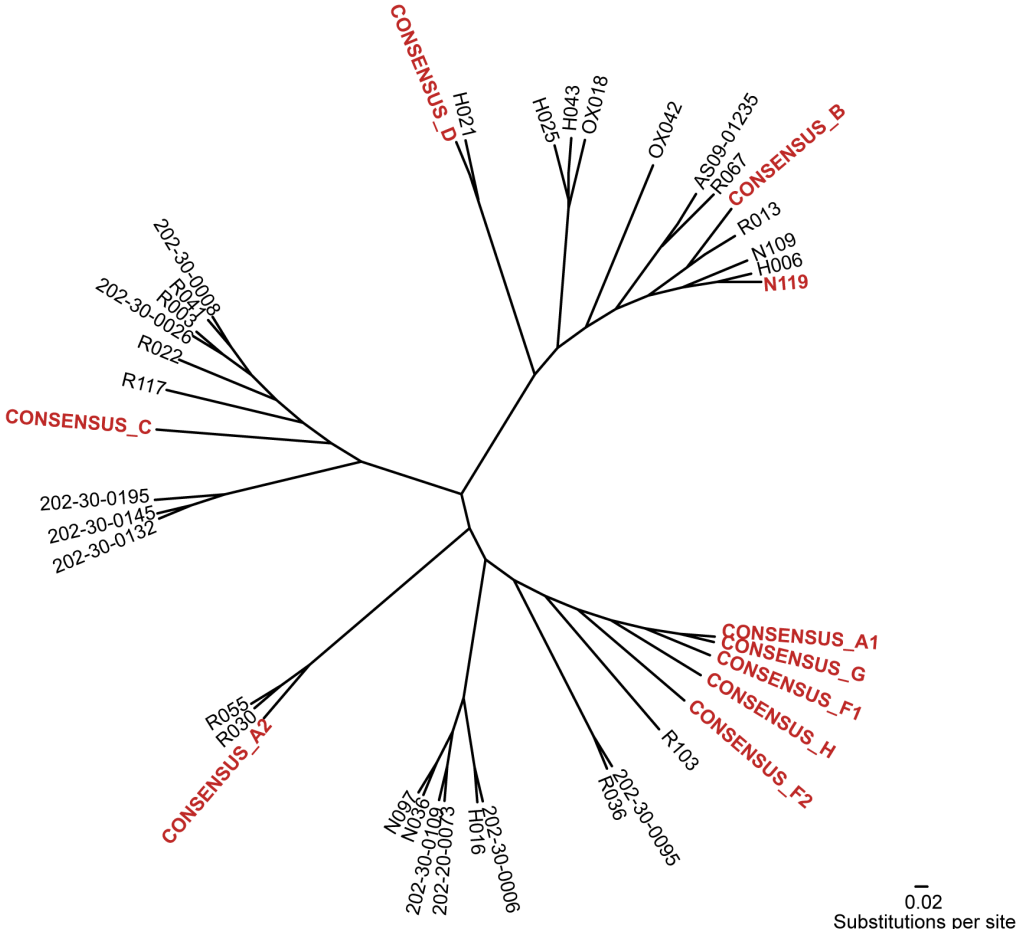


Figure 3.3. Maximum-likelihood phylogenetic tree of Env sequences in HLA-B*14 subjects.

To investigate the role HLA-B*14:02-restricted CD8+ T-cell responses might play in immune control of HIV, we first screened PBMC in this individual for HIV-specific IFN-γ ELISPOT responses using overlapping peptides spanning the entire HIV proteome (Kiepiela et al., 2004) together with previously defined HIV-specific epitopes (Llano et al., 2013). The HLA-B*14:02-restricted responses dominated overall, the highest magnitude responses being to the HLA-B*14:02-restricted Env-EL9 (^{584}ERYLKDQQL^{592}) (Johnson et al., 1992) and its corresponding overlapping peptide Env-366 (^{579}RVLAIERYLKDQQLLGIW^{596}) (**Figures 3.2B,C**). The next highest optimal peptide response was towards the HLA-B*14:02-Gag-DA9 epitope (^{298}DRFYKTLRA^{306}) (Harrer et al., 1996).

To test the hypothesis that suppression of HIV in this patient was mediated principally by HLA-B*14:02-restricted CD8+ T-cell activity, we next compared the antiviral potency of Env-EL9- and Gag-DA9-specific CD8+ T-cells. Bulk CD8+ T-cells were first expanded with the bi-specific CD3.4 antibody (Chen et al., 2009; Jones et al., 2003; Wong and Colvin, 1987), and then depleted of selected CD8+ T-cell specificities using cytotoxic saporin-conjugated tetramers (see Chapter 6 for details) (**Figure 3.2D**). The ability of the bulk or depleted CTL to inhibit viral replication *in vitro* was then evaluated using T1 cells expressing HLA-B*14:02 as CD4+ T-cell targets and the B clade NL4-3 as the test strain of HIV (**Figures 3.2E,F**). Compared to undepleted CD8+ T-cells, the HIV-suppressive capacity of Env-EL9-depleted CD8+ T-cells was significantly reduced (median 0.001% versus 22% of remaining infected target cells, respectively (**Figure 3.2E**); and suppressive capacity was reduced by 27 fold, p=0.02; **Figure 3.2F**), whereas depletion of Gag-DA9-depleted cells made little impact. This result suggests that the presence of Env-EL9 specificity represents the majority of CD8+ T-cell-mediated control of viral suppression in subject N119, and that the Gag-DA9 specificity does not contribute significantly.

A potential caveat of this finding in this study subject is the unequal frequency of Env- and Gag-specific CD8+ T-cells, with Env-specific cells being nearly 20-fold more frequent than Gag-specific cells (**Figure 3.2D**). To address this we adopted two approaches. First, we repeated targeted depletion experiments using cells from another chronically B-clade infected HLA-B*14:02-positive controller (subject AS09-01235, VL=80 copies/ml, CD4=1,355 cells/mm^3), who had equal frequencies of Env-EL9- and Gag-DA9-specific CD8+ T-cells (**Figure 3.2G, left panels)**. As with N119, elimination of the Env-EL9 specificity resulted in preservation of 25% of infected target cells at the peak of viral replication compared to only 1% in bulk CD8+ T-cell coculture (**Figure 3.2H**), representing a 16-fold reduction of suppressive capacity of the Env-EL9-depleted CTL (p=0.03; **Figure 3.2I**). In contrast, Gag-DA9 depletion had only a minor effect, thus supporting the notion that Env-EL9-specific CTL mediate the major antiviral efficacy of the two HLA-B*14:02-restricted responses.

In the second approach we tested antiviral efficacy of Env-EL9- and Gag-DA9-specific CD8+ T-cells directly by generating epitope-specific CTL lines and clones. In the experiments using peptide-specific lines (**Figures 3.4A-C**), once again Env-EL9-specific CTL were significantly more potent at suppressing viral replication at the same effector to target ratio 1:100 (p=0.02; **Figures 3.4B,C**). Similarly, Env-EL9-specific CTL clones were more potent inhibitors of viral replication than were Gag-DA9 clones. This was particularly evident at the lower effector to target ratios (1:1000) (**Figures 3.4D-F**). Taken together, these experiments suggest that Env-EL9-specific CD8+ T-cells are more efficacious at suppressing HIV replication than Gag-DA9-specific cells.

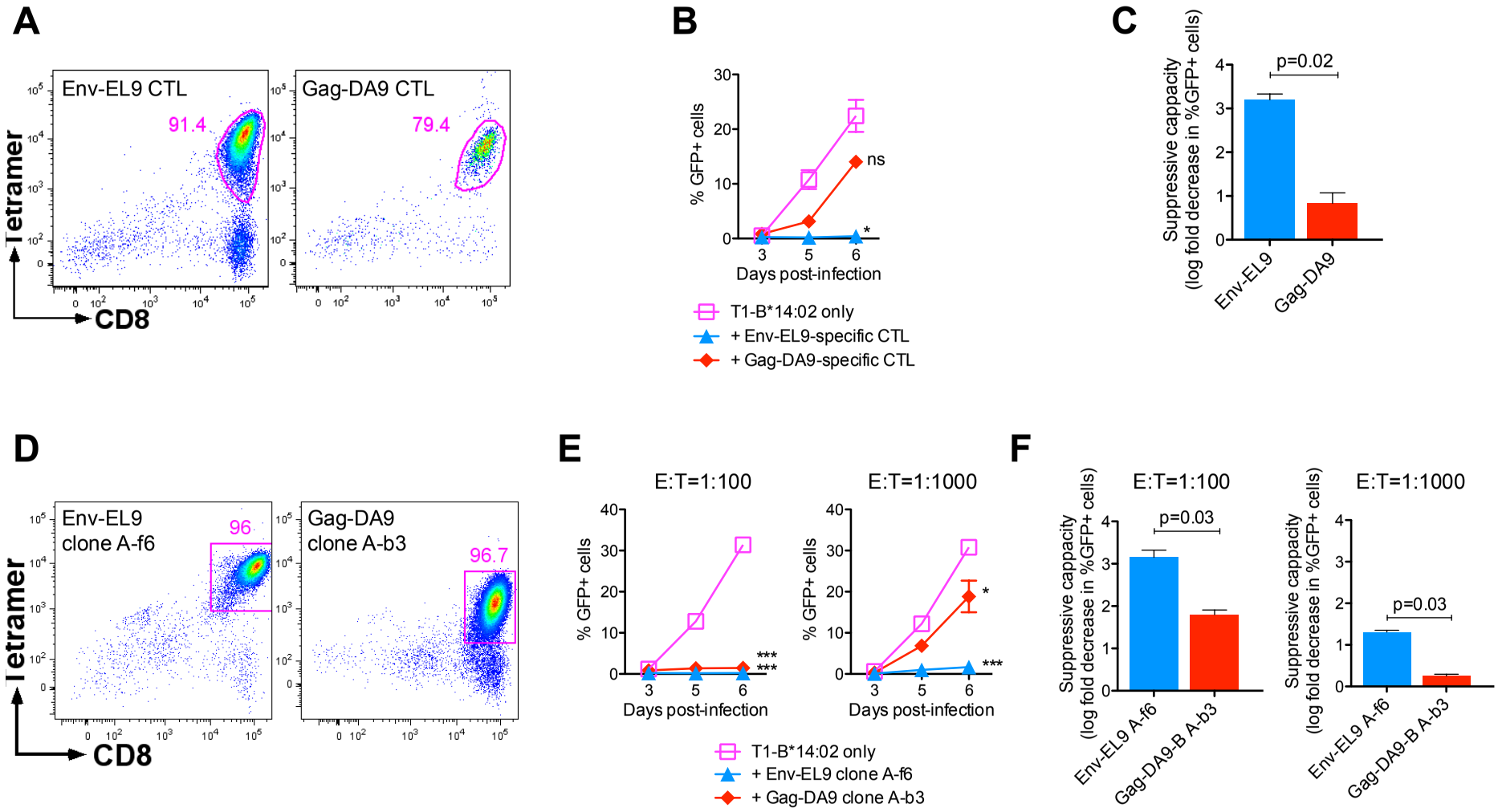

A
Env-EL9 CTL
91.4
Gag-DA9 CTL
79.4
Tetramer
CD8
B
% GFP+ cells
Days post-infection
ns
*
T1-B*14:02 only
+ Env-EL9-specific CTL
+ Gag-DA9-specific CTL
C
Suppressive cappacity
(log fold decrease in %GFP+ cells)
p=0.02
Env-EL9
Gag-DA9
D
Env-EL9
clone A-f6
96
Gag-DA9
clone A-b3
96.7
Tetramer
CD8
E
E:T=1:100
E:T=1:1000
% GFP+ cells
Days post-infection
***
***
*
***
T1-B*14:02 only
+ Env-EL9 clone A-f6
+ Gag-DA9 clone A-b3
F
E:T=1:100
E:T=1:1000
Suppressive cappacity
(log fold decrease in %GFP+ cells)
p=0.03
p=0.03
Env-EL9 A-f6
Gag-DA9-B A-b3

Figure 3.4. Suppressive capacity of epitope-specific Env and Gag CTL lines and clones. Panels **A-C** show results for CTL lines, generated by peptide-stimulation of epitope-specific cells from PBMC, sorting them and further expanding before testing in inhibition assays; panels **D-F** show examples of clones, generated by single-cell sorting of epitope-specific cells and growing them out in culture before testing their antiviral capacity. **A,D.** Confirmatory tetramer stainings of epitope-specific CTL lines (A) and clones (D). Gated on live CD3+CD4- cells around CD8+tetramer+ cells; numbers indicate % tetramer+ cells (of CD3+CD4-). **B,E.** Viral replication in infected T1-HLA-B*14:02-positive target cells with or without effector cells. Results were compared to T1-HLA-B*14:02 target cells only at the peak of viral replication using paired t-tests. *p<0.05, **p<0.01, ***p<0.001, ns, not significant (p>0.05). **C,F.** Suppressive capacity of effector cells. Mann-Whitney U test. B,C,E,F, error bars represent s.e.m.

3.3.3.2 Higher functional avidity, antigen recognition and magnitude of EL9 versus DA9

In order to further investigate this observed antiviral superiority of Env-EL9-specific cells over Gag-DA9-specific cells, we next examined differences between the two specificities in functional avidity, response magnitude and antigen recognition in a larger number of HLA-B*14-positive subjects (n=30). Among all HLA-B*14-positive subjects, functional avidity, or antigen sensitivity (EC50; see Chapter 2, section 2.4.3), of the Env-EL9 response was >24-fold higher than that of the Gag-DA9 response (median 0.84 versus 20.6 μM, p<0.0001; **Figure 3.5A, left panel**). This difference was significant among both HLA-B*14:01-positive (median 3.7 versus 22.3 μM, p=0.002) and HLA-B*14:02-positive subjects (median 0.3 versus 19.8 μM, p<0.0001; **Figure 3.5A, right panel**). However, Env-EL9 functional avidity was 12-fold higher in HLA-B*14:02-positive subjects than in HLA-B*14:01-positive subjects (p=0.005; **Figure 3.5A, right panel**).

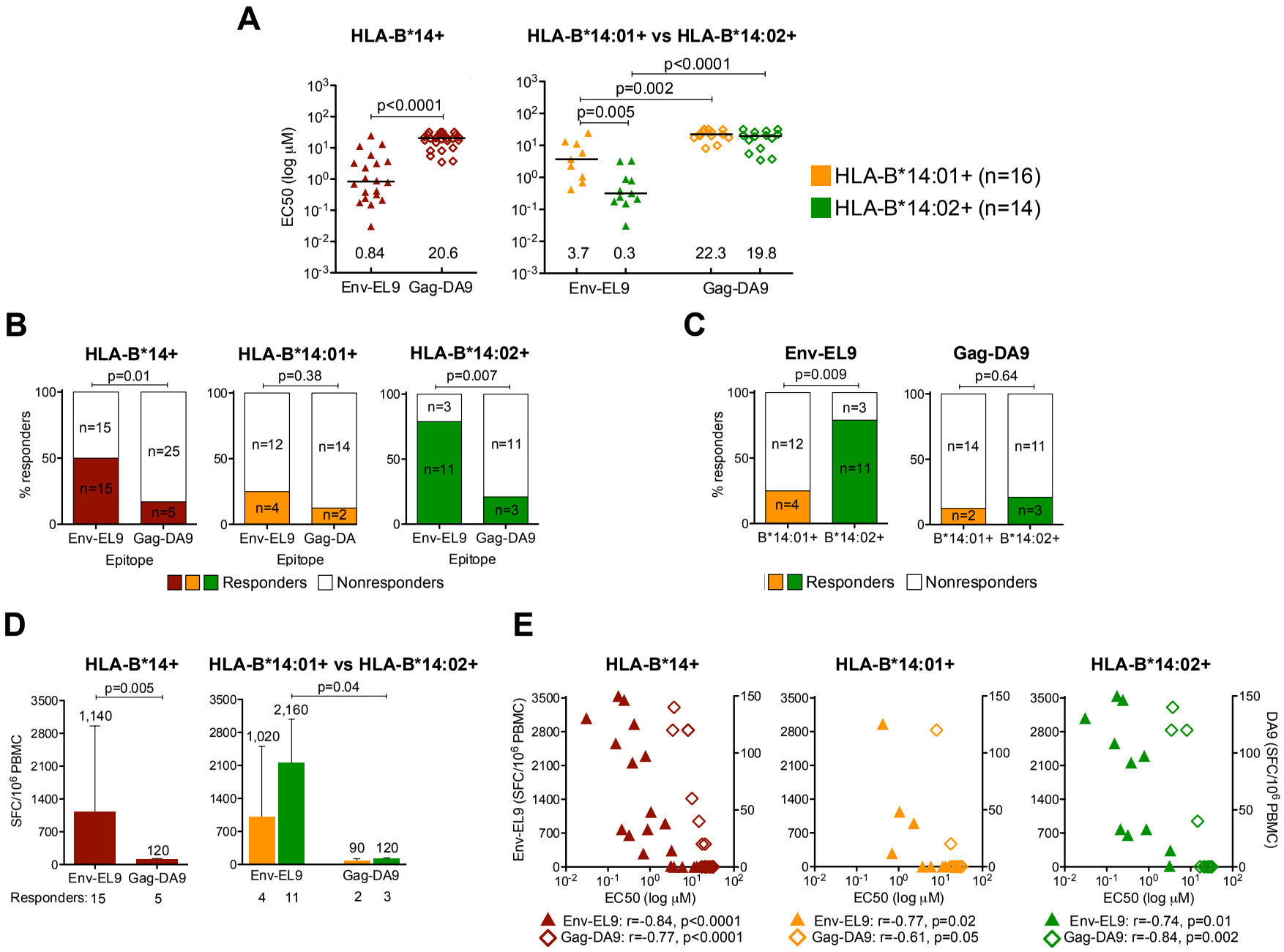

A
HLA-B*14+
HLA-B*14:01+ vs HLA-B*14:02+
EC50 (log μM)
p<0.0001
p=0.002
p=0.005
0.84
20.6
3.7
0.3
22.3
19.8
Env-EL9
Gag-DA9
HLA-B*14:01+ (n=16)
HLA-B*14:02+ (n=14)
B
HLA-B*14+
HLA-B*14:01+
HLA-B*14:02+
p=0.01
p=0.38
p=0.007
% responders
n=15
n=25
n=5
n=12
n=14
n=4
n=2
n=3
n=11
n=3
Epitope
Responders
Nonresponders
C
Env-EL9
Gag-DA9
p=0.009
p=0.64
B*14:01+
B*14:02+
D
HLA-B*14+
HLA-B*14:01+ vs HLA-B*14:02+
p=0.005
p=0.04
SFC/10^6 PBMC
1,140
120
1,020
2,160
90
120
Responders: 15
5
4
11
2
3
E
HLA-B*14+
HLA-B*14:01+
HLA-B*14:02+
Env-EL9 (SFC/10^6 PBMC)
DA9 (SFC/10^6 PBMC)
EC50 (log μM)
Env-EL9: r=-0.84, p<0.0001
Gag-DA9: r=-0.77, p<0.0001
Env-EL9: r=-0.77, p=0.02
Gag-DA9: r=-0.61, p=0.05
Env-EL9: r=-0.74, p=0.01
Gag-DA9: r=-0.84, p=0.002

Figure 3.5. Higher functional avidity, antigen recognition, and magnitude of EL9 versus DA9. **A.** Functional avidity (EC50) of Env-EL9 versus Gag-DA9 CD8+ T-cell responses in all HLA-B*14-positive subjects (n=30, left panel) or separately in HLA-B*14:01-expressing (n=16) or HLA-B*14:02-expressing (n=14) subjects (right panel). Lines and numbers indicate median values. Mann-Whitney U tests. **B.** Frequency of recognition of Env-EL9 versus Gag-DA9 epitopes in all HLA-B*14-positive chronically infected subjects (n=30, left panel) or separately in HLA-B*14:01-positive subjects (n=16, middle panel) and HLA-B*14:02-positive subjects (n=14, right panel). Fisher's Exact Tests. **C.** Frequency of recognition of Env-EL9 or Gag-DA9 epitopes in HLA-B*14:01-positive versus HLA-B*14:02-positive subjects. Fisher's Exact Tests. **D.** Magnitude of Env-EL9 or Gag-DA9 responses determined by IFN-γ ELISPOT assay in all HLA-B*14-positive subjects (n=30; left panel) or in HLA-B*14:01-expressing (n=16) and HLA-B*14:02-expressing (n=14) subjects (right panel). Numbers above the bar graphs indicate median values; error bars show interquartile ranges; Mann-Whitney U tests. **E.** Correlation between response magnitude and functional avidity in HLA-B*14-positive (left), HLA-B*14:01-positive (middle) and HLA-B*14:02-positive subjects. R and p values were obtained by Spearman correlation.

The frequency of epitope recognition was also higher of Env-EL9 than Gag-DA9 (p=0.01; **Figure 3.5B, left panel**). Again, this difference was only significant among HLA-B*14:02-positive subjects (p=0.007). Additionally, HLA-B*14:02-positive subjects recognised Env-EL9 epitope significantly more than HLA-B*14:01-positive subjects (p=0.009), whereas no significant difference in recognition of the Gag-DA9 epitope was observed (**Figure 3.5C**).

Finally, the magnitude of the Env-EL9 response was >9-fold higher than that of the Gag-DA9 response among all HLA-B*14-expressing subjects (p=0.005; **Figure 3.5D, left panel**). Once again this difference was only significant among HLA-B*14:02-positive subjects (**Figure 3.5D, right panel**). Interestingly, the magnitude of both Env-EL9 and Gag-DA9 responses was negatively correlated with EC50 (i.e. positively with functional avidity) (Env-EL9: r=-0.84, p=<0.0001; Gag-DA9: r=-0.77, p<0.0001; **Figure 3.5E**),

indicating that cells with higher functional avidity mounted a response of greater magnitude.

Together, these data demonstrate that the greater antiviral potency of the HLA-B*14-Env-EL9-specific response observed above is associated also with higher functional avidity, recognition frequency and response magnitude compared with Gag-DA9.

*3.3.3.3 Differential Env-EL9 and Gag-DA9 selection pressure in HLA-B*14:01 versus HLA-B*14:02*

To further understand the differences between Env-EL9- and Gag-DA9-specific CD8+ T-cell function, we next investigated what selection pressure is imposed on the virus by these two responses (**Figure 3.6**). Consistent with previously published data describing HLA-associated polymorphisms from analysis of 3,754 HLA-typed treatment-naïve persons (Carlson et al., 2012; Carlson et al., 2014) within the Env-EL9 epitope (**Figure 3.6A**), K588Q is strongly selected among both HLA-B*14:01- and HLA-B*14:02-positive persons, and variants at Env-588 and at other residues within Env-EL9 are observed more commonly in HLA-B*14:02-positive subjects (although here these differences between HLA-B*14:01- and HLA-B*14:02 did not reach statistical significance; **Figure 3.6B**). For the Gag-DA9 epitope, consistent with previous large cohorts studies (Carlson et al., 2012; Carlson et al., 2014; Matthews et al., 2008) showing that the commonest K302R variant is only selected in HLA-B*14:01-positive subjects, we also observed that K302R was the commonest variant and was only selected in HLA-B*14:01-positive subjects ($p=0.005$). Thus there was significantly more variation in HLA-B*14:02-positive subjects in the Env-EL9 epitope than in Gag-DA9 ($p=9.8x10^{-7}$; **Figure 3.6B**), consistent with this being the dominant response among HLA-B*14:02-positive subjects. Among B*14:01-positive subjects the Env-EL9 epitope was not targeted significantly more than the Gag-DA9, and

A

	Consensus B clade	302 303 D R F Y K T L R A	585 588 592 E R Y L K D Q Q L
HLA-associated polymorphisms within DA9 or EL9	B*14:01	– – – – R – – – – – – – – – V – – –	– – – – Q – – – – – – – – – – – – –
	B*14:02	– – – – – V – – –	– – – – Q – – – – – K – – – – – – – – S – – – – – – F
	C*03:04 C*03:02/03/04	– – – – – C – – – – – – – – I – – –	

B

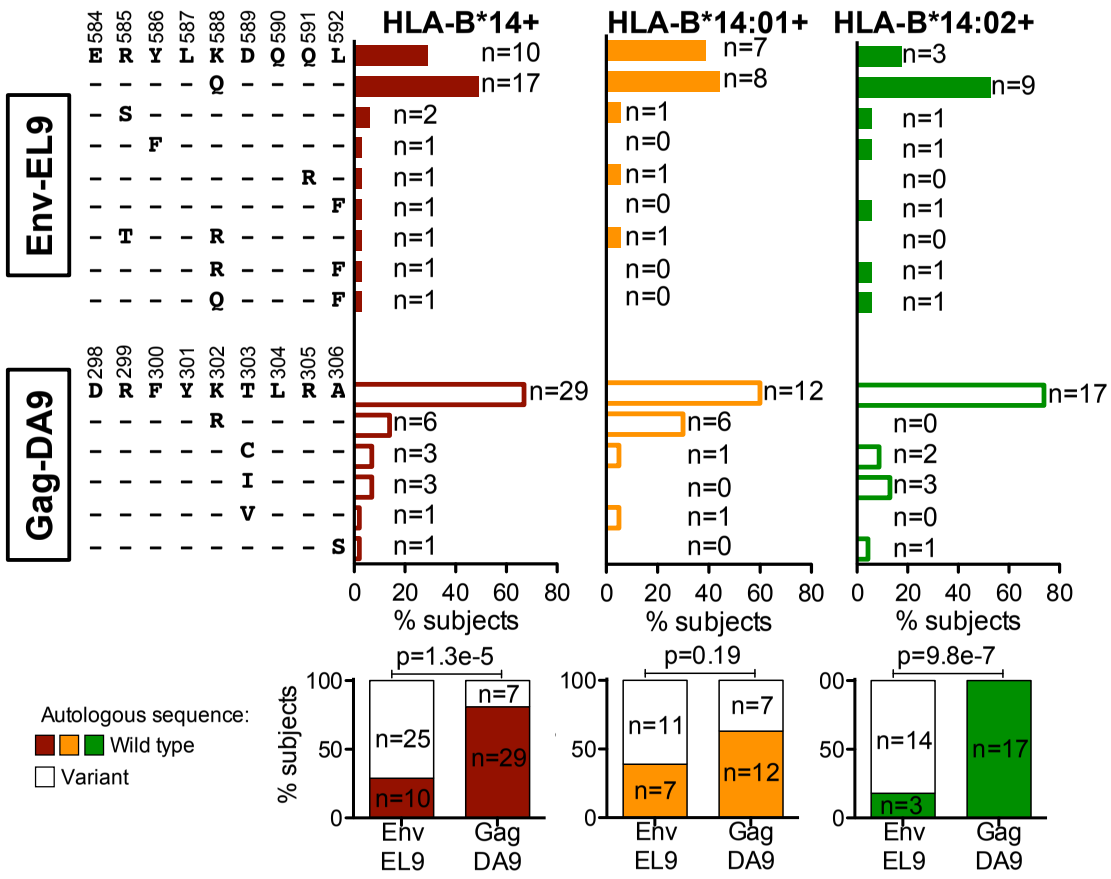


Figure 3.6. Differential Env-EL9 and Gag-DA9 selection pressure in HLA-B*14:01 versus HLA-B*14:02. A. Consensus sequences of Env-EL9 and Gag-DA9 epitopes and polymorphisms associated with HLA-B*14 subtypes; overlapping polymorphisms associated with non-HLA-B*14 alleles are also shown. Data compiled from previously published large cohort studies (Carlson et al., 2012; Carlson et al., 2014; Matthews et al., 2008). **B.** Frequency of Env-EL9 and Gag-DA9 wild type and variant sequences in the studied HLA-B*14-positive subjects. Graphs at the bottom compare frequency of subjects with autologous wild type (filled bars) or mutated (empty bars) sequence of Env-EL9 versus Gag-DA9 epitopes. Fisher's Exact Tests. A,B, residues identical to the wild type are presented as '-', non-identical residues are specified.

correspondingly there was no significant difference in the selection of variants within Env-EL9 and Gag-DA9 in these subjects.

3.3.3.4 Impact of Gag-DA9 and Env-EL9 escape mutants on viral fitness and HIV outcome

Previous studies have indicated that the most effective CTL responses are those capable of driving the selection of escape mutants that significantly reduce viral replicative capacity (Crawford et al., 2009; Martinez-Picado et al., 2006; Miura et al., 2009; Schneidewind et al., 2007). These are more likely in p24 Gag, which is highly conserved as opposed to Env, which is highly variable. We next therefore investigated the impact on viral replicative capacity of the most common escape mutants in p24 Gag-DA9 and Env-EL9 (**Figures 3.7A,B**). In contrast to the general observation of the high cost of p24 Gag mutants, the K302R mutant had little impact on VRC, consistent with previous studies of this variant (Boutwell et al 2013). The Env EL9 mutant if anything marginally decreased VRC. Thus, in this case, the fitness cost resulting from the selection of escape mutants within the capsid protein appears to have little impact on viral replicative capacity.

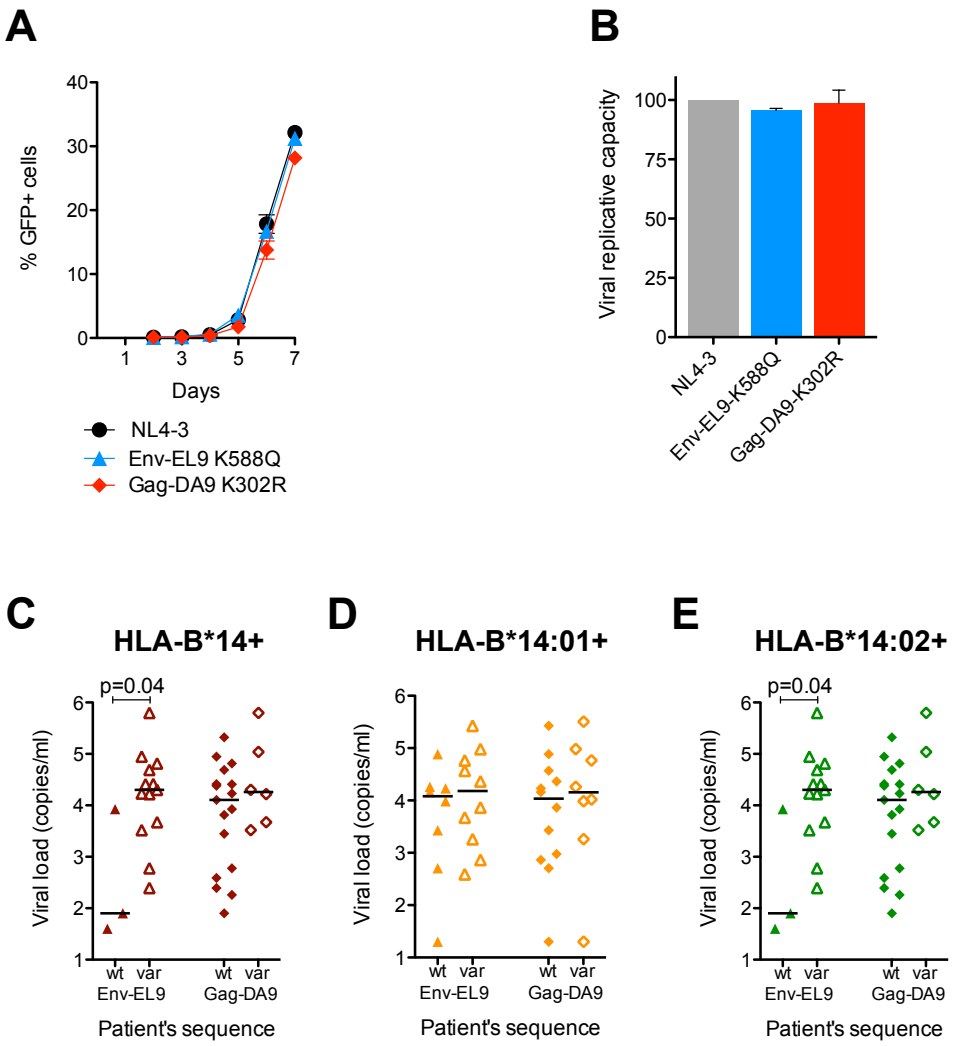


Figure 3.7. Impact of Gag-DA9 and Env-EL9 escape mutants on viral fitness and HIV outcome. **A.** Replication kinetics of NL4-3 containing wild type p24 and Env compared to HLA-B*14-associated Gag and Env mutants. Infectivity is expressed as %GFP-positive GXR reporter cells over 7 days after infection. Error bars represent s.e.m. **B.** Viral replication capacity of the viruses in A. ANOVA with Dunnett's Multiple Comparison Test comparing NL4-3 versus the other viruses. Error bars represent s.e.m. *p<0.05, **p<0.01, ***p<0.001, ns, not significant (p≥0.05). **C,D.** Viral loads in HLA-B*14-positive (C), HLA-B*14:01-positive (D) and HLA-B*14:02-positive (E) subjects with either wild type or mutated autologous sequences in Env-EL9 and Gag-DA9 epitopes. X-axes indicate patients' autologous epitope sequences. Only significant p values (p<0.05), obtained by Mann-Whitney U test, are shown. Horizontal bars indicate medians. Wt, wild type; var, variant sequence.

Furthermore, HLA-B*14-positive subjects who had wild type Env-EL9 had significantly lower viral loads (median 8,435 versus 21,546 copies/ml, p=0.04; **Figure 3.7C**) and higher CD4+ T-cell counts (median 610 versus 455 cells/mm^3, p=0.01; **Figure 3.8A**). Again, this difference was exclusive to HLA-B*14:02-positive subjects among whom individuals with wild type Env-EL9 had lower VL versus those with a variant (median 80 versus 20,003 copies/ml, p=0.04; **Figures 3.7D,E**), and a trend towards higher CD4+ T-cell counts (median 1,340 versus 410 cells/mm^3, p=0.2; **Figures 3.8B,C**), although there were only three subjects with wild type sequence.

Taken together these results suggest that the Env-EL9 response is highly effective and contributes to successful immune control of HIV, whereas Gag-DA9 is not.

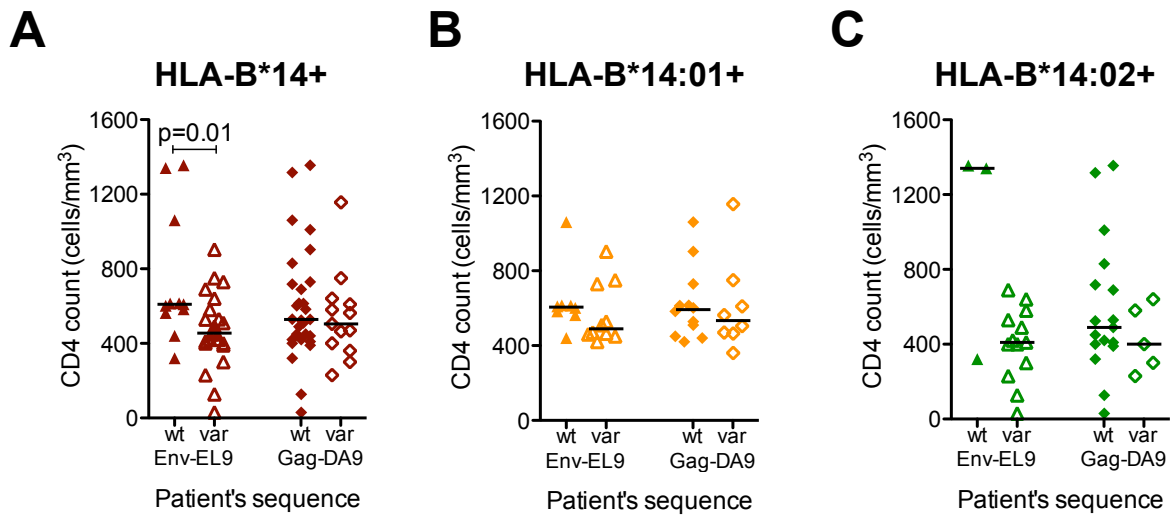


Figure 3.8. CD4+ T-cell counts in HLA-B*14-positive subjects with either wild type or mutated autologous sequences in Env-EL9 and Gag-DA9 epitopes. A. HLA-B*14-positive subjects; **B.** HLA-B*14:01-positive subjects; **C.** HLA-B*14:02-positive subjects. X-axes indicate patients' autologous epitope sequences. Only significant p values (p<0.05), obtained by Mann-Whitney U test, are shown. Horizontal bars indicate medians. Wt, wild type; var, variant sequence.

*3.3.3.5 Stronger association of HLA-B*14:02 than HLA-B*14:01 with HIV immune control*

On this basis of the findings above, one would predict improved immune control of HIV in association with HLA-B*14:02 compared with HLA-B*14:01. In order to test this hypothesis, we first compared, in large, previously well-described cohorts (see section 3.3.2 for details), the frequency of HLA-B*14:01 with that of HLA-B*14:02 in cohorts of viraemic controllers (viral load <2,000 copies/ml) and non-controllers (viral load>10,000 copies/ml). Among HLA-B*14-positive Caucasians ('whites'; n=285) and HLA-B*14-positive African Americans ('blacks'; n=104), the difference between HLA-B*14:01 and HLA-B*14:02 was not significant even after adjusting for the co-expression of HLA-B*57 or HLA-B*27 (**Table 3.1**). We then extended the analysis to the entire cohorts of controllers and non-controllers (whites, n=3,259; blacks, n=1,745) also taking into account the greater frequency of HLA-B*14:02 compared to HLA-B*14:01, by performing stepwise selection on HLA-B alleles having a frequency equal to or greater than HLA-B*14:01. First in the Caucasian cohorts, following this analysis, HLA-B*14:02 was in a group of 6 HLA-B alleles with odds ratios significantly below 1 (i.e. that were significantly enriched amongst non-progressors compared to progressors) (**Table 3.2**). These comprised HLA-B*57:01 (OR 0.25), HLA-B*27:05 (OR 0.34), HLA-B*52:01 (OR 0.40), HLA-B*14:02 (OR 0.44), HLA-B*13:02 (OR 0.47) and HLA-B*40:02 (OR 0.48). Following stepwise selection on HLA-B alleles having a frequency equal to or greater than HLA-B*14:01 among the African American cohort, HLA-B*14:02 was again selected as one of 6 HLA-B alleles significantly enriched in the non-progressor group: HLA-B*57:03 (OR 0.15), HLA-B*81:01 (OR 0.20), HLA-B*39:01 (OR 0.22), HLA-B*57:01 (OR 0.41), HLA-B*27:05 (OR 0.44) and HLA-B*14:02 (OR 0.54). In neither cohort was HLA-B*14:01 among alleles enriched in the controller group. To further validate this result and take into account for lower frequency of HLA-B*14:01 compared to HLA-B*14:02, we repeated this analysis 100 times by randomly

Table 3.1. Frequency of HLA-B*14:01 versus HLA-B*14:02 among viraemic controllers and non-controllers. ART-naïve chronically HIV-infected subjects were categorised as viraemic controllers (viral loads <2,000 copies/ml plasma) or non-controllers (viral loads >10,000 copies/ml plasma). Logistic regression was used to compute significance (p values), OR and 95%CI for the differences in frequency of HLA-B*14 subtypes in controllers versus non-controllers, with adjusting by HLA-B*57/27 expression. OR, odds ratio; CI, confidence interval.

HLA-B*14+ (n=285) from 3,259 whites						HLA-B*14+ (n=104) from 1,745 blacks					
	Controllers, n (%)	Non-controllers, n (%)		OR (95% CI)	P value		Controllers, n (%)	Non-controllers, n (%)		OR (95% CI)	P value
				Not adjusted						Not adjusted	
B*14:01	23 (23%)	54 (29%	B*14:01 vs B*14:02	1.41 (0.80-2.47)	0.23	**B*14:01**	7 (19%)	21 (31%)	B*14:01 vs B*14:02	1.96 (0.74-5.17)	0.18
B*14:02	78 (77%)	130 (71%)				**B*14:02**	30 (81%)	46 (69%)			
				Adjusted for B*27, B*57						Adjusted for B*57, B*81	
B*14:01	23 (23%)	54 (29%)	B*14:01 vs B*14:02	1.54 (0.86-2.77)	0.15	**B*14:01**	7 (19%)	21 (31%)	B*14:01 vs B*14:02	1.52 (0.56-4.13)	0.41
B*14:02	78 (77%)	130 (71%)				**B*14:02**	30 (81%)	46 (69%)			
B*27	7 (7%)	8 (4%)	B*27 vs others	0.49 (0.17-1.42)	0.19	**B*57**	6 (16%)	3 (4%)	B*57 vs others	0.23 (0.05-0.98)	0.05
Others	94 (93%)	176 (96%)				**Others**	31 (84%)	64 (96%)			
B*57	16 (16%)	6 (3%)	B*57 vs others	0.17 (0.06-0.44)	0.0003	**B*81**	4 (11%)	0 (0%)	n/a		
Others	85 *84%)	178 (97%)				**Others**	33 (89%)	67 (100%)			

Table 3.2. HLA-B*14:02 is significantly enriched among viraemic controllers. Presence or absence of individual HLA-B alleles that have a frequency equal to or greater than that of HLA-B*14:01 were tested by logistic regression with stepwise selection. OR, odds ratio; CI, confidence interval.

Whites (n=3,259)				Blacks (n=1,745)			
	Stepwise selection on HLA-B alleles that are of equal or greater frequency as B*14:01				Stepwise selection on HLA-B alleles that are of equal or greater frequency as B*14:01		
	OR	**95%CI**	**P value**		**OR**	**95%CI**	**P value**
B*57:01 vs others	0.25	0.20-0.32	2e-31	**B*57:03 vs others**	0.15	0.11-0.21	2e-29
B*27:05 vs others	0.34	0.26-0.45	2e-15	**B*81:01 vs others**	0.20	0.12-0.33	1e-10
B*52:01 vs others	0.40	0.25-0.63	7e-5	**B*39:10 vs others**	0.22	0.11-0.45	2e-5
B*14:02 vs others	0.44	0.32-0.60	2e-7	**B*57:01 vs others**	0.41	0.19-0.91	3e-2
B*13:02 vs others	0.47	0.33-0.67	3e-5	**B*27:05 vs others**	0.44	0.21-0.91	3e-2
B*40:02 vs others	0.48	0.31-0.75	1e-3	**B*14:02 vs others**	0.54	0.32-0.90	2e-2
B*08:01 vs others	1.66	1.28-2.13	1e-4	**B*07:02 vs others**	1.45	1.01-2.09	4e-2
B*38:01 vs others	1.66	1.04-2.66	3e-2	**B*53:01 vs others**	1.51	1.12-2.03	7e-3
B*40:01 vs others	1.76	1.24-2.50	2e-3	**B*35:01 vs others**	1.92	1.29-2.86	1e-3
B*07:02 vs others	2.04	1.60-2.60	8e-9	**B*15:10 vs others**	2.27	1.33-3.89	3e-3
				B*58:02 vs others	2.63	1.51-4.59	6e-4
				B*45:01 vs others	4.10	2.36-7.13	6e=7

selecting HLA-B*14:02-positive subjects matching the numbers of HLA-B*14:01-positive subjects within the Caucasian and African American cohorts and running the stepwise selection on HLA-B alleles having a frequency equal to or greater than HLA-B*14:01. Again, HLA-B*14:02 was among HLA-B alleles significantly enriched among non-progressors – 100 out of 100 times in the Caucasian cohort, and 31 out of 100 times in the African-American cohort. These analyses of the large cohorts confirm the improved control of HIV in association with HLA-B*14:02 expression and are consistent with our immunological findings.

3.3.4 Discussion

This study investigated HIV control mediated by HLA-B*14. We showed that the HLA-B*14-restricted Env-EL9-specific CD8+ T-cell response was more efficacious against HIV than Gag-DA9-specific response. In association with this, Env-specific response had significantly greater function avidity, was more frequently targeted and was of higher magnitude than the Gag-specific response.

Higher anti-HIV efficacy of Env- compared to Gag-specific CD8+ T-cells responses is unusual; and in fact unreported until the current study. Numerous studies have suggested that Gag-specific CD8+ T-cell responses are associated with better disease outcome in HIV infection, are more efficacious at antiviral activity than other specificities and are often dominant responses in elite controllers (Barouch et al., 2003; Barouch et al., 2002; Edwards et al., 2002; Geldmacher et al., 2007; Janes et al., 2013; Kiepiela et al., 2007; Klein et al., 1995; Masemola et al., 2004; Novitsky et al., 2003; Ogg et al., 1998; Payne et al., 2010; Riviere et al., 1995; Saez-Cirion et al., 2009; Streeck et al., 2007; Zuniga et al., 2006). However, our result is consistent with studies showing that non-Gag responses can

also mediate viral control. In the macaque model of elite control, Env-, Nef- and Vif-specific CD8+ T responses have been shown to be dominant and efficacious in viral clearance (Maness et al., 2008; Mudd et al., 2012; Valentine et al., 2009). In HIV infection, a dominant HLA-B*57-restricted Nef response was present in an elite controller, although antiviral efficacy of that response has not been evaluated (Jessen et al., 2014). Similarly, HLA-B*27:02, allele associated with better protection than HLA-B*27:05 (P. Goulder, unpublished data), restricts dominant CD8+ T-cell response in Nef, although as above its efficacy remains to be determined. Furthermore, effective elimination of infected cells by Env-specific CD8+ T-cells, including HLA-B*14-Env-EL9-restricted cells, has been reported in HIV infection (Chen et al., 2011; Yang et al., 1997). Our finding of the superior Env-specific antiviral efficacy is also in line with one of the most recent reports about HLA-B*57/27-negative HIV elite controllers suggesting that potent cytotoxic capacity (measured by granzyme B expression and infected cell elimination) of HIV-specific CD8+ T-cells rather than epitope-specific targeting is the determining factor in mediating successful control of infection (Migueles et al., 2015).

Our results suggest that an important reason for the superior antiviral efficacy of Env-specific CD8+ T-cell response is its better functional avidity among HLA-B*14-positive subjects in our study. Indeed, this feature has been proposed to be the key CD8+ T-cell characteristic that gives rise to all other CD8+ T-cell functions (Almeida et al., 2009; Lecuroux et al., 2014; Mothe et al., 2012). Functional avidity of the Env-EL9 response was >24-fold better than that of the Gag-DA9-specific response and correlated with response magnitude; Env-specific response was also significantly greater in magnitude and more frequently targeted than Gag-specific response (**Figure 3.5**). Therefore, CD8+ T-cells with higher antigen sensitivity were able to elicit a greater and more rapid and effective antiviral response even at lower antigen concentrations.

Furthermore, these qualitative differences between Env- and Gag-specific CD8+ T-cells were only significant among HLA-B*14:02-positive individuals (**Figure 3.5**). In case of functional avidity, the difference between the Env- and Gag-specific responses was significant even among HLA-B*14:01-positive individuals, although less markedly so and the avidity of the Env-EL9 response was still 12-fold higher in the HLA-B*14:02-positive subjects. These observations suggest that despite restriction of the same epitopes by these two HLA molecules, CD8+ T-cells that recognise HLA-B*14:01 versus HLA-B*14:02 are qualitatively different and the difference is primarily determined by the superior function of HLA-B*14:02-restricted Env-EL9-specific CD8+ T-cells. Interestingly, HLA-B*14 allele has been shown to be associated with modest protection in HIV infection (Hendel et al., 1999; Kiepiela et al., 2004; Pereyra et al., 2010) and Pereyra *et al.* showed that HLA-B*14:02 was marginally more protective than HLA-B*14:01 (Pereyra et al., 2010).

Structurally, HLA-B*14:01 and HLA-B*14:02 differ only at the position 11, where HLA-B*14:01 has a serine and HLA-B*14:02 has an alanine (Domena et al., 1993). Residue 11 is located in the α1 domain of HLA at the C-terminus of the first strand of β-pleated sheet near the C pocket (Bjorkman et al., 1987; Garrett et al., 1989). It does not contribute to any interactions between the HLA domains, is not solvent-accessible (Saper, Bjorkman, and Wiley, 1991), is of low variability and does not form a peptide-binding site or a TCR-binding site (Parham et al., 1988). Peptide-binding motif for HLA-B*14:02 consists of a combination of any 3 preferred anchors: arginine at P2, tyrosine at P3, arginine at P5 and leucine at the carboxy-terminus (DiBrino et al., 1994). Explicitly HLA-B*14:01 motif has not been shown and studies identifying optimal HLA-B*14-restricted epitopes report only 2-digit HLA (Harrer et al., 1996; Johnson et al., 1992). Given the limited contribution of the only distinguishing residue 11, the peptide-binding motif is likely to be the same for both

molecules but this 'buried' position may alter the confirmation of the nearby α1 residues or affect upstream peptide processing (Domena et al., 1993). Of note, HLA-B*14:02 and HLA-B*14:03 share only ~30% of their peptides due to a single amino acid change in the HLA sequence, leucine at the position 156 in HLA-B*14:02 versus arginine in HLA-B*14:03 (Merino et al., 2005). Although unknown in the context of HIV, the difference at the position156, which is essential in D and E peptide-binding pockets (Saper et al., 1991), may play a role in the differential association of HLA-B*14:02 and HLA-B*14:03 with ankylosing spondylitis (Lopez-Larrea et al., 2002; Merino et al., 2005). Previous studies have also shown that one amino acid difference between closely-related HLA subtypes is sufficient to have a significant impact on HIV disease outcome. Examples are HLA-B*35:01 and HLA-B*35:03 (difference at residue 116) (Gao et al., 2001), HLA-B*35:01 and HLA-B*35:08 (difference at residue 156) (Juarez-Molina et al., 2014), HLA-B*42:01 and HLA-B*42:02 (difference at residue 9) (Kloverpris et al., 2012a), HLA-B*57:02 and HLA-B*57:03 (at residue 156) (Kloverpris et al., 2012b).

Another distinguishing feature between HLA-B*14:01 and HLA-B*14:02 alleles appears to be in the selection pressure that they exert on the virus. First, the Gag-DA9 K302R mutation was found exclusively in HLA-B*14:01-positive subjects, consistent with previous large cohort studies involving >3500 study subjects (Carlson et al., 2012; Carlson et al., 2014). This again would point to the lack of antiviral efficacy of HLA-B*14:02-Gag-specific CD8+ T-cells. At the same time, HLA-B*14:02 appeared to have selected Env-EL9 K588Q mutation and there is a hint that this selection is associated with higher viraemia and lower CD4+ T-cell counts (**Figures 3.7C-E, 3.8**). Curiously, however, neither of these mutations had a significant impact on viral replication, although Env-EL9-K588Q tended to have a slightly lower replicative capacity than the wild type, while the opposite was true for Gag-DA9-K302R (**Figures 3.7A,B**). This is particularly interesting in the case of the Gag

epitope. This epitope (Gag 298-306) overlaps with the highly conserved major homology region (Gag 285-304) in the C-terminus of HIV p24 capsid, which is essential for virion assembly and stability (Wagner et al., 1999; Zhao et al., 2013) and previous reports showed rapid reversion of K302R in the absence of HLA-B*14:01 (Koibuchi et al., 2005; Matthews et al., 2008), implying K302R inflicts a significant cost to viral replicative capacity. However, apparent lack of impact of this mutation on viral replication was also recently reported by another group (Boutwell et al., 2013).

In conclusion, these studies indicate that, although Gag-specific CD8+ T-cell responses may usually have greater antiviral efficacy against HIV for the several reasons described above, influences such as functional avidity of individual responses are also critically important factors in contributing to immune control of HIV infection that are independent of protein specificity. This finding is relevant to the development of vaccines designed to generate effective antiviral CD8+ T-cell responses.

CHAPTER 4. CONTRASTING CTL IMPACT IN DISTINCT PHENOTYPES OF NON-PROGRESSING PAEDIATRIC HIV

4.1 Introduction

Patterns of natural progression of HIV infection are strikingly different in adults and children. In adults, in the absence of therapy, AIDS onset typically occurs after 10 years of infection and death after 11 (Babiker et al., 2000). In contrast, without antiretroviral treatment >70% HIV-infected children progress to AIDS within 6 months of age (Mphatswe et al., 2007) and >50% die by 2 years (Newell et al., 2004).

However, a rare minority of HIV-infected ART-naïve adults and children remain disease-free (preserve normal-for-age CD4 counts) for years. In adults, so-called 'elite controllers' (<0.3% of infected individuals) (Lambotte et al., 2005; Lefrere et al., 1999), non-progression is characterised by undetectable viraemia (typically <50 c/ml) and is strongly linked with expression of protective HLA class I alleles and potent HLA-restricted CD8+ T-cell responses (Goulder and Walker, 2012; Migueles et al., 2000; Pereyra et al., 2008). For example, protective HLA-B*57, expressed in 36-68% of elite controllers (Migueles and Connors, 2010), presents Gag-specific epitopes to CD8+ T-cells that in turn drive debilitating escape mutations, attenuating viral ability to replicate (Crawford et al., 2009; Martinez-Picado et al., 2006; Miura et al., 2009). Furthermore, CD8+ T-cells from elite controllers, unlike those in progressors and often irrespective of their HLA class I expression, possess distinctive characteristics, such as potent capacity to suppress viral replication and eliminate infected cells (Chen et al., 2012; Migueles et al., 2015; Migueles et al., 2008; Saez-Cirion et al., 2007), high functional avidity, proliferative capacity, polyfunctionality (Almeida et al., 2007; Migueles et al., 2002) and cross-recognition of

epitope variants (Chen et al., 2012; Ladell et al., 2013) – all of which allow for CD4+ T-cell preservation.

The adult non-progressing phenotype is diametrically opposed to the non-progressing phenotype in the natural hosts of SIV, such as sooty mangabeys. Non-progressing infection in these animals is characterised by preservation of normal peripheral CD4 counts in the face of persistently high viral loads (Rey-Cuille et al., 1998), but minimal role of CD8+ T-cells and MHC class I expression (Barry et al., 2007; Dunham et al., 2006). Major underlying mechanisms of the non-progression in this case have been attributed to low immune activation (Chakrabarti et al., 2000; Silvestri et al., 2005; Silvestri et al., 2003) and decreased CCR5 expression on CD4+ T-cells (Pandrea et al., 2007), particularly on long-lived central memory CD4 subsets (Paiardini et al., 2011). Interestingly, the non-progressing phenotype in a very rare group of HIV-infected adults, so-called 'viraemic non-progressors', resembles that of sooty mangabeys; these individuals also have persistently high viral replication, healthy CD4 counts, low immune activation and decreased infection of long-lived memory cells (Choudhary et al., 2007; Klatt et al., 2014; Rotger et al., 2011).

Non-progressing paediatric HIV infection is poorly characterised. Despite rapid progression in the majority of paediatric infections, a small subset of untreated perinatally infected children (5-7%) remain immunologically healthy and maintain normal-for-age CD4 counts (Blanche et al., 1997; Grubman et al., 1995; Paul et al., 2005). It is unknown whether paediatric non-progression follows the mechanisms implicated either in the adult elite control-type non-progression, sooty mangabey-type non-progression, a combination of the two or an entirely different pathway. The particular HLA class I molecules expressed in children were recently reported to have minimal impact on paediatric disease progression measured by viral load and CD4 counts; neither did it influence replicative

capacity of the transmitted virus in the child (Adland et al., 2015). These findings point to the hypothesis that HLA-mediated CD8+ T-cell activity does not play an instrumental role in paediatric non-progression, at least in the first years of life in the context of Th2-biased immunity and immunological immaturity (Goenka and Kollmann, 2015; Kollmann et al., 2012) – unlike adult elite controllers and more closely resembling sooty mangabey-type approach. However, other features of an effective antiviral CD8+ T-cell response are important in the non-progressive phenotype of adult elite controllers, as described above. To this point, HIV-specific CD8+ T-cell responses are detected in infected children even in the first days of life. Although these responses are dominated by Env- and Nef-specific targeting (Huang et al., 2008; Shalekoff et al., 2009; Thobakgale et al., 2007), suggestive of their lack of potency, some children produce Gag responses very early in life which are potentially of significance in terms of viral containment (Brander et al., 1999; Goulder et al., 2001b; Luzuriaga et al., 1995; Thobakgale et al., 2007). Additionally, the ability of infant CD8+ T-cells to suppress HIV replication is associated with longer survival (Pollack et al., 1997) as well as with the selection of escape mutations (Feeney et al., 2005; Leslie et al., 2004), suggesting that even early in life CD8+ T-cell response can be functional and influence the disease progression in some children.

To further examine the role played by HLA-mediated CD8+ T-cell responses in paediatric non-progressive HIV infection, we investigated the ability of these cells to impose selection pressure on the virus by employing ultra-deep sequencing technology on longitudinal samples from 11 slow progressors from a historical cohort of perinatally infected children and their mothers, recruited in 2003-2005 in the Paediatric Early HAART and Strategic Treatment Interruption Study (PEHSS) (Mphatswe et al., 2007; Prendergast et al., 2008) and followed from birth through the first decade of life. We report here that paediatric slow and non-progressors adopt two broadly contrasting strategies to long-term maintenance of

normal health and CD4 T-cell counts – one taking on the adult elite controller-type route and the other one following the sooty mangabey-type route.

4.2 Chapter-specific materials and methods

4.2.1 Confirmatory analysis of deep sequenced genomes

Eleven PSP mother-child pairs were sequenced (see Chapter 2, section 2.1 for cohort description). Maternal timepoints included closest to delivery, if available, and 5-7 years post-delivery, if available; children's timepoints included earliest available, ~2.5, ~5, ~7 years of age or only the earliest and 5 years of age timepoints (43 full-genomes and 7 partial genomes were generated). To confirm the close relationship between viral sequences from mother-child pairs, a maximum likelihood phylogenetic tree was constructed, using the General Time Reversible models of nucleotide substitution, from the 43 full-genome sequences and 8 clade-specific reference sequences with 1,000 bootstrap replicates in Mega6.06-mac software. The tree was visualised in FigTree v1.4.2 and adjusted (fonts and colours) in Adobe Illustrator CS4 v14.0.0. HIV subtype (subtype C) was confirmed with REGA tool, v3.0.

4.2.2 Escape in HLA-relevant and HLA-irrelevant CD8+ T-cell epitopes in PSPs

The Gene Cutter tool (www.hiv.lanl.gov) was used to extract sequences of the nine HIV proteins from the *de novo* assembled consensus sequences from mother-child pairs; protein-encoding sequences were then translated in Geneious 6.1.8 and aligned in Mega6.06.

A panel of well-characterised epitopes across full HIV proteome restricted by six HLA-A/B/C alleles expressed among the 11 PSPs was compiled (epitopes and sources are

detailed in the Appendix, **Tables 8.1-8.3**). To examine escape in HLA-relevant CD8+ T-cell epitopes, for each child, regions of the virus encoding the CD8+ T-cell epitopes restricted by any of the six HLA alleles expressed by that child were analysed using the panel in **Tables 8.1-8.3**, Appendix I. Only polymorphisms that developed independently in the child (i.e. had not been transmitted by the mother) were included and confirmed using epitope minor variant data.

The extent of HLA-driven escape was quantified as the proportion of HLA-associated sites that were adapted to that allele (i.e. polymorphisms that are enriched in the presence of an HLA allele or polymorphisms that differ from the polymorphisms that are less frequently observed in the presence of that HLA allele), based on previously defined HLA-associated escape sites (Carlson et al., 2012; Carlson et al., 2014). The number of HLA-associated adaptations observed across HIV proteome in each child was divided by the total number of HLA-associated adaptations relevant to that child's HLA repertoire (Payne et al., 2014).

The extent of escape in CD8+ T-cell epitopes that are not restricted by the HLA molecules in a given child (HLA-irrelevant epitopes), children's viral sequences of a pool of 36 epitopes from the described panel were used. These epitopes represented all the HIV proteins; any HLA-relevant epitopes for a given child were omitted. Escape in these HLA-irrelevant epitopes was calculated as above.

4.3 Results

4.3.1 Paediatric slow progressors categorised into high- and low-viraemic groups

Of 75 perinatally infected South African infants, 11 children who were followed longitudinally from birth (Mphatswe et al., 2007; Prendergast, 2008) had failed to meet prevailing clinical (WHO stage III or IV) or CD4 criteria (absolute CD4 count of <350

Table 4.1. Characteristics of the PSPs.

PID	DOB	Transmission	Sex		HLA-A	HLA-A	HLA-B	HLA-B	HLA-C	HLA-C	Early ART duration (years)	Early ART start (age, years)	Early ART stop (age, years)	ART (re)start age (years)	Type of slow progression
133-C	02/11/2003	IU	F	C	68:01	74:01	58:02	81:01	04:01	06:02	none	n/a	n/a	left study at 9y, no ART	Viraemic controller-like
				M	03:01	68:01	42:01	58:02	06:02	12:04					
468-C	07/12/2004	IU	M	C	02:02	68:01	57:03	58:01	06:02	07:01	1.5	0.1	1.6y	6.1	
				M	34:02	68:01	44:03	58:01	04:01	06:02					
349-C	29/11/2004	IU	F	C	23:01	43:01	45:01	58:02	06:02	06:02	none	n/a	n/a	9	
				M	23:01	30:02	45:01	57:02	06:02	07:01					
364-C	23/09/2004	IU	F	C	29:02	30:02	41:02	44:03	07:01	17:01	1.5	0.2	1.7	8	
				M	03:01	29:02	35:01	44:03	04:01	07:01					
385-C	25/01/2005	IP	F	C	30:01	34:02	15:03	58:02	02:10	06:02	1.3	0.3	1.6	left study at 8y, no ART	
				M	30:01	43:01	15:03	58:02	02:02	06:02					
517-C	07/01/2005	IP	M	C	30:02	68:02	15:10	42:01	03:04	17:01	none	n/a	n/a	never	Sooty mangabey-like
				M	30:02	30:04	42:01	58:02	06:02	17:01					
021-C	06/09/2005	IU	F	C	02:05	29:02	42:01	44:03	02:10	17:01	1.0	0.1	1.1	never	
				M	02:05	33:01	42:01	44:03	02:10	17:01					
114-C	25/09/2003	IP	F	C	03:01	24:02	07:02	08:01	07:01	07:02	1.0	0.1	1.1	left study at 7.3y, no ART	
				M	03:01	68:02	08:01	57:02	07:01	18:01					
559-C	03/02/2005	IU	M	C	23:01	68:02	08:01	58:01	07:01	07:01	1.0	0.1	1.1	5.2	
				M	23:01	30:02	08:01	58:02	06:02	07					
380-C	13/10/2004	IU	M	C	23:01	68:02	15:10	15:10	03:04	08:01	1.1	0.1	1.2	7.6	
				M	02:00	23:01	07:02	15:10	03:04	04:01					
081-C	24/08/2003	IU	F	C	29:02	68:02	15:16	44:03	03:04	07:01	1.4	0.1	1.5	6.7	
				M	29:02	30:01	42:02	44:03	07:01	17:01					

PID = participant ID; DOB = date of birth; IU = *in utero* infection; IP = *intra-partum* infection; M = male; F = female; C = child; M = mother; yo = years old. For each subject, child's HLA type is shown on the first row and maternal HLA is on the second row.

cells/mm^3) for ART initiation by the age 5 years. These children we define here as paediatric slow progressors, or PSPs (**Table 4.1**).

We first examined changes in viral load with age among these 11 PSPs. Viral loads declined over the first 5 years of life and then reached a setpoint (**Figure 4.1A**). Correlation analysis showed that viraemia continued to decline during the first five years of life and then plateaued (<5 years: r=-0.23, p<0.0001; >5 years: r=0.06, p=0.5; not shown). The median viral setpoint at age >5 years in all 11 PSPs was 26,731 HIV copies/ml (**Figure 4.1B**). As expected, the subgroup of children whose viral loads were above the median in the first 5 years of life were the same children whose viral loads were above the median at age >5 years. Thus the 11 PSPs could be subdivided into two groups, one with persistently higher, and one with persistently lower viral loads both before (p=0.004) and after reaching the 5-year viral setpoint (p=0.008) (**Figure 4.1C**). These we have termed here, respectively, sooty mangabey-like ('SM-like') and viraemic controller-like ('VC-like'). Viral loads declined less markedly in the first 5 years in the SM-like children than in the VC-like children (**Figure 4.1D**). After 5 years of age, CD4% significantly increased in SM-like children and absolute CD4 count significantly decreased in VC-like children (**Figures 4.1E,F**). CD4% and absolute CD4 count remained healthy and similar in both groups, following the natural CD4 decline in the first 5 years observed in healthy uninfected children (**Table 4.2**) (Lugada et al., 2004; Shearer et al., 2003).

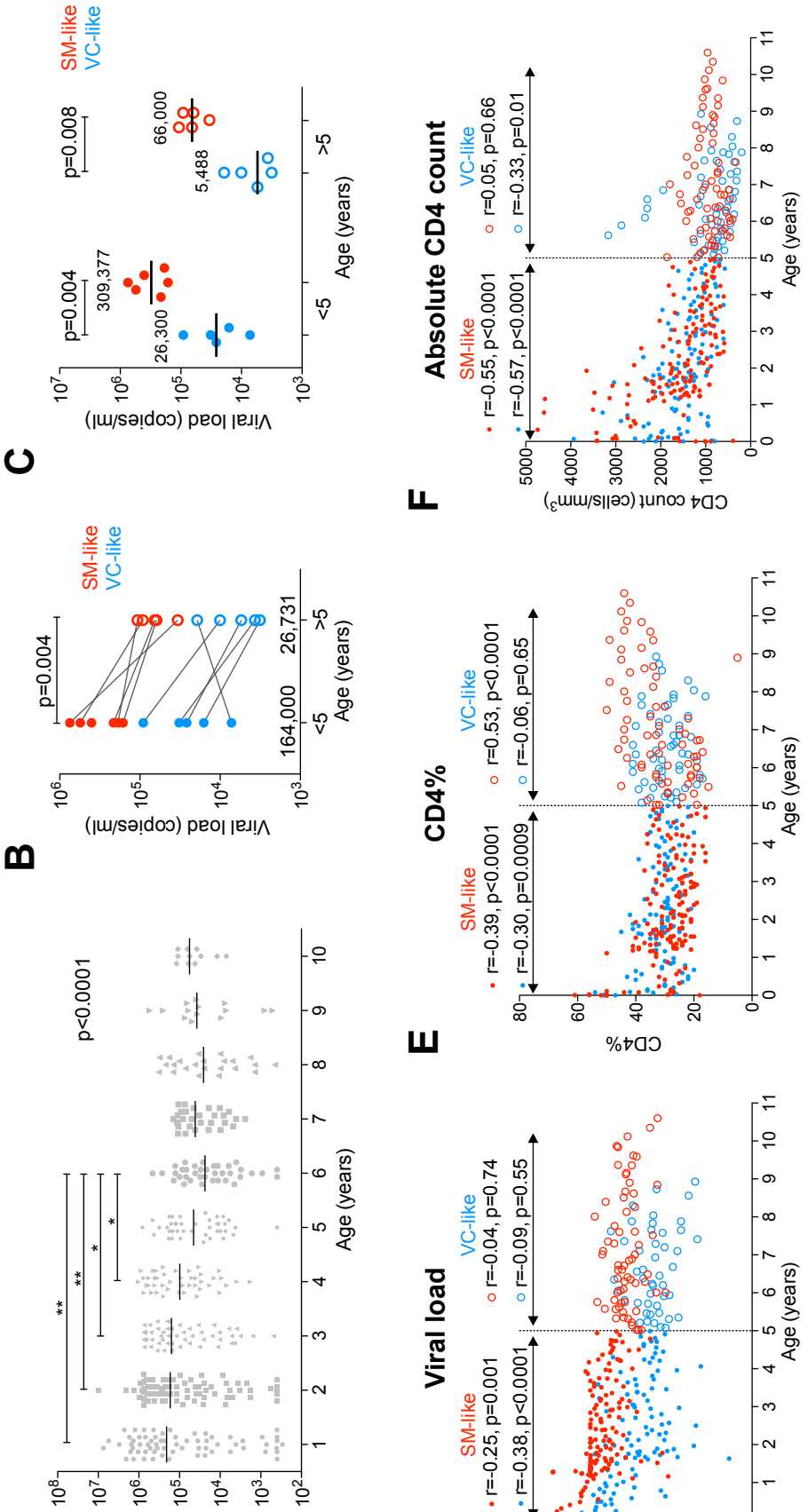

A
p<0.0001
**
**
*
*
Viral load (copies/ml)
Age (years)
B
SM-like
VC-like
p=0.004
164,000
26,731
<5
>5
Viral load (copies/ml)
Age (years)
C
SM-like
VC-like
p=0.004
p=0.008
309,377
26,300
66,000
5,488
<5
>5
Viral load (copies/ml)
Age (years)
D
Viral load
SM-like
r=-0.25, p=0.001
r=-0.38, p<0.0001
VC-like
r=-0.04, p=0.74
r=-0.09, p=0.55
Viral load (copies/ml)
Age (years)
E
CD4%
SM-like
r=-0.39, p<0.0001
r=-0.30, p=0.0009
VC-like
r=0.53, p<0.0001
r=-0.06, p=0.65
CD4%
Age (years)
F
Absolute CD4 count
SM-like
r=-0.55, p<0.0001
r=-0.57, p<0.0001
VC-like
r=0.05, p=0.66
r=-0.33, p=0.01
CD4 count (cells/mm3)
Age (years)

Figure 4.1. PSPs can be separated into two groups based on their virological profile – SM-like and VC-like. A. Viral loads of 11 PSPs broken down by each year of life. Kruskal-Wallis test with Dunn's post-test; *p<0.05, **p<0.01. Only significant differences are shown. **B,C.** Viral loads before and after 5 years of age in 11 PSPs together (B) and split into SM-like versus VC-like (C). SM-like child 559-C is represented only <5 years of age as ART was started at the age of 5.2 years and no pre-ART viral load data are available between 5 and 5.2 years. B, Wilcoxon matched-pairs signed rank test; C, Mann-Whitney U test. Median viral loads are indicated and shown as horizontal lines in C. **D-F.** Spearman correlation between age and viral load (D), CD4% (E) and absolute CD4 count (F) in SM- and VC-like PSPs.

Table 4.2. Virological and CD4+ T-cell profile in VC-like PSPs, SM-like PSPs and healthy HIV-uninfected children.

PID	<5 years old			>5 years old		
	Absolute CD4 count, cells/mm^3, median (IQR)	CD4%, median (IQR)	Viral load, copies/ml, median (IQR)	Absolute CD4 count, cells/mm^3, median (IQR)	CD4%, median (IQR)	Viral load, copies/ml, median (IQR)
Viraemic controller-like						
133-C	1,621 (1,316-2,166)	32.5 (30-37)	26,300 (5,930-118,500)	1,051 (885-1,117)	32 (30-33)	5,488 (2,927-8,714)
468-C	1,628 (1,156-1,837)	31 (30-35)	32,600 (15,900-155,534)	2,301 (1,191-2,747)	38.5 (26-41)	3,699 (1,669-5,728)
349-C	1,377 (1,100-1,650)	30 (28-35)	91,500 (12,023-362,000)	492 (409-661)	30 (23-32)	10,083 (7,725-24,599)
364-C	870 (739-1,302)	26 (23-32)	7,270 (3,530-26,037)	422 (332-510)	25 (20-27)	19,462 (13,579-42,000)
385-C	1,314 (1,086-2,005)	29 (26-36)	16,120 (8,406-163,300)	733 (660-823)	32 (21-38)	3,207 (1,400-88,754)
Total	1,384 (1,057-1,826)	30 (27-35)	28,650 (7,888-139,000)	734 (472-1,051)	29 (25-34)	9,179 (4,279-20,559)
Sooty mangabey-like						
517-C	2,565 (1798-3,008)	32 (29-36)	750,000 (394,000-1,410,000)	1,166 (1,023-1,422)	44 (42-45)	34,000 (13,454-83,000)
021-C	1,047 (849-1,581)	28 (25-33)	214,168 (116,412-562,197)	875 (737-1,000)	34 (32-36)	66,000 (47,000-165,000)
114-C	1,335 (955-1,650)	25 (23-32)	189,000 (92,950-337,250)	736 (624-910)	19 (18.5-21.5)	108,128 (61,925-142,492)
559-C[a]	1,346 (1,137-1,757)	24 (20-28)	404,586 (128,250-750,000)	n/a	n/a	n/a
380-C	1,101 (887-1,471)	28 (26-32)	557,000 (187,677-750,000)	509 (418-772)	30 (29-32)	92,317 (34,000-112,840)
081-C	1,173 (927-1,687)	25 (22-29)	164,000 (53,600-471,500)	657 (475-892)	21 (19-22)	62,540 (35,273-75,475)
Total	1,390 (1,012-1,858)	27 (24-33)	360,000 (122,500-750,000)	875 (728-1,120)	33 (23-43)	64,000 (34,000-110,000)
Healthy HIV-uninfected children[b]						
	2,610 (1,770-2,760)	46 (39.5-49)	-	980 (650-1,500)	37 (31-47)	-

[a] ART was started at the age of 5.2 years, but no pre-ART viral load or CD4 data available between 5 and 5.2 years.
[b] Adapted from Shearer *et al. J Allergy Clin Immunol* 2003.
IQR designates interquartile range; n/a, not applicable.

4.3.2 SM-like PSPs have greater non-Gag-specific CD8+ T-cell responses early in life

Specificity and breadth of the HIV-specific CD8+ T-cell response has been related to viral load in previously reported adult studies, with broad Gag-specific responses associated with lower viral loads, and broad Env-, Nef- and Accessory protein (Vif/Vpr/Vpu/Tat/Rev)-specific responses associated with higher viral loads (Barouch et al., 2003; Barouch et al., 2002; Edwards et al., 2002; Geldmacher et al., 2007; Janes et al., 2013; Kiepiela et al., 2007; Klein et al., 1995; Masemola et al., 2004; Novitsky et al., 2003; Ogg et al., 1998; Riviere et al., 1995; Streeck et al., 2007; Zuniga et al., 2006). We therefore next investigated whether differential CD8+ T-cell activity might explain the distinct viral loads among the two groups of PSPs. Using a panel of 410 overlapping 18mer peptides spanning the clade C proteome, we determined in IFN-g ELISPOT assays which individual peptides were recognised (Addo et al., 2003; Kiepiela et al., 2004). In both groups, HIV-specific CD8+ T-cell responses significantly increased with age in breadth and magnitude (SM-like: $r=0.47$, $p<0.0001$ for breadth, $r=0.47$, $p<0.0001$ for magnitude; VC-like: breadth $r=0.48$, $p<0.0001$; magnitude $r=0.44$, $p<0.0001$; not shown). However, total breadth tended to be higher in SM-like than in VC-like PSPs ($p=0.06$; **Figure 4.2A**). This difference was only significant in Nef-specific responses ($p=0.001$) but not in Gag ($p=0.42$; **Figures 4.2B,C**, **Figure 4.3**), and was most marked in the first 3 years of life, when responses to Env and Vif/Vpr/Vpu/Tat/Rev were also higher in the SM-like children (**Figures 4.2D-I, Figure 4.4**). These paediatric data are therefore consistent with adult studies indicating increased viral loads associated with non-Gag-specific responses, particularly those directed towards Env or Nef.

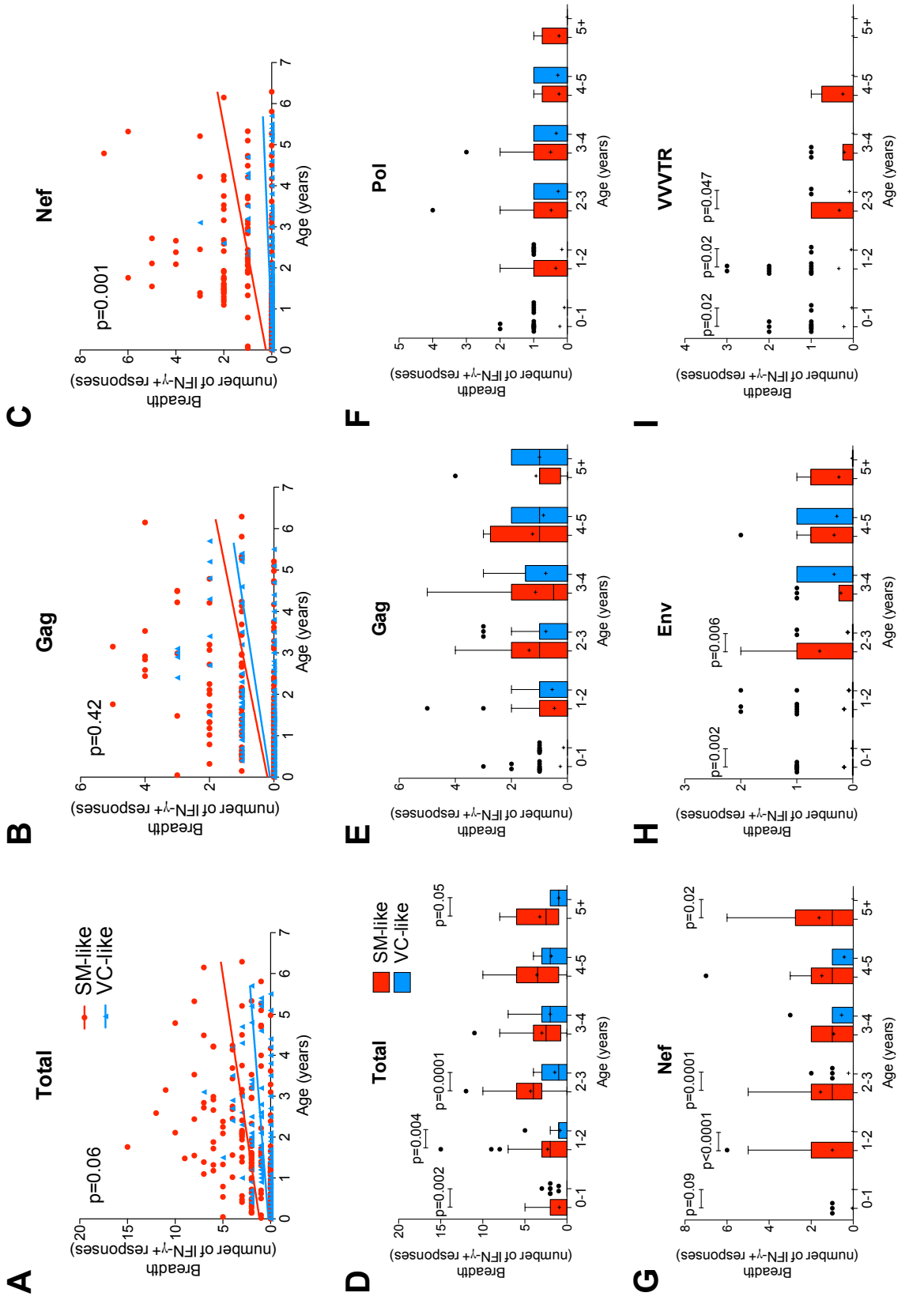

A
Total
SM-like
VC-like
p=0.06
Breadth
(number of IFN-γ+ responses)
Age (years)
B
Gag
p=0.42
C
Nef
p=0.001
D
Total
p=0.004
p=0.002
p=0.0001
p=0.05
E
Gag
F
Pol
G
Nef
p=0.09
p<0.0001
p=0.0001
p=0.02
H
Env
p=0.002
p=0.006
I
VVVTR
p=0.02
p=0.02
p=0.047
0-1
1-2
2-3
3-4
4-5
5+

Figure 4.2. SM-like PSPs have larger non-Gag-specific CD8+ T-cell responses early in life. A-C. Differences in CD8+ T-cell breadth, determined by ELISPOT assays, in SM-like versus VC-like PSPs. **A.** Total breadth; **B.** Gag-specific breadth; **C.** Nef-specific breadth. P-values show differences in slopes determined by linear regression. **D-I.** CD8+ T-cell breadth in SM-like versus VC-like PSPs in each year of life: total (D); Gag-specific (E); Pol-specific (F); Nef-specific (G); Env-specific (H); and Vif/Vpu/Vpr/Tat/Rev-specific breadth (I). Mann-Whitney U test. Tukey boxplots show interquartile ranges, whiskers show minimum and maximum, horizontal lines show medians, 'plus' signs show means and individual dots indicate outliers.

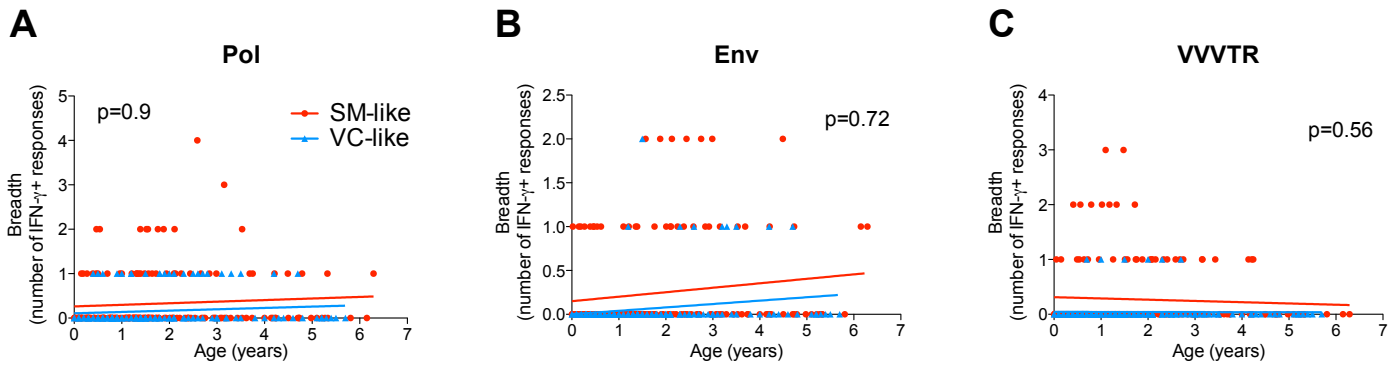


Figure 4.3. Longitudinal breadth of CD8+ T-cell responses in the PSPs. A. Pol-specific; **B.** Env-specific; and **C.** Vif/Vpu/Vpr/Tat/Rev-specific breadth. P-values show differences in slopes determined by linear regression.

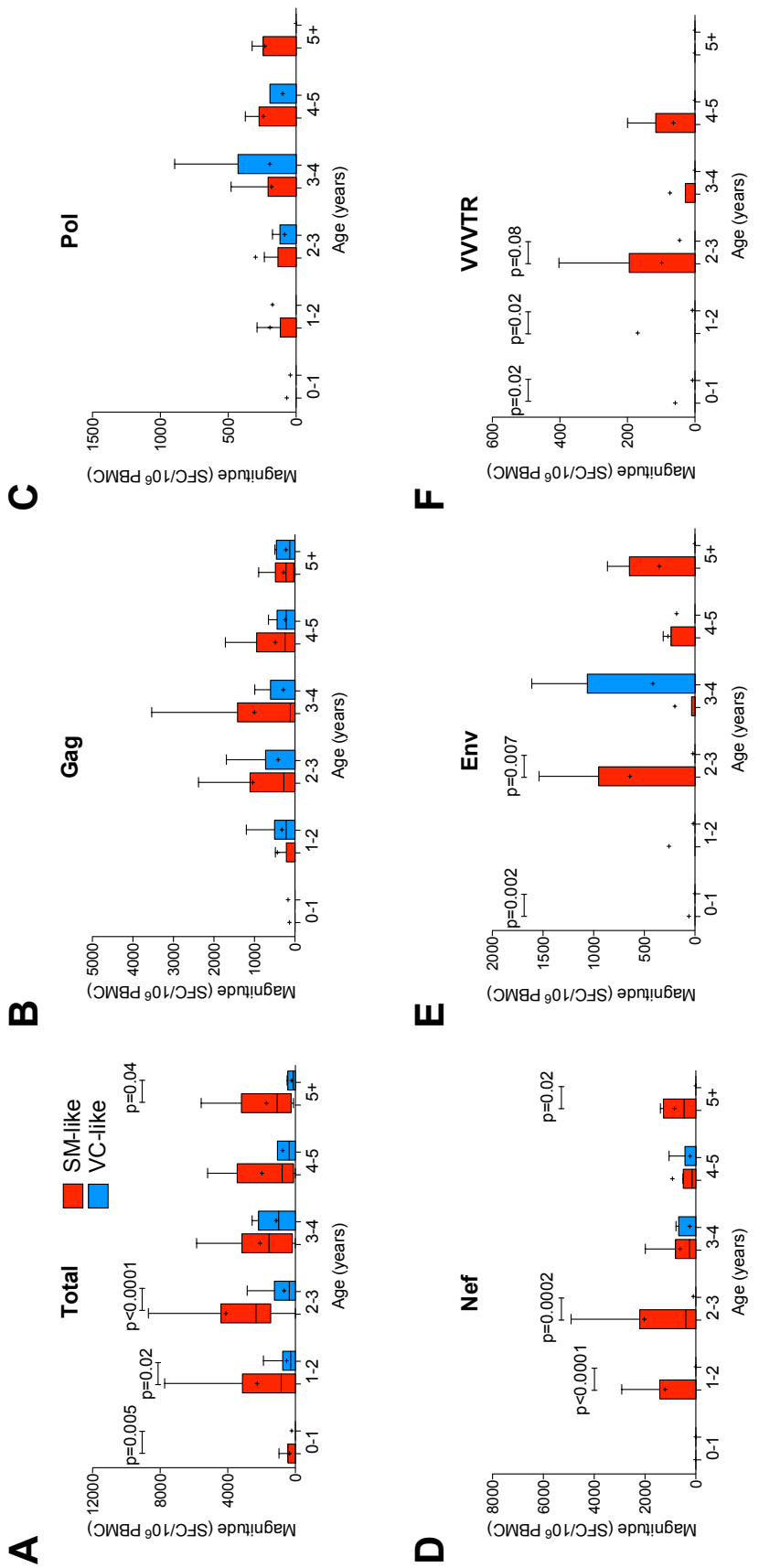

A
Total
SM-like
VC-like
p=0.005
p=0.02
p<0.0001
p=0.04
Magnitude (SFC/10^6 PBMC)
Age (years)
0-1
1-2
2-3
3-4
4-5
5+
B
Gag
C
Pol
D
Nef
p<0.0001
p=0.0002
p=0.02
E
Env
p=0.002
p=0.007
F
VVTR
p=0.02
p=0.02
p=0.08

Figure 4.4. SM-like PSPs have greater non-Gag-specific CD8+ T-cell responses early in life. A-F. CD8+ T-cell magnitude in SM-like versus VC-like PSPs in each year of life: total (A); Gag-specific (B); Pol-specific (C); Nef-specific (D); Env-specific (E); and Vif/Vpu/Vpr/Tat/Rev-specific (F) magnitude. Mann-Whitney U test. Tukey boxplots show interquartile ranges, whiskers show minimum and maximum, horizontal lines show medians, 'plus' sings show means.

4.3.3 Development of CD8+ T-cell-mediated selection pressure with age among PSPs

To further investigate the role of HIV-specific CD8+ T-cells in these two distinct groups of PSPs, we next tracked the kinetics of selection pressure imposed on the virus within HLA-restricted CD8+ T-cell-epitopes from birth through childhood, in each case also having access to samples from the transmitting mother. In order to maximise the resolution of sequence changes that were selected, we deep-sequenced the virus. Phylogenetic analysis of full-length consensus sequence for all 11 mother-child pairs confirmed the close relationship between virus in each mother-child pair (**Figure 4.5**).

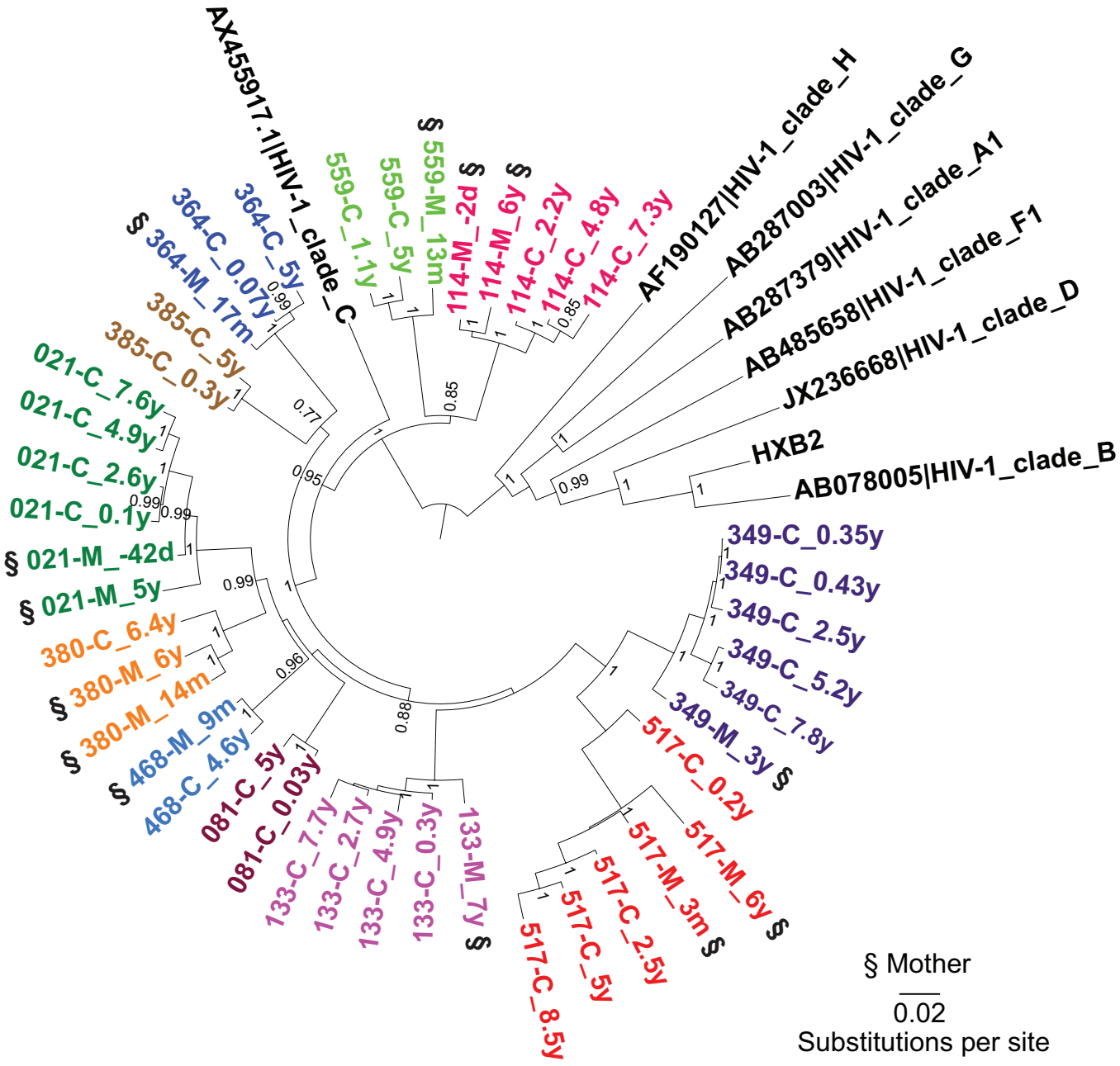


Figure 4.5. Maximum likelihood phylogenetic tree from 43 full-genome sequences of the 11 PSP and their mothers. Partial genomes were not included. Mother-child pairs are distinguished by colours and maternal sequences are marked. HXB2 sequence and reference sequences for clades A, B, C, D, F, G and H are included. Bootstrap values >0.75 based on 1,000 bootstrap replicates are shown. Scale bar shows number of substitutions per site.

In each child we analysed the regions of virus encoding the CD8+ T-cell epitopes restricted by any of the six HLA alleles expressed by that child, using a panel of well-characterised epitopes representing all the HIV proteins (see section 4.2 for details). Variants shared with the mother expressing the same HLA class I molecule were presumed to have been transmitted and not to have arisen *de novo* in the child. In both VC-like and SM-like paediatric groups, there was accumulation of HLA-associated polymorphisms with age (**Figures 4.6A-C**).

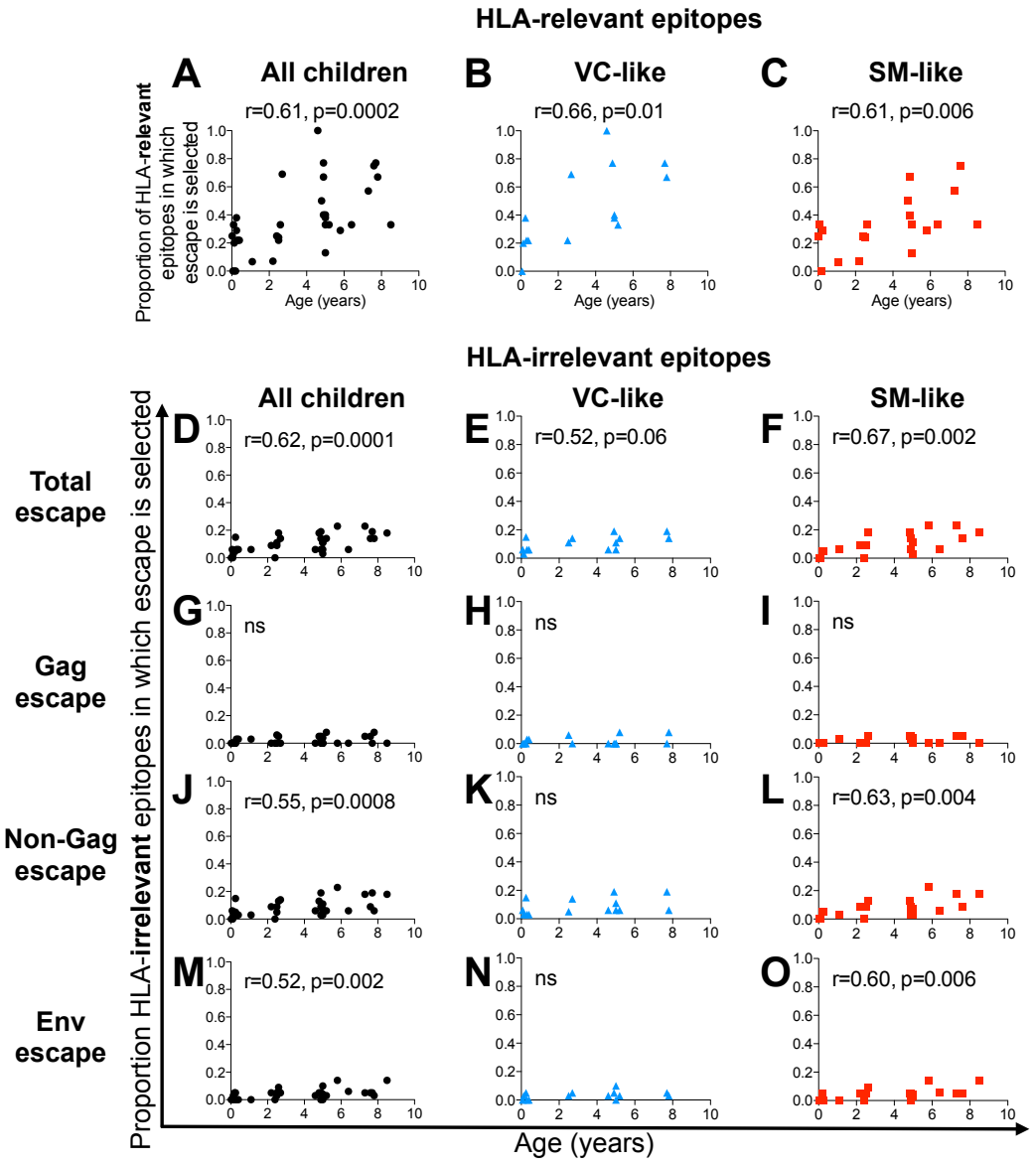


Figure 4.6. Development of CD8 T-cell-mediated selection pressure with age among PSPs. **A-C.** Proportion of polymorphisms across full HIV genome associated with all six HLA class I alleles in each child, developed independently of transmitted variants. **A.** All PSPs together; **B.** VC-like PSPs; **C.** SM-like PSPs. **D-O.** Proportion of polymorphisms in HLA-irrelevant CD8+ T-cell epitopes across full HIV genome (D-F), in Gag-specific epitopes (G-I), in non-Gag-specific epitopes (J-L) and in Env-specific epitopes (M-O). **D,G,J,M.** All PSPs together; **E,H,K,N.** VC-lke PSPs; **F,I,L,O.** SM-like PSPs. Spearman correlation.

The escape was more pronounced in the VC-like group compared to the SM-like groups, although this did not reach significance (**Figure 4.7A**). However, in the VC-like children there was significantly more escape in non-Gag than in Gag epitopes, whereas in SM-like children this difference did not reach significance (**Figures 4.7B,C**), suggesting that the greater escape in non-Gag epitopes in the VC-like children could account for the smaller non-Gag-specific CD8+ T-cell response in the VC-like group versus the SM-like group.

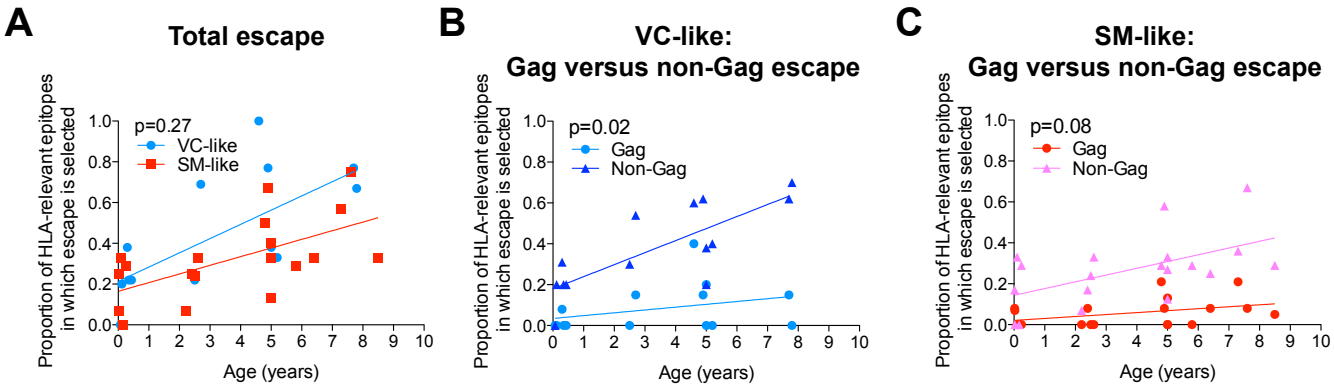


Figure 4.7. Differences in accumulation of HLA-associated polymorphisms in VC-like versus SM-like children. A. Escape mutations across HIV proteome accumulated with age in the VC-like group compared to the SM-like group. **B,C.** Escape in Gag-specific versus non-Gag-specific CD8+ T-cell epitopes in VC-like children (B) and SM-like children (C). Linear regression.

In order to seek further evidence that these differences in accumulation of escape variants in VC-like and SM-like children were due to the HLA-restricted CD8+ T-cell responses, we analysed also the appearance of escape mutations in HLA-irrelevant epitopes, i.e. CD8+ T-cell epitopes that were not restricted by the child's HLA class I molecules. Although in all children there was accumulation of HLA-irrelevant polymorphisms with age, in the VC-like group this did not reach significance, whereas in the SM-like group it was highly significant (**Figures 4.6D-F**). Moreover, the HLA-irrelevant polymorphisms were accumulating in non-Gag, specifically in Env epitopes, and only in the SM-like children (**Figures 4.6G-O**). Finally, comparison of polymorphisms in the HLA-relevant and HLA-irrelevant epitopes within each group of children showed that in the VC-like children there were significantly more HLA-relevant than HLA-irrelevant mutations accumulating with age, particularly in non-Gag regions, but the difference was not significant in the SM-like children (**Figure 4.8**). Together, these findings suggest that CD8+ T-cells in the VC-like PSPs exert stronger HLA-associated pressure on the virus through childhood than the SM-like children, reflected in the relatively high frequency of escape mutants selected in non-Gag HLA-relevant epitopes. In contrast, variants accumulate more in HLA-irrelevant epitopes in the SM-like PSPs, perhaps reflecting the higher viral loads in these children.

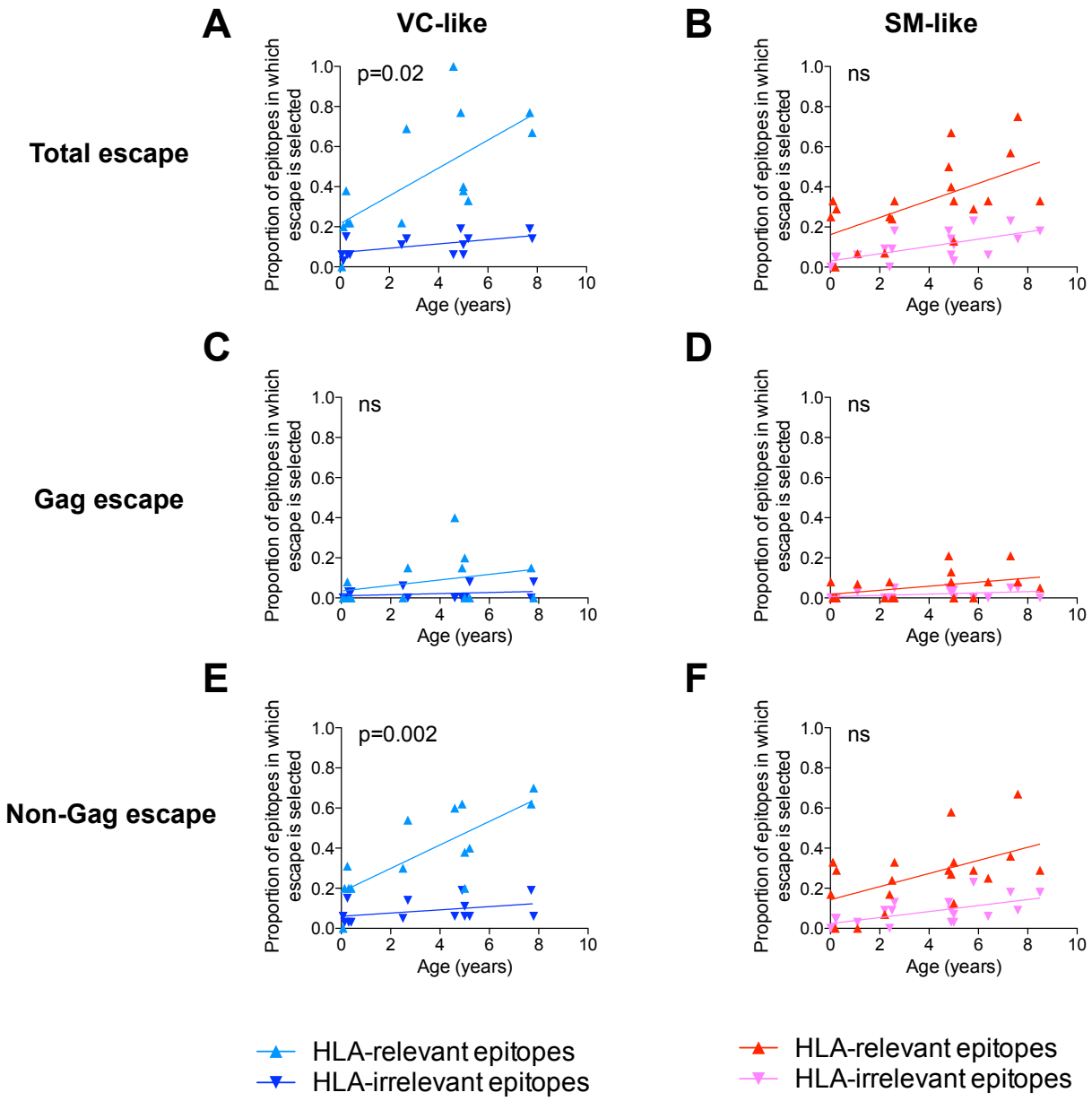


Figure 4.8. Difference in accumulation of polymorphisms in HLA-relevant versus in HLA-irrelevant CD8+ T-cell epitopes in the VC-like PSPs and SM-like PSPs. A,B. Total escape across HIV proteome. **C,D.** Polymorphisms in Gag-specific epitopes. E,F. Polymorphisms in non-Gag epitopes. Linear regression.

4.3.4 Contrasting selection pressure in VC-like and SM-like children targeting Gag-TL9:

i) VC-like child 133-C

To examine in more detail the findings of differential escape within Gag and non-Gag epitopes among VC-like and SM-like slow progressors, we focused on the specific CD8+ T-cell responses and viral sequence changes in 3 selected children. These comprised one VC-like child, 133-C, and two SM-like children, 517-C and 021-C, all of whom targeted the same immunodominant Gag-TL9 epitope (TPQDLNTML, Gag residues 180-188) at the time viral load was reaching a setpoint at ~5 years of age (**Figure 4.9**).

VC-like slow progressor 133-C made a dominant HLA-B*81:01-restricted response from the first timepoint tested at age 206 days. This response remained strongly immunodominant, with other smaller responses transiently detected (**Figures 4.9A,B**). Although Gag-TL9 is also restricted by HLA-B*42:01 expressed in the mother 133-M, the selection pressure imposed on the virus differs, such that typically the HLA-B*81:01-TL9 response selects variants at position 7 (P7) in the epitope (T186X), whereas HLA-B*42:01-TL9 characteristically selects the Q182T variant at P3 in the epitope (Carlson et al., 2014; Wright et al., 2010; Wright et al., 2012). The virus transmitted to the child encoded the wildtype TL9 epitope, but a T186M variant was selected that had almost reached fixation (96% frequency) by 2.7 years of age (**Figure 4.10A**). Lack of available timepoints between 0.3 years and 2.7 years prevented more precise timing of the emergence of the T186M variant, but population sequencing that had been previously undertaken at two additional timepoints showed that T186M mutant arose between 0.7 and 1.3years (Thobakgale et al., 2009). Moreover, the emergence of a T186M variant-specific CD8+ T-cell response by 1.3

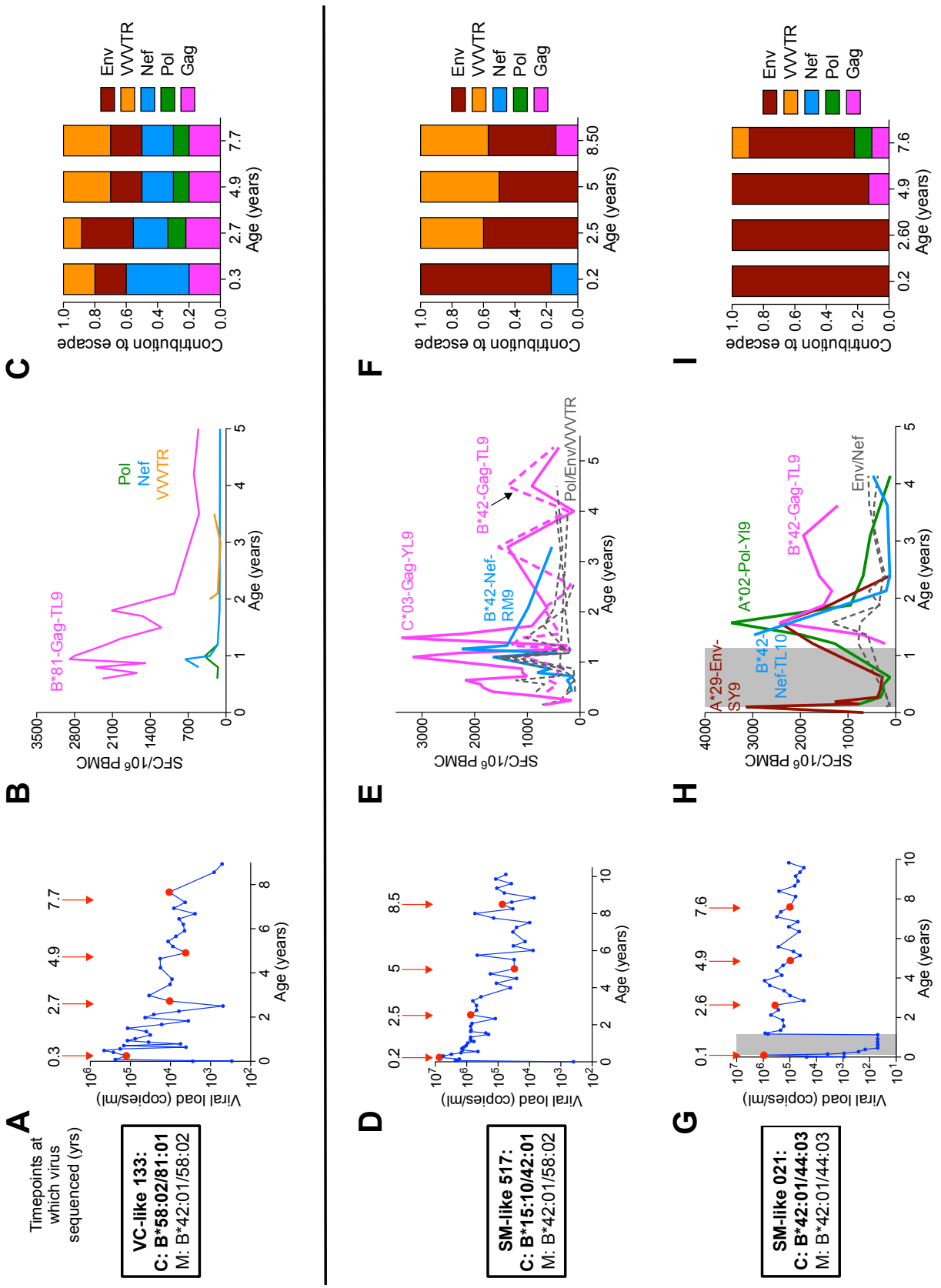

A
Timepoints at which virus sequenced (yrs)
0.3
2.7
4.9
7.7
Viral load (copies/ml)
Age (years)
VC-like 133:
C: B*58:02/81:01
M: B*42:01/58:02
B
B*81-Gag-TL9
Pol
Nef
VVVTR
SFC/10⁶ PBMC
Age (years)
C
Env
VVVTR
Nef
Pol
Gag
Contribution to escape
Age (years)
D
0.2
2.5
5
8.5
Viral load (copies/ml)
Age (years)
SM-like 517:
C: B*15:10/42:01
M: B*42:01/58:02
E
C*03-Gag-YL9
B*42-Nef-RM9
B*42-Gag-TL9
Pol/Env/VVVTR
SFC/10⁶ PBMC
Age (years)
F
Env
VVVTR
Nef
Pol
Gag
Contribution to escape
Age (years)
G
0.1
2.6
4.9
7.6
Viral load (copies/ml)
Age (years)
SM-like 021:
C: B*42:01/44:03
M: B*42:01/44:03
H
A*29-Env-SY9
B*42-Nef-TL10
A*02-Pol-YI9
B*42-Gag-TL9
Env/Nef
SFC/10⁶ PBMC
Age (years)
I
Env
VVVTR
Nef
Pol
Gag
Contribution to escape
Age (years)

Figure 4.9. Differential CD8+ T-cell targeting and selection pressure in VC-like child 133-C and SM-like children 517-C and 021-C. A-C, Data for 133-C; D-F, data for 517-C; G-I, data for 021-C. **A,D,G**. Virological profiles of the three children with deep-sequenced timepoints shown in red and child's age (years) indicated above the arrows. **B,E,H**. ELISPOT CD8+ T-cell responses. **C,F,I.** Contribution of different HIV proteins to HLA-associated escape across HIV proteome. VVVTR, Vif/Vpr/Vpu/Tat/Rev. Gray area in G,H represents 12-month period on ART.

years of age (**Figure 4.10B**) indicates that this variant was present before 1.3 years. Ultimately the T186M variant-specific response dominated and the TL9 wildtype-specific response was substantially diminished (**Figure 4.10B**).

Strikingly, there was also evidence of early CD8+ T-cell-driven escape selection within the first 3 months of life in 133-C (**Figure 4.9C, Figure 4.10A**). In each case, the specific escape mutation selected in the child was precisely the one previously shown in large cohort studies (Carlson et al., 2012; Carlson et al., 2014) to be driven by the particular HLA class I molecule expressed in the child. One of these was within the epitope Gag-SK10 (SILRGGKLDK, Gag residues 6-15) restricted by HLA-A*74, an allele not shared with the mother 133-M. The characteristic HLA-A*74-associated escape mutant is Gag K12N (at P7 in the epitope), in previous studies of C clade infected adults carrying a q value of $6x10^{-17}$ (Carlson et al., 2014). Thus, the observation that this variant was not transmitted by the HLA-A*74-negative mother, but was selected in 100% of sequences in the HLA-A*74-positive child within 3 months of age, is strong evidence of early immune escape driven by the child. Similarly, in two HLA-B*81-restricted epitopes (HLA-B*81 was also not expressed the mother 133-M), in Pol-SL10 (SPIETVPVKL, Pol residues 158-167) and in Nef-RM9 (RPQVPLRPM, Nef residues 71-79), 100% of transmitted sequences encoded wildtype epitopes and escape mutations were selected in 133-C by 3 months of age. Additionally, escape mutations in 4 more epitopes arose later than 3 months but

A

VC-like: 133-C

	Subject	Child's age	B*81 Gag ^{180}TL9^{188} **TPQDLNTML**	Frequency	A*74 Gag ^{6}SK10^{15} **SILRGGKLDK**	Frequency	B*81 Pol ^{158}SL10^{167} **SPIETVPVKL**	Frequency	A*74 Pol ^{423}SR10^{432} **SQIYPGIKVR**	Frequency	B*81 Nef ^{71}RM9^{79} **RPQVPLRPM**	Frequency
A*74-neg/ B*81-neg	133-M	13m	····· ·····	100%	····E··· ····	100%	nd		nd		nd	
		7y	··T···· ·····	65% 35%	·V··E··· ····	100%	····· ·····	100%	·····R·· ····VR·· ···R·R··	81% 13% 6%	·····	100%
A*74-pos/ B*81-pos	133-C	0.3y	····· ·····	100%	····EN··· ····	100%	····· ···D···· ···P···· ···K····	65% 32% 2% 1%	···R·R··	100%	···V··· ····· ···A···· K·····	60% 32% 6% 2%
		0.7y	·····M··	n/a	nd		nd		nd		nd	
		1.3y	·····M··	n/a	nd		nd		nd		nd	
		2.7y	·····M·· ·····	96% 4%	····EN··· ·V··EN···	75% 24%	·S····· ···K···· ·····	92% 5% 3%	·····RIK ·····R·K ···R·R··	55% 42% 3%	····I··· ····V··· K···V··· ·····	54% 36% 8% 2%
		4.9y	·····M··	100%	·V··EN···	99%	·S·····	100%	·····RIK ·····R·K	98.7% 1.3%	····T··· ····V···	89% 11%
		7.7y	·····M··	100%	····EN···	100%	·S····· ·T·····	76% 24%	···R·R·K ·····RIK ·····R·K	81% 17% 2%	····V···	99%
HLA association			HLA-B*42		HLA-A*74		HLA-B*81 HLA-B*81		HLA-A*74		HLA-B*81	
Escape variant			Q182T		K12N		P159S E161X		R432K		L76X	
q value			3 x 10-5		6 x 10-17		3 x 10-39 3 x 10-4		7 x 10-3		2 x 10-38	

B

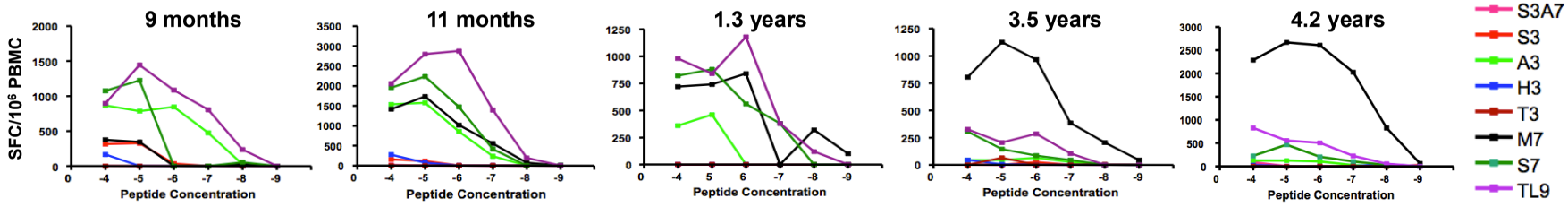


Figure 4.10. HLA-associated Gag-specific escape develops within the first 3 months of life in the VC-like child 133-C. A. Sequences of epitopes in which 133-C developed early escape independently of the transmitted variants, determined by deep sequencing. Highlighted in grey are footprints associated with the HLA class I allele indicated below the table; known escape variants and q values indicating significance of an HLA-polymorphism association are shown (Carlson et al., 2014). M, mother; C, child; neg, negative; pos, positive. **B.** CD8+ T-cell response to the Gag-TL9 wild type epitope and its variants at five different timepoints in 133-C, determined by IFN-γ ELISPOT.

within the first years of life (**Table 4.3**). These data demonstrate that CD8+ T-cell responses in VC-like slow progressor 133-C exerted selection pressure on the virus within the first months of life in Gag and non-Gag epitopes. In addition, variant-specific Gag-TL9 responses were generated, likely in the first year of life, effectively negating the benefit to the virus of the original escape mutant.

Table 4.3. Additional HLA-associated escape mutations that developed in VC-like 133-C within the first years of life.

	Subject	Time point	A*68:01 Vif ^{54}ER10^{63} **EVHIPLGDAR**	Frequency	A*68:01 Vif ^{113}DR9^{121} **DCFADSAIR**	Frequency	C*04 Env ^{614}OLP371^{631} **WSNKSQEDIWDNMTWMQW**	Frequency	C*06:02 Env ^{272}OLP325^{288} **IRSENLTNNAKTIIVHL**	Frequency
A*68:01-pos/ C*04-neg/ C*06-pos	**133-M**	13m	nd		nd		nd		nd	
		7y	·····E··	65%	···T·····	51%	·N····T···N·····	58%	·····D·V·····	40%
			····V·E··	24%	·····	49%	·····T·····	41%	·····I·····	30%
			·····E·K	11%					·····D·I·····	25%
									··T····N·I·····	5%
A*68:01-pos/ C*04-pos/ C*06-pos	**133-C**	0.3y	·····E··	100%	·····	100%	·····T·····	100%	·····D·I·····	98%
									·····D·T·····	2%
		2.7y	·····E··	100%	·····	86%	·····TE·····	66%	·····D·T·····	46%
					···T·····	11%	·····TD·····	34%	·····D·TR·····	44%
					·····G	3%			·····D·I·····	10%
		4.9y	·····E·K	96%	···T·····	65%	····HT·····	86%	·····D·T·····	100%
			····V·E··	4%	····E····	25%	····KS·····	10%		
					·····	10%	·····S·····	4%		
		7.7y	·····E·K	67%	···T·····	64%	·····TE·····	66%	·····D·I·····	76%
			·····EGK	33%	····E····	36%	····YT·····	34%	·····D·T·····	24%

133-M indicates mother of the child 133-C. Frequency represents percentage at which a particular haplotype is present at the indicated timepoint. Nd, not determined; pos, positive; neg, negative.

ii) SM-like children 517-C and 021-C

In both of the SM-like slow progressors, 517-C and 021-C, the Gag-TL9 responses arose later in the course of infection (**Figures 4.9D-I**) and did not become immunodominant for several years. In 517-C the dominant response initially was to the HLA-C*03-restricted Gag-YL9 epitope (YVDRFFKTL, Gag 286-304). Unlike 133-C, early (i.e. at ≤3m age) Gag escape mutants were not observed in 517-C (**Table 4.4A**, **Table 4.5**). However, escape mutants were selected to fixation within 2.4m of birth (in 517-C was intra-partum infected and only became viraemic at 28 days) within the HLA-B*15:10 Rev epitope IL9 (IHSISERIL, Rev residues 52-60) (**Table 4.4B**). HLA-B*15:10 was not expressed in the mother 517-M and, as expected, the maternal virus transmitted encoded the wildtype Rev-IL9 epitope. Other epitopes in which escape to fixation appeared to have occurred by 2.4m of age in 517-C were in two HLA-B*42:01-restricted Env epitopes, RI10 (RPNNNTRKSI, Env residues 298-307) and IF9 (IPRRIRQGF, Env residues 843-851), and in two HLA-A*30:02-restricted Env epitopes, KY9 (KYLGSLVQY, Env residues 794-802) and IY9 (IVNRVRQGY, Env residues 704-712). In all four cases the epitope mutant in the child differed in 100% of sequences from the maternal sequence. The caveat here would be that both mother and child express HLA-A*30:02 and HLA-B*42:01, and that the samples sequenced were of plasma virus 2-3 months after transmission. However, particularly in view of the clear-cut evidence of early escape within the HLA-B*15:10 Rev IL9 epitope, it would seem very likely that early escape is driven to fixation in these four Env epitopes, with additional evidence of early escape in almost 50% of sequences within the HLA-A*30:02-retricted Pol epitope AY9 (AQNPEIVIY, Pol residues 328-366).

Table 4.4. Early escape in SM-like child 517-C develops in non-Gag epitopes. A. Sequences of dominant CD8+ T-cell responses. Escape in HLA-C*03-Gag-YL9 epitope develops only by 5 years of age; no evidence of escape over the first 8.5 years of life in HLA-B*42-Gag-TL9 or B*42-GNef-RM9 epitopes. **B.** Sequences of epitopes showing early escape in non-Gag epitopes. Highlighted in red are sites associated with positive or negative selection of an HLA class I allele. (Carlson et al., 2012; Carlson et al., 2014). M, mother; C, child; neg, negative; pos, positive.

A

SM-like: 517-C

	Subject	Child's age	C*03 Gag ^{296}YL9^{304} YVDRFFKTL	Frequency	B*42 Nef ^{71}RM9^{79} RPQVPLRPM	Frequency	B*42 Gag ^{180}TL9^{188} TPQDLNTML	Frequency
A*68-neg/ B*42-pos/ C*03-neg	517-M	0.25y	•••••••••	100%	•••••••••	100%	••T•••••• ••••••••• ••A••••••	54% 31% 16%
		6y	•••••••••	100%	••••••••••	100%	••A•••••• ••T••••••	73% 27%
A*68-pos/ B*42-pos/ C*03-pos	517-C	0.2y	•••••••••	100%	••••••••••	100%	••••••••••	100%
		2.5y	••••••••• ••••••R••	98% 2%	•••••••••	100%	••••••••••	100%
		5y	••••••••• •••••••V• •••••••A•	58% 39% 3%	•••••••••	100%	••••••••••	100%
		8.5y	•••••••V• ••••••••• ••••••R•• •••••••A•	75% 22% 1.6% 1.5%	•••••••••	100%	••••••••••	100%
HLA association			**HLA-C*03**		**HLA-B*42**		**HLA-B*42**	
Escape variant			**T303X**		**R71X**		**Q182T**	
q value			**4 x 10-18**				**3 x 10-5**	

Table 4.4. Early escape in SM-like child 517-C develops in non-Gag epitopes.

B

SM-like: 517-C

Subject	Child's age	A*30 Pol ^{328}AY9^{366} **AQNPEIVIY**	Frequency	A*30 Env ^{704}IY9^{712} **IVNRVRQGY**	Frequency	A*30 Env ^{794}KY9^{802} **KYLGSLVQY**	Frequency	B*42 Env ^{298}RI10^{307} **RPNNNTRKSI**	Frequency	B*42 Env ^{843}IF9^{851} **IPRRIRQGF**	Frequency	B*15:10 Rev ^{52}IL9^{60} **IHSISERIL**	Frequency
A*30:02-pos/ B*15:10-neg/ B*42:01-pos													
517-M	0.25y	····· ·····	100%	V·R····· V·S····· V····· I·S·····	68% 22% 4% 3%	·····	100%	····· ·····R··	85% 15%	L····· L···V····	86% 13%	·····	100%
	6y	····· ·R····· ·K·····	93% 4% 2%	V·R····· V·RK·····	97% 2%	·····	100%	·····T ·····V ··S·····V ··S·····I	55% 29% 13% 1.6%	L····· L···L···· L···F···· L···V····	36% 29% 29% 5%	·····	100%
A*30:02-pos/ B*15:10-pos/ B*42:01-pos													
517-C	0.2y	····· ·····C	53% 47%	··K·····	100%	····N··L·	100%	·TG····R··	100%	·····L	100%	·RA····· ·RA·····I	94% 6%
	2.5y	····· ·····L···	88% 12%	V·R····· V·RK·····	98.6% 1.2%	····· ····N····	91% 9%	··G····R·· ··G····· ··S·····	51% 40% 9%	L·····	100%	·N····· ·RA····· ·H····· LN·····	76% 12% 10% 1.3%
	5y	·····L··· ····· T····L···	82% 16% 2%	V·R····· ··R·····	86% 13%	····· ····N····	91% 9%	··G····R·· ··G····R·M ··S····R··	82% 14% 2%	L····· L···V····	96% 3%	·N····· ·N·L····· LN····· ·H····· ·RA····· VN·····	59% 17% 11% 7% 4% 2%
	8.5y	·····L··· ····· T····L···	55% 41% 2%	V·R····· V·RK····· ··R·····	97% 1.5% 1.2%	····· ····N····	98% 2%	··G····R·T ··G····R··	69% 31%	L····· L·T····· L···L···· L···F····	49% 21% 17% 14%	LN····· ·N·L····· ·N·····	71% 21% 7%

Table 4.5. Additional HLA-associated escape mutations that developed in SM-like child 517-C.

	Subject	Time point	A*30 Gag ^{76}RY11^{86} **RSLYNTVATLY**	Frequency	A*68 Vpr ^{48}EV10^{57} **ETYGDTWTGV**	Frequency	B*42 Pol ^{743}LI9^{751} **LPPIVAKEI**	Frequency	B*42 Vif ^{48}HI10^{57} **HPKVSSEVHI**	Frequency	B*15:10 Rev ^{65}GL11^{75} **GRPAEPVPLQL**	Frequency
A*30:02-pos/ A*68:02-neg/ B*15:10-neg/ B*42:01-pos/ C*17-pos	517-M	3m	K··F····V··	100%	·······A··	75%	·····R··	86%	··········	73%	···T····F··	80%
					A·····A··	25%	···V·····	6%	·····I··	25%	···T·····	16%
							···V··R··	5%	·····I·V	1.5%	···T···HF··	3%
							··········	3%				
		6y	K··F····V··	100%	A·····A··	64%	···V··R··	68%	·········T	100%	···T····F··	75%
					·····A··	36%	·····R··	25%			···T···SF··	21%
							···V·····	6%			···T···HF··	3%
							··········	1.5%			··LT····F··	1.1%
A*30:02-pos/ A*68:02-pos/ B*15:10-pos/ B*42:01-pos/ C*17-pos	517-C	0.2y	K··F····V··	100%	·····A··	100%	·····R··	100%	··········	100%	·····F··	100%
		2.5y	K·····I·V··	42%	·····A··	55%	·····R··	45%	··········	68%	···T····F··	81%
			K··F····V··	33%	A·····A··	44%	···V·····	38%	N·········	16%	···T·····	13%
			K··F··I·V··	25%			··········	16%	···I·····	15%	··LT····F··	7%
							···V··R··	2%	N··I·····	1.5%		
		5y	K··F··I·V··	34%	·····A··	83%	···V··R··	66%	··········	46%	···T····F··	77%
			K·····IVV··	28%	A·····A·V	9%	·····R··	18%	··R·····	38%	···T···AF··	13%
			K··F····V··	24%	·····A·V	7%	···V·····	10%	···I·····	14%	···T···SL··	4%
			K·····I·V··	13%			··········	6%	··RI·····	2%	··LT····F··	2%
											···T···DF··	1.7%
											···T·····	1.6%
		8.5y	K·····IVV··	42%	·····A··	57%	···V··R··	42%	··········	56%	···T····F··	100%
			K··F··I·V··	32%	A·····A·V	41%	·····R··	35%	··R·····	31%		
			K··F····V··	24%			···V·····	14%	···I·····	13%		
			K·····I·V··	2%			··········	9%				
HLA association			**HLA-A*30**				**HLA-B*42**		**HLA-B*42**			
Escape variant			**303R**				**I746V**		**K749R**			
q value			**2 x 10-5**				**5 x 10-13**		**1 x 10-13**			

517-M indicates mother of the child 517-C. Frequency represents percentage at which a particular haplotype is present at the indicated timepoint. Pos, positive; neg, negative

In the other SM-like child, 021-C, escape in the Gag-TL9 epitope was observed but only relatively late, no epitope variants being evident at 2.6 years (**Table 4.6**). Early escape within 2 months of birth was evident at low frequency of only 2% within the immunodominant HLA-A*29:02-restricted epitope, Env-SY9 (SFDPIPIHY, Env 206-217), HLA-A*29:02 not being expressed in the mother 021-M. This low frequency variant was ultimately replaced by a variant at the P1 residue, characteristic of escape in this epitope. There were no other instances of early escape identified in this child's viral sequences, although many escape mutants were transmitted and in this mother-child pair 5 of the 6 HLA class I molecules were shared.

Thus, in the VC-like child 133-C there was evidence of strong selection pressure within the first 3 months of life, with broad Gag-specific CD8+ T-cell responses generated (i.e. responses to HLA-A*74-Gag-SK10 and HLA-B*81-Gag-TL9) and escape mutants within Gag, Pol and Nef, all reaching fixation in that time. In contrast, although escape mutants were selected within the same time period in the two SM-like children 517-C and 021-C, these were mostly in Env, and none were in Gag. These data are consistent with the notion of control of broad Gag-specific CD8+ T-cell responses contributing to lower viraemia in early paediatric infection, as previously shown in adult infection.

A

SM-like: 021-C

Subject	Child's age	A*29 Env ^{206}SY9^{217} **SFDPIPIHY**	Frequency	A*02 Pol ^{282}YI9^{290} **YTAFTIPSI**	Frequency	B*42 Gag ^{180}TL9^{188} **TPQDLNTML**	Frequency	B*42 Nef ^{128}TL10^{137} **TPGPGVRYPL**	Frequency
A29-neg/ A*02-pos/ B*42-pos									
021-M	-42d	··········	100%	·····V ······	98.6% 1.4%	····· ··T···	61% 39%	····· ·····	100%
021-M	5y	··········	100%	·····V	100%	·····		·····	100%
A*29-pos/ A*02-pos/ B*42-pos									
021-C	0.1y	····· ··N···	98% 2%	·····V	100%	·····	100%	·····	100%
021-C	2.6y	T···	99%	·····V ·····	98% 2%	·····	100%	·····	100%
021-C	4.9y	T···	100%	·····V ·····	95% 5%	··T··· ·····	72% 28%	·····	100%
021-C	7.6y	T···L···	100%	····· ·····V	50% 50%	··T··· ·····	89% 11%	·····	100%
HLA association				**HLA-A*29**		**HLA-B*42**		**HLA-B*42**	
Escape variant				**I290V**		**Q182T**		**P129X**	
q value				**9 x 10-3**		**3 x 10-5**		**0.12**	

B

Subject	Child's age	B*42 Vpr ^{34}FL9^{42} **FPRPWLHGL**	Frequency	B*42 Vif ^{48}HI10^{57} **HPKVSSEVHI**	Frequency	B*42 Env ^{298}RI10^{307} **RPNNNTRKSI**	Frequency	A*02 Pol ^{464}IV9^{472} **ILKEPVHGV**	Frequency
A29-neg/ A*02pos/ B*42-pos									
021-M	-42d	···V····· ···M····· ····· ···V···S·	71% 14% 12% 2%	N····· ····· ···I····· ···L·····	41% 25% 23% 10%	··G·····	100%	····· ·····A	96% 4%
021-M	5y	···V·····	99%	N····· ···I····· ·····	62% 29% 8%	··G····· ··D·····	97% 2%	·····A ····· ··Q·····A ··Q·····	75% 22% 1.6% 1.4%
A*29-pos/ A*02-pos/ B*42-pos									
021-C	0.1y	···M·····	100%	···L·····	100%	··G·····	100%	·····	100%
021-C	2.6y	···M····· ···T·····	98.7% 1.3%	···L····· ·····	95% 5%	··G·····	100%	·····	100%
021-C	4.9y	···V····· ···A····· ···M····· ···T····· ···V··Q··	54% 32% 10% 3% 1.2%	···L····· ····· ·····I·· ···I·····	62% 24% 9% 5%	·HG····· ··G·····	63% 36%	·····A ·····	66% 33%
021-C	7.6y	···V····· ···V···S· ···M····· ···A·····	44% 39% 9% 6%	···I····· ·····I·· ···L····· ····· ··RI·····	39% 28% 23% 6% 2%	·HG····R·· ·YG····R·· ·HG·····	80% 14% 5%	·····A ·····	96% 4%

Table 4.6. Sequence evolution in the SM-like child 021-C. A. Sequences of dominant CD8+ T-cell responses. Escape in the dominant HLA-B*42-Gag-TL9 develops only by 5 years of age. **B.** Sequences of epitopes showing variant had been transmitted by the mother, who shares 5 out of 6 HLA class I alleles with the child. Highlighted in grey are footprints associated with the HLA class I allele indicated below the table; known escape variants and q values indicating significance of an HLA-polymorphism association are shown (Carlson et al., 2014). Highlighted in red are sites associated with positive or negative selection of an HLA class I allele. (Carlson et al., 2012, Carlson et al., 2014). M, mother; C, child; neg, negative; pos, positive.

4.4 Discussion

In this study, we sought to investigate the role of HLA-associated CD8+ T-cell activity in paediatric non-progressing HIV infection. Using state-of-the-art deep-sequencing technology, we examined the evolution of CD8+ T-cell selection pressure on the virus in association with HIV-specific CD8+ T-cell responses in the first decade of life in 11 ART-naïve PSPs. Our findings suggest that two broadly distinct immune strategies exist in non-progressing paediatric infection: adult viraemic controller (VC)-like CD8+ T-cell-mediated suppression of viraemia; and a sooty mangabey (SM)-like approach, in which high viraemia is associated with a minimal role of CD8+ T-cells.

We have followed the evolution of the CD8+ T-cell selective anti-HIV pressure from birth in the very first years of life in a group of therapy-naïve PSPs. Under the current ART-initiation recommendations (Lundgren et al., 2015; WHO, 2015b), it would be impossible to establish such a cohort and study the natural cellular response in a therapy-free context. The longitudinal follow-up in combination with the technology available >13 years after study initiation allows us to gain a much more comprehensive picture of the successful immune response compared to a cross-sectional snapshot at a singular timepoint. The second aspect is that we know exactly who the donor is (i.e. the transmitting mother) and

what immune pressure the virus had been pre-exposed to prior to transmission. The combination of deep sequencing and availability of the maternal donor allows one to determine with a high degree of certainty the selection that is operating in the child, even when HLA types are shared between mother and child.

There are two main findings from this study. The first is the differential HIV protein specificity of the CD8+ T-cell response among VC-like and SM-like non-progressing children, respectively. In the SM-like children, there are significantly broader and higher frequency responses towards Nef and other non-Gag proteins, such as Env and the accessory/regulatory proteins. These non-Gag responses have previously been associated with poor control of viral load, so this is consistent with the high viraemia among the SM-like children.

The second main finding here is the unexpected demonstration that in both groups of children strong selection pressure on the virus can be exerted by the CD8+ T-cell response in the first days and weeks of life. In the VC-like group, there is strong evidence of Gag-specific escape in the first days and weeks of life, whilst among the SM-like children there is greater evidence of escape among non-Gag epitopes. These observations, as stated above, are made possible by the deep sequencing and access to mother-child transmission pairs. Several previous studies have shown some evidence of early CD8+ T-cell-driven escape in the first weeks and months of life (Leslie et al., 2004; Pillay et al., 2005; Sanchez-Merino, Nie, and Luzuriaga, 2005). However, these studies did not examine full-length HIV, or employ deep sequencing with the resolution depth of hundreds and thousands of reads; as a result, especially in cases where mother and child shared the same restriction element it was not possible to be certain that the escape mutation arose in the child. Furthermore, although two examples of escape mutants being

generated in the first 2-3 months of life in some children have been described (Sanchez-Merino et al., 2005), since these studies did not involve full-length virus, the extent of early escape among all groups of HIV-infected children has not been recognised. In the current studies that have followed the children through the first decade of life, it has thus been possible to identify differential patterns of CD8+ T-cell targeting among the two groups identified here (VC-like and SM-like) of non-progressing children. The perception of the immune response in the first weeks of life as being incapable of antiviral efficacy therefore needs to be revised substantially in the light of these data. This is important both to reinforce the benefits of very early ART to limit selection of escape mutations even in children, and also to highlight the potential for T-cell vaccines even in early life to induce effective HIV-specific T-cell responses in children as part of strategies to eradicate the HIV reservoir.

Previous studies of the role of CD8+ T-cells in perinatal HIV infection, particularly in non-progressing infection, have been inconclusive and sparse. HLA was shown to have limited impact on disease progression (Adland et al., 2015). Some benefit to the child was gained if the mother expressed an unshared protective HLA allele and transmitted a pre-adapted virus with lower replicative capacity (Prado et al., 2010; Thobakgale et al., 2009), and no benefit to the child was gained if both the child and the mother shared a protective HLA because the virus may have already been pre-adapted in the key epitopes in the mother prior to transmission, compromising child's potential to generate an effective response to those epitopes (Goulder et al., 2001b). A genomic study examined the association of SNPs (in 17 host genes), previously shown or hypothesised to alter HIV disease progression, with HIV viral load and CD4+ T-cell count in >1,000 vertically infected children in the United States (Qin et al., 2014). They reported a significant association of HLA-B*57/B*27/B*14 (protective in adult infection) with lower viral loads prior to ART

initiation in this paediatric cohort, but the cohort was comprised of symptomatic children of a wide age range from 42 days to 18 years (Qin et al., 2014). In an earlier analysis of a subgroup of this cohort (n=572), HLA-B*27 and HLA-C*02 expression was associated with slow disease progression; HLA-B*27 expression was also associated with protection against CNS impairment, while HLA-A*24 expression predisposed to more rapid CNS impairment (Singh et al., 2011), suggesting at least some role of HLA class I expression in paediatric disease progression. However, none of these studies addressed more directly HLA-associated CD8+ T-cell selection pressure on the virus and its evolution from birth to >5 years in non-progressing paediatric infection.

Similarly, inconclusive observations have been made in terms of the role of HIV-specific CD8+ T-cell responses. Antiviral CD8+ T-cell responses are detected in some children from birth, but are usually less frequent and lower in magnitude than in adolescents or adults (Scott et al., 2001; Shalekoff et al., 2009; Thobakgale et al., 2007), tend to target Env and Nef versus Gag (Huang et al., 2008; Shalekoff et al., 2009) and neither breadth nor magnitude at the age 1 month correlates with survival (Lohman et al., 2005). Higher Gag-specific versus Env-specific responses were found in infants who survived to 1 year (Nqoko et al., 2011); Gag-specific CD8+ T-cell breadth and magnitude inversely correlated with viral load in one study (Huang et al., 2008), but not in another (Prendergast et al., 2011).

In our study, we found that in some PSPs (the VC-like group) HLA-restricted CD8+ T-cells exert strong selection pressure on the virus from the first months of life by targeting key viral epitopes, similar to adult viraemic controllers; in other PSPs (the SM-like subset) CD8+ T-cell responses target a variety of epitopes in Env, Nef and other accessory and regulatory proteins but ignore Gag that is typically a more successful target and generate

dominant responses to non-HLA-B-restricted epitopes – very different from adult slow progression, in whom with a few exceptions HLA-B-restricted Gag responses dominate (Kiepiela et al., 2004). In this latter SM-like group of children, HLA-restricted CD8+ T-cell activity appears to contribute minimally to slow progression; and disease protection is more likely to result from other factors, such as low immune activation and low CCR5 expression, similar to the natural hosts of SIV sooty mangabey (Adland et al., 2014). At least in some of these SM-like children CD8+ T-cells start to exert stronger pressure through HLA-associated selection of mutations in Gag epitopes later in life, ≥5 years, consistent with the age-related immunological maturation, although in 517-C Gag selection occurs in an HLA-C-restricted epitope and the key HLA-B*42:01-restricted epitope Gag-TL9 remains wildtype until at least the age of 8.5 years. The main observation here is however, that neither in 517-C nor in 021-C any of these escape mutations appear to affect viral load, again pointing to the discordancy between CD8+ T-cell activity, high viraemia and non-progression.

Among the VC-like PSPs protective HLA alleles were not enriched, albeit a very small group of children was studied here. However, these findings were consistent with those of a larger cohort of 256 ART-naïve children in whom these same protective HLA alleles were also not related to viral load (Adland et al., 2015). It is possible that the expression of an unshared with the mother protective allele plays a role, as was observed in 133-C expressing protective HLA-B*81:01 and selecting the key escape mutation by 1.3 years of age. The findings of apparently effective Gag-specific responses restricted by the protective HLA-B*81:01 in some children, such as 133-C here, and ineffective Gag-specific responses restricted by protective alleles such as HLA-B*57/58:01 in others (Adland et al., 2015) suggest the hypothesis that factors other than HLA play a critical role, and that even in the VC-like PSPs there is something intrinsically different about CD8+ T-cells, so that

even at a young age they can drive viraemia down independent of the particular HLA class I molecules expressed. This hypothesis is supported by the fact that in adult infection, non-HLA qualitative characteristics of CD8+ T-cell function have been reported to be the distinguishing factors between elite controllers and progressors and that not all adult controllers express HLA-B*57/27 (Migueles et al., 2015). Thus it will be informative to examine functional quality and phenotype of HIV-specific CD8+ T-cells from the VC-like PSPs in terms of their suppressive capacity, proliferative potential, expression of cytolytic granzyme B and perforin, as well as exhaustion and activation profiles, how all these functions evolve from birth and how they compare to those of SM-like PSPs and rapid progressors.

The replicative capacity of perinatally transmitted viruses is also a potentially important factor in influencing paediatric disease outcome. In a small study of 5 slow progressor children and 3 progressors, lower viral replication, linked largely to the inheritance of HLA-B*57/58:01-associated Gag mutations, was associated with slower paediatric progression (Prado et al., 2010). In the larger cohort study (Adland et al., 2015), viral replicative capacity was also shown to play a part in paediatric progression. However variation in CD4 count in non-progressor children was only weakly associated with viral replicative capacity, and factors other than viral fitness would appear to play a more critical role in most cases.

In conclusion, we show two distinct phenotypes in paediatric non-progressing HIV infection with contrasting impact of antiviral CD8+ T-cell response. Future detailed characterisation of CD8+ T-cell function in PSPs of both phenotypes will shed more light on the mechanisms of paediatric HIV disease control. As WHO guidelines now support ART initiation for all HIV-infected children, irrespective of age or CD4 count, the relevance of these studies turns towards the issue of HIV Cure. Since HIV-specific CD8+ T-cells are

likely to play a critical role in strategies designed to bring about viral eradication (Deng et al., 2015), a better understanding of the HIV-specific CD8+ T-cell responses that are generated in children prior to ART initiation and their ability to kill virus-infected cells will be directly relevant to future immunotherapeutic interventions developed with the aim of achieving paediatric cure.

CHAPTER 5. LOWER VIRAL LOADS AND SLOWER CD4 DECLINE IN MRKAD5 HIV VACCINEES EXPRESSING DISEASE-SUSCEPTIBLE HLA-B*58:02

[This work has been published in: **Leitman, E.M**, Hurst, J., Mori, M., Kublin, J., Ndung'u, T., Walker, B.D., Carlson, J., Gray, G.E., Matthews, P.C., Frahm, N., Goulder, P.J.R. **2016**. Lower Viral Loads and Slower CD4 Decline in MRKAd5 HIV-1 Vaccinees Expressing Disease-Susceptible HLA-B*58:02. *J. Infect. Dis.* Pii: jiw093. Epub ahead of print.]

5.1 Introduction

HLA class I alleles are an important predictor of disease course in HIV-1 infection (Goulder and Walker, 2012). In sub-Saharan Africa, HLA-B*57, HLA-B*58:01, and HLA-B*81:01 are protective against disease progression, while HLA-B*18:01 and HLA-B*58:02 are associated with rapid progression (Carlson et al., 2012; Kiepiela et al., 2004; Leslie et al., 2010). One contributory factor is the role of HLA molecules in presenting particular epitopes to induce CD8+ T-cell responses against HIV-1. Gag-specific CD8+ T-cell responses are associated with lower viraemia and are dominant in people with protective HLA alleles, such as HLA-B*57:03 (Goulder and Walker, 2012; Kiepiela et al., 2007). In contrast, disease-susceptible HLA alleles, such as HLA-B*58:02, typically present relatively ineffective non-Gag responses (Ngumbela et al., 2008) associated with high viral setpoints (Kiepiela et al., 2007).

This prompts the hypothesis that a successful vaccine might induce Gag-specific responses in subjects who would not target this protein in natural infection. Two recent

randomised efficacy trials of the MRKAd5 subtype B HIV-1 Gag/Pol/Nef T-cell vaccine provide a unique opportunity to address this question (Buchbinder et al., 2008; Gray et al., 2014).

The first study, Step, was conducted in the Americas, Australia, and the Caribbean, where HIV-1 subtype B predominates (Buchbinder et al., 2008). Both interim and follow-up analyses reported vaccine-enhanced HIV-1 acquisition (Buchbinder et al., 2008; Duerr et al., 2012). The second trial, Phambili, tested the efficacy of the same vaccine in South Africa, where HIV-1 subtype C is endemic (Gray et al., 2011; Gray et al., 2014). Following Step discontinuation, Phambili was terminated 9 months into the study, having enrolled 801 subjects (27%) of the originally scheduled 3,000 (Gray et al., 2011). As in Step, the vaccine increased risk of HIV-1 acquisition and did not reduce viraemia in early infection (Gray et al., 2011; Gray et al., 2014).

Post-hoc Step studies, however, demonstrated lower viraemia in vaccinees with greater breadth of Gag-specific CD8+ T-cell activity (Janes et al., 2012), consistent with the notion of Gag-specific efficacy, but also suggested the possibility of lower viral loads in vaccinees expressing protective HLA alleles (Altfeld and Goulder, 2011; Fitzgerald et al., 2011). In order to examine this question in a population substantially dissimilar in the HLA alleles expressed from that studied in Step, we here tested in the South African Phambili cohort the hypothesis that the MRKAd5 HIV-1 vaccine might indeed have an HLA-specific effect.

Specifically, we hypothesised that subjects expressing HLA-B*58:02, the most prevalent HLA-B allele in South Africans (Kiepiela et al., 2004; Kiepiela et al., 2007), might benefit from the MRKAd5 HIV-1 vaccine. The rationale was that the HLA-B*58:02-restricted CD8+ T-cell response is solely Env-specific, and therefore associated with poor immune control

(Kiepiela et al., 2007; Troyer et al., 2009); HLA-B*58:02 indeed is strongly associated with rapid HIV-1 disease progression in Southern Africa (Kiepiela et al., 2004; Leslie et al., 2010; Ngumbela et al., 2008). Hence, vaccine-mediated induction of Gag-specific responses in subjects expressing HLA-B*58:02 would, hypothetically, improve disease course in vaccinees who subsequently became HIV-1-infected. HLA-B*18:01, also strongly associated with rapid progression (Kiepiela et al., 2004; Leslie et al., 2010), restricts a dominant CD8+ T-cell epitope in Nef (Kiepiela et al., 2007). Although Nef-specific CD8+ T-cell responses have also been associated with poor control of HIV-1 (Betts et al., 2001; Kiepiela et al., 2007; Masemola et al., 2004; Novitsky et al., 2003), the immunodominance of the HLA-B*18:01-restricted CD8+ T-cell response might be unaffected by the MRKAd5 HIV-1 Gag/Pol/Nef vaccine.

We set out, therefore, to investigate the impact of the MRKAd5 HIV-1 vaccine in the Phambili trial, particularly on the HLA-B*58:02-expressing individuals, to determine whether immune control of HIV-1 was improved in vaccinees who subsequently became infected. This study has limitations that we wish to highlight, including post-randomisation bias, sample selection bias, and low subject numbers (see Discussion, section 5.4), but it provides potentially important insights into HLA-dependent vaccine effects on post-infection disease course and immune response to HIV-1.

5.2 Chapter-specific methods

5.2.1 Study design

Phambili Ancillary study investigated HLA-specific effects on disease progression and CD8+ T-cell immune responses in the Phambili trial participants who subsequently became HIV-1-infected. Phambili, described previously (Gray et al., 2011; Gray et al.,

2014), was a double-blind placebo-controlled randomised phase 2b trial that enrolled 801 heterosexual HIV-1-negative South Africans aged 18-35 years, from January to September 2007 (ClinicalTrials.gov: NCT00413725, South African Research Database: DOH-27-0207-1539). There were 100 HIV-1 infections diagnosed after enrolment in the Phambili cohort by 42 months follow-up (**Figure 5.1**) (Gray et al., 2014). Sixty of them, for whom HLA types, PBMC, viral load, and CD4 data were available, comprise the focus of this report (**Table 5.1**). For the remaining 40 individuals, no PBMC were available to assess CD8+ T-cell responses, thus only selected viral load and CD4 data were included in additional analyses; material for HLA typing was available for 25 participants.

Subjects were categorised according to their HLA-B expression: 'Protective' (HLA-B*57:02/57:03/58:01/81:01); 'Disease-susceptible' (HLA-B*18:01/58:02); and 'Neither Protective nor Disease-susceptible' (e.g. HLA-B*42:01/44:03) (Kiepiela et al., 2004; Leslie et al., 2010). We compared viral loads, CD4+ T-cell counts and HIV-1-specific CD8+ T-cell responses (blinded to the vaccine/placebo treatment assignment) between vaccinees and placebo-recipients within each HLA group. For the most prevalent HLA-B allele, HLA-B*58:02 (phenotypic frequency 23%), there were sufficient subject numbers to compare vaccinees (n=7) to placebo-recipients (n=7).

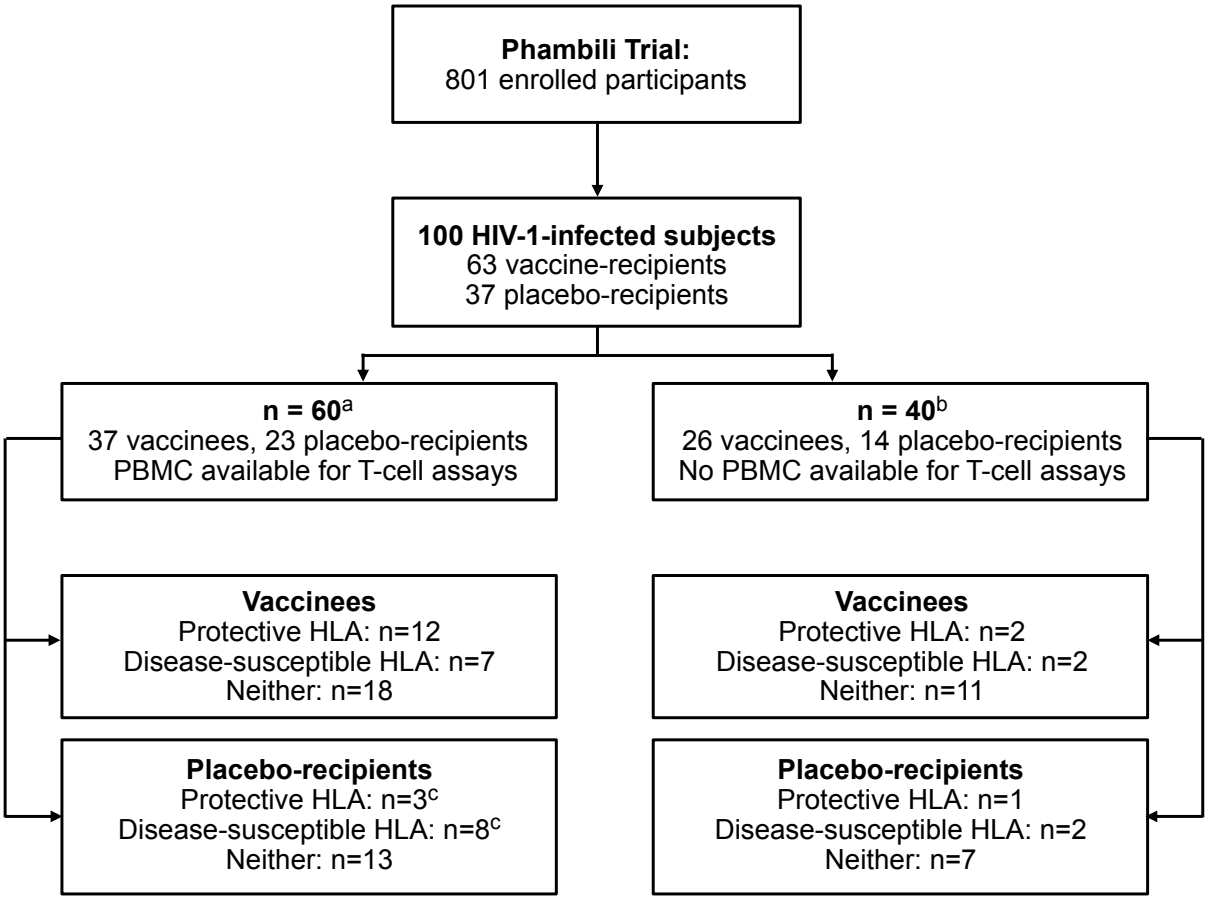


Figure 5.1. Phambili ancillary study profile. [a] These 60 subjects are presented in Tables 5.1 and 5.2. [b] Material available for HLA typing on 25 subjects. [c] One placebo-recipient, co-expressing protective HLA-B*58:01 and disease-susceptible HLA-B*58:02, is included in both HLA subsets in this figure.

To identify associations between HLA expression and recognition of HIV-1-specific peptides, we used ELISPOT data from 1,031 untreated subjects with chronic natural HIV-1 infection from the previously described Sinikithemba (enrolled in 2003-2008) and Gateway (enrolled in 2012-2013) cohorts in Durban, South Africa (Kiepiela et al., 2007; Payne et al., 2014) (see Chapter 2, section 2.1 for cohort details). Median viral load in these subjects was 25,700 [3,690-119,000] copies/ml; median CD4 count was 404 [273-549] cells/mm^3. PBMC from each individual were screened with a panel of peptides spanning the entire C-clade 2001 consensus sequence (Kiepiela et al., 2007) and analysed (section 5.2.3).

To compare the CD8+ T-cell responses in the HLA-B*58:02-positive South African Phambili subjects with HLA-B*58:02-positive South African subjects naturally infected with HIV-1, we used ELISPOT data from 66 HLA-B*58:02-positive subjects from the Sinikithemba cohort as individuals in both groups would have had similar geographical location, genetic background, timing of infection and infection with similar/related viral species (**Table 5.2**).

Table 5.1. Baseline characteristics[a] of the 60 infected Phambili participants studied in this report.

Characteristic	Vaccine (n=37, 62%)	Placebo (n=23, 38%)	Total (n=60)
Age at enrollment (years), median (IQR)	24 (21.5-28.5)	24 (22-32)	24 (22-29)
Sex (n)			
Female	21 (57%)	18 (78%)	39 (65%)
Male	16 (43%)	5 (22%)	21 (35%)
Study site (n)			
Soweto, Johannesburg	15 (41%)	7 (30%)	22 (37%)
Emavundleni, Cape Town	8 (22%)	6 (26%)	14 (23%)
CAPRISA, Klerksdorp	5 (14%)	4 (17%)	9 (15%)
eThekwini, Durban	7 (19%)	3 (13%)	10 (17%)
Medunsa, Polokwane	2 (5%)	3 (13%)	5 (8%)
Timepoint 1: months since diagnosis, median (IQR)	2 (1-2.5)	2 (1-3)	2 (1-3)
Timepoint 2: months since diagnosis, median (IQR)	12 (11-12)	11 (11-12)	12 (11-12)
Duration of follow-up data, months since diagnosis, median (IQR)	17 (16-18)	17 (16-19)	17 (16-18)
Started on ART	5 (14%)	6 (26%)	11 (18%)
HLA[b]			
Protective	12 (32%)	3 (13%)	15 (25%)
B*57:03	2 (5%)	0 (0%)	2 (3%)
B*58:01	7 (19%)	3 (13%)	10 (17%)
B*81:01	4 (11%)	0 (0%)	4 (7%)
Disease-susceptible			
B*18:01	0 (0%)	1 (4%)	1 (2%)
B*58:02	7 (19%)	7 (30%)	14 (23%)
Neither Protective nor Disease-susceptible	18 (49%)	13 (57%)	31 (52%)
Early viral setpoint[c] (copies/ml), median (IQR)	41,850 (3,675-234,075)	88,500 (11,485-238,500)	71,700 (6,475-238,500)

[a] There were no significant differences between vaccine and placebo groups for any of the characteristics. IQR denotes interquartile range.

[b] HLA types were grouped by their association with disease progression as specified in section 5.2.1.

[c] Early viral setpoint defined as the median of HIV-1 viral load measurements at 2-3 months post-diagnosis as specified in section 5.2.3.

Table 5.2. Characteristics of the unvaccinated ART-naïve HLA-B*58:02-positive C-clade infected subjects outside of the trial (n=66).

Characteristic	N (%)
Sex	
Female	52 (79%)
Male	10 (15%)
Unknown	4 (6%)
Country of origin	
South Africa	54 (82%)
Zimbabwe	8 (12%)
Somalia	2 (3%)
Malawi	1 (1.5%)
Kenya	1 (1.5%)
Year of enrolment[a]	
2003	19 (29%)
2004	18 (27%)
2005	14 (21%)
2006	3 (4.5%)
2007	6 (9%)
2008	6 (9%)
Age at enrolment (years), median (IQR)	31 (27-35)
Viral load (copies/ml), median (IQR)	52,850 (9,678-229,250)
CD4 count (cells/mm^3), median (IQR)	337 (227-431)

[a] CD8+ T-cell ELISPOT assays, viral load and CD4+ T-cell measurements were performed at enrolment. IQR denotes interquartile range.

5.2.2 Interferon-γ ELISPOT assays

We screened PBMC from the 60 subjects with available cells, to quantify IFN-γ ELISPOT responses to pools (n=36) of overlapping peptides spanning the entire C-clade HIV-1 proteome based on 2001 C-clade consensus (Kiepiela et al., 2007). For each subject, cells from 2 and 12 months post-diagnosis (**Table 5.1**) were tested (Addo et al., 2003; Altfeld et al., 2000). Responses were divided into four groups: specific to Gag, Pol, Nef, or other

(Env/Tat/Rev/Vpu/Vpr/Vif) proteins. Spots were counted using an automated ELISPOT reader (AID ELISPOT v4.0, Autoimmun Diagnostika, Germany). Breadth was defined as the number of pools testing positive (>50 SFC/10^6PBMC after background subtraction). All assays were carried out blinded to the vaccine/placebo treatment assignments. For the 60 Phambili subjects, for whom cells were available, PBMC from 59 were screened because cells from one placebo-recipient were not viable upon thawing. Additionally, CD8+ T-cell responses of five subjects at the second timepoint were excluded from the analyses because ART had been initiated.

5.2.3 Statistical analysis

Baseline characteristics (**Table 5.1**) between vaccine- and placebo-recipients were analysed using Mann-Whitney U test or Fisher's Exact test (Prism v5.0c).

Only pre-ART viral loads were used. Early viral setpoint was defined as the geometric mean of HIV-1 viral load measurements at 2-3 months post-diagnosis (Buchbinder et al., 2008; Gray et al., 2011). HIV-1 plasma viral load limits of detection were 400 and 1,000,000 copies/ml. In order to determine viral setpoint more accurately, we also defined long-term chronic setpoint as the median of all pre-ART viral load values available in five ways: i) including the diagnostic (acute) measurement; (ii) excluding the diagnostic measurement; (iii) including all measurements from >2 weeks post-diagnosis; (iv) including all measurements from >1 month post-diagnosis; or (v) including all measurements from >3 months post-diagnosis. Chronic setpoints were very similar irrespective of the definition and results using definition (v) are reported here as this may most accurately reflect the beginning of the chronic phase (Gounder et al., 2015; Wright et al., 2011). Setpoint differences between vaccinees and placebo-recipients were analysed using Mann-Whitney U test (Prism v5.0c).

Linear mixed-effects models were constructed to investigate the effects of vaccination, sex, age, Ad5 antibody levels, and HSV-2 serostatus on longitudinal viraemia. Random intercept models were constructed with the grouping by participant ID in R using the lme4 library (Bates, 2014); p values were obtained by comparing models with and without vaccination as a fixed effect (ANOVA) (Long, 2012). Linear mixed effects models were constructed and alanysed by Dr. Jacob Hurst (University of Oxford, UK).

The log-rank test (Prism v5.0c) and univariate Cox regression models (SPSS v22.0) were used to compare time to disease progression between vaccine and placebo groups, defined by CD4<350/mm^3, the WHO CD4+ T-cell criterion for ART initiation (WHO, 2008). Only pre-ART CD4 counts were included; impact of sex/age/Ad5 antibody levels/HSV-2 serostatus was checked.

Differences in ELISPOT responses between vaccinees and placebo-recipients were analysed in Prism v5.0c by Mann-Whitney U test (two-group analyses) or Kruskal-Wallis test (three-group analyses).

We used a decision tree based on Fisher's Exact Test to identify associations between expression of HLA alleles and recognition of HIV-1-specific peptides, as previously described (Kloverpris et al., 2012a) (performed by Dr. Jonathan Carlson, Microsoft Research, Redmond, WA, USA). For each peptide, we computed the Fisher's Exact Test p-value against all four-digit HLA alleles observed in the Sinikithemba and Gateway cohorts and added the most significant HLA allele to the decision tree. We next removed all individuals who expressed that allele and repeated the process until the most significant HLA allele had a p-value of >0.2. False-discovery rates (Benjamini, 1995) were calculated

using a procedure-specific to Fisher's Exact Test that analytically computes the null distribution for all permutation of the data, as previously described (Carlson, 2009).

Spearman correlation analyses of breadth or magnitude of CD8+ T-cell responses with either viral loads or CD4 counts were performed in Prism (v5.0c, GraphPad).

5.3 Results

5.3.1 HLA-independent vaccine effects

We first compared the baseline characteristics between vaccine- and placebo-recipients in the selected subgroup of 60 subjects for whom PBMC were available to test the impact of the MRKAd5 HIV-1 vaccine on post-infection CD8+ T-cell activity. These showed no significant differences in age, gender, HLA-B genotype, or early viral setpoint (**Table 5.1**). As previously reported (Buchbinder et al., 2008; Gray, Buchbinder, and Duerr, 2010; Gray et al., 2011), early viral setpoint did not differ significantly between vaccine- and placebo-recipients, in these 60 patients (early setpoint: 41,850 [3,657-234,075] versus 88,500 [11,485-238,500] copies/ml, p=0.34; **Table 5.1**). We observed a trend towards a lower chronic setpoint in vaccinees in the 60 subjects (median 12,055 [3,805-137,500] versus 103,600 [9,190-141,800], p=0.055; **Figure 5.2A**). However, this difference did not reach statistical significance, even when all the viral load data were analysed using a linear mixed-effects model (p=0.058, **Figure 5.2B**). It is important to take note of the fact that 12 of the vaccinees expressed protective alleles (HLA-B*57/58:01/81:01) versus 3 of the placebo recipient, although this also did not reach statistical significance (p=0.13). Additionally, there was no significant difference in time to disease progression (CD4<350/mm^3) between vaccine and placebo groups (p=0.25, **Figure 5.2C**).

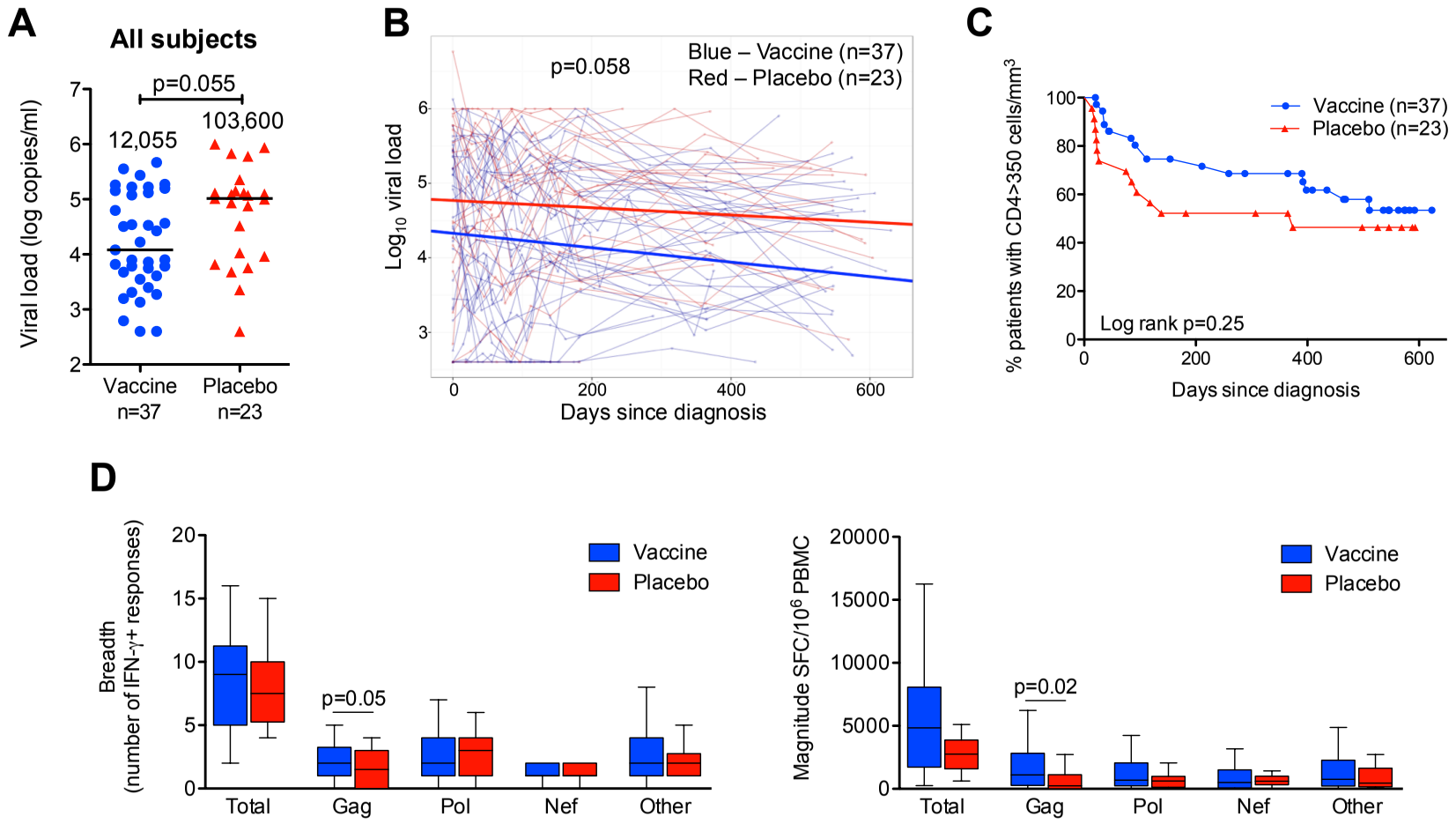

A
All subjects
p=0.055
12,055
103,600
Viral load (log copies/ml)
Vaccine n=37
Placebo n=23
B
p=0.058
Blue – Vaccine (n=37)
Red – Placebo (n=23)
Log10 viral load
Days since diagnosis
C
Vaccine (n=37)
Placebo (n=23)
% patients with CD4>350 cells/mm3
Log rank p=0.25
Days since diagnosis
D
Breadth (number of IFN-γ+ responses)
Vaccine
Placebo
p=0.05
Total
Gag
Pol
Nef
Other
Magnitude SFC/10^6 PBMC
p=0.02

Figure 5.2. Longitudinal viraemia, CD4+ T-cell counts, and CD8+ T-cell responses in the 60 infected vaccinees and placebo-recipients, irrespective of HLA. A. Chronic viral setpoint (defined for each individual as the median of all measurements from >3months post-diagnosis). Each patient's setpoint is shown as blue circles (vaccine-recipients) or red triangles (placebo-recipients), horizontal lines and numbers denote median values; Mann-Whitney U test. **B.** Examination of the effect of vaccination on longitudinal pre-ART viraemia: the slopes (thick lines) generated from a linear mixed-effects model are plotted on top of the individual patient's data points and viral load trajectories (thin lines). Vaccinees (n=37) are in blue, placebo-recipients (n=23) are in red; ANOVA. **C.** Kaplan-Meier curves showing time to reach CD4<350 cells/mm^3 in vaccinees (blue) and placebo-recipients (red); log-rank test. **D.** Breadth and magnitude of CD8+ T-cell responses at the second timepoint in vaccinees (blue bars) and placebo-recipients (red bars); Tukey box-and-whisker plots: horizontal lines indicate median values, boxes show IQR, whiskers show minimum and maximum; Mann-Whitney U test. 'Total' is combined values of responses to all proteins; 'Other' includes responses to Env/Rev/Tat/Vpu/Vif/Vpr.

Examining the impact of the MRKAd5 HIV-1 vaccine on CD8+ T-cell IFN-γ responses post-infection in Phambili subjects with available PBMC, we observed that vaccinees had significantly higher Gag-specific breadth and magnitude than placebo-recipients (p=0.03 and p=0.02, respectively, at 2m post-diagnosis; and p=0.05 and p=0.02, respectively, at 12m post-diagnosis; **Figure 5.2D**). These assays were undertaken blinded to the subjects' vaccination assignments. There was no difference between the two groups in the responses towards proteins not included in the vaccine (Env/Vif/Vpr/Vpu/Tat/Rev). However, there was no significant difference in the Pol- or Nef-specific responses between vaccine- and placebo-recipients either, despite *pol*/*nef* inclusion in the vaccine.

5.3.2 HLA-specific vaccine effects on viral load and CD4+ T-cell counts: Protective HLA alleles

To investigate whether these vaccine-mediated effects on the CD8+ T-cell responses were associated with HLA-specific immune control, as observed for protective HLA alleles in the

Step trial (Fitzgerald et al., 2011), we first compared chronic viral setpoints and time to CD4<350 cells/mm^3 in the subset of infected Phambili subjects expressing any of the protective alleles HLA-B*57/58:01/81:01 (**Table 5.3**). Although subject numbers provided limited power (three placebo-recipients versus 12 vaccinees expressed HLA-B*57/58:01/81:01), nonetheless there was evidence of vaccine-mediated immune protection through these HLA alleles (**Figures 5.3A,B**), with significantly more rapid time to disease progression (CD4<350/mm^3), in placebo-recipients (p=0.009). Placebo-/vaccine-treatment assignment was the only significant contributor to this difference, in a univariate analysis that included sex, age, Ad5 antibody levels, and HSV-2 status (**Table 5.4**).

Table 5.3. Demographic table[a] stratified by HLA groups.

	Protective HLA		Neither Protective nor Disease-susceptible HLA		Disease-susceptible HLA-B*58:02	
Characteristic	**Vaccine (n=12)**	**Placebo (n=3)**	**Vaccine (n=18)**	**Placebo (n=13)**	**Vaccine (n=7)**	**Placebo (n=7)**
Age at enrolment (years), median (IQR)	25.5 (22.5-30.5)	32 (22-32)	22.5 (21.5-30.5)	23 (22-26)	22 (21-27)	26 (21-34)
Sex (n)						
Female	7 (58%)	3 (100%)	9 (50%)	10 (77%)	5 (71%)	5 (71%)
Male	5 (42%)	0 (0%)	9 (50%)	3 (23%)	2 (29%)	2 (29%)
Circumcision status (for men) (n)						
Circumcised[b]	2 (40%)	--	5 (56%)	1 (33%)	0 (0%)	0 (0%)
Uncircumcised[c]	3 (60%)	--	4 (44%)	2 (67%)	2 (100%)	2 (100%)
Adenovirus 5 status[d] (n)						
Seropositive	9 (75%)	2 (67%)	17 (94%)	12 (92%)	6 (86%)	4 (57%)
Seronegative	3 (25%)	1 (33%)	1 (6%)	1 (8%)	1 (14%)	3 (43%)
HSV-2 status at enrolment (n)						
Positive	9 (75%)	2 (67%)	10 (56%)	5 (38%)	2 (29%)	5 (71%)
Negative	3 (25%)	1 (33%)	8 (44%)	8 (62%)	5 (71%)	2 (29%)

[a] There were no significant differences between vaccine and placebo groups within each HLA subset for any characteristic. IQR denotes interquartile range, HSV-2 denotes herpes simplex virus 2.

[b] Men circumcised at baseline or during study but before infection.

[c] Men uncircumcised throughout study or before infection.

[d] Adenovirus 5 seropositive: titer >18; seronegative: titer ≤18.

5.3.3 HLA-specific vaccine effects on viral load and CD4+ T-cell counts: Disease-susceptible HLA alleles

With respect to the disease-susceptible HLA alleles, HLA-B*18:01 and HLA-B*58:02, none of the vaccinees with available PBMC and HLA expressed HLA-B*18:01, and analyses were limited to the HLA-B*58:02-positive subjects (seven vaccinees and seven placebo-recipients, **Table 5.3**). Chronic viral setpoint was significantly lower in HLA-B*58:02-positive vaccinees (median 7,240 [4,090-63,000] versus 122,500 [103,600-677,500], p=0.01; **Figure 5.3C**). This difference was especially clear when all pre-ART longitudinal datapoints were interrogated using a mixed-effects model (p=0.01; **Figure 5.3C**). These data show that vaccination in the HLA-B*58:02-positive subjects on average resulted in a 0.76 $\log_{10}$ reduction in chronic viral setpoint and no other factors (sex/age/Ad5 antibody levels/HSV-2 serostatus) had a significant impact. The viral load differences between vaccinees and placebo-recipients remained significant when the three additional HLA-B*58:02-positive subjects were added from the Phambili participants with determined HLA types but unavailable PBMC (p=0.03, Mann-Whitney U test; p=0.03, ANOVA, mixed-effects model).

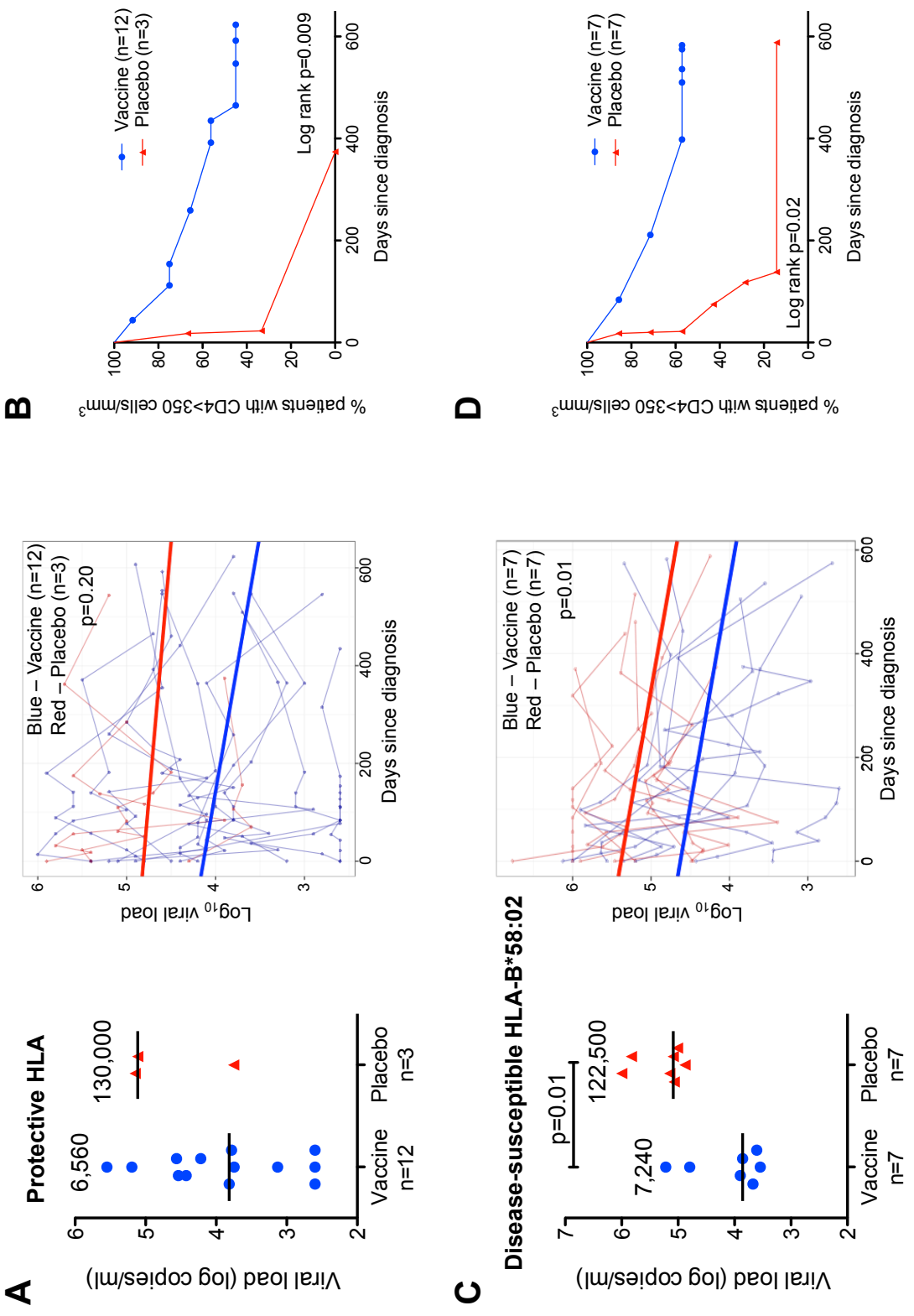

A
Protective HLA
6,560
130,000
Viral load (log copies/ml)
Vaccine n=12
Placebo n=3
Blue – Vaccine (n=12)
Red – Placebo (n=3)
p=0.20
Log10 viral load
Days since diagnosis
B
Vaccine (n=12)
Placebo (n=3)
Log rank p=0.009
% patients with CD4>350 cells/mm3
Days since diagnosis
C
Disease-susceptible HLA-B*58:02
p=0.01
122,500
7,240
Viral load (log copies/ml)
Vaccine n=7
Placebo n=7
Blue – Vaccine (n=7)
Red – Placebo (n=7)
p=0.01
Log10 viral load
Days since diagnosis
D
Vaccine (n=7)
Placebo (n=7)
Log rank p=0.02
% patients with CD4>350 cells/mm3
Days since diagnosis

Figure 5.3. Chronic viral setpoint and CD4+ T-cell counts in the infected Phambili subjects expressing protective HLA-B*57/58:01/81:01 or disease-susceptible HLA-B*58:02 alleles. Data for the participants expressing protective alleles are shown in A-C (vaccinees: n=12, placebo-recipients: n=3); data for the participants expressing HLA-B*58:02 are shown in D-F (vaccinees: n=7, placebo-recipients: n=7). **A, C. Left panels:** chronic viral setpoint (defined for each individual as the median of all measurements from >3months post-diagnosis). Each patient's setpoint is shown as blue circles (vaccine-recipients) or red triangles (placebo-recipients), horizontal lines and numbers denote median values for vaccine and placebo groups; Mann-Whitney U test. **Right panels:** examination of the effect of vaccination on longitudinal pre-ART viral load values: the slopes (thick lines) generated from a linear mixed-effects model are plotted on top of the individual patient's data points and viral load trajectories (thin lines). Vaccinees are in blue, placebo-recipients are in red; ANOVA. **B,D.** Kaplan-Meier curves showing time to reach CD4<350 cells/mm^3 in vaccinees (blue) and placebo-recipients (red); log-rank test.

Table 5.4. Univariate Cox regression model comparing time to reach CD4+ T-cell count of <350 cells/mm^3 in vaccinees versus placebo-recipients expressing protective HLA-B*57/58:01/81:01.

Variable (indicator)	HR (95% CI)	p value
Protective HLA: vaccinees (n=12) and placebo-recipients (n=3) out of 60 (univariate Cox)		
Placebo- or vaccine-treatment arm (vaccine)	0.17 (0.04-0.78)	0.02
Sex (female)	1.27 (0.31-5.17)	0.74
Age (continuous)	1.12 (0.96-1.30)	0.17
Ad5 (Ad5>18)	2.59 (0.32-20.41)	0.38
HSV-2 at enrolment (HSV-2+)	0.45 (0.11-1.86)	0.27

Ad5 denotes adenovirus type 5; HSV-2 denotes herpes simplex virus 2; HR denotes hazard ratio; CI denotes confidence interval.

Progression to CD4<350 cells/mm^3 was also significantly slower in HLA-B*58:02-positive vaccinees compared to placebo-recipients (p=0.02, log-rank test, **Fig. 5.3D**; HR=0.22, 95%CI 0.05-0.91, p=0.04, Cox regression model, **Table 5.5**). Again, the only significant contributor to this difference was placebo-/vaccine-treatment assignment and the difference between vaccine- and placebo-recipients remained significant with addition of the three HLA-B*58:02-positive subjects with determined HLA types but unavailable PBMC (p=0.03, log-rank test; HR=0.29, 95%CI 0.06-0.99, p=0.04, Cox regression model, **Table 5.5**). Finally, among the HLA-B*58:02-positive subjects studied, one individual also expressed protective HLA-B*58:01, and exclusion of this subject did not materially alter the findings described (viral setpoint difference, p=0.01; time to CD4<350 cells/mm^3, p=0.04). Similarly, no significant difference was observed with respect to HLA-C alleles expressed among the HLA-B*58:02-positive subjects studied; in each case HLA-C*06:02 was expressed in linkage disequilibrium with HLA-B*58:02.

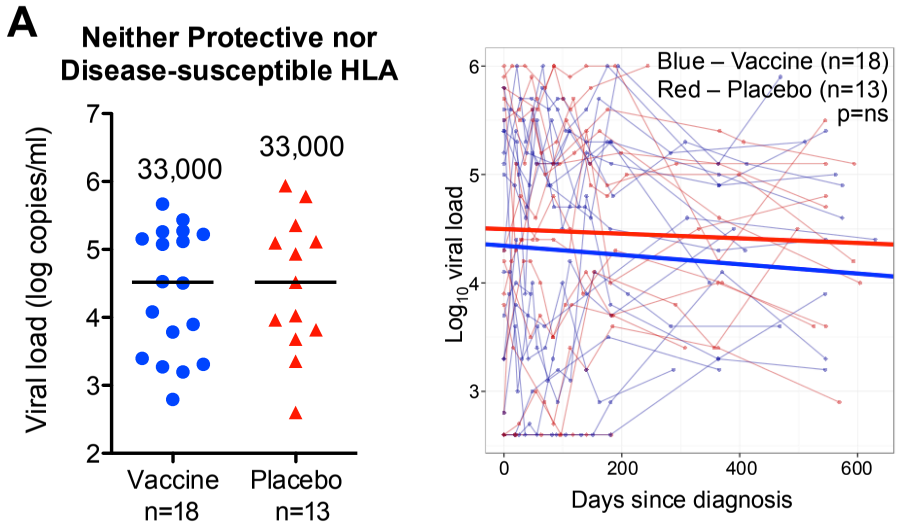
5.3.4 HLA-specific vaccine effects on viral load and CD4+ T-cell counts: Neither protective nor disease-susceptible HLA alleles

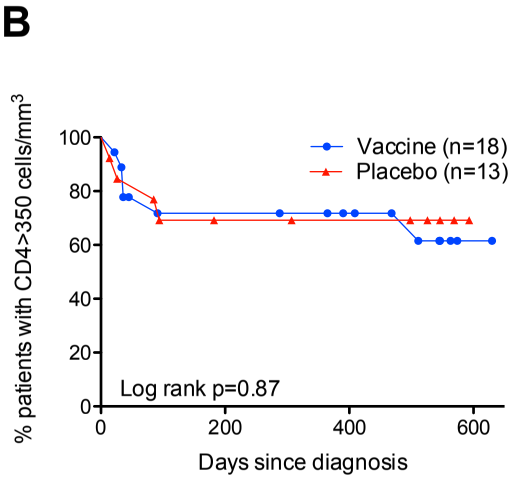
Analysis of the subjects expressing neither protective nor disease-susceptible alleles showed no differences between vaccine and placebo groups in chronic viral setpoints or time to CD4<350 cells/mm^3 (**Figures 5.4A,B**). Representative observations are illustrated by the HLA-B*44:03-expressing subjects (n=6 in each group; **Figures 5.4C,D**).

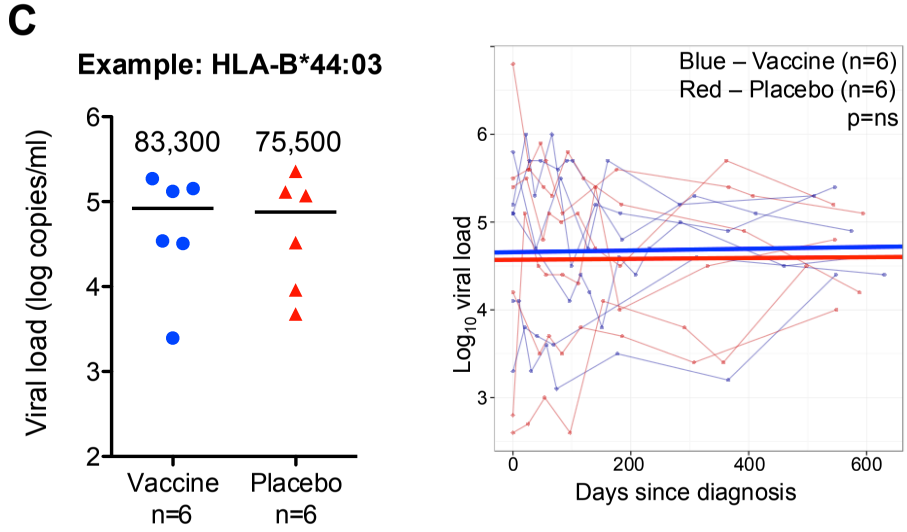
Table 5.5. Univariate Cox regression model comparing time to reach CD4+ T-cell count of <350 cells/mm^3 in vaccinees versus placebo-recipients expressing disease-susceptible HLA-B*58:02.

Variable (indicator)	HR (95% CI)	p value
HLA-B*58:02-positive vaccinees (n=7) and placebo-recipients (n=7) out of 60 (univariate Cox)		
Placebo- or vaccine-treatment arm (vaccine)	0.22 (0.05-0.91)	0.04
Sex (female)	1.90 (0.39-9.26)	0.43
Age (continuous)	1.05 (0.93-1.18)	0.44
Ad5 (Ad5>18)	0.56 (0.14-2.32)	0.44
HSV-2 at enrolment (HSV2+)	1.69 (0.45-6.39)	0.44
HLA-B*58:02-positive vaccinees (n=8) and placebo-recipients (n=9) out of 100 (univariate Cox)		
Placebo- or vaccine-treatment arm (vaccine)	0.29 (0.06-0.99)	0.04
Sex (female)	1.55 (0.33-7.34)	0.58
Age (continuous)	1.01 (0.89-1.15)	0.84
Ad5 (Ad5>18)	0.52 (0.13-2.04)	0.35
HSV-2 at enrolment (HSV-2+)	1.28 (0.36-4.56)	0.70

Ad5 denotes adenovirus type 5; HSV-2 denotes herpes simplex virus 2; HR denotes hazard ratio; CI denotes confidence interval.


A
Neither Protective nor Disease-susceptible HLA
Viral load (log copies/ml)
33,000
33,000
Vaccine n=18
Placebo n=13
Blue – Vaccine (n=18)
Red – Placebo (n=13)
p=ns
Log10 viral load
Days since diagnosis


B
% patients with CD4>350 cells/mm3
Vaccine (n=18)
Placebo (n=13)
Log rank p=0.87
Days since diagnosis


C
Example: HLA-B*44:03
Viral load (log copies/ml)
83,300
75,500
Vaccine n=6
Placebo n=6
Blue – Vaccine (n=6)
Red – Placebo (n=6)
p=ns
Log10 viral load
Days since diagnosis

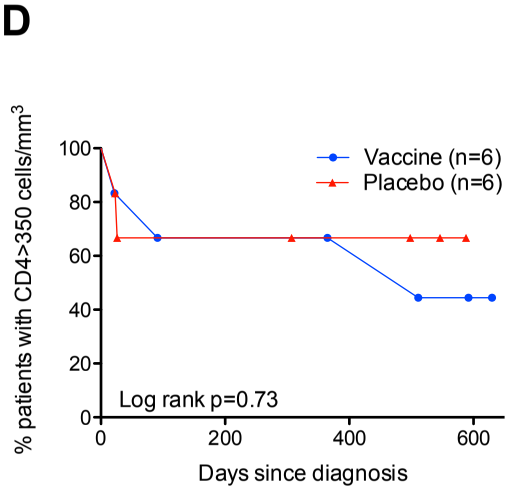

D
% patients with CD4>350 cells/mm3
Vaccine (n=6)
Placebo (n=6)
Log rank p=0.73
Days since diagnosis

Figure 5.4. Chronic viral setpoint and CD4+ T-cell counts in the infected Phambili subjects expressing neither protective nor disease-susceptible HLA alleles. Data for the participants expressing neither protective nor disease-susceptible alleles overall are shown in A,C (vaccinees: n=18, placebo-recipients: n=13); C,D is an example of a subset of the subjects from A-C, who express HLA-B*44:03 and for whom there were sufficient subject numbers to compare vaccine (n=6) and placebo (n=6) groups. **A, C. Left panels:** chronic viral setpoint (defined for each individual as the median of all measurements from >3months post-diagnosis). Each patient's setpoint is shown as blue circles (vaccine-recipients) or red triangles (placebo-recipients), horizontal lines and numbers denote median values for vaccine and placebo groups; Mann-Whitney U test. **Right panels:** examination of the effect of vaccination on longitudinal pre-ART viral load values: the slopes (thick lines) generated from a linear mixed-effects model are plotted on top of the individual patient's data points and viral load trajectories (thin lines). Vaccinees are in blue, placebo-recipients are in red; ANOVA. Ns = not significant. **B,D.** Kaplan-Meier curves showing time to reach CD4<350 cells/mm^3 in vaccinees (blue) and placebo-recipients (red); log-rank test.

5.3.5 HLA-specific vaccine effects on anti-HIV CD8+ T-cell responses

To investigate whether the apparent effects on reduced viral load and slower time to CD4<350 cells/mm^3 observed might be related to HLA-specific induction of altered CD8+ T-cell responses in the vaccinees versus placebo-recipients, we first analysed these in HLA-B*58:02-positive study subjects. Gag-specific breadth was 4.5-fold higher in vaccinees (median 4.5 [2-5] responses versus 1 [0-3], p=0.04; **Figure 5.5A**), and Gag-specific magnitude was 32-fold higher (median 2,300 [603-6,105] versus 70 [0-1,520] SFC/10^6 PBMC, p=0.06; **Figure 5.5A**). Additionally, we compared the CD8+ T-cell responses in the Phambili subjects to those of HLA-B*58:02-positive unvaccinated individuals with natural chronic HIV-1 C-clade infection (n=66; **Figure 5.5A**), mostly females (79%) recruited in South Africa (**Table 5.2**). Here also we observed that the Phambili HLA-B*58:02-positive vaccinees had significantly higher Gag-specific breadth compared to non-Phambili infected subjects (p=0.04), while the difference between HLA-

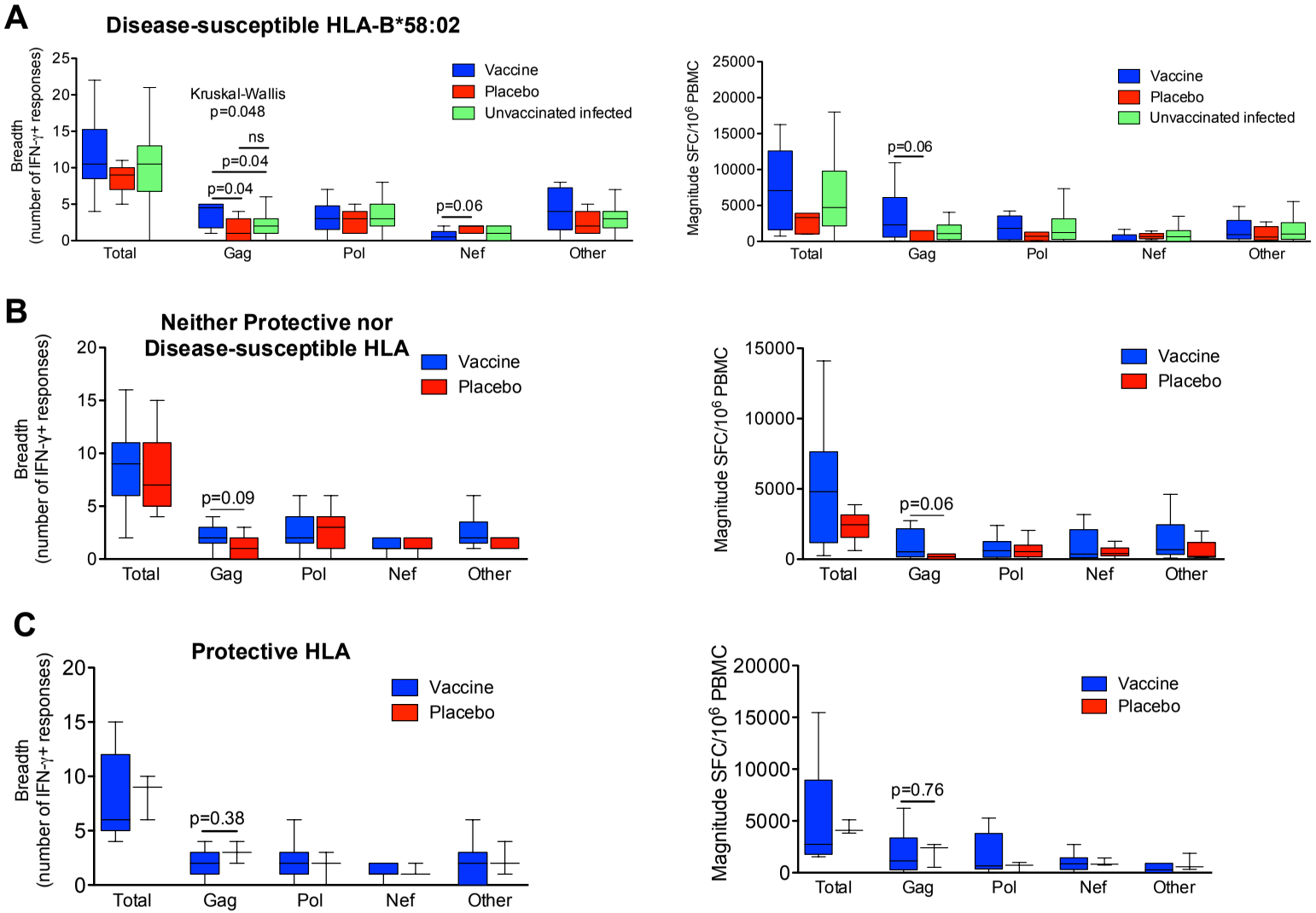

A
Disease-susceptible HLA-B*58:02
Breadth (number of IFN-γ+ responses)
Kruskal-Wallis p=0.048
ns
p=0.04
p=0.04
p=0.06
Vaccine
Placebo
Unvaccinated infected
Total
Gag
Pol
Nef
Other
Magnitude SFC/10^6 PBMC
p=0.06
B
Neither Protective nor Disease-susceptible HLA
p=0.09
p=0.06
C
Protective HLA
p=0.38
p=0.76

Figure 5.5. CD8+ T-cell responses in the infected Phambili subjects expressing disease-susceptible HLA-B*58:02 or those expressing neither protective nor disease-susceptible alleles. A. Breadth and magnitude of CD8+ T-cell responses at the second timepoint in HLA-B*58:02-positive vaccinees (blue bars), placebo-recipients (red bars) and C-clade chronically infected unvaccinated B*58:02-positive individuals (green bars). **B.** Breadth and magnitude of CD8+ T-cell responses at the second timepoint in vaccinees (blue bars) and placebo-recipients (red bars) expressing neither protective nor disease-susceptible HLA-B alleles. **C.** Breadth and magnitude of CD8+ T-cell responses at the second timepoint in vaccinees (blue bars) and placebo-recipients (red bars) expressing protective HLA-B alleles. Tukey box-and-whisker plots: horizontal lines indicate median values, boxes show IQR, whiskers show minimum and maximum; Kruskal-Wallis and Mann-Whitney U tests. 'Total' is combined values of responses to all proteins; 'Other' includes responses to Env/Rev/Tat/Vpu/Vif/Vpr.

B*58:02-positive placebo-recipients and non-Phambili subjects was not significant. Gag-specific magnitude was >2-fold higher in HLA-B*58:02-positive vaccinees compared to non-Phambili HLA-B*58:02-positive subjects (median 1,100 [255-2,050] SFC/million PBMC, p=0.2). No significant associations were found between Gag-specific breadth/magnitude and viral loads or CD4 count in HLA-B*58:02-positive vaccinees (**Figures 5.6, 5.7**).

In contrast, in subjects expressing neither protective nor disease-susceptible alleles, the difference between the groups in Gag-specific breadth and magnitude was more modest (median 2 [1.5-3] responses versus 1 [0-2], p=0.09; and median 529 [166-2,163] versus 180 [0-377] SFC/million PBMC, p=0.06; **Figure 5.5B**). No significant differences were observed in Gag breadth and magnitude in the subjects expressing protective HLA (**Figure 5.5C**).

Figure 5.6

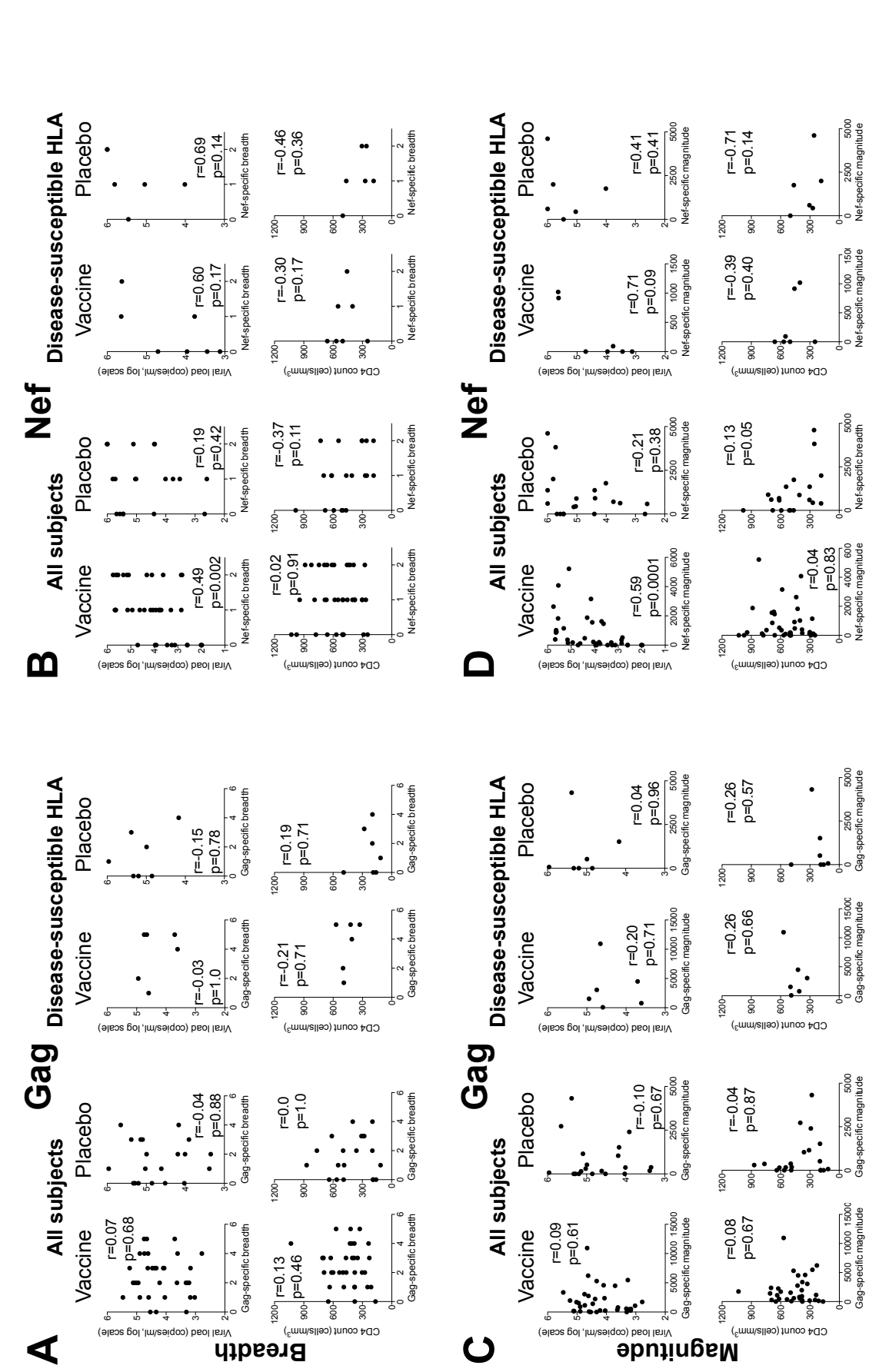

A
Gag
All subjects
Disease-susceptible HLA
Vaccine
Placebo
Breadth
Magnitude
Viral load (copies/ml, log scale)
CD4 count (cells/mm3)
Gag-specific breadth
Gag-specific magnitude
r=0.07 p=0.68
r=-0.04 p=0.88
r=-0.03 p=1.0
r=-0.15 p=0.78
r=0.13 p=0.46
r=0.0 p=1.0
r=-0.21 p=0.71
r=0.19 p=0.71
r=0.09 p=0.61
r=-0.10 p=0.67
r=0.20 p=0.71
r=0.04 p=0.96
r=0.08 p=0.67
r=-0.04 p=0.87
r=0.26 p=0.66
r=0.26 p=0.57
B
Nef
Nef-specific breadth
Nef-specific magnitude
r=0.49 p=0.002
r=0.19 p=0.42
r=0.60 p=0.17
r=0.69 p=0.14
r=0.02 p=0.91
r=-0.37 p=0.11
r=-0.30 p=0.17
r=-0.46 p=0.36
D
r=0.59 p=0.0001
r=0.21 p=0.38
r=0.71 p=0.09
r=0.41 p=0.41
r=0.04 p=0.83
r=0.13 p=0.05
r=-0.39 p=0.40
r=-0.71 p=0.14

Figure 5.7

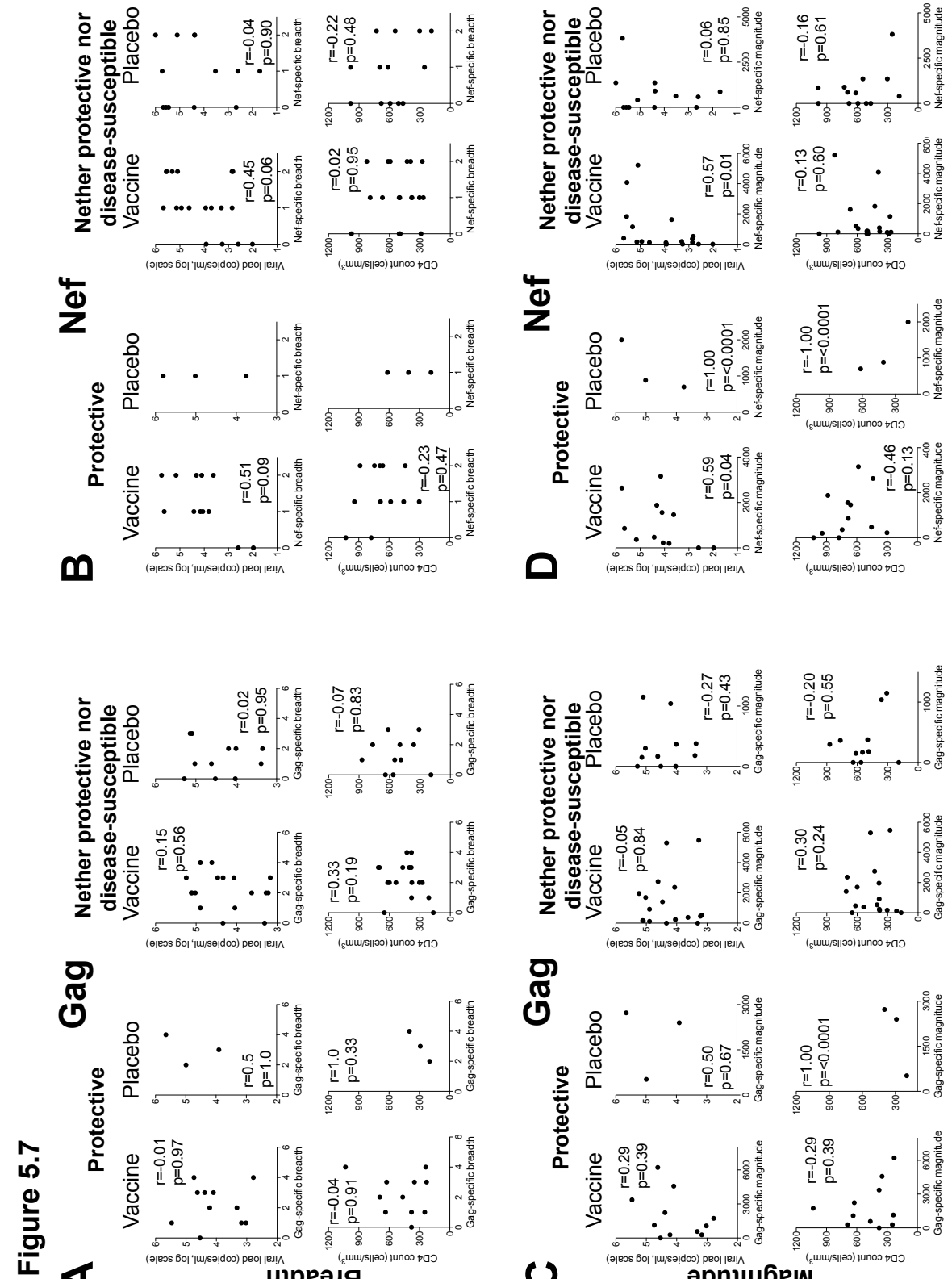

A
Gag
Protective
Vaccine
Placebo
Nether protective nor disease-susceptible
Vaccine
Placebo
Breadth
r=-0.01 p=0.97
r=0.5 p=1.0
r=0.15 p=0.56
r=0.02 p=0.95
r=-0.04 p=0.91
r=1.0 p=0.33
r=0.33 p=0.19
r=-0.07 p=0.83
B
Nef
Protective
Vaccine
Placebo
Nether protective nor disease-susceptible
Vaccine
Placebo
r=0.51 p=0.09
r=0.45 p=0.06
r=-0.04 p=0.90
r=-0.23 p=0.47
r=0.02 p=0.95
r=-0.22 p=0.48
C
Gag
Protective
Vaccine
Placebo
Nether protective nor disease-susceptible
Vaccine
Placebo
Magnitude
r=0.29 p=0.39
r=0.50 p=0.67
r=-0.05 p=0.84
r=-0.27 p=0.43
r=-0.29 p=0.39
r=1.00 p=<0.0001
r=0.30 p=0.24
r=-0.20 p=0.55
D
Nef
Protective
Vaccine
Placebo
Nether protective nor disease-susceptible
Vaccine
Placebo
r=0.59 p=0.04
r=1.00 p=<0.0001
r=0.57 p=0.01
r=0.06 p=0.85
r=-0.46 p=0.13
r=-1.00 p=<0.0001
r=0.13 p=0.60
r=-0.16 p=0.61
Viral load (copies/ml, log scale)
CD4 count (cells/mm3)
Gag-specific breadth
Nef-specific breadth
Gag-specific magnitude
Nef-specific magnitude

Figure 5.6. Correlations of Gag- and Nef-specific breadth and magnitude with viral load or CD4 counts in all subjects irrespective of HLA expression and subjects expressing disease-susceptible HLA. In all panels, correlations with viral load are presented in the top rows and with CD4 counts in the bottom rows. **A.** Correlations between Gag-specific breadth and viral load or CD4 counts in vaccinees and placebo-recipients. **B.** Correlations between Nef-specific breadth and viral load or CD4 counts in vaccinees and placebo-recipients. **C.** Correlations between Gag-specific magnitude and viral load or CD4 counts in vaccinees and placebo-recipients. **D.** Correlations between Nef-specific magnitude and viral load or CD4 counts in vaccinees and placebo-recipients. P and r-values were obtained from Spearman correlation analyses.

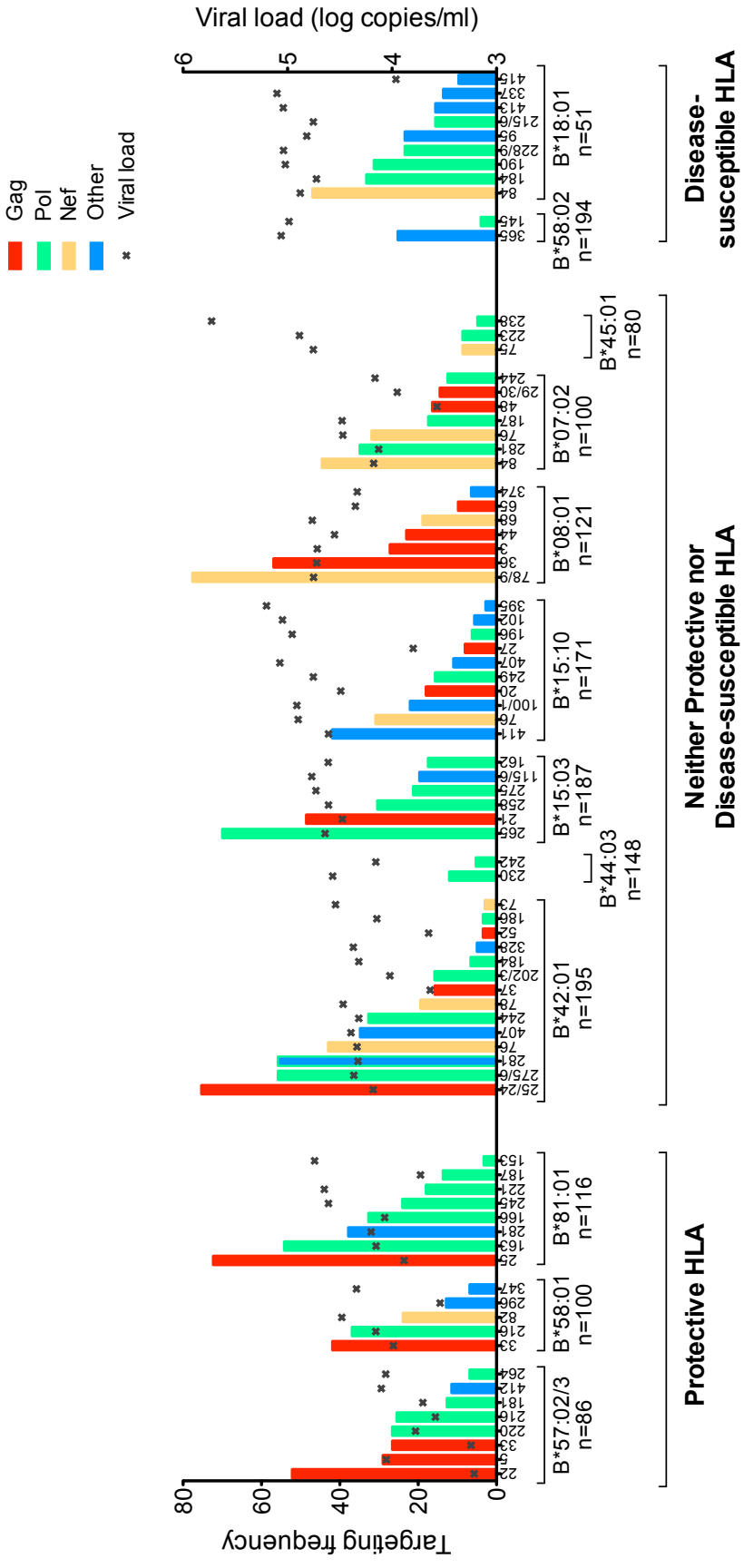
Figure 5.7. Correlations of Gag- and Nef-specific breadth and magnitude with viral load or CD4 counts in subjects expressing protective HLA and neither protective nor disease-susceptible HLA. In all panels, correlations with viral load are presented in the top rows and with CD4 counts in the bottom rows. **A.** Correlations between Gag-specific breadth and viral load or CD4 counts in vaccinees and placebo-recipients. **B.** Correlations between Nef-specific breadth and viral load or CD4 counts in vaccinees and placebo-recipients. **C.** Correlations between Gag-specific magnitude and viral load or CD4 counts in vaccinees and placebo-recipients. **D.** Correlations between Nef-specific magnitude and viral load or CD4 counts in vaccinees and placebo-recipients. P and r-values were obtained from Spearman correlation analyses.

Although the MRKAd5 HIV-1 Gag/Pol/Nef vaccine appeared to boost Gag-specific responses overall in vaccinees within the 60 subjects studied here (**Figure 5.2D**), there were no significant differences for the CD8+ T-cell responses towards Pol, Nef, or Env/Vif/Vpr/Vpu/Tat/Rev in the three HLA groups (**Figure 5.5**). However, of note, in addition to having a significantly broader Gag-specific response, HLA-B*58:02-positive vaccinees tended to have a narrower Nef-specific response (p=0.06; **Figure 5.5A**). The potential relevance of this is discussed below.

Together, our findings support the original hypothesis that the MRKAd5 HIV-1 vaccine could improve disease outcome by boosting beneficial Gag-specific responses (Kiepiela et

al., 2007) in HLA-B*58:02-positive individuals who in natural infection do not generate HLA-B*58:02-restricted Gag responses but produce predominantly Env-specific ineffective responses (**Figure 5.8**).

(Next page) **Figure 5.8. HLA-dependent differential immunodominance hierarchy of CD8+ T-cell responses in chronically C-clade infected, ART-naïve, South African adults.** CD8+ T-cell immunodominance hierarchy in subjects in the three HLA groups (allele frequency ≥5%), expressing: protective HLA, neither protective nor disease-susceptible HLA, and disease-susceptible HLA. Targeting frequency: percentage of subjects making detectable responses in IFN-γ ELISPOT assays to the named HIV-1 peptide. Numbers on x-axis refer to the particular overlapping peptide (of 410 spanning the C clade proteome) to which a response was detected. The x in each column denotes the median viral load of responders to that peptide.


Viral load (log copies/ml)
6
5
4
3
Gag
Pol
Nef
Other
Viral load
Targeting frequency
80
60
40
20
0
Protective HLA
Neither Protective nor Disease-susceptible HLA
Disease-susceptible HLA
B*57:02/3 n=86
B*58:01 n=100
B*81:01 n=116
B*42:01 n=195
B*44:03 n=148
B*15:03 n=187
B*15:10 n=171
B*08:01 n=121
B*07:02 n=100
B*45:01 n=80
B*58:02 n=194
B*18:01 n=51

5.4 Discussion

This study set out to investigate whether the HLA-specific vaccine effects suggested in the Step trial (Altfeld and Goulder, 2011; Fitzgerald et al., 2011; Janes et al., 2013) could be demonstrated in the ethnically dissimilar Phambili cohort. Half of the Step trial participants who subsequently became infected were Caucasian, whereas none of the Phambili cohort was Caucasian. Expression of HLA class I molecules, such as HLA-B*42:01, HLA-B*58:02, and HLA-B*81:01, for example, is observed in 0% of Caucasians (Cao et al., 2001), and in 20%, 23%, and 10%, respectively, of Black South Africans (Kiepiela et al., 2004; Kiepiela et al., 2007). The principal finding in the current study is an HLA-specific vaccine effect in subjects expressing the disease-susceptible HLA-B*58:02. HLA-B*58:02-positive vaccinees had significantly lower viral setpoint and progressed more slowly to CD4<350 cells/mm^3 compared to HLA-matched placebo-recipients. This result was associated with an increased breadth and magnitude of Gag-specific CD8+ T-cell responses in vaccinees expressing HLA-B*58:02. In contrast, in Phambili subjects expressing neither protective nor disease-susceptible alleles, these vaccine effects were not observed.

The described HLA-specific vaccine effect was suggested in the Step study in relation to the protective HLA-B*27:05/B*57:01/B*58:01 (Altfeld and Goulder, 2011; Fitzgerald et al., 2011; Janes et al., 2013). Analysis here also showed a 1.3log_{10} lower viral load and significantly slower progression to CD4<350 cells/mm^3 (p=0.009) in vaccinees expressing protective HLA-B*57:02/57:03/58:01/81:01 (Kiepiela et al., 2004; Leslie et al., 2010), compared to HLA-matched placebo-recipients. However, these analyses were limited by numbers (only three placebo-recipients).

Our finding of reduced viral load and slower time to CD4<350 cells/mm^3 in HLA-B*58:02-positive vaccinees is significant. First, viral load in natural infection is 4.9-5.2 log_{10} copies/ml (Lazaryan et al., 2006; Ngumbela et al., 2008), similar to that in the HLA-B*58:02-positive placebo-recipients here (5.1 log_{10} copies/ml), corresponding to rapid progression and a high risk of further transmissions (Carlson et al., 2012; Fraser et al., 2007; Kiepiela et al., 2004; Leslie et al., 2010). The 17-fold reduction in viral setpoint in HLA-B*58:02-positive vaccinees observed here equates to >5-year AIDS-free without ART and >2-fold reduction in onward transmission risk (Fraser et al., 2007). Second, HLA-B*58:02 is highly prevalent in sub-Saharan Africa, expressed in 20-25% of South Africans (Kiepiela et al., 2004; Kiepiela et al., 2007). Thus, a vaccine effect on post-infection disease progression in subjects expressing protective HLA-B*57/58:01/81:01 (24% of South Africans (Kiepiela et al., 2004; Kiepiela et al., 2007)) and in those expressing HLA-B*58:02, would favourably affect disease course in approximately half of the population.

The HLA-B*58:02-specific effect observed supports the original hypothesis. HLA-B*58:02-restricted CD8+ T-cell responses are almost exclusively directed against Env, associated with high viral load (Kiepiela et al., 2007) (**Figure 5.8**). The MRKAd5 HIV-1 vaccine might therefore be expected to improve outcome by boosting beneficial Gag responses (Janes et al., 2012; Kiepiela et al., 2007). 70-fold higher magnitude and 4-5-fold greater breadth of Gag-specific responses were indeed observed in HLA-B*58:02-positive vaccine-recipients, however the necessary samples were unavailable to determine whether these were restricted by HLA-B*58:02 or by other HLA alleles expressed by these subjects.

Although previous studies have shown a correlation between increasing Gag breadth and decreasing viral load (Geldmacher et al., 2007; Kiepiela et al., 2007; Masemola et al., 2004; Radebe et al., 2015) including vaccinees of the Step study (Janes et al., 2013), this

was not observed here (**Figures 5.6, 5.7**). In part this is due to our small study numbers. In addition, Gag-specific responses are not equally potent. For example, p24-specific responses are associated with better viremic control than p17- or p15-specific responses (Honeyborne et al., 2007). However, in this study the design of the Gag peptide pools made these subanalyses not possible. Furthermore, sample non-availability prevented the HLA restriction of the CD8+ T-cell responses in the vaccinees to be determined. In large cohort studies, on average Gag-specific breadth is associated with lower viral load, but in small studies the variation between the different Gag and non-Gag responses will strongly influence these analyses. Furthermore, the vaccine-mediated increase in Gag breadth may be associated with changes in the non-Gag-specific responses. On average Nef-specific and Env-specific responses are associated with higher viral loads (Kiepiela et al., 2007; Masemola et al., 2004). In our study, Nef-specific breadth in infected HLA-B*58:02-positive vaccinees was four-fold *lower* than in HLA-B*58:02-positive placebo-recipients (p=0.06). Nef-specific breath has been consistently shown in previous studies to be associated with higher viral loads and the same observation is made here (**Figures 5.6, 5.7**). Thus the finding of lower viral loads in B*58:02-positive subjects with both higher Gag- and lower Nef-specific responses may be the result of a combination of these effects.

The limitations of this study include small subject numbers, potential for post-randomisation bias (Mehrotra, Li, and Gilbert, 2006) and the caveats that apply to any post-hoc analysis. To address the possibility that the differences in post-infection outcomes were caused by the differences in characteristics associated with infection risk, not by vaccination, we investigated HLA impact on HIV-1 acquisition among 329 (out of 801) Phambili subjects with available HLA data. There was none, in either vaccine- or placebo-recipients. This suggests that HLA does not confound the association of vaccination status with disease progression (Shepherd et al., 2006) and is consistent with

ample data showing HLA impact on disease progression but not on HIV-1 acquisition (Goulder and Walker, 2012; Vince et al., 2014). Skewing could have been introduced by unintended sample selection bias: PBMC were only available for 60 of the 100 HIV-1-infected subjects, and the 40 subjects with unavailable samples and thus unknown CD8+ T-cell responses, showed faster time to CD4<350 cells/mm^3. However, absence of the CD8+ T-cell-response data in this group of 40 more rapidly progressing subjects does not alter the validity of the finding in relation to the 60 we were able to study.

Finally, although low CD4 count and high viral load are, separately, strongly correlated with increased risk of opportunistic infections and mortality (Mellors et al., 1996; Seage et al., 2002), these measures do not necessarily equate with disease (Abrams et al., 2009). However, the observation of progression to CD4<350 cells/mm^3 within 6 months of infection in >80% of the HLA-B*58:02-positive placebo-recipients, together with a viral setpoint of 5.1 log_{10} copies/ml in these subjects, is consistent with rapid progression observed in natural infection in HLA-B*58:02-positive individuals (Lazaryan et al., 2006; Ngumbela et al., 2008). The 1.3log_{10} lower viral setpoint in HLA-B*58:02-positive vaccinees, and >50% failing to meet the CD4 ART-initiation criteria by 600 days post-infection, are consistent with vaccine-mediated protection against rapid progression.

In conclusion, although the MRKAd5 HIV-1 Gag/Pol/Nef vaccine increased infection risk among vaccine-recipients in both Step and Phambili trials (Buchbinder et al., 2008; Gray et al., 2011; Gray et al., 2014), these data suggest its potential role as a therapeutic vaccine operating in an HLA-specific manner, with the capacity to benefit individuals expressing disease-susceptible alleles. Even in ART-treated individuals, CD8+ T cells may contribute to suppression of viraemia (Silvestri, 2015) and 'shock and kill' cure strategies (Deeks, 2012) may likely require effective anti-HIV-1 CD8+ T-cell activity to achieve successful

eradication of viral reservoirs (Deng et al., 2015). Any theoretical increased risk of HIV-1 infection resulting from adenoviral-based vaccines in already HIV-1-infected subjects would be low compared to the potential therapeutic benefit of inducing an effective anti-HIV-1 T-cell response. These studies indicate that the dramatic differences in HLA composition between distinct populations may contribute to variation in vaccine efficacy.

CHAPTER 6. SAPORIN-CONJUGATED TETRAMERS IDENTIFY EFFICACIOUS ANTI-HIV CD8+ T-CELL SPECIFICITIES

6.1 Introduction

The notion of selective T-cell depletion, most frequently aiming to purge autoreactivity, has recently gained substantial traction in the immunological field (Clark et al., 1994; Hess et al., 2007; Hess et al., 2013; Kappel et al., 2006; Penaloza-MacMaster, Masopust, and Ahmed, 2009; Schutz et al., 2010; Vincent et al., 2010; Yuan et al., 2004). The development of fluorescently-labeled tetrameric peptide-MHC complexes (tetramers) allowed binding and visualisation of antigen-specific T-cells (Altman et al., 1996; Leisner et al., 2008; Sims, Willberg, and Klenerman, 2010) and has led to the generation of modified tetramers that are coupled to a toxin, such as a ribosome inactivating protein saporin (SAP), that can selectively kill antigen-specific cells of interest. Being highly specific for their cognate T-cells and rapidly internalised upon engagement of the TCR, peptide-MHC tetramers can deliver any coupled moiety in a very selective manner (Whelan et al., 1999). The potential to cause death of selected antigen-specific T-cell target cells makes SAP-conjugated tetramers (tet-SAP) a powerful tool not only to eliminate auto-reactive T-cells causing disease but also by which to identify antiviral T cell specificities that are effective in preventing disease (Hess et al., 2007).

An elegant proof-of-concept study in the mouse-LCMV model exploited the idea of SAP-conjugated tetramers and demonstrated tetramer-mediated selective depletion of certain CD8+ T-cells *in vitro* and *in vivo* (Hess et al., 2007). These cytotoxic tetramers were later used *in vivo* in further murine studies to delete diabetogenic T-cells (Vincent et al., 2010),

encephalopathogenic T-cells (Penaloza-MacMaster et al., 2009), or minor histocompatibility HY-specific T-cells to prevent organ rejection (Hess et al., 2013).

To date, however, the tet-SAP technology has not been applied in human studies. We here set out to demonstrate that this tool can be used to selectively deplete HIV-specific CD8+ T-cells *in vitro*, thereby to evaluate the contribution and efficacy of a particular CD8+ T-cell specificity to viral inhibition. Although the importance of CD8+ T-cells in HIV control has been established for some decades (Borrow et al., 1994; Koup et al., 1994), a long-standing question – and one that is critical to HIV vaccine design – remains, namely, which of the many different HIV-specific responses are effective in mediating effective and durable immune control of HIV infection.

6.2 Chapter-specific materials and methods

6.2.1 Tetramer generation

In addition to the tetramers produced in the laboratory of Prof. Soren Buus (University of Copenhagen, Copenhagen, Denmark; Chapter 2, section 2.5.3), tetramers were also generated in the Goulder laboratory during optimisation of the method. Biotinylated MHC class I monomers were tetramerised by stepwise addition (1/10th volume every 10 minutes) of streptavidin-PE (Sigma), streptavidin-APC (Sigma) or streptavidin-SAP (Advanced Targeting Systems) at a 1:1 molar ratio of biotynilated MHC to biotin binding sites (Altman, 2003). [MHC monomers were kindly provided by Dr. Rebecca Payne (HIV HLA-B*27:05-KK10) and Dr. Stuart Sims (CMV HLA-B*07-TM10, EBV HLA-A*02:01-GL9 and EBV HLA-B*07:02-RL9.] Between additions, tetramerisation reaction was left on a rotor at 4°C in the dark. Tetramers were stored at 4°C protected from light. Tetramerisation was confirmed by staining anti-mouse Ig κ beads (BD Biosciences) with an anti-HLA

antibody, followed by tetramer staining (**Figure 6.1A**). Specificity was confirmed using cells from HLA-matched HIV-negative subjects (**Figure 6.1B**).

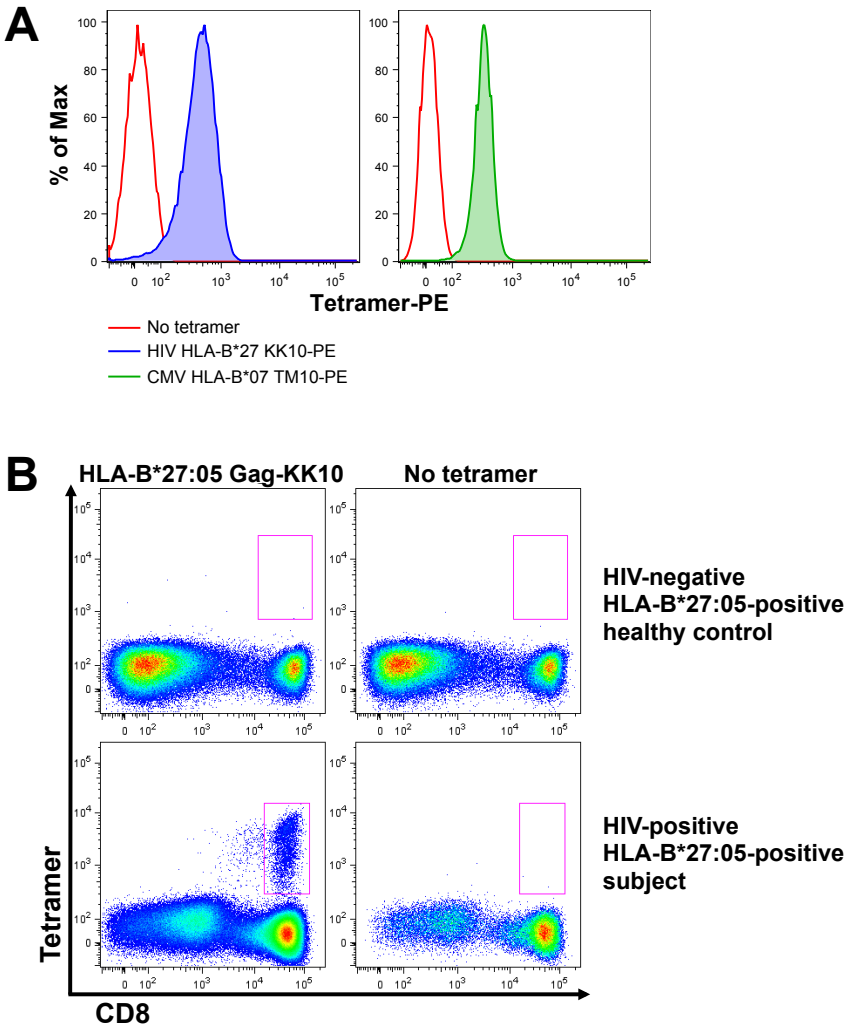


Figure 6.1. Example of tetramer validation. A. To confirm tetramerisation of MHC-monomers, anti-mouse Ig κ beads were stained with an anti-HLA antibody, then incubated with or without a tetramer-PE and acquired on a flow cytometer. Shift in PE fluorescence when a tetramer-PE was added to beads (blue and green histograms) compared to 'no tetramer' control (red histograms) indicates successful tetramerisation. **B.** Representative dot plot confirming tetramer specificity using either cells from an HIV-negative HLA-mismatched control or an HIV-positive HLA-matched donor. Gated on live CD3+CD8+ cells around tetramer+ population. Numbers indicate %tetramer+ cells (of CD8+).

6.2.2 Tetramer staining

Staining with fluorescently-conjugated tetramers were performed as described in Chapter 2, section 2.5.4. For staining with SAP-conjugated tetramers, cells were incubated with tetramers for 30 minutes at room temperature, washed, fixed and permeabilised with BD Cytofix/Cytoperm kit (BD Biosciences) and then incubated with antibodies, including a secondary anti-SAP antibody (see **Table 2.1** for details). Controls included cells incubated with no tetramer, HLA-mismatched SAP-conjugated tetramers and free unconjugated SAP. Negative gates during analysis were set up based on no tetramer and HLA-mismatched tetramer stainings. Samples were hierarchically gated on singlets, lymphocytes, live cells and CD3+ cells and gated around SAP-positive CD8+ cell populations.

6.2.3 Tetramer internalisation experiments

To establish the kinetics of tetramer interactions with human PBMCs, internalisation experiments were performed as previously described (Hess et al., 2007). Briefly, cells were incubated with tetramers at 4°C for 30 minutes to allow binding, further incubated at either 37°C or 4°C to promote or inhibit internalisation, respectively, for up to 3 hours, stripped of external fluorescence with 0.5M NaCl/0.5M acetic acid (pH 2.5) and immediately acquired by flow cytometry.

6.2.4 Timecourse of cell-depletion mediated by tetramer-SAP

To establish the timecourse and efficiency of selective tetramer-mediated cell depletion, PBMCs or expanded CD8+ T-cells were treated with tetramer-SAP (5-10 nM) for 2 hours at 37°C in R10, washed 3 times with R10 and further cultured in R10 (PBMCs) or R10/50 (expanded CD8+ T-cells). Control treatments included: free SAP, HLA-mismatched tetramer-SAP, tetramer-PE and no treatment. Every 24 hours aliquots of cells from each

condition were stained with the relevant fluorochrome-conjugated tetramer and analysed by flow cytometry. For comparison with the conventional cell-depletion method using anti-PE magnetic beads (Keenan et al., 2001), cells were incubated with tetramer-PE for 30 minutes on ice to allow surface binding and inhibit internalisation; tetramer-PE-bound cells were then removed using anti-PE beads (positive selection) (EasySep, StemCell Technologies) according to the manufacturer's protocol.

6.3 Results and Discussion

6.3.1 Recognition and internalisation of conventional and cytotoxic tetramers

We first confirmed that SAP conjugation to tetramers did not compromise tetramer recognition and internalisation by cognate CD8+ T-cells. Stainings with conventional, fluorescently labeled peptide-MHC tetramers (tet-PE or tet-APC) and with cytotoxic tetramers (tet-SAP) of the same specificity showed comparable levels of responses (**Figure 6.2**).

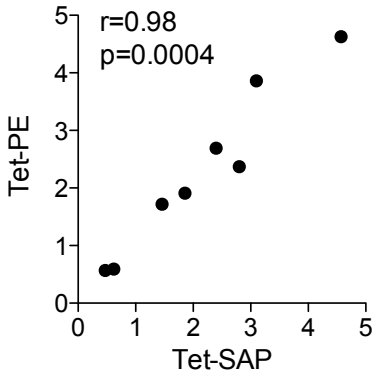


Figure 6.2. Similar levels of CD8+ T-cell responses are detected with both conventional tet-PE and tet-SAP. Spearman correlation of stainings of PBMC from 8 different donors with tetramers of different specificities and restricted by different HLA types.

An example in **Figures 6.3A,B** illustrates that a similar level of the immunodominant Gag-KK10 (^{263}KRWIILGLNK^{272}) response was detected when PBMCs from an HLA-B*27:05-positive, HIV-infected donor were stained with either KK10-PE or KK10-SAP. Visualisation of tet-SAP-specific cells required permeabilisation and staining with an anti-SAP fluorescent antibody following incubation with tet-SAP (**Figures 6.3B,C**). HLA-mismatched tetramers (in this case HLA-B*07:02-specific tetramers) showed low background staining (≤0.03% of CD8+ T-cells), similar to conventional tetramers (**Figures 6.3D,E**). Free SAP, not conjugated to tetramers and therefore lacking the means of cell entry, did not show CD8+ T-cell binding or internalisation (**Figure 6.3F**). The kinetics of tetramer binding and internalisation was strongly temperature-dependent (**Figure 6.3G**), consistent with murine studies (Hess et al., 2007), and reached maximum within 2 hours of tetramer-PBMC incubation at 37˚C.

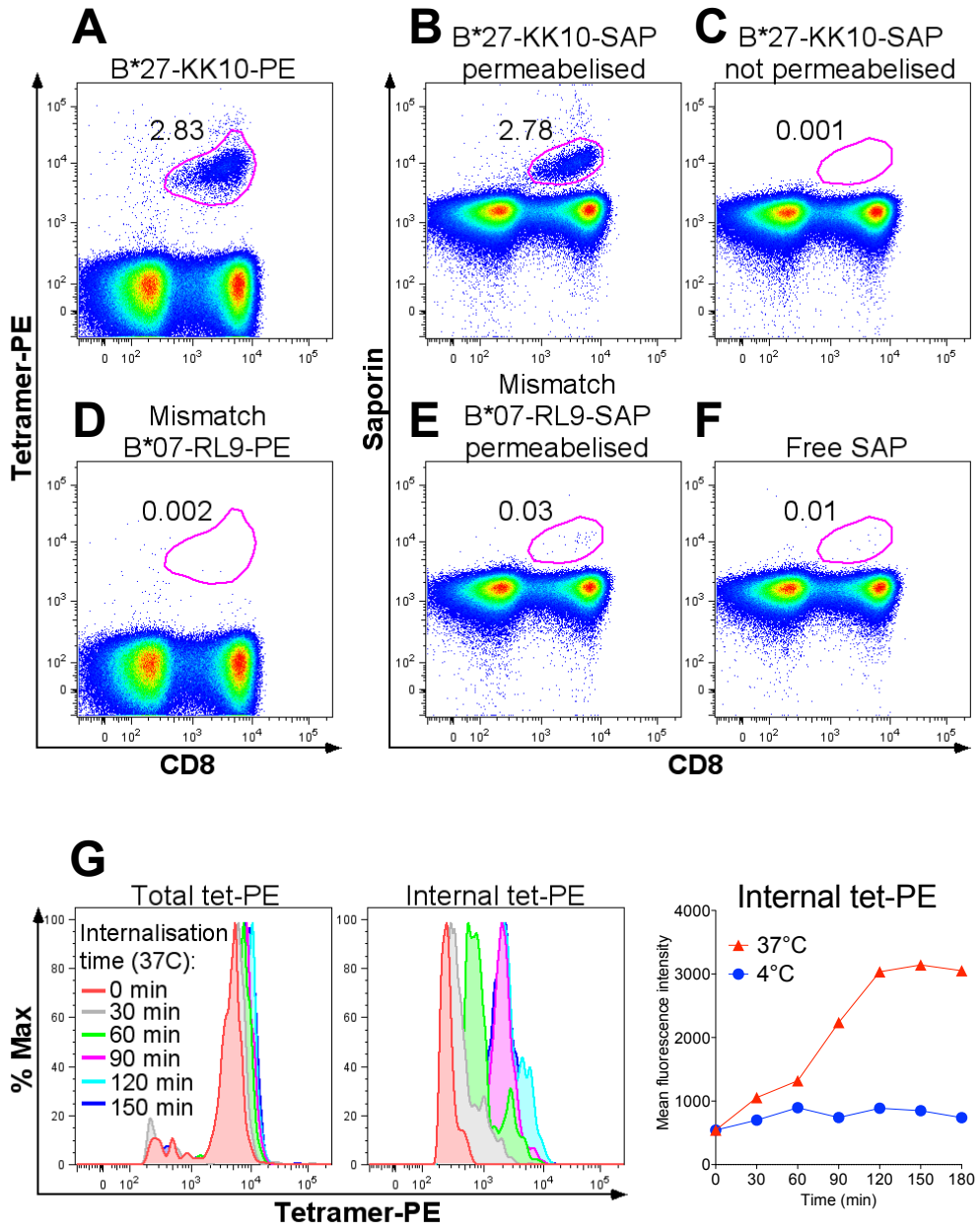


Figure 6.3. Recognition and internalisation of conventional and cytotoxic tetramers. A-F. Representative dot plots of PBMC staining in an HIV-infected HLA-B*27:05-positive subject with conventional fluorescently labeled tetramer HLA-B*27:05-Gag-KK10-PE **(A)** or SAP-coupled HLA-B*27:05-Gag-KK10-SAP tetramer, detected with a secondary Alexa Fluor 488 anti-SAP antibody in permeabelised **(B)** or not permeabelised **(C)** cells. Absence of non-specific binding of HLA-mismatched tet-PE **(D)** and tet-SAP **(E)** and free unconjugated SAP **(F)** is shown. Gated on live CD3+ cells around CD8+tet+ cells; numbers indicate % tet+ cells (of CD8+). **G.** Kinetics of tetramer

binding and internalisation, determined by measurements of total and internal tetramer fluorescence in cells at internalisation-promoting (37°C) or internalisation-inhibiting (4°C) conditions. No further increase in internal fluorescence is observed after 90-120 minutes of internalisation time, suggesting that nearly all cognate metabolically active (37°C) CD8+ T cells have internalised the tetramer. PBMC from an HIV-negative healthy donor with an EBV-HLA-A*02:01-GL9 response were used here. 'Total tet-PE' = surface-bound and internal tetramer fluorescence measured in cells not stripped of any surface-bound tetramer; 'internal tet-PE' = internal tetramer fluorescence measured in acid-stripped cells. A-F, representative of 8 independent experiments with PBMC from different donors. G, representative of 2 independent experiments with cells from two individuals.

6.3.2 Tet-SAP effectively and specifically depletes cognate CD8+ T-cells

We next assessed whether cytotoxic tetramers could deplete specific populations of human CD8+ T-cells. An illustrative example in **Figure 6.4A**, involving the same HLA-B*27:05-KK10 tetramers, shows staining of PBMCs with conventional KK10-PE tetramers following either no treatment, or treatment with KK10-SAP tetramer, HLA-mismatched tetramer or free SAP. This demonstrated that, by 24 hours post-treatment, nearly all KK10-specific cells had been depleted by tet-SAP, and did not re-emerge later in the time course (up to 72hrs). Similar observations were made in relation to 4 other SAP-conjugated tetramers, to represent a range of different HLA class I types and to include CD8+ T-cell responses to CMV and EBV in addition to HIV (**Figure 6.4B**).

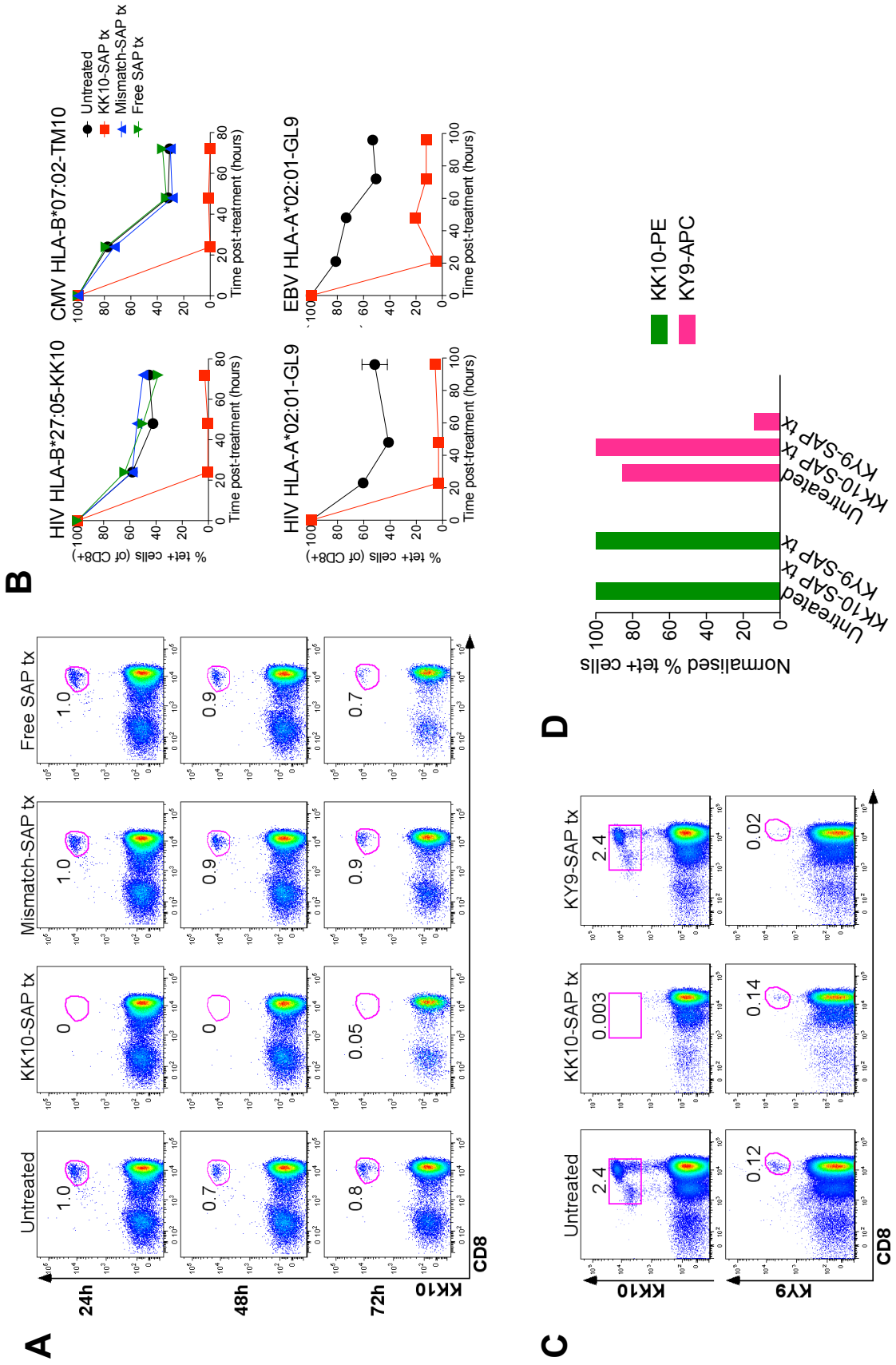

A
Untreated
KK10-SAP tx
Mismatch-SAP tx
Free SAP tx
24h
48h
72h
KK10
CD8
B
HIV HLA-B*27:05-KK10
CMV HLA-B*07:02-TM10
HIV HLA-A*02:01-GL9
EBV HLA-A*02:01-GL9
Untreated
KK10-SAP tx
Mismatch-SAP tx
Free SAP tx
% tet+ cells (of CD8+)
Time post-treatment (hours)
C
Untreated
KK10-SAP tx
KY9-SAP tx
KK10
KY9
CD8
D
KK10-PE
KY9-APC
Normalised % tet+ cells
Untreated
KK10-SAP tx
KY9-SAP tx

Figure 6.4. Tet-SAP effectively and specifically depletes cognate CD8+ T cells. A. Representative dot plots of a time course, showing depletion of HIV HLA-B*27:05-Gag-KK10-specific CD8+ T cells mediated by KK10-SAP. Controls included no treatment, HLA-mismatched tet-SAP and free SAP. Gated on live CD3+ cells around CD8+tet+ cells; numbers indicate % tet+ cells (of CD8+) assessed at indicated times after treatment. **B.** Graphical representation of 4 depletion time courses with tet-SAP of different HIV, CMV and EBV specificities and restricted by different HLA class I molecules. % tet+ cells is normalised to baseline pre-treatment levels (t=-2h). Tx = treatment. **C,D.** KK10-SAP-mediated depletion (assessed 48 hours post-treatment) of HLA-B*27:05-restricted KK10-specific CD8+ T cells does not have an off-target effect on HLA-B*27:05-restricted KY9-specific CD8+ T cells, while KY9-SAP-mediated elimination of KY9-specific cells does not affect KK10-specific cells. A,B, representative of at least 10 separate experiments with cells from different individuals with different HLA types and with tetramers of different specificities. C,D, representative of 3 independent experiments with cells from different HIV-positive HLA-B*27:05-positive donors.

To address the possibility that tetramer-mediated depletion of CD8+ T-cells of one specificity has any off-target effects on other CD8+ T-cell specificities, in particular those restricted by the same HLA class I molecule, we studied the impact of the HLA-B*27:05-KK10 tet-SAP on CD8+ T-cells recognising the HLA-B*27:05-restricted, subdominant HIV Pol epitope KY9 (^{901}KRKGGIGGY^{909}) (Payne et al., 2010). Treatment with KK10-SAP resulted in effective depletion of KK10-specific cells, but did not affect KY9-specific cells (**Figures 6.4C,D**). Similarly, KY9-SAP-mediated depletion of KY9-specific cells did not have an effect on KK10-specific cells. These data underscore the high degree of specificity maintained by the cytotoxic tetramers.

6.3.3 Contribution of KK10 to immune control of HIV determined by tet-SAP

We next applied cytotoxic tetramers to determine the contribution of specific CD8+ T-cell responses to immune control of viral infections such as HIV. To evaluate the contribution of the HLA-B*27:05-KK10 response in an HIV-infected HLA-B*27:05-positive subject, we non-specifically expanded, from PBMCs, 'bulk' CD8+ T-cells using the bi-specific

monoclonal CD3.4 antibody (Chen et al., 2009; Jones et al., 2003; Wong and Colvin, 1987), and then treated with either the KK10-tet-SAP or treatments that did not affect the HLA-B*27:05-KK10 CD8+ T-cells (no treatment, treatment with KK10-PE tetramer or with an HLA-mismatched tet-SAP; **Figure 6.5A**). We then assessed inhibition of HIV replication in HLA-B*27:05-expressing target cells by CD8+ T-cells with or without Gag-KK10 depletion. The example in **Figures 6.5B,C** illustrates that the CD8+ T-cells with unaffected HLA-B*27:05-KK10-specific cells inhibited viral replication by 3-4 $\log_{10}$ compared to the KK10-depleted CD8+ T-cells that lost the inhibitory capacity.

In a separate experiment, we ran the same tet-SAP depletion procedure in parallel with depletion using anti-PE magnetic beads (Keenan et al., 2001) (**Figures 6.5D-F**). This showed that depletion efficiency and loss of viral inhibition were similar irrespective of the method of depletion (see Discussion below).

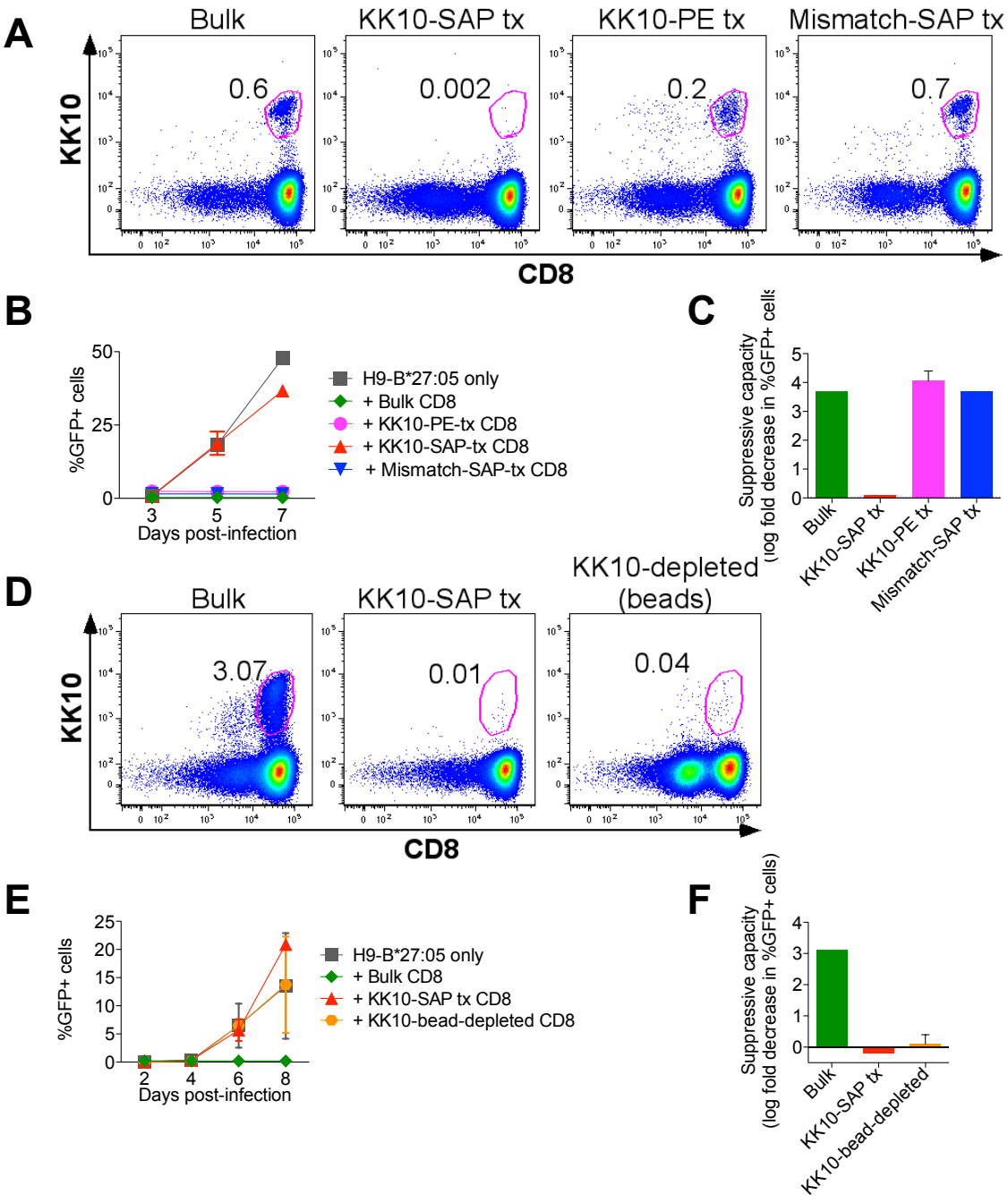


Figure 6.5. Contribution of KK10 to immune control of HIV determined by tet-SAP.

Panels A-C and D-F show results with cells from two different HIV-infected HLA-B*27:05-positive donors. **A.** Tetramer staining 48h post-treatment with KK10-SAP to confirm depletion of KK10-specific cells. Gated on live CD3+ cells around CD8+tet+ cells; numbers indicate % tet+ cells (of CD8+). **B.** Viral replication in HLA-B*27:05-expressing H9 cells without or with added untreated bulk, KK10-SAP-treated, KK10-PE-treated or mismatch-tet-SAP-treated CD8+ T cells. Infected cells were measured by NL4-3-GFP expression. **C.** Suppressive capacity of bulk, KK10-SAP-treated or

mismatch SAP-treated CD8+ T cells. **D.** Tetramer staining to confirm KK10-SAP-mediated depletion of KK10-specific CD8+ T cells (48 hours post-treatment) or depletion of KK10-PE-stained cells with anti-PE magnetic beads. **E.** Viral replication (as in B) in H9-HLA-B*27:05-positive infected target cells alone or with bulk, KK10-SAP-treated or KK10-bead-depleted CD8+ T cells. **F.** Suppressive capacity of bulk, KK10-SAP-treated or KK10-bead-depleted CD8+ T cells. B,C,E,F, error bars represent s.e.m. Representatives 2 separate experiments with two HLA-B*27:05-positive donors.

6.3.4. Definition of antiviral efficacy of different CD8+ T-cell responses using tet-SAP

We next employed the tet-SAP reagents to compare simultaneously HIV-suppressive capacity of several CD8+ T-cell specificities following this approach (**Figure 6.6**). We used samples from an HLA-B*27:05-positive HIV-infected donor who initially controlled viraemia and had three wild type HLA-B*27-restricted dominant responses, as determined by IFN-γ ELISPOT assays and confirmed by tetramer staining (**Figures 6.7A-C**): Gag-KK10, Pol-KY9 and Vpr-VL9 (^{31}VRHFPRPWL^{39}). Responses to the wild type epitopes diminished over time, while viraemia progressively increased and well-characterised HLA-B*27-associated mutations emerged in the dominant responses (**Figure 7.6D**). Viral sequence encoding the Vpr epitope was not available for the earliest timepoint, but the R32K escape mutant present at months 39 and 78 is characteristically selected specifically in HLA-B*27-positive subjects (Carlson et al., 2012).

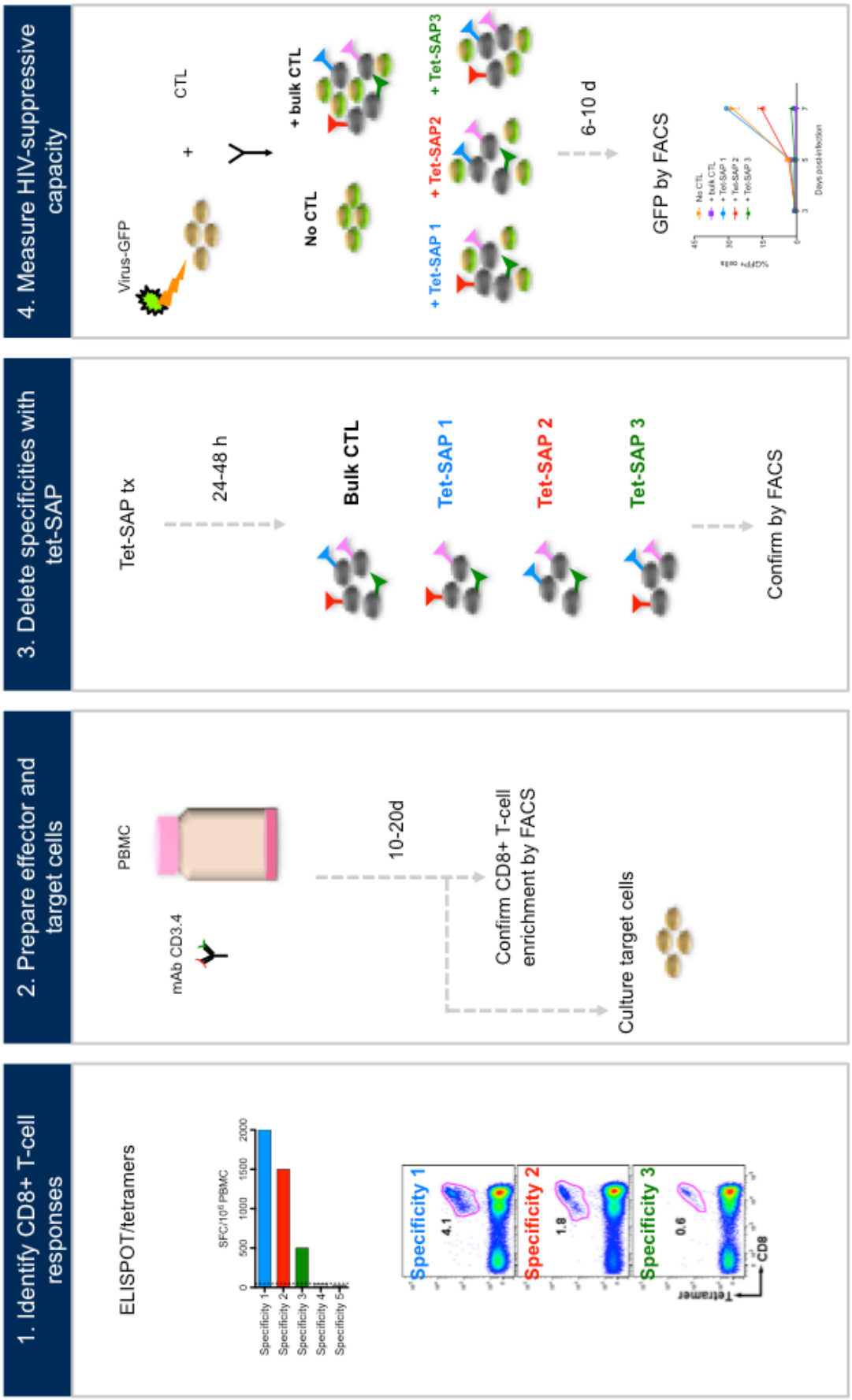
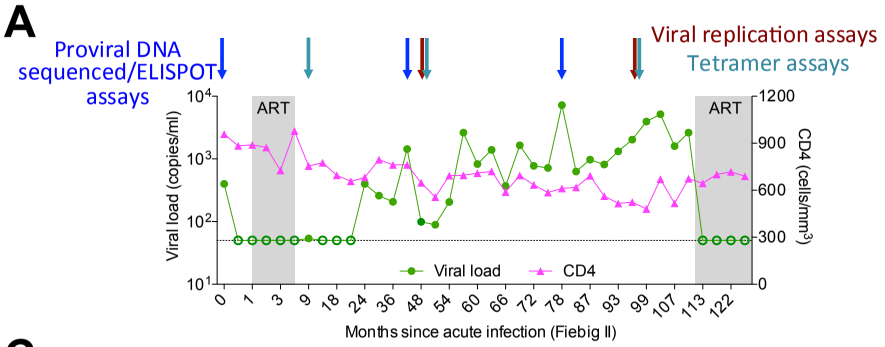
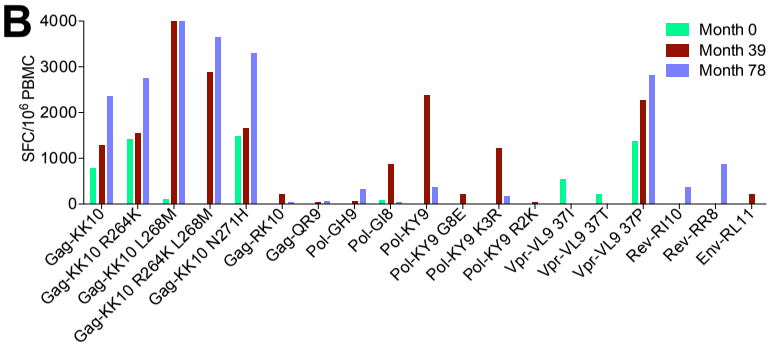

1. Identify CD8+ T-cell responses
ELISPOT/tetramers
SFC/10^6 PBMC
0
500
1000
1500
2000
Specificity 1
Specificity 2
Specificity 3
Specificity 4
Specificity 5
Specificity 1
4.1
Specificity 2
1.8
Specificity 3
0.6
Tetramer
CD8
2. Prepare effector and target cells
PBMC
mAb CD3.4
10-20d
Confirm CD8+ T-cell enrichment by FACS
Culture target cells
3. Delete specificities with tet-SAP
Tet-SAP tx
24-48 h
Bulk CTL
Tet-SAP 1
Tet-SAP 2
Tet-SAP 3
Confirm by FACS
4. Measure HIV-suppressive capacity
Virus-GFP
+
CTL
No CTL
+ bulk CTL
+ Tet-SAP 1
+ Tet-SAP2
+ Tet-SAP3
6-10 d
GFP by FACS
No CTL
+ bulk CTL
+ Tet-SAP 1
+ Tet-SAP 2
+ Tet-SAP 3
Days post-infection

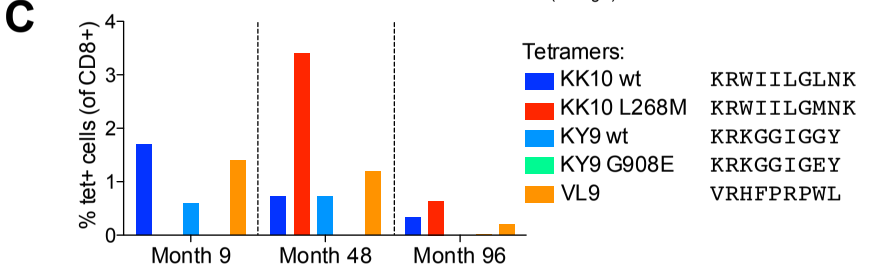
Figure 6.6. Workflow of the method to assess anti-HIV efficacy of different CD8+ T-cell specificities in human cells using tet-SAP. The proposed method consists of four main steps:

1. Identify CD8+ T-cell responses by IFN-γ ELISPOT and/or tetramer staining.
2. Expand CD8+ T cells with bi-specific CD3.4 monoclonal antibody and confirm targeted specificities by tetramer staining
   2.1. Include an anti-CD4 antibody in the panel to assess CD8+ T-cell purity.
   2.2. Use this period to generate SAP-conjugated tetramers.
   2.3. Prepare target cells: (i) if using HIV-permissive cell lines (e.g. H9, U937, T1), start the cultures a week before infection; (ii) if using primary CD4+ T cells, start their activation 3-4 days before superinfection.
3. Remove desired specificities with tet-SAP and confirm by tetramer staining. Include controls (HLA-mismatched tet-SAP, free SAP).
4. Perform viral inhibition assay using tet-SAP-treated CTL as effector cells. Use intracellular Gag-p24 staining or ELISA as a read-out if the virus used for infection does not have a GFP reporter.

We next evaluated the impact on viral inhibition of tet-SAP-mediated depletion of CD8+ T-cell responses present, studying two timepoints, 4 and 8 years after infection. At 4 years (48 months) post-infection, Pol-KY9 and Vpr-VL9 depletion made little difference to viral replication, while Gag-KK10 depletion significantly attenuated the ability of CD8+ T-cells to suppress viral replication, suggesting that the majority of bulk CD8+ T-cell-mediated inhibition was Gag-KK10-specific (**Figures 6.7E-G**). At 8 years (96 months) post-infection (**Figures 6.7H-J**), the contribution of the Pol-KY9 response to inhibition of viral replication was lost altogether; Vpr-VL9 continued not to contribute significantly to viral inhibition, and the Gag-KK10-specific cells contributed the most. Of note, the Gag-KK10 effect was seen with both the wild type-specific and mutant L268M-specific tet-SAP mediated depletion (**Figures 6.7G,J**). This can be explained by cross-recognition of the variant by the wild type-specific cells that are highly effective against both wild type



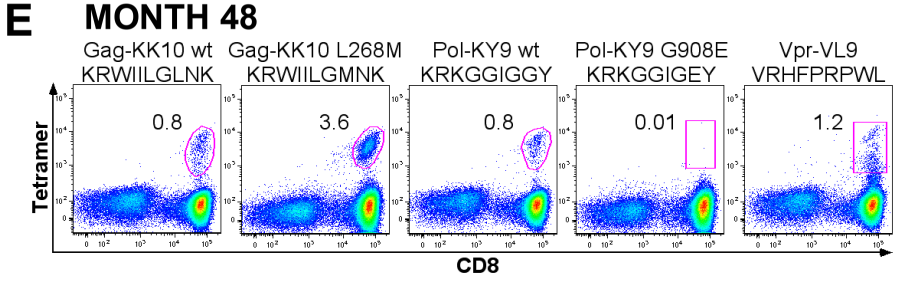


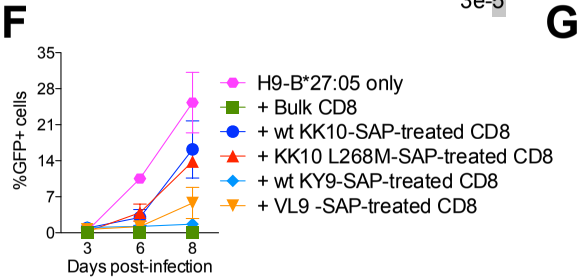


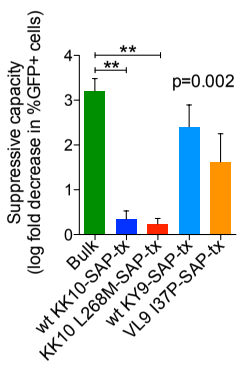
D

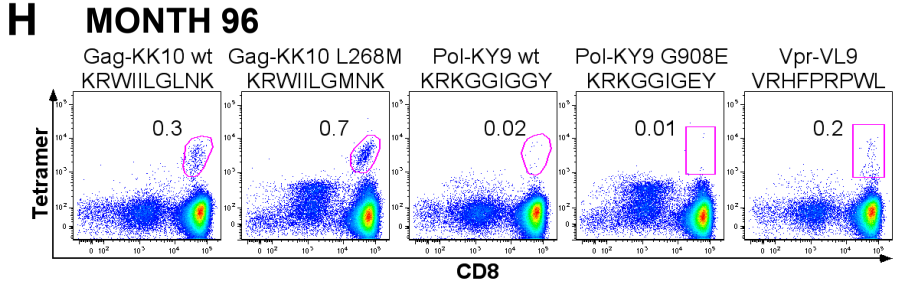
	B*27 Gag ^{263}KK10^{272} KRWIILGLNK	B*27 Gag ^{901}KY9^{909} KRKGGIGGY	B*27 Vpr ^{31}VL9^{39} VRHFPRPWL
Month 0	·····M··	·····E·	nd
Month 39	·····M··	·····E·	·K·····
Month 78	·····M··	·····E·	·K·····

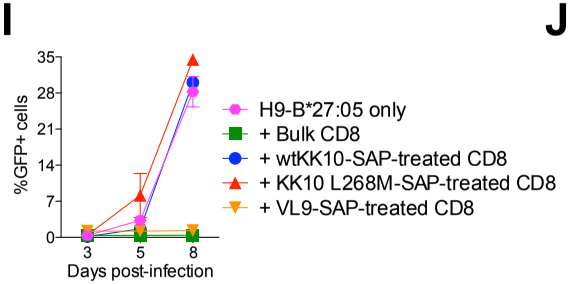
Escape variant	R264K	L268M	R902K	G908E	R32K	P37G
q value	8e-5	9e-5	5e-3	8e-21	6e-14	2e-4
			K903R 3e-5			











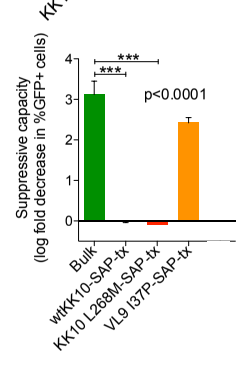


Figure 6.7. Definition of antiviral efficacy of different CD8+ T-cell responses using tet-SAP. All panels show data from one HIV-infected HLA-B*27:05-positive subject. **A.** Viral loads, CD4+ T-cell counts with timepoints of assays indicated. **B.** IFN-γ ELISPOT CD8+ T-cell responses to HLA-B*27-restricted optimal epitopes. Only responses >50 SFC/10^6 PBMC are shown. **C.** Frequency of antigen-specific cells of three dominant specificities determined by tetramer staining. **D.** Proviral sequences of the three dominant responses. Known HLA-B*27:05-associated footprints and the significance of the associations (q value) are shown (Carlson et al., 2012). Nd, not done. **E-G.** Results from timepoint 48 months post-infeciton; (H-J) results from timepoint 96 months post-infecition. **E,H.** Dot plots showing tetramer staining of existing in this donor HLA-B*27:05-restricted responses at the timepoint assayed. Gated on live CD3+ cells around CD8+tet+ cells; numbers indicate % tet+ cells (of CD8+). **F,I.** Viral replication in H9-HLA-B*27:05-positive infected target cells alone or with bulk CD8+ T cells or CD8+ T-cells depleted of a particular specificity with tet-SAP. Infected cells were measured by NL4-3-GFP expression. **(G,H)** Suppressive capacity of bulk or tet-SAP-depleted CD8+ T cells. F,G,I,J, error bars represent s.e.m. G,J, ANOVA with Dunnett's Multiple comparisons test to compare suppressive capacity of bulk versus tet-SAP-treated CD8+ T cells. *p<0.05, **p<0.01, ***p<0.001.

and L268M viruses, express an anti-apoptotic phenotype and are long-lived (Ladell et al., 2013; van Bockel et al., 2011). Although in this case the subject initiated ART through choice after 9 years of infection, viral load was well contained for much of this time at <2,000 copies/ml, and absolute CD4 counts were maintained at high levels of 500-700 cells/mm^3 until ART intervention. This is representative of 2 similar experiments involving HLA-B*27:05-positive HIV-infected individuals, showing that in subjects with low viral loads (e.g. 73 copies/ml, 518 copies/ml), inhibition of viral replication was highly dependent upon the Gag-KK10 response (**Figure 6.8**).

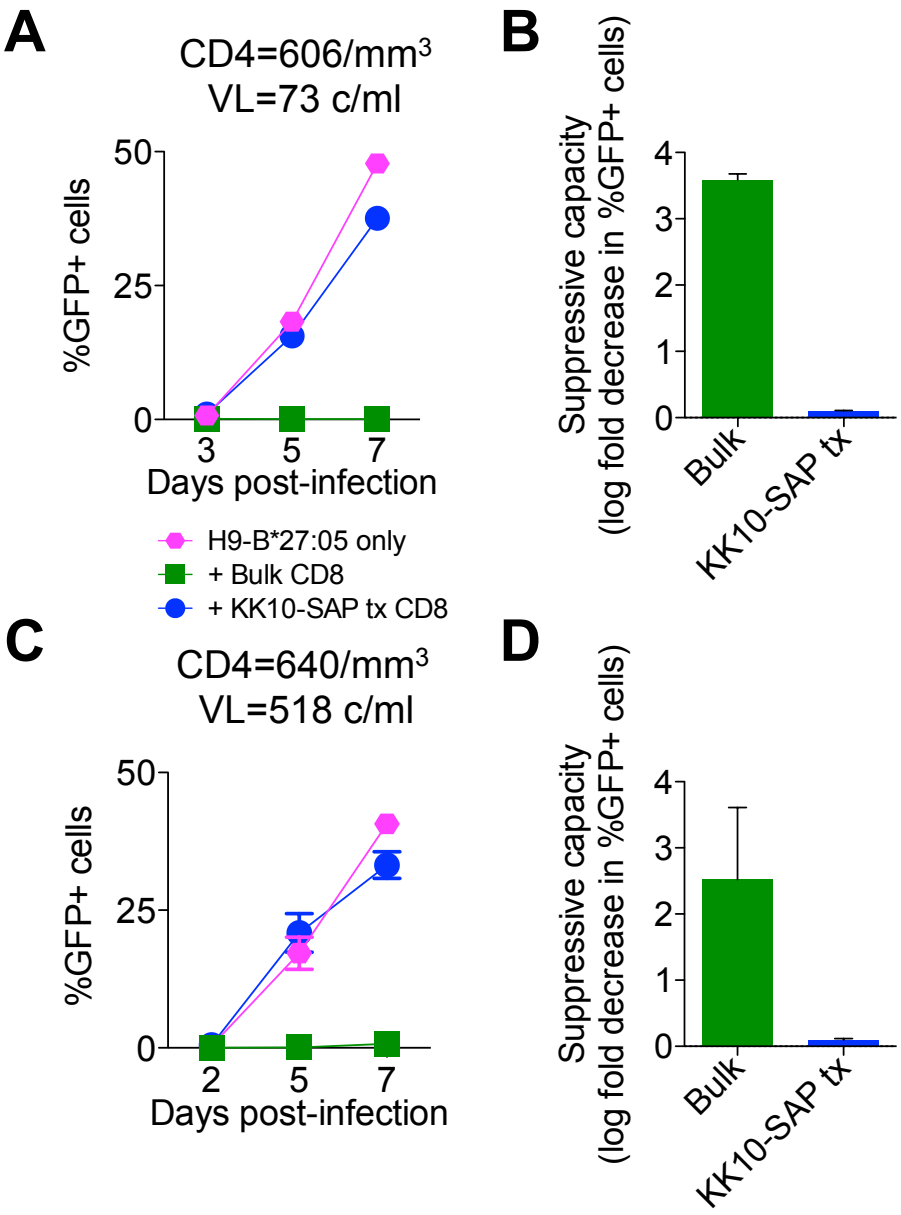


Figure 6.8. Examples of HIV-infected HLA-B*27:05-positive individuals with low viral loads in whom control of viral replication was dependent on Gag-KK10 response. Panels A,B show data for an HLA-B*27:05-positive controller with viral load of 73 copies/ml; panels C,D show data for another HLA-B*27:05-positive controller with viral load of 518 copies/ml. **A,C.** Viral replication in H9-HLA-B*27:05-positive infected target cells alone or with bulk CD8+ T cells or CD8+ T-cells depleted of Gag-KK10 specificity with tet-SAP. Infected cells were measured by NL4-3-GFP expression. **B,D.** Suppressive capacity of bulk or KK10-tet-SAP-depleted CD8+ T cells. Error bars represent s.e.m.

6.3.5 Discussion

In summary, we here show, for the first time, that cytotoxic saporin-conjugated tetramers can be used in *in vitro* studies with human cells. These tetramers bind and are internalised by cognate CD8+ T-cells, resulting in their effective elimination by as little as 24 hours. We did not observe an off-target effect and found that the tet-SAP approach is considerably simpler and less time-consuming than the conventional method using magnetic beads, especially if more than one CD8+ T-cell specificity is being assessed. These reagents can facilitate identification of effective HIV-specific CD8+ T-cell responses that could be induced by a successful vaccine, can also be used in other viral infections, such as CMV or HCV, and finally, as shown in murine studies (Hess et al., 2007), they have the potential for *in vivo* depletions to be undertaken immunotherapeutically in humans.

CHAPTER 7. CONCLUSIONS

CD8+ T-cells are critical mediators of the host immune protection against an array of viral pathogens. These cells have the intrinsic ability to expand immensely upon antigen encounter, effectively eliminate infected cells and persist for up to 75 years in humans to deal rapidly with any reappearing pathogen (Hammarlund et al., 2003). Yet in some infections, HIV being a case in point, CD8+ T-cell immunity in most cases fails to clear the infection. Only in extremely rare cases of elite control the cellular anti-HIV response succeeds, with a caveat that even in these instances the virus has not been completely eliminated. The unresolved questions of what allows the rare CD8+ T-cell responses to succeed against the virus, what their identities are and how to elicit this degree of antiviral efficacy in the majority of the remaining cases continue to be a priority.

In this thesis I have focused on the specific aspects of the interplay between host and virus in HIV infection to extend our understanding of the HLA-restricted CD8+ T-cell-mediated immune response. I dissected the contribution of particular antiviral HLA-B*57- and HLA-B*14-restricted CD8+ T-cell specificities to immune control in adult infection; I followed the evolution of CD8+ T-cell immune pressure on the virus over the first years of life in paediatric non-progressing infection; I examined the potential of a vaccine to alter natural CD8+ T-cell targeting to generate more beneficial antiviral responses; and finally, I developed a novel tool to evaluate the contribution of an individual CD8+ T-cell response to viral control.

In light of the new WHO recommendations to initiate ART for any HIV-infected person, irrespective of CD4 count and in children irrespective of age (Lundgren et al., 2015; WHO,

2015b), the relevance of these studies turns towards the issue of HIV cure, whether it is 'sterilising' or 'functional' cure. While early initiated ART reduces viral reservoir both in adult and paediatric infection, it does not eradicate it (Chun et al., 1997; Finzi et al., 1997; Luzuriaga et al., 2015). Many 'cure' strategies have focused on reactivation of this latent reservoir. However, since the reactivated latently infected cells do not die of viral cytopathic effects, the role that HIV-specific CD8+ T-cell response will play in eliminating the reactivated proviruses is likely to be critical (Deng et al., 2015; Shan et al., 2012). A better understanding of the successful CD8+ T-cell responses in natural infection is therefore essential to our ability to induce such responses therapeutically.

Of particular importance is the need to gain more insights into CD8+ T-cell activity during infection in early life. Little is known about the role of the CD8+ T-cell immune response in HIV-infected children. Similarly, while multiple strategies and immunotherapeutic interventions are being investigated in adults, such studies, even *ex vivo*, are rarely undertaken in children. However, the immune environment in early life – immunotolerance, T_H2 bias, low immune activation – provides a different background for the host-virus interactions and may present us with unique opportunities for achieving 'cure' in children. One of such opportunities is the so-called 'honeymoon period' (Ahmed, Oldstone, and Palese, 2007) – a period from ~3 to ~9 years of age during which the immune response is optimally adapted against a range of infections, including tuberculosis, influenza, malaria, Epstein-Barr virus, varicella zoster virus, mumps, measles and perhaps also HIV, such that it is sufficient to control the infection without causing immunopathology. Indeed, by 2 years of age levels of type I IFNs are similar to those in adults, levels of the immunosuppressive IL10 and T_H17-polarising IL6 and IL23 are lower than in neonates and T_{Reg} cell numbers are similar to those in adults (Kollmann et al., 2012). It is therefore possible that during this 'honeymoon period' there is a window of opportunity for

immunotherapeutic interventions to eradicate the viral reservoir prior to the onset of adolescence and linked to the adolescence high levels of ART non-adherence (Nsheha et al., 2014).

Given the high potential for cell-mediated immunity in the eradication strategies, further paediatric studies need to gain a better understanding of the role and function of the HIV-specific CD8+ T-cell responses generated in children and how these responses can be modulated with immunotherapeutic interventions. Similarly, in adult studies the focus on understanding and harnessing the 'best' CD8+ T-cell qualities is essential. Finally, development of effective therapeutic Gag-specific T-cell vaccines is an important step towards achieving HIV cure.

With that being said, it is crucial to keep in mind, however, that the future success will very likely depend on a multifaceted approach, in which the contributions of the innate and humoral immunity and other factors are just as important as those of the T-cell responses. It is also necessary to approach the results that we obtain in the laboratory with a grain of caution as they cannot always fully reflect the real-life scenarios.

The scale and scope of my D.Phil. studies, spanned a range of methods and topics, including application of the next generation sequencing to a unique historical cohort, development of a novel assay, exploration of individual case studies versus large population-level cohorts extending all the way to an HIV vaccine trial and, of course, writing original and review articles. Some of my work has already been published and several more manuscripts are in preparation – the HLA-B*14 project, tet-SAP method and the CD8+ T-cell selection pressure in early life. This latter theme will, in fact, be continued in the next several months, as I will examine directly the evolution of the anti-HIV

functionality and the phenotype of the CD8+ T-cells in paediatric slow and rapid progressors in the first decade of life. In a different subset of children from the PEHSS cohort who received treatment during the first year of life, I will have the opportunity to also examine in parallel the development and activity of the CD8+ T-cells and the dynamics of the viral reservoir size during treatment, after treatment interruption and upon treatment re-initiation.

I believe that the skills and the expertise that I have gained thanks to the depth and the breadth of my D.Phil. will enable me to contribute to the scientific knowledge in the near and far future both in the role of a scientist and a physician.

"You must do the things you think you cannot do."

Eleanor Roosevelt

APPENDIX

Table 8.1. Epitopes restricted by HLA-A alleles used in the analysis of paediatric deep sequence data (Chapter 4).

Epitope	Protein	Sequence	HXB2 location	Source
A*02-Env-IT10	Env	IGPGQTFYAT	311-320	a
A*02-Env-LV10	Env	LLDTIAIAV	814-822	a
A*02-Gag-FK10	Gag	FLGKIWPSHK	433-442	a
A*02-Gag-OLP4	Gag	GKKHYMLKHLVWASREL	24-41	a
A*02-Gag-SL9	p17	SLYNTVATL	77-85	b
A*02-Nef-PL10	Nef	PLTFGWCFKL	136-145	b
A*02-Pol-AM9	Pol	ALTAICEEM	188-196	a
A*02-Pol-IV9	Pol	ILKEPVHGV	464-472	b
A*02-Pol-VL9	Pol	VIYQYMDDL	334-342	a
A*02-Pol-YI9	Pol	YTAFTIPSI	282-290	a
A*02-Vpr-AL9	Vpr	AIIRILQQL	59-67	b
A*02:05-Gag-FK10	Gag	FLGKIWPSHK	433-442	a
A*02:05-Gag-OLP48	Gag	ACQGVGGPSHKARVLAEA	349-366	a
A*02:05-Gag-OLP58	Gag	QMKDCTERQANFLGKIW	422-438	a
A*02:05-Nef-OLP78	Nef	FKGAFDLSFFLKEKGGL	81-97	a
A*02:05-Pol-OLP162	Pol	GKKAIGTVLVGPTPVNII	124-141	a
A*02:05-Pol-OLP200	Pol	EKDSWTVNDIQKLVGKL	403-419	a
A*02:05-Pol-OLP202	Pol	SKLNWASQIYPGIKVRQL	417-434	a
A*02:05-Pol-OLP262	Pol	ELKKIIGQVRDQAEHLK	872-888	a
A*02:05-Rev-OLP96	Rev	QAVRIIKILYQSNPY	14-28	a
A*03:01-Gag-KK9	Gag	KIRLRPGGK	18-28	b
A*03:01-Pol-KK9	Pol	KLAGRWPVK	818-826	a
A*03:01-Pol-LK11	Pol	LVSIKVGGQIK	66-76	a
A*03:01-Pol-RK11	Pol	RVYLSWVPAHK	685-695	a
A*23:01-Env-KY9	Env	KYLGSLVQY	794-802	a
A*23:01-Env-NL10	Env	NYTNTIYRLL	637-646	a
A*23:01-Env-RL9	Env	RYLKDQQLL	585-593	b
A*23:01-Env-VW8	Env	VYYGVPVW	38-46	a
A*23:01-Gag-OLP4	Gag	GKKHYMLKHLVWASREL	25-41	a
A*23:01-Nef-OLP84	Nef	NYTPGPGVRYPLTFGWCF	126-143	a
A*23:01-Nef-OLP85	Nef	RYPLTFGWCFKLVPV	134-148	a
A*23:01-Pol-IL9	Pol	IYQEPFKNL	496-504	a
A*24-Env-LY10	Env	LFCASDAKAY	52-61	b
A*24-Env-RL9	Env	RYLKDQQLL	585-593	b
A*24-Nef-RW8	Nef	RYPLTFGW	134-141	c
A*24:02-Gag-OLP4	Gag	GKKHYMLKHLVWASREL	25-41	a
A*24:02-Pol-IL9	Pol	IYQEPFKNL	496-504	a
A*24:02-Pol-OLP211	Pol	GHDQWTYQIYQEPFKNLK	488-505	a
A*24:02-Pol-OLP212	Pol	IYQEPFKNLKTGKYAKMR	496-513	a
A*29:02-Env-SY10	Env	SFNCGGEFFY	375-384	d
A*29:02-Env-SY9	Env	SFDPIPIHY	209-217	d
A*29:02-Gag-LY9	Gag	LYNTVALTY	78-86	d
A*29:02-Nef-YY8	Nef	FFPDWQNY	120-127	d
A*30:02-Env-IY9	Env	IVNRVRQGY	704-712	e
A*30:02-Env-KY9	Env	KYLGSLVQY	794-802	e
A*30:02-Gag-RY11	Gag	RSLYNTVATLY	76-86	e
A*30:02-Nef-OLP83	Nef	QGYFPDWQNYTPGPGVRY	118-135	a
A*30:02-Pol-AY9	Pol	AQNPEIVIY	328-336	e

Epitope	Protein	Sequence	HXB2 location	Source
A*30:02-Pol-KY9	Pol	KLNWASQIY	418-426	e
A*30:02-Pol-OLP269	Pol	TKELQKQIIKIQNFRVYY	925-942	a
A*30:02-Pol-OLP270	Pol	IKIQNFRVYYRDSRDPIW	933-950	a
A*30:02-Vif-OLP406	Vif	RRANGWFYRHHYESRHPK	33-50	a
A*32-Env-RW9	Env	RIKQIINMW	419-427	b
A*32-Pol-PSW10	Pol	PIQLPEKDSW	398-407	f
A*32-Pol-PTW10	RT	PIQKETWETW	547-556	b
A*33-Pol-OLP261	Pol	VVESMNKELKKIIGQVR	865-882	a
A*33:01-Pol-OLP274	Pol	VIQDNSDIKVVPRRKAKI	965-982	a
A*34:02-Gag-OLP19	Gag	IVQNLQGQMVHQAISPR	134-150	a
A*34:02-Nef-OLP81	Nef	KKRQEILDLWVYHTQGYF	104-121	a
A*43-Env-OLP293	Env	VVGNLWVTVYYGVPVWK	30-46	a
A*43-Env-OLP294	Env	TVYYGVPVWKEAKTTLF	37-53	a
A*66-Pol-ER11	Pol	ETFYVDGAANR	593-603	a
A*66-Vpr-OLP-283	Vpr	GLGQYIYETYGDTWTGV	41-57	a
A*66:01-Tat-OLP-111	Tat	MEPVDPNLEPWNHPGSQPK	1-19	a
A*68:01-Gag-DR12	Gag	DTINEEAAEWDR	203-214	a
A*68:01-Gag-OLP28	Gag	LKDTINEEAAEWDRLHPV	201-218	a
A*68:01-Nef-IR10	Nef	IVGWPAVRER	10-19	a
A*68:01-Nef-OLP68	Nef	SSIVGWPAVRERIRR	8-22	a
A*68:01-Pol-EK13	Pol	EVQLGIPHPAGLK	244-256	a
A*68:01-Pol-NK10	Pol	NTPVFAIKKK	212-221	a
A*68:01-Pol-OLP178	Pol	FWEVQLGIPHPAGLKKKK	242-259	a
A*68:01-Vif-DR9	Vif	DCFADSAIR	113-121	a
A*68:01-Vif-ER10	Vif	EVHIPLGEAR	54-63	a
A*68:01-Vif-OLP408	Vif	HPKVSSEVHIPLGEARLV	48-65	a
A*68:01-Vif-OLP416	Vif	LIHMHYFDCFADSAIRKA	106-123	a
A*68:01-Vpu-OLP131	Vpu	STMVDMGHLRLLDVNDL	66-82	a
A*68:01-Vpu-SR10	Vpu	STMVDMGHLR	66-75	a
A*68:02-Gag-EI9	Gag	ETSEGCKQI	52-60	g
A*68:02-Gag-TA10	Gag	TTSTLQEQIA	239-248	g
A*68:02-Nef-ML9	Nef	MTYKAAFDL	79-87	g
A*68:02-Pol-EA8	Pol	AETFYVDGAANRETKIG	592-608	g
A*68:02-Pol-Int-EA10	Pol	ETAYYILKLA	811-820	g
A*68:02-Pol-RT-EA10	Pol	ETWWTDYWQA	554-563	g
A*68:02-Rev-SA8	Rev	STCLGRPA	61-68	g
A*68:02-Vpr-EV10	Vpr	ETYGDTWTGV	48-57	g
A*74:01-Gag-GR11	Gag	GQMVHQAISPR	140-150	h
A*74:01-Gag-KR9	Gag	KLDKWEKIR	12-20	h
A*74:01-Gag-SK10	Gag	SILRGEKLDK	6-15	h
A*74:01-Nef-SR9	Nef	SLARRHLAR	188-196	h
A*74:01-Pol-NR10	Pol	NLAFPQGEAR	5-14	h
A*74:01-Pol-SK9	Pol	SLTETTNQK	623-631	h
A*74:01-Pol-SR10	Pol	SQIYPGIKVR	423-432	h
A*74:01-Rev-RR9	Rev	RQIHSISER	50-58	h

Table 8.2 Epitopes restricted by HLA-B alleles used in the analysis of paediatric deep sequence data (Chapter 4).

Epitope	Protein	Sequence	HXB2 location	Source
B*07:02-Env-IF9	Env	IPRRIRQGF	843-851	i
B*07:02-Env-RI10	Env	RPNNNTRKSI	298-307	i
B*07:02-Gag-GL9	Gag	GPSHKARVL	355-363	i
B*07:02-Gag-HA9	Gag	HPVHAGPIA	216-224	i
B*07:02-Gag-RM9	Gag	RPGGKKHYM	22-30	i
B*07:02-Gag-SV9	Gag	SPRTLNAWV	148-156	i
B*07:02-Gag-TL9	Gag	TPQDLNTML	180-188	i
B*07:02-Nef-FL9	Nef	FPVRPQVPL	68-76	i
B*07:02-Nef-RF9	Nef	RPMTFKGAF	77-85	i
B*07:02-Nef-RM9	Nef	RPQVPLRPM	71-79	i
B*07:02-Nef-TL10	Nef	TPGPGVRYPL	128-137	i
B*07:02-Pol-LI9	Pol	LPPIVAKEI	743-751	i
B*07:02-Pol-SM9	Pol	SPAIFQSSM	311-319	i
B*07:02-Rev-RL10	Rev	RPAEPVPLQL	66-75	i
B*07:02-Vif-HI10	Vif	HPKVSSEVHI	48-57	i
B*07:02-Vpr-FL9	Vpr	FPRPWLHGL	34-42	i
B*08-Env-YL8	gp41	YLKDQQLL	586-593	b
B*08-Gag-DI8	p24	DIYKRWII	260-267	a
B*08-Gag-DL9	p24	DCKTILRAL	329-337	b
B*08-Gag-EL8	Gag	EPKDREPL	477-486	a
B*08-Gag-EV9	p17	ELRSLYNTV	74-82	b
B*08-Gag-GL8	Gag	GGKKHYML	24-31	a
B*08-Nef-FL8	Nef	FLKEKGGL	90-97	b
B*08-Nef-WM8	Nef	WPAVRERI	13-20	b
B*08-Pol-GL9	Pol	GPKVKQWPL	173-181	b
B*14-Env-EL9	Env	ERYLKDQQL	584-592	b
B*14-Gag-DA9	Gag	DRFFKTLRA	298-306	b
B*14:02-Gag-OLP37	Gag	WIILGLNKIVRMYSPVSI	265-282	a
B*15:03-Gag-VF9 (p24)	Gag	VKVIEEKAF	156-164	j
B*15:03-Nef-WF9	Nef	WKFDSHLAF	183-191	a
B*15:03-Pol-FY10	Pol	FKRKGGIGGY	900-909	j
B*15:03-Pol-GL9	Pol	GKKAIGTVL	124-132	a
B*15:03-Pol-IY9	Pol	IQQEFGIPY	850-858	j
B*15:03-Pol-RY9	Pol	RKAKIIKDY	978-986	b
B*15:03-Pol-VI10	Pol	VKAACWWAGI	841-850	a
B*15:03-Tat-FY10	Tat	FQTKGLGISY	38-47	j
B*15:10-Env-OLP395	Env	LGSLVQYWGLELKKSAVSLL	796-815	a
B*15:10-Gag-GL9	Gag	GHQAAMQML	193-201	b
B*15:10-Gag-HL9	Gag	HQAISPRTL	144-152	b
B*15:10-Gag-KL8	Gag	KHYMLKHL	27-34	a
B*15:10-Nef-OLP76	Nef	EVGFPVRPQVPLRPMTFK	65-82	a
B*15:10-Pol-KL9	Pol	KHQKEPPFL	375-383	a
B*15:10-Pol-OLP249	Pol	GIWQLDCTHLEGKIILVA	774-791	a
B*15:10-Rev-GL11	Rev	GRPAEPVPLQL	65-75	a
B*15:10-Rev-IL9	Rev	IHSISERIL	52-60	a
B*15:10-Vif-OLP407	Vif	RHHYESRHPKVSSEVHI	41-57	a
B*15:10-Vif-WI9	Vif	DWHLGHGVSI	78-87	b
B*15:16-Env-SF9	Env	SFNCGGEFF	375-383	b
B*15:16-Pol-163	Pol	LVGPTPVNIIGRNMLTQL	132-149	a
B*15:16-Pol-226	Pol	ETKIGKAGYVTDRGRQKI	604-621	a
B*18-Env-GF10	Env	GDLEITTHSF	367-376	a

Epitope	Protein	Sequence	HXB2 location	Source
B*18-Nef-YY9	Nef	YPLTFGWCY	135-143	a
B*18-Pol-NY10	RT	NETPGIRYQY	292-301	b
B*18-Pol-NY9	RT	NPEIVIYQY	330-338	b
B*18-Pol-SY11	RT	SEVNIVTDSQY	646-656	a
B*18-Pol-TL10	RT	TETTNQKTEL	625-634	a
B*18-Pol-VL9	Pol	VASCDKLQL	752-760	a
B*18-Rev-DI10	Rev	DEALLQAVRI	9-18	a
B*18-Vif-IY8	Vif	IEWRLRRY	87-94	a
B*18-Vif-LY10	Vif	LADQLIHLHY	102-111	b
B*18:01-AY9	Vif	ADQLIHMHY	103-111	a
B*18:01-Nef-QY9	Nef	QEILDLWVY	107-115	a
B*18:01-Nef-YF9	Nef	YPLTFGWCF	135-143	a
B*35:01Pol-EY10	Pol	EPIAGAETFY	587-596	k
B*35:01-Env-DL9	Env	DPNPQEMVL	78-86	k
B*35:01-Env-TW9	Env	TAVPWNSSW	606-614	k
B*35:01-Env-VL11	Env	VPVWKEATTTL	42-52	k
B*35:01-Gag-HA9	Gag	H**P**VHAGPIA	216-224	k
B*35:01-Gag-NY10	Gag	NPPIPVGDIY	253-262	k
B*35:01-Nef-VF9	Nef	VPLRPMTF	73-81	k
B*35:01-Nef-YF9	Nef	YPLTFGWCY	135-143	k
B*35:01-Pol-IY11	Pol	IPAETGQETAY	804-814	k
B*35:01-Pol-NY9	Pol	NPEIVIYQY	330-338	k
B*35:01-Pol-TY9	Pol	TVLDVGDAY	262-270	k
B*35:01-Rev-QY10	Rev	QAVRIIKILY	14-23	k
B*35:01-Pol-VY10	Pol	VPLDKEFRKY	273-282	k
B*39-Pol-PA10	Pol	PPIVAKEIVA	744-753	a
B*39-Rev-QY10	Rev	QAVRIIKILY	14-23	a
B*39:01-Gag-GL9	Gag	GHQAAMQML	193-201	a
B*39:10-Env-OLP321	Env	QCTHGI**KPVVSTQLL**L	246-261	a
B*39:10-Env-OLP322	Env	**KPVVSTQLL**LNGSLA	252-266	a
B*39:10-Gag-HA9	Gag	HPVHAGPIA	216-224	a
B*39:10-Gag-NL11	Gag	NPDCKTILRAL	327-337	a
B*39:10-Gag-TL9	Gag	TPQDLNTML	180-188	d
B*39:10-Pol-LI11	Pol	LPSGWKGSPAI	304-314	a
B*39:10-Pol-OLP231	Pol	EVNIVTDSQYALGII	647-661	a
B*39:10-Pol-OLP233	Pol	ALGIIQAQPDKSESEL	657-672	a
B*39:10-Pol-OLP234	Pol	AQPDKSESELVNQIIEQL	663-680	a
B*39:10-Pol-SL10	Pol	SPIETVPVKL	158-167	a
B*41-Pol-OLP206	Pol	PLTEEAELELAENREILK	449-466	a
B*42-Pol-OLP-184	Pol	PSINNETPGIRYQYNVL	288-304	a
B*42:01-Env-IF9	Env	IPRRIRQGF	843-851	l
B*42:01-Env-RI10	Env	RPNNNTRKSI	298-307	l
B*42:01-Gag-GF9	Gag	GPKRIVKCF	385-393	l
B*42:01-Gag-GL9	Gag	GPSHKARVL	355-363	l
B*42:01-Gag-OLP-37	Gag	WIILGLNKIVRMYSPVSI	265-282	a
B*42:01-Gag-OLP-65	Gag	PKQEPKDREPLTSLK	473-490	a
B*42:01-Gag-RM9	Gag	RPGGKKHYM	22-30	l
B*42:01-Gag-TL9	Gag	TPQDLNTML	180-188	l
B*42:01-Nef-OLP-73	Nef	GALTSSNTDTTNADCAWL	41-58	a
B*42:01-Nef-OLP-78	Nef	FKGAFDLSFFLKEKGGL	81-97	a
B*42:01-Nef-RF9	Nef	RPMTYKAAF	77-85	l
B*42:01-Nef-RM9	Nef	RPQVPLRPM	71-79	l
B*42:01-Nef-RM9	Nef	RPQVPLRPM	71-79	l
B*42:01-Nef-TL10	Nef	TPGPGVRYPL	128-137	l

Epitope	Protein	Sequence	HXB2 location	Source
B*42:01-Pol-IM9	Pol	IIKDYGKQM	982-990	l
B*42:01-Pol-LI9	Pol	LPPIVAKEI	743-751	l
B*42:01-Pol-OLP-186	Pol	QYNVLPQGWKGSPAIF	300-315	a
B*42:01-Pol-YL9	Pol	YPGIKVRQL	426-434	l
B*42:01-Vif-HI10	Vif	HPKVSSEVHI	48-57	l
B*42:01-Vpr-FL9	Vpr	FPRPWLHSL	34-42	l
B*42:02-Env-KL9	Env	KPCVKLIPL	117-125	l
B*42:02-Env-RI10	Env	RPNNNTRKSI	298-307	l
B*42:02-Gag-RM9	Gag	RPGGKKHYM	22-30	l
B*42:02-Nef-RF9	Nef	RPMTYKAAF	77-85	l
B*42:02-Nef-RM9	Nef	RPQVPLRPM	71-79	l
B*42:02-Nef-TL10	Nef	TPGPGVRYPL	128-137	l
B*42:02-Pol-GL9	Pol	GPKVKQWPL	173-180	l
B*42:02-Pol-SM9	Pol	SPAIFQSSM	311-319	l
B*42:02-Pol-TL11	Pol	TPGIRYQYNVL	294-304	l
B*42:02-Pol-YL9	Pol	YPGIKVRQL	426-434	l
B*42:02-Rev-RL10	Rev	RPAEPVPLQL	66-75	l
B*42:02-Vpr-FL9	Vpr	FPRPWLHSL	34-42	l
B*44-Env-AY9	Env	AENLWVTVY/VGNLWVTVY	31-39	b
B*44-Gag-AW11	Gag	AEQASQDVKNW	306-316	b
B*44-Pol-EW10	Pol	EEHEKYHSNW	725-734	a
B*44-Pol-SY11	Pol	SEVNIVTDSQY	646-656	a
B*45:01-Nef-EV11	Nef	EEVGFPVRPQV	64-74	a
B*45:01-Pol-AA9	Pol	AETFYVDGA	592-600	a
B*45:01-Pol-NV8	Pol	NEQVDKLV	700-707	a
B*57:02-Gag-IW9	Gag	ISPRTLNAW	147-155	m
B*57:02-Gag-QW9	Gag	QATQDVKNW	308-316	m
B*57:02-Gag-TW10	Gag	TSTLQEQIAW	240-249	m
B*57:02-Nef-KF9	Nef	KAAFDLSFF	82-90	m
B*57:02-Pol-FF9	Pol	FSVPLDEGF	271-279	m
B*57:02-Pol-IW9	Pol	IAMESIVIW	530-538	m
B*57:02-Pol-QF10	Pol	QATWIPEWEF	562-571	m
B*57:03-Env-KW11	Env	KAYEKEVHNVW	59-69	m
B*57:03-Env-TW9	Env	TVYYGVPVW	37-44	m
B*57:03-Gag-IW9	Gag	ISPRTLNAW	147-154	m
B*57:03-Gag-KF11	Gag	KAFSPEVIPMF	162-172	m
B*57:03-Gag-LF11	Gag	LVWASRELERF	34-44	m
B*57:03-Gag-QW9	Gag	QATQDVKNW	308-316	m
B*57:03-Gag-TW10	Gag	TSTLQEQIAW	240-249	m
B*57:03-Nef-HW9	Nef	HTQGFFPDW	116-124	m
B*57:03-Nef-KF9	Nef	KAAFDLSFF	82-90	m
B*57:03-Pol-FF9	Pol	FSVPLDEGF	271-279	m
B*57:03-Pol-IW9	Pol	IAMESIVIW	530-538	m
B*57:03-Pol-KF9	Pol	KTAVQMAVF	888-896	m
B*57:03-Pol-QF10	Pol	QATWIPEWEF	562-571	m
B*57:03-Rev-QY10	Rev	QAVRIIKILY	14-22	m
B*57:03-Vif-LW9	Vif	LGHGVSIEW	81-88	m
B*58:01-Env-KW11	Env	KAYEKEVHNVW	59-69	m
B*58:01-Env-OLP-347	Env	AGNITCKSNITGLLLTR	440-456	m
B*58:01-Env-TW9	Env	TVYYGVPVW	37-45	m
B*58:01-Gag-DW10	Gag	DTINEEAAEW	203-212	m
B*58:01-Gag-QW9	Gag	QATQDVKNW	308-316	m
B*58:01-Gag-TW10	Gag	TSTLQEQIAW	240-249	m
B*58:01-Nef-HW9	Nef	HTQGFFPDW	116-124	m

Epitope	Protein	Sequence	HXB2 location	Source
B*58:01-Nef-KF9	Nef	KAAFDLSFF	82-90	m
B*58:01-Pol-IW9	Pol	IAMESIVIW	530-538	m
B*58:01-Pol-KF9	Pol	KTAVQMAVF	888-896	m
B*58:01-Pol-SW9	Pol	SAAVKAACW	838-846	m
B*58:01-Rev-QY10	Rev	QAVRIIKILY	14-23	m
B*58:02-Env-IL10	Env	ITLTVQARQL	535-544	a
B*58:02-Env-QL11	Env	QTRVLAIERYL	577-587	n
B*58:02-Pol-LF11	Pol	LAFPQGEAREF	6-16	a
B*81-Gag-TL9	Gag	TPQDLNTML	180-188	o
B*81-Nef-RM9	Nef	RPQVPLRPM	71-79	a
B*81-Pol-LA9	Pol	LFLDGIDKA	715-723	a
B*81-Pol-TL10	Pol	TPVNIIGRNL	136-145	a
B*81-Pol-TL11	Pol	TPVNIIGRNLL	136-146	a
B*81-Vpr-FL9	Vpr	FPRIWLHGL	34-42	b
B*81:01-Pol-PI8	Pol	PPIVAKEI	744-751	a
B*81:01-Pol-SL10	Pol	SPIETVPVKL	158-167	a
B*81:01-Pol-SM9	Pol	SPAIFQSSM	311-319	a
B*81:01-Pol-TL11	Pol	TPPLVKLWYQL	574-584	a

Table 8.3. Epitopes restricted by HLA-C alleles used in the analysis of paediatric deep sequence data (Chapter 4).

Epitope	Protein	Sequence	HXB2 location	Source
C*02:02-Pol-OLP207	Pol	ELAENREILKEPVHGVYY	457-474	a
C*03-Gag-YL9	Gag	YVDRFFKTL	296-304	a
C*04-Env-OLP371	Env	WSNKSQEEIWDNMTWMQW	614-631	a
C*04-Env-OLP372	Env	IWDNMTWMQWDREISNY	622-638	a
C*04-Env-SF9	Env	SFNCGGEFF	375-383	b
C*04:01-Env-OLP316	Env	KVSFDPIPIHYCAPAGYA	207-224	a
C*04:01-Pol-OLP180	Pol	KKKSVTVLDVGDAYFSV	257-273	a
C*06:02-Env-OLP325	Env	IRSENLTNNAKTIIVHL	272-288	a
C*06:02-Pol-OLP213	Pol	LKTGKYAKMRTAHTNDVK	504-521	a
C*07-Nef-KY11	Nef	KRQEILDLWVY	105-115	a
C*08-Rev-SL9	Rev	PAEPVPLQL	67-75	a
C*08:01-Env-OLP-357	Env	RAVGIGAVFLGFLGAA	511-526	a
C*08:01-Env-OLP-362	Env	IVQQQSNLLRAIEAQQHM	548-565	a
C*08:01-Gag-OLP46	Gag	TILRALGPGASLEEMMTA	332-349	a
C*08:02-Gag-TL9	Gag	TPQDLNTML	180-188	o
C*08:02-Pol-OLP268	Pol	DIIATDIQTKELQKQIIK	917-934	a
C*08:02-Vif-OLP417	Vif	CFADSAIRKAILGHIV	114-129	a
C*12:03-Gag-OLP45	Gag	NANPDCKTILRALGPGA	325-341	a
C*12:03-Nef-OLP76	Nef	EVGFPVRPQVPLRPMTYK	65-82	a
C*12:03-Pol-OLP190	Pol	RAQNPEIVIYQYMDDLYV	327-344	a
C*12:03-Pol-OLP216	Pol	QKIAMESIVIWGKTPKFR	528-545	a
C*18:01-Gag-FF9	Gag	FRDYVDRFF	293-301	d
C*18:01-Gag-VI9	Gag	VRMYSPVSI	274-282	d
C*18:01-Pol-VL8	Pol	VRDQAEHL	880-887	d
C*18:01-Vpu-YI9	Vpu	YRLGVGALI	12-20	d

Sources used in Tables 8.1-8.3:

a: Goulder group, unpublished; additionally overlapping peptides that do not contain defined optimal epitopes, but for which significant associations between expression of HLA alleles and recognition of the overlapping peptides have been compiled in the Goulder group. These were based on ELISPOT and HLA data of >1,000 individuals from the Sinikithemba and Gateway cohorts and statistically determined by Dr. Jonathan Carlson, Microsoft Research, Redmond, WA, USA (see the description in Chapter 5, Methods). Underlined sequences indicated predicted optimal epitopes; **b**: Los Alamos A-list (LLano A, 2013); **c**: (Goulder et al., 1997); **d**: (Honeyborne et al., 2006); **e**: (Goulder et al., 2001a); **f**: (Matthews et al., 2008); **g**: (Kloverpris et al., 2013b); **h**: (Matthews et al., 2011); **i**: (Kloverpris et al., 2014a); **i**: (Kloverpris et al., 2014b); **k**: (Matthews et al., 2012); **l**: (Kloverpris et al., 2012a); **m**: (Kloverpris et al., 2012b); **n**: (Ngumbela et al., 2008); **o**: (Goulder et al., 2000).

REFERENCES

Abrams, D., Y. Levy, M.H. Losso, A. Babiker, G. Collins, D.A. Cooper, J. Darbyshire, S. Emery, L. Fox, F. Gordin, H.C. Lane, J.D. Lundgren, R. Mitsuyasu, J.D. Neaton, A. Phillips, J.P. Routy, G. Tambussi, and D. Wentworth. **2009**. Interleukin-2 therapy in patients with HIV infection. *N Engl J Med* 361:1548-1559.

Addo, M.M., X.G. Yu, A. Rathod, D. Cohen, R.L. Eldridge, D. Strick, M.N. Johnston, C. Corcoran, A.G. Wurcel, C.A. Fitzpatrick, M.E. Feeney, W.R. Rodriguez, N. Basgoz, R. Draenert, D.R. Stone, C. Brander, P.J. Goulder, E.S. Rosenberg, M. Altfeld, and B.D. Walker. **2003**. Comprehensive epitope analysis of human immunodeficiency virus type 1 (HIV-1)-specific T-cell responses directed against the entire expressed HIV-1 genome demonstrate broadly directed responses, but no correlation to viral load. *J Virol* 77:2081-2092.

Adland, E., J.M. Carlson, P. Paioni, H. Kloverpris, R. Shapiro, A. Ogwu, L. Riddell, G. Luzzi, F. Chen, T. Balachandran, D. Heckerman, A. Stryhn, A. Edwards, T. Ndung'u, B.D. Walker, S. Buus, P. Goulder, and P.C. Matthews. **2013**. Nef-specific CD8+ T cell responses contribute to HIV-1 immune control. *PLoS One* 8:e73117.

Adland, E., L. Laker, M. Mori, J. Hurst, P. Jooste, and P. Goulder. 2014. Mechanisms of non-pathogenicity in HIV: Lessons from paediatric infection. In 20th International AIDS Conference. International AIDS Society, Melbourne, Australia.

Adland, E., P. Paioni, C. Thobakgale, L. Laker, L. Mori, M. Muenchhoff, A. Csala, M. Clapson, J. Flynn, V. Novelli, J. Hurst, V. Naidoo, R. Shapiro, K.H. Huang, J. Frater, A. Prendergast, J.G. Prado, T. Ndung'u, B.D. Walker, M. Carrington, P. Jooste, and P.J. Goulder. **2015**. Discordant Impact of HLA on Viral Replicative Capacity and Disease Progression in Pediatric and Adult HIV Infection. *PLoS Pathog.* 11:e1004954.

Ahmed, R., M.B. Oldstone, and P. Palese. **2007**. Protective immunity and susceptibility to infectious diseases: lessons from the 1918 influenza pandemic. *Nature Immunol.* 8:1188-1193.

Almeida, J.R., D.A. Price, L. Papagno, Z.A. Arkoub, D. Sauce, E. Bornstein, T.E. Asher, A. Samri, A. Schnuriger, I. Theodorou, D. Costagliola, C. Rouzioux, H. Agut, A.G. Marcelin, D. Douek, B. Autran, and V. Appay. **2007**. Superior control of HIV-1 replication by CD8+ T cells is reflected by their avidity, polyfunctionality, and clonal turnover. *J Exp Med* 204:2473-2485.

Almeida, J.R., D. Sauce, D.A. Price, L. Papagno, S.Y. Shin, A. Moris, M. Larsen, G. Pancino, D.C. Douek, B. Autran, A. Saez-Cirion, and V. Appay. **2009**. Antigen sensitivity is a major determinant of CD8+ T-cell polyfunctionality and HIV-suppressive activity. *Blood* 113:6351-6360.

Altfeld, M., M.M. Addo, R.L. Eldridge, X.G. Yu, S. Thomas, A. Khatri, D. Strick, M.N. Phillips, G.B. Cohen, S.A. Islam, S.A. Kalams, C. Brander, P.J. Goulder, E.S.

Rosenberg, and B.D. Walker. **2001**. Vpr is preferentially targeted by CTL during HIV-1 infection. *J Immunol* 167:2743-2752.

Altfeld, M., and P.J. Goulder. **2011**. The STEP study provides a hint that vaccine induction of the right CD8+ T cell responses can facilitate immune control of HIV. *J Infect Dis* 203:753-755.

Altfeld, M.A., A. Trocha, R.L. Eldridge, E.S. Rosenberg, M.N. Phillips, M.M. Addo, R.P. Sekaly, S.A. Kalams, S.A. Burchett, K. McIntosh, B.D. Walker, and P.J. Goulder. **2000**. Identification of dominant optimal HLA-B60- and HLA-B61-restricted cytotoxic T-lymphocyte (CTL) epitopes: rapid characterization of CTL responses by enzyme-linked immunospot assay. *J Virol* 74:8541-8549.

Altman, J., Davis, M. 2003. MHC-Peptide Tetramers to Visualize Antigen-Specific T Cells. In Current Protocols in Immunology. 1-33.

Altman, J.D., P.A. Moss, P.J. Goulder, D.H. Barouch, M.G. McHeyzer-Williams, J.I. Bell, A.J. McMichael, and M.M. Davis. **1996**. Phenotypic analysis of antigen-specific T lymphocytes. *Science* 274:94-96.

Alvarez, Y., M. Tuen, G. Shen, F. Nawaz, J. Arthos, M.J. Wolff, M.A. Poles, and C.E. Hioe. **2013**. Preferential HIV infection of CCR6+ Th17 cells is associated with higher levels of virus receptor expression and lack of CCR5 ligands. *J. Virol.* 87:10843-10854.

Ananworanich, J., T. Puthanakit, P. Suntarattiwong, K. Chokephaibulkit, S.J. Kerr, R. Fromentin, W. Bakeman, J. Intasan, A. Mahanontharit, S. Sirivichayakul, and N. Chomont. **2014**. Reduced markers of HIV persistence and restricted HIV-specific immune responses after early antiretroviral therapy in children. *AIDS* 28:1015-1020.

AVERT. 2016. Global HIV and AIDS statistics. In http://www.avert.org/professionals/hiv-around-world/global-statistics - footnote2_e2c543m. Accessed 16 March 2016.

Babiker, A., S. Darby, D. De Angelis, D. Ewart, and K. Porter. **2000**. Collaborative Group on AIDS Incubation and HIV Survival including the CASCADE EU Concerted Action. Concerted Action on SeroConversion to AIDS and Death in Europe. Time from HIV-1 seroconversion to AIDS and death before widespread use of highly-active antiretroviral therapy: a collaborative re-analysis. *Lancet* 355:1131-1137.

Barouch, D.H., J. Kunstman, J. Glowczwskie, K.J. Kunstman, M.A. Egan, F.W. Peyerl, S. Santra, M.J. Kuroda, J.E. Schmitz, K. Beaudry, G.R. Krivulka, M.A. Lifton, D.A. Gorgone, S.M. Wolinsky, and N.L. Letvin. **2003**. Viral escape from dominant simian immunodeficiency virus epitope-specific cytotoxic T lymphocytes in DNA-vaccinated rhesus monkeys. *J Virol* 77:7367-7375.

Barouch, D.H., J. Kunstman, M.J. Kuroda, J.E. Schmitz, S. Santra, F.W. Peyerl, G.R. Krivulka, K. Beaudry, M.A. Lifton, D.A. Gorgone, D.C. Montefiori, M.G. Lewis,

S.M. Wolinsky, and N.L. Letvin. **2002**. Eventual AIDS vaccine failure in a rhesus monkey by viral escape from cytotoxic T lymphocytes. *Nature* 415:335-339.

Barre-Sinoussi, F., J.C. Chermann, F. Rey, M.T. Nugeyre, S. Chamaret, J. Gruest, C. Dauguet, C. Axler-Blin, F. Vezinet-Brun, C. Rouzioux, W. Rozenbaum, and L. Montagnier. **1983**. Isolation of a T-lymphotropic retrovirus from a patient at risk for acquired immune deficiency syndrome (AIDS). *Science* 220:868-871.

Barry, A.P., G. Silvestri, J.T. Safrit, B. Sumpter, N. Kozyr, H.M. McClure, S.I. Staprans, and M.B. Feinberg. **2007**. Depletion of CD8+ cells in sooty mangabey monkeys naturally infected with simian immunodeficiency virus reveals limited role for immune control of virus replication in a natural host species. *J Immunol* 178:8002-8012.

Bashirova, A.A., E. Martin-Gayo, D.C. Jones, Y. Qi, R. Apps, X. Gao, P.S. Burke, C.J. Taylor, J. Rogich, S. Wolinsky, J.H. Bream, P. Duggal, S. Hussain, J. Martinson, A. Weintrob, G.D. Kirk, J. Fellay, S.P. Buchbinder, J.J. Goedert, S.G. Deeks, F. Pereyra, J. Trowsdale, M. Lichterfeld, A. Telenti, B.D. Walker, R.L. Allen, M. Carrington, and X.G. Yu. **2014**. LILRB2 interaction with HLA class I correlates with control of HIV-1 infection. *PLoS Genet.* 10:e1004196.

Bates, D., Maechler M., Bolker B., and Walker S. 2014. lme4: Linear mixed-effects models using Eigen and S4. R package version 1.1-7. In.

Benjamini, Y., Hochberg, Y. 1995. Controlling the false discovery rate: a practical and powerful approach to multiple testing. *Journal of the Royal Statistical Society. Series B* 57:289-300.

Besson, G.J., C.M. Lalama, R.J. Bosch, R.T. Gandhi, M.A. Bedison, E. Aga, S.A. Riddler, D.K. McMahon, F. Hong, and J.W. Mellors. **2014**. HIV-1 DNA decay dynamics in blood during more than a decade of suppressive antiretroviral therapy. *Clin. Infect. Dis.* 59:1312-1321.

Betts, M.R., D.R. Ambrozak, D.C. Douek, S. Bonhoeffer, J.M. Brenchley, J.P. Casazza, R.A. Koup, and L.J. Picker. **2001**. Analysis of total human immunodeficiency virus (HIV)-specific CD4(+) and CD8(+) T-cell responses: relationship to viral load in untreated HIV infection. *J Virol* 75:11983-11991.

Betts, M.R., M.C. Nason, S.M. West, S.C. De Rosa, S.A. Migueles, J. Abraham, M.M. Lederman, J.M. Benito, P.A. Goepfert, M. Connors, M. Roederer, and R.A. Koup. **2006**. HIV nonprogressors preferentially maintain highly functional HIV-specific CD8+ T cells. *Blood* 107:4781-4789.

Bitnun, A., L. Samson, T.W. Chun, F. Kakkar, J. Brophy, D. Murray, S. Justement, H. Soudeyns, M. Ostrowski, S. Mujib, P.R. Harrigan, J. Kim, P. Sandstrom, and S.E. Read. **2014**. Early initiation of combination antiretroviral therapy in HIV-1-infected newborns can achieve sustained virologic suppression with low frequency of CD4+ T cells carrying HIV in peripheral blood. *Clin. Infect. Dis.* 59:1012-1019.

Bjorkman, P.J., M.A. Saper, B. Samraoui, W.S. Bennett, J.L. Strominger, and D.C. Wiley. **1987**. Structure of the human class I histocompatibility antigen, HLA-A2. *Nature* 329:506-512.

Blanche, S., M.L. Newell, M.J. Mayaux, D.T. Dunn, J.P. Teglas, C. Rouzioux, and C.S. Peckham. **1997**. Morbidity and mortality in European children vertically infected by HIV-1. The French Pediatric HIV Infection Study Group and European Collaborative Study. *J. Acquir. Immune Defic. Syndr. Hum. Retrovirol.* 14:442-450.

Blanco-Gelaz, M.A., B. Suarez-Alvarez, S. Gonzalez, A. Lopez-Vazquez, J. Martinez-Borra, and C. Lopez-Larrea. **2006**. The amino acid at position 97 is involved in folding and surface expression of HLA-B27. *Int Immunol* 18:211-220.

Blazkova, J., K. Trejbalova, F. Gondois-Rey, P. Halfon, P. Philibert, A. Guiguen, E. Verdin, D. Olive, C. Van Lint, J. Hejnar, and I. Hirsch. **2009**. CpG methylation controls reactivation of HIV from latency. *PLoS Pathog* 5:e1000554.

Bleul, C.C., M. Farzan, H. Choe, C. Parolin, I. Clark-Lewis, J. Sodroski, and T.A. Springer. **1996**. The lymphocyte chemoattractant SDF-1 is a ligand for LESTR/fusin and blocks HIV-1 entry. *Nature* 382:829-833.

Bobat, R., M. Archary, and M. Lawler. **2015**. An update on the HIV treatment cascade in children and adolescents. *Curr Opin HIV AIDS* 10:411-419.

Borrow, P., H. Lewicki, B.H. Hahn, G.M. Shaw, and M.B. Oldstone. **1994**. Virus-specific CD8+ cytotoxic T-lymphocyte activity associated with control of viremia in primary human immunodeficiency virus type 1 infection. *J Virol* 68:6103-6110.

Bosselut, R. 2004. CD4/CD8-lineage differentiation in the thymus: from nuclear effectors to membrane signals. *Nat Rev Immunol* 4:529-540.

Boutwell, C.L., J.M. Carlson, T.H. Lin, A. Seese, K.A. Power, J. Peng, Y. Tang, Z.L. Brumme, D. Heckerman, A. Schneidewind, and T.M. Allen. **2013**. Frequent and variable cytotoxic-T-lymphocyte escape-associated fitness costs in the human immunodeficiency virus type 1 subtype B Gag proteins. *J Virol* 87:3952-3965.

Brahmer, J.R., S.S. Tykodi, L.Q. Chow, W.J. Hwu, S.L. Topalian, P. Hwu, C.G. Drake, L.H. Camacho, J. Kauh, K. Odunsi, H.C. Pitot, O. Hamid, S. Bhatia, R. Martins, K. Eaton, S. Chen, T.M. Salay, S. Alaparthy, J.F. Grosso, A.J. Korman, S.M. Parker, S. Agrawal, S.M. Goldberg, D.M. Pardoll, A. Gupta, and J.M. Wigginton. **2012**. Safety and activity of anti-PD-L1 antibody in patients with advanced cancer. *N Engl J Med* 366:2455-2465.

Brander, C., P.J. Goulder, K. Luzuriaga, O.O. Yang, K.E. Hartman, N.G. Jones, B.D. Walker, and S.A. Kalams. **1999**. Persistent HIV-1-specific CTL clonal expansion despite high viral burden post in utero HIV-1 infection. *J Immunol* 162:4796-4800.

Brockman, M.A., A. Schneidewind, M. Lahaie, A. Schmidt, T. Miura, I. Desouza, F. Ryvkin, C.A. Derdeyn, S. Allen, E. Hunter, J. Mulenga, P.A. Goepfert, B.D. Walker, and T.M. Allen. **2007**. Escape and compensation from early HLA-B57-

mediated cytotoxic T-lymphocyte pressure on human immunodeficiency virus type 1 Gag alter capsid interactions with cyclophilin A. *J Virol* 81:12608-12618.

Buchbinder, S.P., D.V. Mehrotra, A. Duerr, D.W. Fitzgerald, R. Mogg, D. Li, P.B. Gilbert, J.R. Lama, M. Marmor, C. Del Rio, M.J. McElrath, D.R. Casimiro, K.M. Gottesdiener, J.A. Chodakewitz, L. Corey, and M.N. Robertson. **2008**. Efficacy assessment of a cell-mediated immunity HIV-1 vaccine (the Step Study): a double-blind, randomised, placebo-controlled, test-of-concept trial. *Lancet* 372:1881-1893.

Butler, K.M., P. Gavin, S. Coughlan, A. Rochford, S.M. Donagh, O. Cunningham, H. Poulsom, S. Watters, and N. Klein. **2015**. Rapid Viral Rebound after 4 Years of Suppressive Therapy in a Seronegative HIV-1 Infected Infant Treated from Birth. *Pediatr. Infect. Dis. J.* 34:e48-e51.

Cano, P., W. Klitz, S.J. Mack, M. Maiers, S.G. Marsh, H. Noreen, E.F. Reed, D. Senitzer, M. Setterholm, A. Smith, and M. Fernandez-Vina. **2007**. Common and well-documented HLA alleles: report of the Ad-Hoc committee of the american society for histocompatiblity and immunogenetics. *Hum Immunol* 68:392-417.

Cao, K., J. Hollenbach, X. Shi, W. Shi, M. Chopek, and M.A. Fernandez-Vina. **2001**. Analysis of the frequencies of HLA-A, B, and C alleles and haplotypes in the five major ethnic groups of the United States reveals high levels of diversity in these loci and contrasting distribution patterns in these populations. *Hum Immunol* 62:1009-1030.

Carlson, J. 2012. Widespread implications. Phoebe Putney decision could affect future deals. *Mod Healthc* 42:26.

Carlson, J., Heckerman, D., Shani, G. 2009. Estimating false discovery rates for contingency tables. *Microsoft, Redmond, WA.*

Carlson, J.M., C.J. Brumme, E. Martin, J. Listgarten, M.A. Brockman, A.Q. Le, C.K. Chui, L.A. Cotton, D.J. Knapp, S.A. Riddler, R. Haubrich, G. Nelson, N. Pfeifer, C.E. Deziel, D. Heckerman, R. Apps, M. Carrington, S. Mallal, P.R. Harrigan, M. John, and Z.L. Brumme. **2012**. Correlates of protective cellular immunity revealed by analysis of population-level immune escape pathways in HIV-1. *J Virol* 86:13202-13216.

Carlson, J.M., M. Schaefer, D.C. Monaco, R. Batorsky, D.T. Claiborne, J. Prince, M.J. Deymier, Z.S. Ende, N.R. Klatt, C.E. DeZiel, T.H. Lin, J. Peng, A.M. Seese, R. Shapiro, J. Frater, T. Ndung'u, J. Tang, P. Goepfert, J. Gilmour, M.A. Price, W. Kilembe, D. Heckerman, P.J. Goulder, T.M. Allen, S. Allen, and E. Hunter. **2014**. HIV transmission. Selection bias at the heterosexual HIV-1 transmission bottleneck. *Science* 345:1254031.

Carrington, M., G.W. Nelson, M.P. Martin, T. Kissner, D. Vlahov, J.J. Goedert, R. Kaslow, S. Buchbinder, K. Hoots, and S.J. O'Brien. **1999**. HLA and HIV-1: heterozygote advantage and B*35-Cw*04 disadvantage. *Science* 283:1748-1752.

Cartwright, E.K., T. Vanderford, K. Easley, J.E. Schmitz, A. Chahroudi, S.E. Bosinger, M. Paiardini, J. Estes, and G. Silvestri. 2016. CD8 T Cells Are

Required to Suppress Viremia in SIV-Infected ART Treated Macaques. Abstract 22. In Conference on Retroviruses and Opportunistic Infections, February 22-25, 2016. Boston, MA, USA.

Chakrabarti, L.A., S.R. Lewin, L. Zhang, A. Gettie, A. Luckay, L.N. Martin, E. Skulsky, D.D. Ho, C. Cheng-Mayer, and P.A. Marx. **2000**. Normal T-cell turnover in sooty mangabeys harboring active simian immunodeficiency virus infection. *J Virol* 74:1209-1223.

Chen, D.Y., A. Balamurugan, H.L. Ng, and O.O. Yang. **2011**. Antiviral activity of human immunodeficiency virus type 1 Gag-specific cytotoxic T lymphocyte targeting is not necessarily intrinsically superior to envelope targeting. *J Virol* 85:2474-2478.

Chen, H., Z.M. Ndhlovu, D. Liu, L.C. Porter, J.W. Fang, S. Darko, M.A. Brockman, T. Miura, Z.L. Brumme, A. Schneidewind, A. Piechocka-Trocha, K.T. Cesa, J. Sela, T.D. Cung, I. Toth, F. Pereyra, X.G. Yu, D.C. Douek, D.E. Kaufmann, T.M. Allen, and B.D. Walker. **2012**. TCR clonotypes modulate the protective effect of HLA class I molecules in HIV-1 infection. *Nat Immunol* 13:691-700.

Chen, H., A. Piechocka-Trocha, T. Miura, M.A. Brockman, B.D. Julg, B.M. Baker, A.C. Rothchild, B.L. Block, A. Schneidewind, T. Koibuchi, F. Pereyra, T.M. Allen, and B.D. Walker. **2009**. Differential neutralization of human immunodeficiency virus (HIV) replication in autologous CD4 T cells by HIV-specific cytotoxic T lymphocytes. *J Virol* 83:3138-3149.

Choe, H., M. Farzan, Y. Sun, N. Sullivan, B. Rollins, P.D. Ponath, L. Wu, C.R. Mackay, G. LaRosa, W. Newman, N. Gerard, C. Gerard, and J. Sodroski. **1996**. The beta-chemokine receptors CCR3 and CCR5 facilitate infection by primary HIV-1 isolates. *Cell* 85:1135-1148.

Choudhary, S.K., N. Vrisekoop, C.A. Jansen, S.A. Otto, H. Schuitemaker, F. Miedema, and D. Camerini. **2007**. Low immune activation despite high levels of pathogenic human immunodeficiency virus type 1 results in long-term asymptomatic disease. *J Virol* 81:8838-8842.

Chun, T.W., J.S. Justement, D. Murray, C.W. Hallahan, J. Maenza, A.C. Collier, P.M. Sheth, R. Kaul, M. Ostrowski, S. Moir, C. Kovacs, and A.S. Fauci. **2010**. Rebound of plasma viremia following cessation of antiretroviral therapy despite profoundly low levels of HIV reservoir: implications for eradication. *AIDS* 24:2803-2808.

Chun, T.W., L. Stuyver, S.B. Mizell, L.A. Ehler, J.A. Mican, M. Baseler, A.L. Lloyd, M.A. Nowak, and A.S. Fauci. **1997**. Presence of an inducible HIV-1 latent reservoir during highly active antiretroviral therapy. *Proc Natl Acad Sci U S A* 94:13193-13197.

Clark, B.R., S.V. Deshpande, S.D. Sharma, and B. Nag. **1994**. Antigen-specific deletion of cloned T cells using peptide-toxin conjugate complexed with purified class II major histocompatibility complex antigen. *J Biol Chem* 269:94-99.

Clavel, F., D. Guetard, F. Brun-Vezinet, S. Chamaret, M.A. Rey, M.O. Santos-Ferreira, A.G. Laurent, C. Dauguet, C. Katlama, C. Rouzioux, D. Klatzmann, J.L. Champalimaud, and L. Montagnier. **1986**. Isolation of a new human retrovirus from West African patients with AIDS. *Science* 233:343-346.

Collins, K.L., B.K. Chen, S.A. Kalams, B.D. Walker, and D. Baltimore. **1998**. HIV-1 Nef protein protects infected primary cells against killing by cytotoxic T lymphocytes. *Nature* 391:397-401.

Connor, R.I., K.E. Sheridan, D. Ceradini, S. Choe, and N.R. Landau. **1997**. Change in coreceptor use correlates with disease progression in HIV-1--infected individuals. *J Exp Med* 185:621-628.

Contreras, X., M. Barboric, T. Lenasi, and B.M. Peterlin. **2007**. HMBA releases P-TEFb from HEXIM1 and 7SK snRNA via PI3K/Akt and activates HIV transcription. *PLoS Pathog* 3:1459-1469.

Cook, M.A., S.E. Jobson, D.C. Atkinson, D.P. Lowe, S.L. Farmer, W.J. Alvi-Ali, N.A. Smith, and D.C. Briggs. **2003**. Used leucodepletion filters as a source of large quantities of DNA suitable for the study of genetic variations in human populations. *Transfus Med* 13:77-81.

Coovadia, H.M., N.C. Rollins, R.M. Bland, K. Little, A. Coutsoudis, M.L. Bennish, and M.L. Newell. **2007**. Mother-to-child transmission of HIV-1 infection during exclusive breastfeeding in the first 6 months of life: an intervention cohort study. *Lancet* 369:1107-1116.

Crawford, H., W. Lumm, A. Leslie, M. Schaefer, D. Boeras, J.G. Prado, J. Tang, P. Farmer, T. Ndung'u, S. Lakhi, J. Gilmour, P. Goepfert, B.D. Walker, R. Kaslow, J. Mulenga, S. Allen, P.J. Goulder, and E. Hunter. **2009**. Evolution of HLA-B*5703 HIV-1 escape mutations in HLA-B*5703-positive individuals and their transmission recipients. *J Exp Med* 206:909-921.

Crawford, H., J.G. Prado, A. Leslie, S. Hue, I. Honeyborne, S. Reddy, M. van der Stok, Z. Mncube, C. Brander, C. Rousseau, J.I. Mullins, R. Kaslow, P. Goepfert, S. Allen, E. Hunter, J. Mulenga, P. Kiepiela, B.D. Walker, and P.J. Goulder. **2007**. Compensatory mutation partially restores fitness and delays reversion of escape mutation within the immunodominant HLA-B*5703-restricted Gag epitope in chronic human immunodeficiency virus type 1 infection. *J Virol* 81:8346-8351.

Crooks, A.M., R. Bateson, A.B. Cope, N.P. Dahl, M.K. Griggs, J.D. Kuruc, C.L. Gay, J.J. Eron, D.M. Margolis, R.J. Bosch, and N.M. Archin. **2015**. Precise Quantitation of the Latent HIV-1 Reservoir: Implications for Eradication Strategies. *J. Infect. Dis.* 212:1361-1365.

Davey, R.T., Jr., N. Bhat, C. Yoder, T.W. Chun, J.A. Metcalf, R. Dewar, V. Natarajan, R.A. Lempicki, J.W. Adelsberger, K.D. Miller, J.A. Kovacs, M.A. Polis, R.E. Walker, J. Falloon, H. Masur, D. Gee, M. Baseler, D.S. Dimitrov, A.S. Fauci, and H.C. Lane. **1999**. HIV-1 and T cell dynamics after interruption of highly active antiretroviral therapy (HAART) in patients with a history of sustained viral suppression. *Proc Natl Acad Sci U S A* 96:15109-15114.

Dean, M., M. Carrington, C. Winkler, G.A. Huttley, M.W. Smith, R. Allikmets, J.J. Goedert, S.P. Buchbinder, E. Vittinghoff, E. Gomperts, S. Donfield, D. Vlahov, R. Kaslow, A. Saah, C. Rinaldo, R. Detels, and S.J. O'Brien. **1996**. Genetic restriction of HIV-1 infection and progression to AIDS by a deletion allele of the CKR5 structural gene. Hemophilia Growth and Development Study, Multicenter AIDS Cohort Study, Multicenter Hemophilia Cohort Study, San Francisco City Cohort, ALIVE Study. *Science* 273:1856-1862.

Deeks, S.G. 2012. HIV: Shock and kill. *Nature* 487:439-440.

Deeks, S.G., and B.D. Walker. **2007**. Human immunodeficiency virus controllers: mechanisms of durable virus control in the absence of antiretroviral therapy. *Immunity* 27:406-416.

Deng, H., R. Liu, W. Ellmeier, S. Choe, D. Unutmaz, M. Burkhart, P. Di Marzio, S. Marmon, R.E. Sutton, C.M. Hill, C.B. Davis, S.C. Peiper, T.J. Schall, D.R. Littman, and N.R. Landau. **1996**. Identification of a major co-receptor for primary isolates of HIV-1. *Nature* 381:661-666.

Deng, K., M. Pertea, A. Rongvaux, L. Wang, C.M. Durand, G. Ghiaur, J. Lai, H.L. McHugh, H. Hao, H. Zhang, J.B. Margolick, C. Gurer, A.J. Murphy, D.M. Valenzuela, G.D. Yancopoulos, S.G. Deeks, T. Strowig, P. Kumar, J.D. Siliciano, S.L. Salzberg, R.A. Flavell, L. Shan, and R.F. Siliciano. **2015**. Broad CTL response is required to clear latent HIV-1 due to dominance of escape mutations. *Nature* 517:381-385.

DiBrino, M., K.C. Parker, D.H. Margulies, J. Shiloach, R.V. Turner, W.E. Biddison, and J.E. Coligan. **1994**. The HLA-B14 peptide binding site can accommodate peptides with different combinations of anchor residues. *J Biol Chem* 269:32426-32434.

Dickover, R.E., E.M. Garratty, S.A. Herman, M.S. Sim, S. Plaeger, P.J. Boyer, M. Keller, A. Deveikis, E.R. Stiehm, and Y.J. Bryson. **1996**. Identification of levels of maternal HIV-1 RNA associated with risk of perinatal transmission. Effect of maternal zidovudine treatment on viral load. *JAMA* 275:599-605.

Doitsh, G., N.L. Galloway, X. Geng, Z. Yang, K.M. Monroe, O. Zepeda, P.W. Hunt, H. Hatano, S. Sowinski, I. Munoz-Arias, and W.C. Greene. **2014**. Cell death by pyroptosis drives CD4 T-cell depletion in HIV-1 infection. *Nature* 505:509-514.

Domena, J.D., K. Azumi, W.B. Bias, and P. Parham. **1993**. B*1401 encodes the B64 antigen: the B64 and B65 splits of B14 differ only at residue 11, a buried amino acid. *Tissue Antigens* 41:110-111.

Duerr, A., Y. Huang, S. Buchbinder, R.W. Coombs, J. Sanchez, C. del Rio, M. Casapia, S. Santiago, P. Gilbert, L. Corey, and M.N. Robertson. **2012**. Extended follow-up confirms early vaccine-enhanced risk of HIV acquisition and demonstrates waning effect over time among participants in a randomized trial of recombinant adenovirus HIV vaccine (Step Study). *J Infect Dis* 206:258-266.

Dunham, R., P. Pagliardini, S. Gordon, B. Sumpter, J. Engram, A. Moanna, M. Paiardini, J.N. Mandl, B. Lawson, S. Garg, H.M. McClure, Y.X. Xu, C. Ibegbu,

K. Easley, N. Katz, I. Pandrea, C. Apetrei, D.L. Sodora, S.I. Staprans, M.B. Feinberg, and G. Silvestri. **2006**. The AIDS resistance of naturally SIV-infected sooty mangabeys is independent of cellular immunity to the virus. *Blood* 108:209-217.

Edwards, B.H., A. Bansal, S. Sabbaj, J. Bakari, M.J. Mulligan, and P.A. Goepfert. **2002**. Magnitude of functional CD8+ T-cell responses to the gag protein of human immunodeficiency virus type 1 correlates inversely with viral load in plasma. *J Virol* 76:2298-2305.

Eisele, E., and R.F. Siliciano. **2012**. Redefining the viral reservoirs that prevent HIV-1 eradication. *Immunity* 37:377-388.

Elyaman, W., E.M. Bradshaw, C. Uyttenhove, V. Dardalhon, A. Awasthi, J. Imitola, E. Bettelli, M. Oukka, J. van Snick, J.C. Renauld, V.K. Kuchroo, and S.J. Khoury. **2009**. IL-9 induces differentiation of TH17 cells and enhances function of FoxP3+ natural regulatory T cells. *Proc. Natl Acad. Sci. U. S. A.* 106:12885-12890.

Eriksson, S., E.H. Graf, V. Dahl, M.C. Strain, S.A. Yukl, E.S. Lysenko, R.J. Bosch, J. Lai, S. Chioma, F. Emad, M. Abdel-Mohsen, R. Hoh, F. Hecht, P. Hunt, M. Somsouk, J. Wong, R. Johnston, R.F. Siliciano, D.D. Richman, U. O'Doherty, S. Palmer, S.G. Deeks, and J.D. Siliciano. **2013**. Comparative analysis of measures of viral reservoirs in HIV-1 eradication studies. *PLoS Pathog.* 9:e1003174.

Eron, J.J., C. Gay, R. Bosch, J. Ritz, J. Hataye, C. Hwang, R.L. Tressler, S.W. Mason, R. Koup, and J.W. Mellors. 2016. Safety, Immunologic and Virologic Activity of Anti-PD-L1 in HIV-1 Participants on ART. Abstract 25. In Conference on Retroviruses and Opportunistic Infections, February 22-25, 2016. Boston, MA, USA.

Ewer, K. 2014. Potent cellular and humoral immunogenicity of ChAd63 MVA ME-TRAP in African infants and children. In 63rd American Society of Tropical Medicine and Hygiene Meeting. New Orleans, LA, USA.

Ewer, K.J., G.A. O'Hara, C.J. Duncan, K.A. Collins, S.H. Sheehy, A. Reyes-Sandoval, A.L. Goodman, N.J. Edwards, S.C. Elias, F.D. Halstead, R.J. Longley, R. Rowland, I.D. Poulton, S.J. Draper, A.M. Blagborough, E. Berrie, S. Moyle, N. Williams, L. Siani, A. Folgori, S. Colloca, R.E. Sinden, A.M. Lawrie, R. Cortese, S.C. Gilbert, A. Nicosia, and A.V. Hill. **2013**. Protective CD8+ T-cell immunity to human malaria induced by chimpanzee adenovirus-MVA immunisation. *Nat Commun* 4:2836.

Farahani, M., H. Mulinder, A. Farahani, and R. Marlink. **2016**. Prevalence and distribution of non-AIDS causes of death among HIV-infected individuals receiving antiretroviral therapy: a systematic review and meta-analysis. pii: 0956462416632428. [Epub ahead of print.]. *International Journal of STD and AIDS*

Faria, N.R., A. Rambaut, M.A. Suchard, G. Baele, T. Bedford, M.J. Ward, A.J. Tatem, J.D. Sousa, N. Arinaminpathy, J. Pepin, D. Posada, M. Peeters, O.G. Pybus,

and P. Lemey. **2014**. HIV epidemiology. The early spread and epidemic ignition of HIV-1 in human populations. *Science* 346:56-61.

Feeney, M.E., Y. Tang, K. Pfafferott, K.A. Roosevelt, R. Draenert, A. Trocha, X.G. Yu, C. Verrill, T. Allen, C. Moore, S. Mallal, S. Burchett, K. McIntosh, S.I. Pelton, M.A. St John, R. Hazra, P. Klenerman, M. Altfeld, B.D. Walker, and P.J. Goulder. **2005**. HIV-1 viral escape in infancy followed by emergence of a variant-specific CTL response. *J Immunol* 174:7524-7530.

Feeney, M.E., Y. Tang, A. Rathod, C. Kneut, and K. McIntosh. **2006**. Absence of detectable viremia in a perinatally HIV-1-infected teenager after discontinuation of antiretroviral therapy. *J. Allergy Clin. Immunol.* 118:324-330.

Fellay, J., K.V. Shianna, D. Ge, S. Colombo, B. Ledergerber, M. Weale, K. Zhang, C. Gumbs, A. Castagna, A. Cossarizza, A. Cozzi-Lepri, A. De Luca, P. Easterbrook, P. Francioli, S. Mallal, J. Martinez-Picado, J.M. Miro, N. Obel, J.P. Smith, J. Wyniger, P. Descombes, S.E. Antonarakis, N.L. Letvin, A.J. McMichael, B.F. Haynes, A. Telenti, and D.B. Goldstein. **2007**. A whole-genome association study of major determinants for host control of HIV-1. *Science* 317:944-947.

Ferrand, R.A., R. Luethy, F. Bwakura, H. Mujuru, R.F. Miller, and E.L. Corbett. **2007**. HIV infection presenting in older children and adolescents: a case series from Harare, Zimbabwe. *Clin. Infect. Dis.* 44:874-878.

Fiebig, E.W., D.J. Wright, B.D. Rawal, P.E. Garrett, R.T. Schumacher, L. Peddada, C. Heldebrant, R. Smith, A. Conrad, S.H. Kleinman, and M.P. Busch. **2003**. Dynamics of HIV viremia and antibody seroconversion in plasma donors: implications for diagnosis and staging of primary HIV infection. *AIDS* 17:1871-1879.

Finzi, D., J. Blankson, J.D. Siliciano, J.B. Margolick, K. Chadwick, T. Pierson, K. Smith, J. Lisziewicz, F. Lori, C. Flexner, T.C. Quinn, R.E. Chaisson, E. Rosenberg, B. Walker, S. Gange, J. Gallant, and R.F. Siliciano. **1999**. Latent infection of CD4+ T cells provides a mechanism for lifelong persistence of HIV-1, even in patients on effective combination therapy. *Nature Med.* 5:512-517.

Finzi, D., M. Hermankova, T. Pierson, L.M. Carruth, C. Buck, R.E. Chaisson, T.C. Quinn, K. Chadwick, J. Margolick, R. Brookmeyer, J. Gallant, M. Markowitz, D.D. Ho, D.D. Richman, and R.F. Siliciano. **1997**. Identification of a reservoir for HIV-1 in patients on highly active antiretroviral therapy. *Science* 278:1295-1300.

Fitzgerald, D.W., H. Janes, M. Robertson, R. Coombs, I. Frank, P. Gilbert, M. Loufty, D. Mehrotra, and A. Duerr. **2011**. An Ad5-vectored HIV-1 vaccine elicits cell-mediated immunity but does not affect disease progression in HIV-1-infected male subjects: results from a randomized placebo-controlled trial (the Step study). *J Infect Dis* 203:765-772.

Flores-Villanueva, P.O., E.J. Yunis, J.C. Delgado, E. Vittinghoff, S. Buchbinder, J.Y. Leung, A.M. Uglialoro, O.P. Clavijo, E.S. Rosenberg, S.A. Kalams, J.D. Braun, S.L. Boswell, B.D. Walker, and A.E. Goldfeld. **2001**. Control of HIV-1 viremia and

protection from AIDS are associated with HLA-Bw4 homozygosity. *Proc Natl Acad Sci U S A* 98:5140-5145.

Foley, G.E., H. Lazarus, S. Farber, B.G. Uzman, B.A. Boone, and R.E. McCarthy. **1965**. Continuous Culture of Human Lymphoblasts from Peripheral Blood of a Child with Acute Leukemia. *Cancer* 18:522-529.

Frahm, N., P. Kiepiela, S. Adams, C.H. Linde, H.S. Hewitt, K. Sango, M.E. Feeney, M.M. Addo, M. Lichterfeld, M.P. Lahaie, E. Pae, A.G. Wurcel, T. Roach, M.A. St John, M. Altfeld, F.M. Marincola, C. Moore, S. Mallal, M. Carrington, D. Heckerman, T.M. Allen, J.I. Mullins, B.T. Korber, P.J. Goulder, B.D. Walker, and C. Brander. **2006**. Control of human immunodeficiency virus replication by cytotoxic T lymphocytes targeting subdominant epitopes. *Nat Immunol* 7:173-178.

Frange, P., A. Faye, V. Avettand-Fenoel, E. Bellaton, D. Deschamps, M. Angin, A. David, S. Caillat-Zucman, G. Peytavin, C. Dollfus, J. Le Chenadec, J. Warszawski, C. Rouzioux, and A. Saez-Cirion. **2016**. HIV-1 virological remission lasting more than 12 years after interruption of early antiretroviral therapy in a perinatally infected teenager enrolled in the French ANRS EPF-CO10 paediatric cohort: a case report. *Lancet HIV* 3:e49-e54.

Fraser, C., T.D. Hollingsworth, R. Chapman, F. de Wolf, and W.P. Hanage. **2007**. Variation in HIV-1 set-point viral load: epidemiological analysis and an evolutionary hypothesis. *Proc Natl Acad Sci U S A* 104:17441-17446.

Fukazawa, Y., R. Lum, A.A. Okoye, H. Park, K. Matsuda, J.Y. Bae, S.I. Hagen, R. Shoemaker, C. Deleage, C. Lucero, D. Morcock, T. Swanson, A.W. Legasse, M.K. Axthelm, J. Hesselgesser, R. Geleziunas, V.M. Hirsch, P.T. Edlefsen, M. Piatak, Jr., J.D. Estes, J.D. Lifson, and L.J. Picker. **2015**. B cell follicle sanctuary permits persistent productive simian immunodeficiency virus infection in elite controllers. *Nature Med.* 21:132-139.

Gall, A., B. Ferns, C. Morris, S. Watson, M. Cotten, M. Robinson, N. Berry, D. Pillay, and P. Kellam. **2012**. Universal amplification, next-generation sequencing, and assembly of HIV-1 genomes. *J Clin Microbiol* 50:3838-3844.

Gallo, R.C., P.S. Sarin, E.P. Gelmann, M. Robert-Guroff, E. Richardson, V.S. Kalyanaraman, D. Mann, G.D. Sidhu, R.E. Stahl, S. Zolla-Pazner, J. Leibowitch, and M. Popovic. **1983**. Isolation of human T-cell leukemia virus in acquired immune deficiency syndrome (AIDS). *Science* 220:865-867.

Gao, X., G.W. Nelson, P. Karacki, M.P. Martin, J. Phair, R. Kaslow, J.J. Goedert, S. Buchbinder, K. Hoots, D. Vlahov, S.J. O'Brien, and M. Carrington. **2001**. Effect of a single amino acid change in MHC class I molecules on the rate of progression to AIDS. *N Engl J Med* 344:1668-1675.

Gardner, M.R., L.M. Kattenhorn, H.R. Kondur, M. von Schaewen, T. Dorfman, J.J. Chiang, K.G. Haworth, J.M. Decker, M.D. Alpert, C.C. Bailey, E.S. Neale, Jr., C.H. Fellinger, V.R. Joshi, S.P. Fuchs, J.M. Martinez-Navio, B.D. Quinlan, A.Y. Yao, H. Mouquet, J. Gorman, B. Zhang, P. Poignard, M.C. Nussenzweig, D.R. Burton, P.D. Kwong, M. Piatak, Jr., J.D. Lifson, G. Gao, R.C. Desrosiers, D.T.

Evans, B.H. Hahn, A. Ploss, P.M. Cannon, M.S. Seaman, and M. Farzan. **2015**. AAV-expressed eCD4-Ig provides durable protection from multiple SHIV challenges. *Nature* 519:87-91.

Garrett, T.P., M.A. Saper, P.J. Bjorkman, J.L. Strominger, and D.C. Wiley. **1989**. Specificity pockets for the side chains of peptide antigens in HLA-Aw68. *Nature* 342:692-696.

Geldmacher, C., J.R. Currier, E. Herrmann, A. Haule, E. Kuta, F. McCutchan, L. Njovu, S. Geis, O. Hoffmann, L. Maboko, C. Williamson, D. Birx, A. Meyerhans, J. Cox, and M. Hoelscher. **2007**. CD8 T-cell recognition of multiple epitopes within specific Gag regions is associated with maintenance of a low steady-state viremia in human immunodeficiency virus type 1-seropositive patients. *J Virol* 81:2440-2448.

Germain, R.N. 2002. T-cell development and the CD4-CD8 lineage decision. *Nat Rev Immunol* 2:309-322.

Giacomet, V., D. Trabattoni, N. Zanchetta, M. Biasin, M. Gismondo, M. Clerici, and G. Zuccotti. **2014**. No cure of HIV infection in a child despite early treatment and apparent viral clearance. *Lancet* 384:1320.

Goedert, J.J., C.M. Kessler, L.M. Aledort, R.J. Biggar, W.A. Andes, G.C. White, 2nd, J.E. Drummond, K. Vaidya, D.L. Mann, M.E. Eyster, M.V. Ragni, M.M. Lederman, A.R. Cohen, G.L. Bray, P.S. Rosenberg, R.M. Friedman, M.W. Hilgartner, W.A. Blattner, B. Kroner, and M.H. Gail. **1989**. A prospective study of human immunodeficiency virus type 1 infection and the development of AIDS in subjects with hemophilia. *N Engl J Med* 321:1141-1148.

Goenka, A., and T.R. Kollmann. **2015**. Development of immunity in early life. *J Infect* 71 Suppl 1:S112-120.

Goonetilleke, N., M.K. Liu, J.F. Salazar-Gonzalez, G. Ferrari, E. Giorgi, V.V. Ganusov, B.F. Keele, G.H. Learn, E.L. Turnbull, M.G. Salazar, K.J. Weinhold, S. Moore, C.C.C. B, N. Letvin, B.F. Haynes, M.S. Cohen, P. Hraber, T. Bhattacharya, P. Borrow, A.S. Perelson, B.H. Hahn, G.M. Shaw, B.T. Korber, and A.J. McMichael. **2009**. The first T cell response to transmitted/founder virus contributes to the control of acute viremia in HIV-1 infection. *J. Exp. Med.* 206:1253-1272.

Gosselin, A., P. Monteiro, N. Chomont, F. Diaz-Griffero, E.A. Said, S. Fonseca, V. Wacleche, M. El-Far, M.R. Boulassel, J.P. Routy, R.P. Sekaly, and P. Ancuta. **2010**. Peripheral blood CCR4+CCR6+ and CXCR3+CCR6+CD4+ T cells are highly permissive to HIV-1 infection. *J. Immunol.* 184:1604-1616.

Gottlieb, M.S., H.M. Schanker, P.T. Fan, A. Saxon, and J.D. Weisman. **1981**. Pneumocystis Pneumonia—Los Angeles; Centers for Disease Control (CDC). *MMWR Morbidity and Mortality Weekly Report* 30:250-252.

Goulder, P., C. Conlon, K. McLntyre, and A. McMichael. **1996**. Identification of a novel human leukocyte antigen A26-restricted epitope in a conserved region of Gag. *AIDS* 10:1441-1443.

Goulder, P.J., M.M. Addo, M.A. Altfeld, E.S. Rosenberg, Y. Tang, U. Govender, N. Mngqundaniso, K. Annamalai, T.U. Vogel, M. Hammond, M. Bunce, H.M. Coovadia, and B.D. Walker. **2001a**. Rapid definition of five novel HLA-A*3002-restricted human immunodeficiency virus-specific cytotoxic T-lymphocyte epitopes by elispot and intracellular cytokine staining assays. *J Virol* 75:1339-1347.

Goulder, P.J., C. Brander, K. Annamalai, N. Mngqundaniso, U. Govender, Y. Tang, S. He, K.E. Hartman, C.A. O'Callaghan, G.S. Ogg, M.A. Altfeld, E.S. Rosenberg, H. Cao, S.A. Kalams, M. Hammond, M. Bunce, S.I. Pelton, S.A. Burchett, K. McIntosh, H.M. Coovadia, and B.D. Walker. **2000**. Differential narrow focusing of immunodominant human immunodeficiency virus gag-specific cytotoxic T-lymphocyte responses in infected African and caucasoid adults and children. *J Virol* 74:5679-5690.

Goulder, P.J., C. Brander, Y. Tang, C. Tremblay, R.A. Colbert, M.M. Addo, E.S. Rosenberg, T. Nguyen, R. Allen, A. Trocha, M. Altfeld, S. He, M. Bunce, R. Funkhouser, S.I. Pelton, S.K. Burchett, K. McIntosh, B.T. Korber, and B.D. Walker. **2001b**. Evolution and transmission of stable CTL escape mutations in HIV infection. *Nature* 412:334-338.

Goulder, P.J., A. Edwards, R.E. Phillips, and A.J. McMichael. **1997**. Identification of a novel HLA-A24-restricted cytotoxic T-lymphocyte epitope within HIV-1 Nef. *AIDS* 11:1883-1884.

Goulder, P.J., and B.D. Walker. **2012**. HIV and HLA class I: an evolving relationship. *Immunity* 37:426-440.

Gounder, K., N. Padayachi, J.K. Mann, M. Radebe, M. Mokgoro, M. van der Stok, L. Mkhize, Z. Mncube, M. Jaggernath, T. Reddy, B.D. Walker, and T. Ndung'u. **2015**. High Frequency of Transmitted HIV-1 Gag HLA Class I-Driven Immune Escape Variants but Minimal Immune Selection over the First Year of Clade C Infection. *PLoS One* 10:e0119886.

Gray, G., S. Buchbinder, and A. Duerr. **2010**. Overview of STEP and Phambili trial results: two phase IIb test-of-concept studies investigating the efficacy of MRK adenovirus type 5 gag/pol/nef subtype B HIV vaccine. *Curr Opin HIV AIDS* 5:357-361.

Gray, G.E., M. Allen, Z. Moodie, G. Churchyard, L.G. Bekker, M. Nchabeleng, K. Mlisana, B. Metch, G. de Bruyn, M.H. Latka, S. Roux, M. Mathebula, N. Naicker, C. Ducar, D.K. Carter, A. Puren, N. Eaton, M.J. McElrath, M. Robertson, L. Corey, and J.G. Kublin. **2011**. Safety and efficacy of the HVTN 503/Phambili study of a clade-B-based HIV-1 vaccine in South Africa: a double-blind, randomised, placebo-controlled test-of-concept phase 2b study. *Lancet Infect Dis* 11:507-515.

Gray, G.E., Z. Moodie, B. Metch, P.B. Gilbert, L.G. Bekker, G. Churchyard, M. Nchabeleng, K. Mlisana, F. Laher, S. Roux, K. Mngadi, C. Innes, M. Mathebula, M. Allen, M.J. McElrath, M. Robertson, J. Kublin, and L. Corey. **2014**. Recombinant adenovirus type 5 HIV gag/pol/nef vaccine in South Africa: unblinded,

long-term follow-up of the phase 2b HVTN 503/Phambili study. *Lancet Infect. Dis.* 14:388-396.

Grubman, S., E. Gross, N. Lerner-Weiss, M. Hernandez, G.D. McSherry, L.G. Hoyt, M. Boland, and J.M. Oleske. **1995**. Older children and adolescents living with perinatally acquired human immunodeficiency virus infection. *Pediatrics* 95:657-663.

Guyader, M., M. Emerman, P. Sonigo, F. Clavel, L. Montagnier, and M. Alizon. **1987**. Genome organization and transactivation of the human immunodeficiency virus type 2. *Nature* 326:662-669.

Hammarlund, E., M.W. Lewis, S.G. Hansen, L.I. Strelow, J.A. Nelson, G.J. Sexton, J.M. Hanifin, and M.K. Slifka. **2003**. Duration of antiviral immunity after smallpox vaccination. *Nat Med* 9:1131-1137.

Hammer, S.M., M.E. Sobieszczyk, H. Janes, S.T. Karuna, M.J. Mulligan, D. Grove, B.A. Koblin, S.P. Buchbinder, M.C. Keefer, G.D. Tomaras, N. Frahm, J. Hural, C. Anude, B.S. Graham, M.E. Enama, E. Adams, E. DeJesus, R.M. Novak, I. Frank, C. Bentley, S. Ramirez, R. Fu, R.A. Koup, J.R. Mascola, G.J. Nabel, D.C. Montefiori, J. Kublin, M.J. McElrath, L. Corey, and P.B. Gilbert. **2013**. Efficacy trial of a DNA/rAd5 HIV-1 preventive vaccine. *N Engl J Med* 369:2083-2092.

Hansen, S.G., J.C. Ford, M.S. Lewis, A.B. Ventura, C.M. Hughes, L. Coyne-Johnson, N. Whizin, K. Oswald, R. Shoemaker, T. Swanson, A.W. Legasse, M.J. Chiuchiolo, C.L. Parks, M.K. Axthelm, J.A. Nelson, M.A. Jarvis, M. Piatak, Jr., J.D. Lifson, and L.J. Picker. **2011**. Profound early control of highly pathogenic SIV by an effector memory T-cell vaccine. *Nature* 473:523-527.

Hansen, S.G., M. Piatak, Jr., A.B. Ventura, C.M. Hughes, R.M. Gilbride, J.C. Ford, K. Oswald, R. Shoemaker, Y. Li, M.S. Lewis, A.N. Gilliam, G. Xu, N. Whizin, B.J. Burwitz, S.L. Planer, J.M. Turner, A.W. Legasse, M.K. Axthelm, J.A. Nelson, K. Fruh, J.B. Sacha, J.D. Estes, B.F. Keele, P.T. Edlefsen, J.D. Lifson, and L.J. Picker. **2013**. Immune clearance of highly pathogenic SIV infection. *Nature* 502:100-104.

Hansen, S.G., H.L. Wu, B.J. Burwitz, C.M. Hughes, K.B. Hammond, A.B. Ventura, J.S. Reed, R.M. Gilbride, E. Ainslie, D.W. Morrow, J.C. Ford, A.N. Selseth, R. Pathak, D. Malouli, A.W. Legasse, M.K. Axthelm, J.A. Nelson, G.M. Gillespie, L.C. Walters, S. Brackenridge, H.R. Sharpe, C.A. Lopez, K. Fruh, B.T. Korber, A.J. McMichael, S. Gnanakaran, J.B. Sacha, and L.J. Picker. **2016**. Broadly targeted CD8(+) T cell responses restricted by major histocompatibility complex E. *Science* 351:714-720.

Harada, S., Y. Koyanagi, and N. Yamamoto. **1985**. Infection of HTLV-III/LAV in HTLV-I-carrying cells MT-2 and MT-4 and application in a plaque assay. *Science* 229:563-566.

Harrer, T., E. Harrer, S.A. Kalams, P. Barbosa, A. Trocha, R.P. Johnson, T. Elbeik, M.B. Feinberg, S.P. Buchbinder, and B.D. Walker. **1996**. Cytotoxic T lymphocytes in asymptomatic long-term nonprogressing HIV-1 infection. Breadth

and specificity of the response and relation to in vivo viral quasispecies in a person with prolonged infection and low viral load. *J Immunol* 156:2616-2623.

Hemelaar, J., E. Gouws, P.D. Ghys, and S. Osmanov. **2011**. Global trends in molecular epidemiology of HIV-1 during 2000-2007. *AIDS* 25:679-689.

Hendel, H., S. Caillat-Zucman, H. Lebuanec, M. Carrington, S. O'Brien, J.M. Andrieu, F. Schachter, D. Zagury, J. Rappaport, C. Winkler, G.W. Nelson, and J.F. Zagury. **1999**. New class I and II HLA alleles strongly associated with opposite patterns of progression to AIDS. *J Immunol* 162:6942-6946.

Henn, M.R., C.L. Boutwell, P. Charlebois, N.J. Lennon, K.A. Power, A.R. Macalalad, A.M. Berlin, C.M. Malboeuf, E.M. Ryan, S. Gnerre, M.C. Zody, R.L. Erlich, L.M. Green, A. Berical, Y. Wang, M. Casali, H. Streeck, A.K. Bloom, T. Dudek, D. Tully, R. Newman, K.L. Axten, A.D. Gladden, L. Battis, M. Kemper, Q. Zeng, T.P. Shea, S. Gujja, C. Zedlack, O. Gasser, C. Brander, C. Hess, H.F. Gunthard, Z.L. Brumme, C.J. Brumme, S. Bazner, J. Rychert, J.P. Tinsley, K.H. Mayer, E. Rosenberg, F. Pereyra, J.Z. Levin, S.K. Young, H. Jessen, M. Altfeld, B.W. Birren, B.D. Walker, and T.M. Allen. **2012**. Whole genome deep sequencing of HIV-1 reveals the impact of early minor variants upon immune recognition during acute infection. *PLoS Pathog* 8:e1002529.

Henrich, T.J., E. Hanhauser, F.M. Marty, M.N. Sirignano, S. Keating, T.H. Lee, Y.P. Robles, B.T. Davis, J.Z. Li, A. Heisey, A.L. Hill, M.P. Busch, P. Armand, R.J. Soiffer, M. Altfeld, and D.R. Kuritzkes. **2014**. Antiretroviral-free HIV-1 remission and viral rebound after allogeneic stem cell transplantation: report of 2 cases. *Ann. Intern. Med.* 161:319-327.

Hersperger, A.R., F. Pereyra, M. Nason, K. Demers, P. Sheth, L.Y. Shin, C.M. Kovacs, B. Rodriguez, S.F. Sieg, L. Teixeira-Johnson, D. Gudonis, P.A. Goepfert, M.M. Lederman, I. Frank, G. Makedonas, R. Kaul, B.D. Walker, and M.R. Betts. **2010**. Perforin expression directly ex vivo by HIV-specific CD8 T-cells is a correlate of HIV elite control. *PLoS Pathog* 6:e1000917.

Hess, P.R., C. Barnes, M.D. Woolard, M.D. Johnson, J.M. Cullen, E.J. Collins, and J.A. Frelinger. **2007**. Selective deletion of antigen-specific CD8+ T cells by MHC class I tetramers coupled to the type I ribosome-inactivating protein saporin. *Blood* 109:3300-3307.

Hess, S.M., E.F. Young, K.R. Miller, B.G. Vincent, A.S. Buntzman, E.J. Collins, J.A. Frelinger, and P.R. Hess. **2013**. Deletion of naive T cells recognizing the minor histocompatibility antigen HY with toxin-coupled peptide-MHC class I tetramers inhibits cognate CTL responses and alters immunodominance. *Transpl Immunol* 29:138-145.

Hocqueloux, L., V. Avettand-Fenoel, S. Jacquot, T. Prazuck, E. Legac, A. Melard, M. Niang, C. Mille, G. Le Moal, J.P. Viard, and C. Rouzioux. **2013**. Long-term antiretroviral therapy initiated during primary HIV-1 infection is key to achieving both low HIV reservoirs and normal T cell counts. *J. Antimicrob. Chemother.* 68:1169-1178.

Honeyborne, I., A. Prendergast, F. Pereyra, A. Leslie, H. Crawford, R. Payne, S. Reddy, K. Bishop, E. Moodley, K. Nair, M. van der Stok, N. McCarthy, C.M. Rousseau, M. Addo, J.I. Mullins, C. Brander, P. Kiepiela, B.D. Walker, and P.J. Goulder. **2007**. Control of human immunodeficiency virus type 1 is associated with HLA-B*13 and targeting of multiple gag-specific CD8+ T-cell epitopes. *J Virol* 81:3667-3672.

Honeyborne, I., A. Rathod, R. Buchli, D. Ramduth, E. Moodley, P. Rathnavalu, S. Chetty, C. Day, C. Brander, W. Hildebrand, B.D. Walker, P. Kiepiela, and P.J. Goulder. **2006**. Motif inference reveals optimal CTL epitopes presented by HLA class I alleles highly prevalent in southern Africa. *J Immunol* 176:4699-4705.

Horton, H., I. Frank, R. Baydo, E. Jalbert, J. Penn, S. Wilson, J.P. McNevin, M.D. McSweyn, D. Lee, Y. Huang, S.C. De Rosa, and M.J. McElrath. **2006**. Preservation of T cell proliferation restricted by protective HLA alleles is critical for immune control of HIV-1 infection. *J Immunol* 177:7406-7415.

Huang, S., J. Dunkley-Thompson, Y. Tang, E.A. Macklin, J. Steel-Duncan, I. Singh-Minott, E.G. Ryland, M. Smikle, B.D. Walker, C.D. Christie, and M.E. Feeney. **2008**. Deficiency of HIV-Gag-specific T cells in early childhood correlates with poor viral containment. *J Immunol* 181:8103-8111.

Huang, Y., W.A. Paxton, S.M. Wolinsky, A.U. Neumann, L. Zhang, T. He, S. Kang, D. Ceradini, Z. Jin, K. Yazdanbakhsh, K. Kunstman, D. Erickson, E. Dragon, N.R. Landau, J. Phair, D.D. Ho, and R.A. Koup. **1996**. The role of a mutant CCR5 allele in HIV-1 transmission and disease progression. *Nat Med* 2:1240-1243.

Hunt, M., A. Gall, S.H. Ong, J. Brener, B. Ferns, P. Goulder, E. Nastouli, J.A. Keane, P. Kellam, and T.D. Otto. **2015**. IVA: accurate de novo assembly of RNA virus genomes. *Bioinformatics* 31:2374-2376.

Hunt, P.W., J.N. Martin, E. Sinclair, B. Bredt, E. Hagos, H. Lampiris, and S.G. Deeks. **2003**. T cell activation is associated with lower CD4+ T cell gains in human immunodeficiency virus-infected patients with sustained viral suppression during antiretroviral therapy. *J Infect Dis* 187:1534-1543.

Hurst, J., M. Hoffmann, M. Pace, J.P. Williams, J. Thornhill, E. Hamlyn, J. Meyerowitz, C. Willberg, K.K. Koelsch, N. Robinson, H. Brown, M. Fisher, S. Kinloch, D.A. Cooper, M. Schechter, G. Tambussi, S. Fidler, A. Babiker, J. Weber, A.D. Kelleher, R.E. Phillips, and J. Frater. **2015**. Immunological biomarkers predict HIV-1 viral rebound after treatment interruption. *Nature Commun.* 6:8495.

Hutter, G., D. Nowak, M. Mossner, S. Ganepola, A. Mussig, K. Allers, T. Schneider, J. Hofmann, C. Kucherer, O. Blau, I.W. Blau, W.K. Hofmann, and E. Thiel. **2009**. Long-term control of HIV by CCR5 Delta32/Delta32 stem-cell transplantation. *N. Engl. J. Med.* 360:692-698.

Iliff, P.J., E.G. Piwoz, N.V. Tavengwa, C.D. Zunguza, E.T. Marinda, K.J. Nathoo, L.H. Moulton, B.J. Ward, and J.H. Humphrey. **2005**. Early exclusive breastfeeding

reduces the risk of postnatal HIV-1 transmission and increases HIV-free survival. *AIDS* 19:699-708.

Janes, H., N. Frahm, A. DeCamp, M. Rolland, E. Gabriel, J. Wolfson, T. Hertz, E. Kallas, P. Goepfert, D.P. Friedrich, L. Corey, J.I. Mullins, M.J. McElrath, and P. Gilbert. **2012**. MRKAd5 HIV-1 Gag/Pol/Nef vaccine-induced T-cell responses inadequately predict distance of breakthrough HIV-1 sequences to the vaccine or viral load. *PLoS One* 7:e43396.

Janes, H., D.P. Friedrich, A. Krambrink, R.J. Smith, E.G. Kallas, H. Horton, D.R. Casimiro, M. Carrington, D.E. Geraghty, P.B. Gilbert, M.J. McElrath, and N. Frahm. **2013**. Vaccine-induced gag-specific T cells are associated with reduced viremia after HIV-1 infection. *J Infect Dis* 208:1231-1239.

Jessen, H., T.M. Allen, and H. Streeck. **2014**. How a single patient influenced HIV research--15-year follow-up. *N. Engl. J. Med.* 370:682-683.

Jin, X., D.E. Bauer, S.E. Tuttleton, S. Lewin, A. Gettie, J. Blanchard, C.E. Irwin, J.T. Safrit, J. Mittler, L. Weinberger, L.G. Kostrikis, L. Zhang, A.S. Perelson, and D.D. Ho. **1999**. Dramatic rise in plasma viremia after CD8(+) T cell depletion in simian immunodeficiency virus-infected macaques. *J Exp Med* 189:991-998.

Johnson, R.P., A. Trocha, T.M. Buchanan, and B.D. Walker. **1992**. Identification of overlapping HLA class I-restricted cytotoxic T cell epitopes in a conserved region of the human immunodeficiency virus type 1 envelope glycoprotein: definition of minimum epitopes and analysis of the effects of sequence variation. *J Exp Med* 175:961-971.

Jones, N., D. Agrawal, M. Elrefaei, A. Hanson, V. Novitsky, J.T. Wong, and H. Cao. **2003**. Evaluation of antigen-specific responses using in vitro enriched T cells. *J Immunol Methods* 274:139-147.

Juarez-Molina, C.I., H. Valenzuela-Ponce, S. Avila-Rios, D. Garrido-Rodriguez, T. Garcia-Tellez, M. Soto-Nava, C. Garcia-Morales, P. Goulder, and G. Reyes-Teran. **2014**. Impact of HLA-B*35 subtype differences on HIV disease outcome in Mexico. *AIDS* 28:1687-1690.

Judd, A., R.A. Ferrand, E. Jungmann, C. Foster, J. Masters, B. Rice, H. Lyall, P.A. Tookey, and K. Prime. **2009**. Vertically acquired HIV diagnosed in adolescence and early adulthood in the United Kingdom and Ireland: findings from national surveillance. *HIV Med.* 10:253-256.

Kalams, S.A., R.P. Johnson, A.K. Trocha, M.J. Dynan, H.S. Ngo, R.T. D'Aquila, J.T. Kurnick, and B.D. Walker. **1994**. Longitudinal analysis of T cell receptor (TCR) gene usage by human immunodeficiency virus 1 envelope-specific cytotoxic T lymphocyte clones reveals a limited TCR repertoire. *J Exp Med* 179:1261-1271.

Kappel, B.J., J. Pinilla-Ibarz, A.A. Kochman, J.M. Eng, V.M. Hubbard, I. Leiner, E.G. Pamer, G. Heller, M.R. van den Brink, and D.A. Scheinberg. **2006**. Remodeling specific immunity by use of MHC tetramers: demonstration in a graft-versus-host disease model. *Blood* 107:2045-2051.

Kaslow, R.A., M. Carrington, R. Apple, L. Park, A. Munoz, A.J. Saah, J.J. Goedert, C. Winkler, S.J. O'Brien, C. Rinaldo, R. Detels, W. Blattner, J. Phair, H. Erlich, and D.L. Mann. **1996**. Influence of combinations of human major histocompatibility complex genes on the course of HIV-1 infection. *Nature Med.* 2:405-411.

Keele, B.F., F. Van Heuverswyn, Y. Li, E. Bailes, J. Takehisa, M.L. Santiago, F. Bibollet-Ruche, Y. Chen, L.V. Wain, F. Liegeois, S. Loul, E.M. Ngole, Y. Bienvenue, E. Delaporte, J.F. Brookfield, P.M. Sharp, G.M. Shaw, M. Peeters, and B.H. Hahn. **2006**. Chimpanzee reservoirs of pandemic and nonpandemic HIV-1. *Science* 313:523-526.

Keenan, R.D., J. Ainsworth, N. Khan, R. Bruton, M. Cobbold, M. Assenmacher, D.W. Milligan, and P.A. Moss. **2001**. Purification of cytomegalovirus-specific CD8 T cells from peripheral blood using HLA-peptide tetramers. *Br J Haematol* 115:428-434.

Kiepiela, P., A.J. Leslie, I. Honeyborne, D. Ramduth, C. Thobakgale, S. Chetty, P. Rathnavalu, C. Moore, K.J. Pfafferott, L. Hilton, P. Zimbwa, S. Moore, T. Allen, C. Brander, M.M. Addo, M. Altfeld, I. James, S. Mallal, M. Bunce, L.D. Barber, J. Szinger, C. Day, P. Klenerman, J. Mullins, B. Korber, H.M. Coovadia, B.D. Walker, and P.J. Goulder. **2004**. Dominant influence of HLA-B in mediating the potential co-evolution of HIV and HLA. *Nature* 432:769-775.

Kiepiela, P., K. Ngumbela, C. Thobakgale, D. Ramduth, I. Honeyborne, E. Moodley, S. Reddy, C. de Pierres, Z. Mncube, N. Mkhwanazi, K. Bishop, M. van der Stok, K. Nair, N. Khan, H. Crawford, R. Payne, A. Leslie, J. Prado, A. Prendergast, J. Frater, N. McCarthy, C. Brander, G.H. Learn, D. Nickle, C. Rousseau, H. Coovadia, J.I. Mullins, D. Heckerman, B.D. Walker, and P. Goulder. **2007**. CD8+ T-cell responses to different HIV proteins have discordant associations with viral load. *Nature Med.* 13:46-53.

Klatt, N.R., S.E. Bosinger, M. Peck, L.E. Richert-Spuhler, A. Heigele, J.P. Gile, N. Patel, J. Taaffe, B. Julg, D. Camerini, C. Torti, J.N. Martin, S.G. Deeks, E. Sinclair, F.M. Hecht, M.M. Lederman, M. Paiardini, F. Kirchhoff, J.M. Brenchley, P.W. Hunt, and G. Silvestri. **2014**. Limited HIV infection of central memory and stem cell memory CD4+ T cells is associated with lack of progression in viremic individuals. *PLoS Pathog* 10:e1004345.

Klein, M.R., C.A. van Baalen, A.M. Holwerda, S.R. Kerkhof Garde, R.J. Bende, I.P. Keet, J.K. Eeftinck-Schattenkerk, A.D. Osterhaus, H. Schuitemaker, and F. Miedema. **1995**. Kinetics of Gag-specific cytotoxic T lymphocyte responses during the clinical course of HIV-1 infection: a longitudinal analysis of rapid progressors and long-term asymptomatics. *J Exp Med* 181:1365-1372.

Kloverpris, H.N., E. Adland, M. Koyanagi, A. Stryhn, M. Harndahl, P.C. Matthews, R. Shapiro, B.D. Walker, T. Ndung'u, C. Brander, M. Takiguchi, S. Buus, and P. Goulder. **2014a**. HIV subtype influences HLA-B*07:02-associated HIV disease outcome. *AIDS Res Hum Retroviruses* 30:468-475.

Kloverpris, H.N., M. Harndahl, A.J. Leslie, J.M. Carlson, N. Ismail, M. van der Stok, K.H. Huang, F. Chen, L. Riddell, D. Steyn, D. Goedhals, C. van Vuuren, J.

Frater, B.D. Walker, M. Carrington, T. Ndung'u, S. Buus, and P. Goulder. **2012a**. HIV control through a single nucleotide on the HLA-B locus. *J Virol* 86:11493-11500.

Kloverpris, H.N., R. McGregor, J.E. McLaren, K. Ladell, A. Stryhn, C. Koofhethile, J. Brener, F. Chen, L. Riddell, L. Graziano, P. Klenerman, A. Leslie, S. Buus, D.A. Price, and P. Goulder. **2014b**. Programmed death-1 expression on HIV-1-specific CD8+ T cells is shaped by epitope specificity, T-cell receptor clonotype usage and antigen load. *AIDS* 28:2007-2021.

Kloverpris, H.N., R.P. Payne, J.B. Sacha, J.T. Rasaiyaah, F. Chen, M. Takiguchi, O.O. Yang, G.J. Towers, P. Goulder, and J.G. Prado. **2013a**. Early antigen presentation of protective HIV-1 KF11Gag and KK10Gag epitopes from incoming viral particles facilitates rapid recognition of infected cells by specific CD8+ T cells. *J Virol* 87:2628-2638.

Kloverpris, H.N., A. Stryhn, M. Harndahl, J.M. Carlson, A.J. Leslie, F. Chen, L. Riddell, J. Mulenga, B.D. Walker, T. Ndung'u, S. Buus, and P. Goulder. **2013b**. HLA-A*68:02-restricted Gag-specific cytotoxic T lymphocyte responses can drive selection pressure on HIV but are subdominant and ineffective. *AIDS* 27:1717-1723.

Kloverpris, H.N., A. Stryhn, M. Harndahl, M. van der Stok, R.P. Payne, P.C. Matthews, F. Chen, L. Riddell, B.D. Walker, T. Ndung'u, S. Buus, and P. Goulder. **2012b**. HLA-B*57 Micropolymorphism shapes HLA allele-specific epitope immunogenicity, selection pressure, and HIV immune control. *J Virol* 86:919-929.

Koibuchi, T., T.M. Allen, M. Lichterfeld, S.K. Mui, K.M. O'Sullivan, A. Trocha, S.A. Kalams, R.P. Johnson, and B.D. Walker. **2005**. Limited sequence evolution within persistently targeted CD8 epitopes in chronic human immunodeficiency virus type 1 infection. *J Virol* 79:8171-8181.

Kollmann, T.R., J. Crabtree, A. Rein-Weston, D. Blimkie, F. Thommai, X.Y. Wang, P.M. Lavoie, J. Furlong, E.S. Fortuno, 3rd, A.M. Hajjar, N.R. Hawkins, S.G. Self, and C.B. Wilson. **2009**. Neonatal innate TLR-mediated responses are distinct from those of adults. *J. Immunol.* 183:7150-7160.

Kollmann, T.R., O. Levy, R.R. Montgomery, and S. Goriely. **2012**. Innate immune function by Toll-like receptors: distinct responses in newborns and the elderly. *Immunity* 37:771-783.

Kosmrlj, A., E.L. Read, Y. Qi, T.M. Allen, M. Altfeld, S.G. Deeks, F. Pereyra, M. Carrington, B.D. Walker, and A.K. Chakraborty. **2010**. Effects of thymic selection of the T-cell repertoire on HLA class I-associated control of HIV infection. *Nature* 465:350-354.

Koup, R.A., J.T. Safrit, Y. Cao, C.A. Andrews, G. McLeod, W. Borkowsky, C. Farthing, and D.D. Ho. **1994**. Temporal association of cellular immune responses with the initial control of viremia in primary human immunodeficiency virus type 1 syndrome. *J Virol* 68:4650-4655.

Kourtis, A.P., C.C. Ibegbu, J. Wiener, C.C. King, G. Tegha, D. Kamwendo, J. Kumwenda, S.P. Kaur, V. Flax, S. Ellington, Z. Kacheche, D. Kayira, C. Chasela, C. van der Horst, and D.J. Jamieson. **2013**. Role of intestinal mucosal integrity in HIV transmission to infants through breast-feeding: the BAN study. *J. Infect. Dis.* 208:653-661.

Ladell, K., M. Hashimoto, M.C. Iglesias, P.G. Wilmann, J.E. McLaren, S. Gras, T. Chikata, N. Kuse, S. Fastenackels, E. Gostick, J.S. Bridgeman, V. Venturi, Z.A. Arkoub, H. Agut, D.J. van Bockel, J.R. Almeida, D.C. Douek, L. Meyer, A. Venet, M. Takiguchi, J. Rossjohn, D.A. Price, and V. Appay. **2013**. A molecular basis for the control of preimmune escape variants by HIV-specific CD8+ T cells. *Immunity* 38:425-436.

Laidlaw, B.J., J.E. Craft, and S.M. Kaech. **2016**. The multifaceted role of CD4(+) T cells in CD8(+) T cell memory. *Nat Rev Immunol* 16:102-111.

Lambotte, O., F. Boufassa, Y. Madec, A. Nguyen, C. Goujard, L. Meyer, C. Rouzioux, A. Venet, and J.F. Delfraissy. **2005**. HIV controllers: a homogeneous group of HIV-1-infected patients with spontaneous control of viral replication. *Clin Infect Dis* 41:1053-1056.

Lazaryan, A., E. Lobashevsky, J. Mulenga, E. Karita, S. Allen, J. Tang, and R.A. Kaslow. **2006**. Human leukocyte antigen B58 supertype and human immunodeficiency virus type 1 infection in native Africans. *J Virol* 80:6056-6060.

Lecuroux, C., A. Saez-Cirion, I. Girault, P. Versmisse, F. Boufassa, V. Avettand-Fenoel, C. Rouzioux, L. Meyer, G. Pancino, O. Lambotte, M. Sinet, and A. Venet. **2014**. Both HLA-B*57 and plasma HIV RNA levels contribute to the HIV-specific CD8+ T cell response in HIV controllers. *J Virol* 88:176-187.

Lefrere, J.J., M. Mariotti, L. Morand-Joubert, M. Thauvin, and F. Roudot-Thoraval. **1999**. Plasma human immunodeficiency virus RNA below 40 Copies/mL is rare in untreated persons even in the first years of infection. *J Infect Dis* 180:526-529.

Leisner, C., N. Loeth, K. Lamberth, S. Justesen, C. Sylvester-Hvid, E.G. Schmidt, M. Claesson, S. Buus, and A. Stryhn. **2008**. One-pot, mix-and-read peptide-MHC tetramers. *PLoS One* 3:e1678.

Leslie, A., D. Kavanagh, I. Honeyborne, K. Pfafferott, C. Edwards, T. Pillay, L. Hilton, C. Thobakgale, D. Ramduth, R. Draenert, S. Le Gall, G. Luzzi, A. Edwards, C. Brander, A.K. Sewell, S. Moore, J. Mullins, C. Moore, S. Mallal, N. Bhardwaj, K. Yusim, R. Phillips, P. Klenerman, B. Korber, P. Kiepiela, B. Walker, and P. Goulder. **2005**. Transmission and accumulation of CTL escape variants drive negative associations between HIV polymorphisms and HLA. *J Exp Med* 201:891-902.

Leslie, A., P.C. Matthews, J. Listgarten, J.M. Carlson, C. Kadie, T. Ndung'u, C. Brander, H. Coovadia, B.D. Walker, D. Heckerman, and P.J. Goulder. **2010**. Additive contribution of HLA class I alleles in the immune control of HIV-1 infection. *J Virol* 84:9879-9888.

Leslie, A.J., K.J. Pfafferott, P. Chetty, R. Draenert, M.M. Addo, M. Feeney, Y. Tang, E.C. Holmes, T. Allen, J.G. Prado, M. Altfeld, C. Brander, C. Dixon, D. Ramduth, P. Jeena, S.A. Thomas, A. St John, T.A. Roach, B. Kupfer, G. Luzzi, A. Edwards, G. Taylor, H. Lyall, G. Tudor-Williams, V. Novelli, J. Martinez-Picado, P. Kiepiela, B.D. Walker, and P.J. Goulder. **2004**. HIV evolution: CTL escape mutation and reversion after transmission. *Nat Med* 10:282-289.

Leth, S., J. Hojen, M. Schleimann, S. Nissen, A. Mork, M. Sommerfelt, L. Ostergaard, T. Rasmussen, M. Tolstrup, and O.S. Sogaard. 2016. Effect of Sequential Vacc-4x/GM-CSF Immunization and Romidepsin on the HIV Reservoir. Abstract 26LB. In Conference on Retroviruses and Opportunistic Infections, February 22-25, 2016. Boston, MA, USA.

Levy, O., M. Coughlin, B.N. Cronstein, R.M. Roy, A. Desai, and M.R. Wessels. **2006**. The adenosine system selectively inhibits TLR-mediated TNF-alpha production in the human newborn. *J. Immunol.* 177:1956-1966.

Liu, R., W.A. Paxton, S. Choe, D. Ceradini, S.R. Martin, R. Horuk, M.E. MacDonald, H. Stuhlmann, R.A. Koup, and N.R. Landau. **1996**. Homozygous defect in HIV-1 coreceptor accounts for resistance of some multiply-exposed individuals to HIV-1 infection. *Cell* 86:367-377.

Llano, A., J. Carrillo, B. Mothe, L. Ruiz, S. Marfil, E. Garcia, E. Yuste, V. Sanchez, B. Clotet, J. Blanco, and C. Brander. **2013**. Expansion of antibody secreting cells and modulation of neutralizing antibody activity in HIV infected individuals undergoing structured treatment interruptions. *J Transl Med* 11:48.

LLano A, W.A., Overa A, Silva-Arrieta A, Brander C. 2013. Best-characterized HIV-1 CTL epitopes: the 2013 update. In HIV Molecular Immunology 2013. Theoretical Biology and Biophysics Group, Los Alamos National Laboratory, Los Alamos, NM. 3-19.

Lohman, B.L., J.A. Slyker, B.A. Richardson, C. Farquhar, J.M. Mabuka, C. Crudder, T. Dong, E. Obimbo, D. Mbori-Ngacha, J. Overbaugh, S. Rowland-Jones, and G. John-Stewart. **2005**. Longitudinal assessment of human immunodeficiency virus type 1 (HIV-1)-specific gamma interferon responses during the first year of life in HIV-1-infected infants. *J Virol* 79:8121-8130.

Long, J.D. 2012. Longitudinal Data Analysis for the Behavioral Sciences Using R. SAGE Publications, Inc., 568 pp.

Lopez-Larrea, C., M. Mijiyawa, S. Gonzalez, J.L. Fernandez-Morera, M.A. Blanco-Gelaz, J. Martinez-Borra, and A. Lopez-Vazquez. **2002**. Association of ankylosing spondylitis with HLA-B*1403 in a West African population. *Arthritis Rheum* 46:2968-2971.

Lugada, E.S., J. Mermin, F. Kaharuza, E. Ulvestad, W. Were, N. Langeland, B. Asjo, S. Malamba, and R. Downing. **2004**. Population-based hematologic and immunologic reference values for a healthy Ugandan population. *Clin Diagn Lab Immunol* 11:29-34.

Lundgren, J.D., A.G. Babiker, F. Gordin, S. Emery, B. Grund, S. Sharma, A. Avihingsanon, D.A. Cooper, G. Fatkenheuer, J.M. Llibre, J.M. Molina, P. Munderi, M. Schechter, R. Wood, K.L. Klingman, S. Collins, H.C. Lane, A.N. Phillips, and J.D. Neaton. **2015**. Initiation of Antiretroviral Therapy in Early Asymptomatic HIV Infection. *N Engl J Med* 373:795-807.

Luzuriaga, K., H. Gay, C. Ziemniak, K.B. Sanborn, M. Somasundaran, K. Rainwater-Lovett, J.W. Mellors, D. Rosenbloom, and D. Persaud. **2015**. Viremic relapse after HIV-1 remission in a perinatally infected child. *N. Engl. J. Med.* 372:786-788.

Luzuriaga, K., D. Holmes, A. Hereema, J. Wong, D.L. Panicali, and J.L. Sullivan. **1995**. HIV-1-specific cytotoxic T lymphocyte responses in the first year of life. *J. Immunol.* 154:433-443.

Luzuriaga, K., B. Tabak, M. Garber, Y.H. Chen, C. Ziemniak, M.M. McManus, D. Murray, M.C. Strain, D.D. Richman, T.W. Chun, C.K. Cunningham, and D. Persaud. **2014**. HIV type 1 (HIV-1) proviral reservoirs decay continuously under sustained virologic control in HIV-1-infected children who received early treatment. *J. Infect. Dis.* 210:1529-1538.

Lyles, R.H., A. Munoz, T.E. Yamashita, H. Bazmi, R. Detels, C.R. Rinaldo, J.B. Margolick, J.P. Phair, and J.W. Mellors. **2000**. Natural history of human immunodeficiency virus type 1 viremia after seroconversion and proximal to AIDS in a large cohort of homosexual men. Multicenter AIDS Cohort Study. *J Infect Dis* 181:872-880.

Madden, D.R., J.C. Gorga, J.L. Strominger, and D.C. Wiley. **1992**. The three-dimensional structure of HLA-B27 at 2.1 A resolution suggests a general mechanism for tight peptide binding to MHC. *Cell* 70:1035-1048.

Maness, N.J., L.J. Yant, C. Chung, J.T. Loffredo, T.C. Friedrich, S.M. Piaskowski, J. Furlott, G.E. May, T. Soma, E.J. Leon, N.A. Wilson, H. Piontkivska, A.L. Hughes, J. Sidney, A. Sette, and D.I. Watkins. **2008**. Comprehensive immunological evaluation reveals surprisingly few differences between elite controller and progressor Mamu-B*17-positive simian immunodeficiency virus-infected rhesus macaques. *J Virol* 82:5245-5254.

Mann, D.L., S.J. O'Brien, D.A. Gilbert, Y. Reid, M. Popovic, E. Read-Connole, R.C. Gallo, and A.F. Gazdar. **1989**. Origin of the HIV-susceptible human CD4+ cell line H9. *AIDS Res Hum Retroviruses* 5:253-255.

Martin, M.P., X. Gao, J.H. Lee, G.W. Nelson, R. Detels, J.J. Goedert, S. Buchbinder, K. Hoots, D. Vlahov, J. Trowsdale, M. Wilson, S.J. O'Brien, and M. Carrington. **2002**. Epistatic interaction between KIR3DS1 and HLA-B delays the progression to AIDS. *Nat Genet* 31:429-434.

Martin, M.P., Y. Qi, X. Gao, E. Yamada, J.N. Martin, F. Pereyra, S. Colombo, E.E. Brown, W.L. Shupert, J. Phair, J.J. Goedert, S. Buchbinder, G.D. Kirk, A. Telenti, M. Connors, S.J. O'Brien, B.D. Walker, P. Parham, S.G. Deeks, D.W. McVicar, and M. Carrington. **2007**. Innate partnership of HLA-B and KIR3DL1 subtypes against HIV-1. *Nat Genet* 39:733-740.

Martinez-Bonet, M., M.C. Puertas, C. Fortuny, D. Ouchi, M.J. Mellado, P. Rojo, A. Noguera-Julian, M.A. Munoz-Fernandez, and J. Martinez-Picado. **2015**. Establishment and Replenishment of the Viral Reservoir in Perinatally HIV-1-infected Children Initiating Very Early Antiretroviral Therapy. *Clin. Infect. Dis.* 61:1169-1178.

Martinez-Picado, J., J.G. Prado, E.E. Fry, K. Pfafferott, A. Leslie, S. Chetty, C. Thobakgale, I. Honeyborne, H. Crawford, P. Matthews, T. Pillay, C. Rousseau, J.I. Mullins, C. Brander, B.D. Walker, D.I. Stuart, P. Kiepiela, and P. Goulder. **2006**. Fitness cost of escape mutations in p24 Gag in association with control of human immunodeficiency virus type 1. *J Virol* 80:3617-3623.

Masemola, A., T. Mashishi, G. Khoury, P. Mohube, P. Mokgotho, E. Vardas, M. Colvin, L. Zijenah, D. Katzenstein, R. Musonda, S. Allen, N. Kumwenda, T. Taha, G. Gray, J. McIntyre, S.A. Karim, H.W. Sheppard, and C.M. Gray. **2004**. Hierarchical targeting of subtype C human immunodeficiency virus type 1 proteins by CD8+ T cells: correlation with viral load. *J Virol* 78:3233-3243.

Matthews, P.C., E. Adland, J. Listgarten, A. Leslie, N. Mkhwanazi, J.M. Carlson, M. Harndahl, A. Stryhn, R.P. Payne, A. Ogwu, K.H. Huang, J. Frater, P. Paioni, H. Kloverpris, P. Jooste, D. Goedhals, C. van Vuuren, D. Steyn, L. Riddell, F. Chen, G. Luzzi, T. Balachandran, T. Ndung'u, S. Buus, M. Carrington, R. Shapiro, D. Heckerman, and P.J. Goulder. **2011**. HLA-A*7401-mediated control of HIV viremia is independent of its linkage disequilibrium with HLA-B*5703. *J Immunol* 186:5675-5686.

Matthews, P.C., M. Koyanagi, H.N. Kloverpris, M. Harndahl, A. Stryhn, T. Akahoshi, H. Gatanaga, S. Oka, C. Juarez Molina, H. Valenzuela Ponce, S. Avila Rios, D. Cole, J. Carlson, R.P. Payne, A. Ogwu, A. Bere, T. Ndung'u, K. Gounder, F. Chen, L. Riddell, G. Luzzi, R. Shapiro, C. Brander, B. Walker, A.K. Sewell, G. Reyes Teran, D. Heckerman, E. Hunter, S. Buus, M. Takiguchi, and P.J. Goulder. **2012**. Differential clade-specific HLA-B*3501 association with HIV-1 disease outcome is linked to immunogenicity of a single Gag epitope. *J Virol* 86:12643-12654.

Matthews, P.C., A. Prendergast, A. Leslie, H. Crawford, R. Payne, C. Rousseau, M. Rolland, I. Honeyborne, J. Carlson, C. Kadie, C. Brander, K. Bishop, N. Mlotshwa, J.I. Mullins, H. Coovadia, T. Ndung'u, B.D. Walker, D. Heckerman, and P.J. Goulder. **2008**. Central role of reverting mutations in HLA associations with human immunodeficiency virus set point. *J. Virol.* 82:8548-8559.

Mehrotra, D.V., X. Li, and P.B. Gilbert. **2006**. A comparison of eight methods for the dual-endpoint evaluation of efficacy in a proof-of-concept HIV vaccine trial. *Biometrics* 62:893-900.

Mellors, J.W., C.R. Rinaldo, Jr., P. Gupta, R.M. White, J.A. Todd, and L.A. Kingsley. **1996**. Prognosis in HIV-1 infection predicted by the quantity of virus in plasma. *Science* 272:1167-1170.

Merino, E., V. Montserrat, A. Paradela, and J.A. Lopez de Castro. **2005**. Two HLA-B14 subtypes (B*1402 and B*1403) differentially associated with ankylosing spondylitis

differ substantially in peptide specificity but have limited peptide and T-cell epitope sharing with HLA-B27. *J Biol Chem* 280:35868-35880.

Michael, N.L., L.G. Louie, A.L. Rohrbaugh, K.A. Schultz, D.E. Dayhoff, C.E. Wang, and H.W. Sheppard. **1997**. The role of CCR5 and CCR2 polymorphisms in HIV-1 transmission and disease progression. *Nat Med* 3:1160-1162.

Migueles, S.A., and M. Connors. **2010**. Long-term nonprogressive disease among untreated HIV-infected individuals: clinical implications of understanding immune control of HIV. *JAMA* 304:194-201.

Migueles, S.A., A.C. Laborico, H. Imamichi, W.L. Shupert, C. Royce, M. McLaughlin, L. Ehler, J. Metcalf, S. Liu, C.W. Hallahan, and M. Connors. **2003**. The differential ability of HLA B*5701+ long-term nonprogressors and progressors to restrict human immunodeficiency virus replication is not caused by loss of recognition of autologous viral gag sequences. *J Virol* 77:6889-6898.

Migueles, S.A., A.C. Laborico, W.L. Shupert, M.S. Sabbaghian, R. Rabin, C.W. Hallahan, D. Van Baarle, S. Kostense, F. Miedema, M. McLaughlin, L. Ehler, J. Metcalf, S. Liu, and M. Connors. **2002**. HIV-specific CD8+ T cell proliferation is coupled to perforin expression and is maintained in nonprogressors. *Nat Immunol* 3:1061-1068.

Migueles, S.A., D. Mendoza, M.G. Zimmerman, K.M. Martins, S.A. Toulmin, E.P. Kelly, B.A. Peterson, S.A. Johnson, E. Galson, K.O. Poropatich, A. Patamawenu, H. Imamichi, A. Ober, C.A. Rehm, S. Jones, C.W. Hallahan, D.A. Follmann, and M. Connors. **2015**. CD8(+) T-cell Cytotoxic Capacity Associated with Human Immunodeficiency Virus-1 Control Can Be Mediated through Various Epitopes and Human Leukocyte Antigen Types. *EBioMedicine* 2:46-58.

Migueles, S.A., C.M. Osborne, C. Royce, A.A. Compton, R.P. Joshi, K.A. Weeks, J.E. Rood, A.M. Berkley, J.B. Sacha, N.A. Cogliano-Shutta, M. Lloyd, G. Roby, R. Kwan, M. McLaughlin, S. Stallings, C. Rehm, M.A. O'Shea, J. Mican, B.Z. Packard, A. Komoriya, S. Palmer, A.P. Wiegand, F. Maldarelli, J.M. Coffin, J.W. Mellors, C.W. Hallahan, D.A. Follman, and M. Connors. **2008**. Lytic granule loading of CD8+ T cells is required for HIV-infected cell elimination associated with immune control. *Immunity* 29:1009-1021.

Migueles, S.A., M.S. Sabbaghian, W.L. Shupert, M.P. Bettinotti, F.M. Marincola, L. Martino, C.W. Hallahan, S.M. Selig, D. Schwartz, J. Sullivan, and M. Connors. **2000**. HLA B*5701 is highly associated with restriction of virus replication in a subgroup of HIV-infected long term nonprogressors. *Proc Natl Acad Sci U S A* 97:2709-2714.

Migueles, S.A., K.A. Weeks, E. Nou, A.M. Berkley, J.E. Rood, C.M. Osborne, C.W. Hallahan, N.A. Cogliano-Shutta, J.A. Metcalf, M. McLaughlin, R. Kwan, J.M. Mican, R.T. Davey, Jr., and M. Connors. **2009**. Defective human immunodeficiency virus-specific CD8+ T-cell polyfunctionality, proliferation, and cytotoxicity are not restored by antiretroviral therapy. *J Virol* 83:11876-11889.

Miles, D.J., M. van der Sande, D. Jeffries, S. Kaye, J. Ismaili, O. Ojuola, M. Sanneh, E.S. Touray, P. Waight, S. Rowland-Jones, H. Whittle, and A. Marchant. **2007**. Cytomegalovirus infection in Gambian infants leads to profound CD8 T-cell differentiation. *J. Virol.* 81:5766-5776.

Misrahi, M., J.P. Teglas, N. N'Go, M. Burgard, M.J. Mayaux, C. Rouzioux, J.F. Delfraissy, and S. Blanche. **1998**. CCR5 chemokine receptor variant in HIV-1 mother-to-child transmission and disease progression in children. French Pediatric HIV Infection Study Group. *JAMA* 279:277-280.

Miura, T., M.A. Brockman, A. Schneidewind, M. Lobritz, F. Pereyra, A. Rathod, B.L. Block, Z.L. Brumme, C.J. Brumme, B. Baker, A.C. Rothchild, B. Li, A. Trocha, E. Cutrell, N. Frahm, C. Brander, I. Toth, E.J. Arts, T.M. Allen, and B.D. Walker. **2009**. HLA-B57/B*5801 human immunodeficiency virus type 1 elite controllers select for rare gag variants associated with reduced viral replication capacity and strong cytotoxic T-lymphocyte [corrected] recognition. *J Virol* 83:2743-2755.

Mold, J.E., J. Michaelsson, T.D. Burt, M.O. Muench, K.P. Beckerman, M.P. Busch, T.H. Lee, D.F. Nixon, and J.M. McCune. **2008**. Maternal alloantigens promote the development of tolerogenic fetal regulatory T cells in utero. *Science* 322:1562-1565.

Monteiro, P., A. Gosselin, V.S. Wacleche, M. El-Far, E.A. Said, H. Kared, N. Grandvaux, M.R. Boulassel, J.P. Routy, and P. Ancuta. **2011**. Memory CCR6+CD4+ T cells are preferential targets for productive HIV type 1 infection regardless of their expression of integrin beta7. *J. Immunol.* 186:4618-4630.

Mori, M., E. Adland, P. Paioni, A. Swordy, L. Mori, L. Laker, M. Muenchhoff, P.C. Matthews, G. Tudor-Williams, N. Lavandier, A. van Zyl, J. Hurst, B.D. Walker, T. Ndung'u, A. Prendergast, P. Goulder, and P. Jooste. **2015**. Sex Differences in Antiretroviral Therapy Initiation in Pediatric HIV Infection. *PLoS One* 10:e0131591.

Mothe, B., A. Llano, J. Ibarrondo, J. Zamarreno, M. Schiaulini, C. Miranda, M. Ruiz-Riol, C.T. Berger, M.J. Herrero, E. Palou, M. Plana, M. Rolland, A. Khatri, D. Heckerman, F. Pereyra, B.D. Walker, D. Weiner, R. Paredes, B. Clotet, B.K. Felber, G.N. Pavlakis, J.I. Mullins, and C. Brander. **2012**. CTL responses of high functional avidity and broad variant cross-reactivity are associated with HIV control. *PLoS One* 7:e29717.

Mphatswe, W., N. Blanckenberg, G. Tudor-Williams, A. Prendergast, C. Thobakgale, N. Mkhwanazi, N. McCarthy, B.D. Walker, P. Kiepiela, and P. Goulder. **2007**. High frequency of rapid immunological progression in African infants infected in the era of perinatal HIV prophylaxis. *AIDS* 21:1253-1261.

Mudd, P.A., M.A. Martins, A.J. Ericsen, D.C. Tully, K.A. Power, A.T. Bean, S.M. Piaskowski, L. Duan, A. Seese, A.D. Gladden, K.L. Weisgrau, J.R. Furlott, Y.I. Kim, M.G. Veloso de Santana, E. Rakasz, S. Capuano, 3rd, N.A. Wilson, M.C. Bonaldo, R. Galler, D.B. Allison, M. Piatak, Jr., A.T. Haase, J.D. Lifson, T.M. Allen, and D.I. Watkins. **2012**. Vaccine-induced CD8+ T cells control AIDS virus replication. *Nature* 491:129-133.

Munoz-Arias, I., G. Doitsh, Z. Yang, S. Sowinski, D. Ruelas, and W.C. Greene. **2015**. Blood-Derived CD4 T Cells Naturally Resist Pyroptosis during Abortive HIV-1 Infection. *Cell Host Microbe* 18:463-470.

Mylvaganam, G., S. Hicks, B. Lawson, M. Nega, V. Velu, R. Ahmed, G.J. Freeman, and R. Amara. 2016. PD-1 Blockade as an Adjunct Therapy to ART and Potential to Destabilize SIV Reservoir. Abstract 93LB. In Conference on Retroviruses and Opportunistic Infections, February 22-25, 2016. Boston, MA, USA.

Nabel, G., and D. Baltimore. **1987**. An inducible transcription factor activates expression of human immunodeficiency virus in T cells. *Nature* 326:711-713.

Nahmias, A.J., J. Weiss, X. Yao, F. Lee, R. Kodsi, M. Schanfield, T. Matthews, D. Bolognesi, D. Durack, A. Motulsky, P. Kanki, and M. Essex. **1986**. Evidence for human infection with an HTLV III/LAV-like virus in Central Africa, 1959. *Lancet* 1:1279-1280.

Ndhlovu, Z.M., P. Kamya, N. Mewalal, H.N. Kloverpris, T. Nkosi, K. Pretorius, F. Laher, F. Ogunshola, D. Chopera, K. Shekhar, M. Ghebremichael, N. Ismail, A. Moodley, A. Malik, A. Leslie, P.J. Goulder, S. Buus, A. Chakraborty, K. Dong, T. Ndung'u, and B.D. Walker. **2015a**. Magnitude and Kinetics of CD8(+) T Cell Activation during Hyperacute HIV Infection Impact Viral Set Point. *Immunity* 43:591-604.

Ndhlovu, Z.M., J. Proudfoot, K. Cesa, D.M. Alvino, A. McMullen, S. Vine, E. Stampouloglou, A. Piechocka-Trocha, B.D. Walker, and F. Pereyra. **2012**. Elite controllers with low to absent effector CD8+ T cell responses maintain highly functional, broadly directed central memory responses. *J Virol* 86:6959-6969.

Ndhlovu, Z.M., E. Stampouloglou, K. Cesa, O. Mavrothalassitis, D.M. Alvino, J.Z. Li, S. Wilton, D. Karel, A. Piechocka-Trocha, H. Chen, F. Pereyra, and B.D. Walker. **2015b**. The breadth of expandable memory CD8+ T cells inversely correlates with residual viral loads in HIV elite controllers. *J Virol* 89:10735-10747.

NDOH, S.A. 2010. Clinical guidelines: PMTCT (prevention of mother-to-child transmission. National Department of Health, South Africa; South African National AIDS Council. 2010. In http://www.sahivsoc.org/practise-guidelines/national-dept-of-health-guidelines. Accessed on 19 March 2016.

Newell, M.L., H. Coovadia, M. Cortina-Borja, N. Rollins, P. Gaillard, and F. Dabis. **2004**. Mortality of infected and uninfected infants born to HIV-infected mothers in Africa: a pooled analysis. *Lancet* 364:1236-1243.

Ngumbela, K.C., C.L. Day, Z. Mncube, K. Nair, D. Ramduth, C. Thobakgale, E. Moodley, S. Reddy, C. de Pierres, N. Mkhwanazi, K. Bishop, M. van der Stok, N. Ismail, I. Honeyborne, H. Crawford, D.G. Kavanagh, C. Rousseau, D. Nickle, J. Mullins, D. Heckerman, B. Korber, H. Coovadia, P. Kiepiela, P.J. Goulder, and B.D. Walker. **2008**. Targeting of a CD8 T cell env epitope presented by HLA-B*5802 is associated with markers of HIV disease progression and lack of selection pressure. *AIDS Res. Hum. Retroviruses* 24:72-82.

Novitsky, V., P. Gilbert, T. Peter, M.F. McLane, S. Gaolekwe, N. Rybak, I. Thior, T. Ndung'u, R. Marlink, T.H. Lee, and M. Essex. **2003**. Association between virus-specific T-cell responses and plasma viral load in human immunodeficiency virus type 1 subtype C infection. *J Virol* 77:882-890.

Nowak, E.C., C.T. Weaver, H. Turner, S. Begum-Haque, B. Becher, B. Schreiner, A.J. Coyle, L.H. Kasper, and R.J. Noelle. **2009**. IL-9 as a mediator of Th17-driven inflammatory disease. *J. Exp. Med.* 206:1653-1660.

Nqoko, B., C.L. Day, N. Mansoor, M. De Kock, E.J. Hughes, T. Hawkridge, G. Kaplan, W.H. Boom, G.D. Hussey, and W.A. Hanekom. **2011**. HIV-specific gag responses in early infancy correlate with clinical outcome and inversely with viral load. *AIDS Res Hum Retroviruses* 27:1311-1316.

Nsheha, A.H., D.E. Dow, G.E. Kapanda, B.C. Hamel, and L.J. Msuya. **2014**. Adherence to antiretroviral therapy among HIV-infected children receiving care at Kilimanjaro Christian Medical Centre (KCMC), Northern Tanzania: A cross- sectional analytical study. *Pan Afr. Med. J.* 17:238.

Oberlin, E., A. Amara, F. Bachelerie, C. Bessia, J.L. Virelizier, F. Arenzana-Seisdedos, O. Schwartz, J.M. Heard, I. Clark-Lewis, D.F. Legler, M. Loetscher, M. Baggiolini, and B. Moser. **1996**. The CXC chemokine SDF-1 is the ligand for LESTR/fusin and prevents infection by T-cell-line-adapted HIV-1. *Nature* 382:833-835.

Ogg, G.S., X. Jin, S. Bonhoeffer, P.R. Dunbar, M.A. Nowak, S. Monard, J.P. Segal, Y. Cao, S.L. Rowland-Jones, V. Cerundolo, A. Hurley, M. Markowitz, D.D. Ho, D.F. Nixon, and A.J. McMichael. **1998**. Quantitation of HIV-1-specific cytotoxic T lymphocytes and plasma load of viral RNA. *Science* 279:2103-2106.

Paiardini, M., B. Cervasi, E. Reyes-Aviles, L. Micci, A.M. Ortiz, A. Chahroudi, C. Vinton, S.N. Gordon, S.E. Bosinger, N. Francella, P.L. Hallberg, E. Cramer, T. Schlub, M.L. Chan, N.E. Riddick, R.G. Collman, C. Apetrei, I. Pandrea, J. Else, J. Munch, F. Kirchhoff, M.P. Davenport, J.M. Brenchley, and G. Silvestri. **2011**. Low levels of SIV infection in sooty mangabey central memory CD(4)(+) T cells are associated with limited CCR5 expression. *Nat Med* 17:830-836.

Pandrea, I., C. Apetrei, S. Gordon, J. Barbercheck, J. Dufour, R. Bohm, B. Sumpter, P. Roques, P.A. Marx, V.M. Hirsch, A. Kaur, A.A. Lackner, R.S. Veazey, and G. Silvestri. **2007**. Paucity of CD4+CCR5+ T cells is a typical feature of natural SIV hosts. *Blood* 109:1069-1076.

Papasavvas, E., L. Azzoni, A. Foulkes, A. Violari, M.F. Cotton, M. Pistilli, G. Reynolds, X. Yin, D.K. Glencross, W.S. Stevens, J.A. McIntyre, and L.J. Montaner. **2011**. Increased microbial translocation in </= 180 days old perinatally human immunodeficiency virus-positive infants as compared with human immunodeficiency virus-exposed uninfected infants of similar age. *Pediatr. Infect. Dis. J.* 30:877-882.

Parham, P., C.E. Lomen, D.A. Lawlor, J.P. Ways, N. Holmes, H.L. Coppin, R.D. Salter, A.M. Wan, and P.D. Ennis. **1988**. Nature of polymorphism in HLA-A, -B, and -C molecules. *Proc Natl Acad Sci U S A* 85:4005-4009.

Paul, M.E., C. Mao, M. Charurat, L. Serchuck, M. Foca, K. Hayani, E.L. Handelsman, C. Diaz, K. McIntosh, and W.T. Shearer. **2005**. Predictors of immunologic long-term nonprogression in HIV-infected children: implications for initiating therapy. *J. Allergy Clin. Immunol.* 115:848-855.

Payne, R., M. Muenchhoff, J. Mann, H.E. Roberts, P. Matthews, E. Adland, A. Hempenstall, K.H. Huang, M. Brockman, Z. Brumme, M. Sinclair, T. Miura, J. Frater, M. Essex, R. Shapiro, B.D. Walker, T. Ndung'u, A.R. McLean, J.M. Carlson, and P.J. Goulder. **2014**. Impact of HLA-driven HIV adaptation on virulence in populations of high HIV seroprevalence. *Proc Natl Acad Sci U S A* 111:E5393-5400.

Payne, R.P., H. Kloverpris, J.B. Sacha, Z. Brumme, C. Brumme, S. Buus, S. Sims, S. Hickling, L. Riddell, F. Chen, G. Luzzi, A. Edwards, R. Phillips, J.G. Prado, and P.J. Goulder. **2010**. Efficacious early antiviral activity of HIV Gag- and Pol-specific HLA-B 2705-restricted CD8+ T cells. *J Virol* 84:10543-10557.

Penaloza-MacMaster, P., D. Masopust, and R. Ahmed. **2009**. T-cell reconstitution without T-cell immunopathology in two models of T-cell-mediated tissue destruction. *Immunology* 128:164-171.

Pereyra, F., M.M. Addo, D.E. Kaufmann, Y. Liu, T. Miura, A. Rathod, B. Baker, A. Trocha, R. Rosenberg, E. Mackey, P. Ueda, Z. Lu, D. Cohen, T. Wrin, C.J. Petropoulos, E.S. Rosenberg, and B.D. Walker. **2008**. Genetic and immunologic heterogeneity among persons who control HIV infection in the absence of therapy. *J. Infect. Dis.* 197:563-571.

Pereyra, F., X. Jia, P.J. McLaren, A. Telenti, P.I. de Bakker, B.D. Walker, S. Ripke, C.J. Brumme, S.L. Pulit, M. Carrington, C.M. Kadie, J.M. Carlson, D. Heckerman, R.R. Graham, R.M. Plenge, S.G. Deeks, L. Gianniny, G. Crawford, J. Sullivan, E. Gonzalez, L. Davies, A. Camargo, J.M. Moore, N. Beattie, S. Gupta, A. Crenshaw, N.P. Burtt, C. Guiducci, N. Gupta, X. Gao, Y. Qi, Y. Yuki, A. Piechocka-Trocha, E. Cutrell, R. Rosenberg, K.L. Moss, P. Lemay, J. O'Leary, T. Schaefer, P. Verma, I. Toth, B. Block, B. Baker, A. Rothchild, J. Lian, J. Proudfoot, D.M. Alvino, S. Vine, M.M. Addo, T.M. Allen, M. Altfeld, M.R. Henn, S. Le Gall, H. Streeck, D.W. Haas, D.R. Kuritzkes, G.K. Robbins, R.W. Shafer, R.M. Gulick, C.M. Shikuma, R. Haubrich, S. Riddler, P.E. Sax, E.S. Daar, H.J. Ribaudo, B. Agan, S. Agarwal, R.L. Ahern, B.L. Allen, S. Altidor, E.L. Altschuler, S. Ambardar, K. Anastos, B. Anderson, V. Anderson, U. Andrady, D. Antoniskis, D. Bangsberg, D. Barbaro, W. Barrie, J. Bartczak, S. Barton, P. Basden, N. Basgoz, S. Bazner, N.C. Bellos, A.M. Benson, J. Berger, N.F. Bernard, A.M. Bernard, C. Birch, S.J. Bodner, R.K. Bolan, E.T. Boudreaux, M. Bradley, J.F. Braun, J.E. Brndjar, S.J. Brown, K. Brown, S.T. Brown, J. Burack, L.M. Bush, V. Cafaro, O. Campbell, J. Campbell, R.H. Carlson, J.K. Carmichael, K.K. Casey, C. Cavacuiti, G. Celestin, S.T. Chambers, N. Chez, L.M. Chirch, P.J. Cimoch, D. Cohen, L.E. Cohn, B. Conway, D.A. Cooper, B. Cornelson, D.T. Cox, M.V. Cristofano, G. Cuchural,

Jr., J.L. Czartoski, J.M. Dahman, J.S. Daly, B.T. Davis, K. Davis, S.M. Davod, E. DeJesus, C.A. Dietz, E. Dunham, M.E. Dunn, T.B. Ellerin, J.J. Eron, J.J. Fangman, C.E. Farel, H. Ferlazzo, S. Fidler, A. Fleenor-Ford, R. Frankel, K.A. Freedberg, N.K. French, J.D. Fuchs, J.D. Fuller, J. Gaberman, J.E. Gallant, R.T. Gandhi, E. Garcia, D. Garmon, J.C. Gathe, Jr., C.R. Gaultier, W. Gebre, F.D. Gilman, I. Gilson, P.A. Goepfert, M.S. Gottlieb, C. Goulston, R.K. Groger, T.D. Gurley, S. Haber, R. Hardwicke, W.D. Hardy, P.R. Harrigan, T.N. Hawkins, S. Heath, F.M. Hecht, W.K. Henry, M. Hladek, R.P. Hoffman, J.M. Horton, R.K. Hsu, G.D. Huhn, P. Hunt, M.J. Hupert, M.L. Illeman, H. Jaeger, R.M. Jellinger, M. John, J.A. Johnson, K.L. Johnson, H. Johnson, K. Johnson, J. Joly, W.C. Jordan, C.A. Kauffman, H. Khanlou, R.K. Killian, A.Y. Kim, D.D. Kim, C.A. Kinder, J.T. Kirchner, L. Kogelman, E.M. Kojic, P.T. Korthuis, W. Kurisu, D.S. Kwon, M. LaMar, H. Lampiris, M. Lanzafame, M.M. Lederman, D.M. Lee, J.M. Lee, M.J. Lee, E.T. Lee, J. Lemoine, J.A. Levy, J.M. Llibre, M.A. Liguori, S.J. Little, A.Y. Liu, A.J. Lopez, M.R. Loutfy, D. Loy, D.Y. Mohammed, A. Man, M.K. Mansour, V.C. Marconi, M. Markowitz, R. Marques, J.N. Martin, H.L. Martin, Jr., K.H. Mayer, M.J. McElrath, T.A. McGhee, B.H. McGovern, K. McGowan, D. McIntyre, G.X. McLeod, P. Menezes, G. Mesa, C.E. Metroka, D. Meyer-Olson, A.O. Miller, K. Montgomery, K.C. Mounzer, E.H. Nagami, I. Nagin, R.G. Nahass, M.O. Nelson, C. Nielsen, D.L. Norene, D.H. O'Connor, B.O. Ojikutu, J. Okulicz, O.O. Oladehin, E.C. Oldfield, 3rd, S.A. Olender, M. Ostrowski, W.F. Owen, Jr., E. Pae, J. Parsonnet, A.M. Pavlatos, A.M. Perlmutter, M.N. Pierce, J.M. Pincus, L. Pisani, L.J. Price, L. Proia, R.C. Prokesch, H.C. Pujet, M. Ramgopal, A. Rathod, M. Rausch, J. Ravishankar, F.S. Rhame, C.S. Richards, D.D. Richman, B. Rodes, M. Rodriguez, R.C. Rose, 3rd, E.S. Rosenberg, D. Rosenthal, P.E. Ross, D.S. Rubin, E. Rumbaugh, L. Saenz, M.R. Salvaggio, W.C. Sanchez, V.M. Sanjana, S. Santiago, W. Schmidt, H. Schuitemaker, P.M. Sestak, P. Shalit, W. Shay, V.N. Shirvani, V.I. Silebi, J.M. Sizemore, Jr., P.R. Skolnik, M. Sokol-Anderson, J.M. Sosman, P. Stabile, J.T. Stapleton, S. Starrett, F. Stein, H.J. Stellbrink, F.L. Sterman, V.E. Stone, D.R. Stone, G. Tambussi, R.A. Taplitz, E.M. Tedaldi, A. Telenti, W. Theisen, R. Torres, L. Tosiello, C. Tremblay, M.A. Tribble, P.D. Trinh, A. Tsao, P. Ueda, A. Vaccaro, E. Valadas, T.J. Vanig, I. Vecino, V.M. Vega, W. Veikley, B.H. Wade, C. Walworth, C. Wanidworanun, D.J. Ward, D.A. Warner, R.D. Weber, D. Webster, S. Weis, D.A. Wheeler, D.J. White, E. Wilkins, A. Winston, C.G. Wlodaver, A. van't Wout, D.P. Wright, O.O. Yang, D.L. Yurdin, B.W. Zabukovic, K.C. Zachary, B. Zeeman, and M. Zhao. **2010**. The major genetic determinants of HIV-1 control affect HLA class I peptide presentation. *Science* 330:1551-1557.

Persaud, D., H. Gay, C. Ziemniak, Y.H. Chen, M. Piatak, Jr., T.W. Chun, M. Strain, D. Richman, and K. Luzuriaga. **2013**. Absence of detectable HIV-1 viremia after treatment cessation in an infant. *N. Engl. J. Med.* 369:1828-1835.

Persaud, D., P.E. Palumbo, C. Ziemniak, M.D. Hughes, C.G. Alvero, K. Luzuriaga, R. Yogev, E.V. Capparelli, and E.G. Chadwick. **2012**. Dynamics of the resting CD4(+) T-cell latent HIV reservoir in infants initiating HAART less than 6 months of age. *AIDS* 26:1483-1490.

Phair, J., L. Jacobson, R. Detels, C. Rinaldo, A. Saah, L. Schrager, and A. Munoz. **1992**. Acquired immune deficiency syndrome occurring within 5 years of infection

with human immunodeficiency virus type-1: the Multicenter AIDS Cohort Study. *J Acquir Immune Defic Syndr* 5:490-496.

Phillips, R.E., S. Rowland-Jones, D.F. Nixon, F.M. Gotch, J.P. Edwards, A.O. Ogunlesi, J.G. Elvin, J.A. Rothbard, C.R. Bangham, C.R. Rizza, and A.J. McMichael. **1991**. Human immunodeficiency virus genetic variation that can escape cytotoxic T cell recognition. *Nature* 354:453-459.

Pillay, T., H.T. Zhang, J.W. Drijfhout, N. Robinson, H. Brown, M. Khan, J. Moodley, M. Adhikari, K. Pfafferott, M.E. Feeney, A. St John, E.C. Holmes, H.M. Coovadia, P. Klenerman, P.J. Goulder, and R.E. Phillips. **2005**. Unique acquisition of cytotoxic T-lymphocyte escape mutants in infant human immunodeficiency virus type 1 infection. *J Virol* 79:12100-12105.

Plantier, J.C., M. Leoz, J.E. Dickerson, F. De Oliveira, F. Cordonnier, V. Lemee, F. Damond, D.L. Robertson, and F. Simon. **2011**. A new human immunodeficiency virus derived from gorillas. *Nature Med.* 15:871-872.

Pollack, H., M.X. Zhan, J.T. Safrit, S.H. Chen, G. Rochford, P.Z. Tao, R. Koup, K. Krasinski, and W. Borkowsky. **1997**. CD8+ T-cell-mediated suppression of HIV replication in the first year of life: association with lower viral load and favorable early survival. *AIDS* 11:F9-13.

Pollard, V.W., and M.H. Malim. **1998**. The HIV-1 Rev protein. *Annu Rev Microbiol* 52:491-532.

Popovic, M., M.G. Sarngadharan, E. Read, and R.C. Gallo. **1984**. Detection, isolation, and continuous production of cytopathic retroviruses (HTLV-III) from patients with AIDS and pre-AIDS. *Science* 224:497-500.

Prado, J.G., A. Prendergast, C. Thobakgale, C. Molina, G. Tudor-Williams, T. Ndung'u, B.D. Walker, and P. Goulder. **2010**. Replicative capacity of human immunodeficiency virus type 1 transmitted from mother to child is associated with pediatric disease progression rate. *J Virol* 84:492-502.

Prendergast, A. 2008. Randomised, controlled trial of 3 approaches to management of HIV-infected infants. In 15th Conference on Retroviruses and Opportunistic Infections, 2008. Boston, MA, USA.

Prendergast, A., H. Goodliffe, M. Clapson, R. Cross, G. Tudor-Williams, A. Riddell, J. Daniels, A. Williams, and P. Goulder. **2011**. Gag-specific CD4+ T-cell responses are associated with virological control of paediatric HIV-1 infection. *AIDS* 25:1329-1331.

Prendergast, A., W. Mphatswe, G. Tudor-Williams, M. Rakgotho, V. Pillay, C. Thobakgale, N. McCarthy, L. Morris, B.D. Walker, and P. Goulder. **2008**. Early virological suppression with three-class antiretroviral therapy in HIV-infected African infants. *AIDS* 22:1333-1343.

Procopio, F.A., R. Fromentin, D.A. Kulpa, J.H. Brehm, A.G. Bebin, M.C. Strain, D.D. Richman, U. O'Doherty, S. Palmer, F.M. Hecht, R. Hoh, R.J. Barnard, M.D.

Miller, D.J. Hazuda, S.G. Deeks, R.P. Sekaly, and N. Chomont. **2015**. A Novel Assay to Measure the Magnitude of the Inducible Viral Reservoir in HIV-infected Individuals. *EBioMedicine* 2:872-881.

Qin, M., S. Brummel, K.K. Singh, T. Fenton, and S.A. Spector. **2014**. Associations of host genetic variants on CD4(+) lymphocyte count and plasma HIV-1 RNA in antiretroviral naive children. *Pediatr Infect Dis J* 33:946-952.

Radebe, M., K. Gounder, M. Mokgoro, Z.M. Ndhlovu, Z. Mncube, L. Mkhize, M. van der Stok, M. Jaggernath, B.D. Walker, and T. Ndung'u. **2015**. Broad and persistent Gag-specific CD8+ T-cell responses are associated with viral control but rarely drive viral escape during primary HIV-1 infection. *AIDS* 29:23-33.

Rey-Cuille, M.A., J.L. Berthier, M.C. Bomsel-Demontoy, Y. Chaduc, L. Montagnier, A.G. Hovanessian, and L.A. Chakrabarti. **1998**. Simian immunodeficiency virus replicates to high levels in sooty mangabeys without inducing disease. *J Virol* 72:3872-3886.

Riviere, Y., M.B. McChesney, F. Porrot, F. Tanneau-Salvadori, P. Sansonetti, O. Lopez, G. Pialoux, V. Feuillie, M. Mollereau, S. Chamaret, F. Tekaja, and L. Montagnier. **1995**. Gag-specific cytotoxic responses to HIV type 1 are associated with a decreased risk of progression to AIDS-related complex or AIDS. *AIDS Res Hum Retroviruses* 11:903-907.

Rizvi, N.A., J. Mazieres, D. Planchard, T.E. Stinchcombe, G.K. Dy, S.J. Antonia, L. Horn, H. Lena, E. Minenza, B. Mennecier, G.A. Otterson, L.T. Campos, D.R. Gandara, B.P. Levy, S.G. Nair, G. Zalcman, J. Wolf, P.J. Souquet, E. Baldini, F. Cappuzzo, C. Chouaid, A. Dowlati, R. Sanborn, A. Lopez-Chavez, C. Grohe, R.M. Huber, C.T. Harbison, C. Baudelet, B.J. Lestini, and S.S. Ramalingam. **2015**. Activity and safety of nivolumab, an anti-PD-1 immune checkpoint inhibitor, for patients with advanced, refractory squamous non-small-cell lung cancer (CheckMate 063): a phase 2, single-arm trial. *Lancet Oncol* 16:257-265.

Robertson, D.L., J.P. Anderson, J.A. Bradac, J.K. Carr, B. Foley, R.K. Funkhouser, F. Gao, B.H. Hahn, M.L. Kalish, C. Kuiken, G.H. Learn, T. Leitner, F. McCutchan, S. Osmanov, M. Peeters, D. Pieniazek, M. Salminen, P.M. Sharp, S. Wolinsky, and B. Korber. **2000**. HIV-1 nomenclature proposal. *Science* 288:55-56.

Rotger, M., J. Dalmau, A. Rauch, P. McLaren, S.E. Bosinger, R. Martinez, N.G. Sandler, A. Roque, J. Liebner, M. Battegay, E. Bernasconi, P. Descombes, I. Erkizia, J. Fellay, B. Hirschel, J.M. Miro, E. Palou, M. Hoffmann, M. Massanella, J. Blanco, M. Woods, H.F. Gunthard, P. de Bakker, D.C. Douek, G. Silvestri, J. Martinez-Picado, and A. Telenti. **2011**. Comparative transcriptomics of extreme phenotypes of human HIV-1 infection and SIV infection in sooty mangabey and rhesus macaque. *J Clin Invest* 121:2391-2400.

Sacha, J.B., C. Chung, E.G. Rakasz, S.P. Spencer, A.K. Jonas, A.T. Bean, W. Lee, B.J. Burwitz, J.J. Stephany, J.T. Loffredo, D.B. Allison, S. Adnan, A. Hoji, N.A. Wilson, T.C. Friedrich, J.D. Lifson, O.O. Yang, and D.I. Watkins. **2007a**. Gag-specific CD8+ T lymphocytes recognize infected cells before AIDS-virus integration and viral protein expression. *J Immunol* 178:2746-2754.

Sacha, J.B., C. Chung, J. Reed, A.K. Jonas, A.T. Bean, S.P. Spencer, W. Lee, L. Vojnov, R. Rudersdorf, T.C. Friedrich, N.A. Wilson, J.D. Lifson, and D.I. Watkins. **2007b**. Pol-specific CD8+ T cells recognize simian immunodeficiency virus-infected cells prior to Nef-mediated major histocompatibility complex class I downregulation. *J Virol* 81:11703-11712.

Saez-Cirion, A., C. Bacchus, L. Hocqueloux, V. Avettand-Fenoel, I. Girault, C. Lecuroux, V. Potard, P. Versmisse, A. Melard, T. Prazuck, B. Descours, J. Guergnon, J.P. Viard, F. Boufassa, O. Lambotte, C. Goujard, L. Meyer, D. Costagliola, A. Venet, G. Pancino, B. Autran, and C. Rouzioux. **2013**. Post-treatment HIV-1 controllers with a long-term virological remission after the interruption of early initiated antiretroviral therapy ANRS VISCONTI Study. *PLoS Pathog* 9:e1003211.

Saez-Cirion, A., C. Lacabaratz, O. Lambotte, P. Versmisse, A. Urrutia, F. Boufassa, F. Barre-Sinoussi, J.F. Delfraissy, M. Sinet, G. Pancino, and A. Venet. **2007**. HIV controllers exhibit potent CD8 T cell capacity to suppress HIV infection ex vivo and peculiar cytotoxic T lymphocyte activation phenotype. *Proc Natl Acad Sci U S A* 104:6776-6781.

Saez-Cirion, A., S.Y. Shin, P. Versmisse, F. Barre-Sinoussi, and G. Pancino. **2010**. Ex vivo T cell-based HIV suppression assay to evaluate HIV-specific CD8+ T-cell responses. *Nat Protoc* 5:1033-1041.

Saez-Cirion, A., M. Sinet, S.Y. Shin, A. Urrutia, P. Versmisse, C. Lacabaratz, F. Boufassa, V. Avettand-Fenoel, C. Rouzioux, J.F. Delfraissy, F. Barre-Sinoussi, O. Lambotte, A. Venet, and G. Pancino. **2009**. Heterogeneity in HIV suppression by CD8 T cells from HIV controllers: association with Gag-specific CD8 T cell responses. *J Immunol* 182:7828-7837.

Salter, R.D., D.N. Howell, and P. Cresswell. **1985**. Genes regulating HLA class I antigen expression in T-B lymphoblast hybrids. *Immunogenetics* 21:235-246.

Sanchez-Merino, V., S. Nie, and K. Luzuriaga. **2005**. HIV-1-specific CD8+ T cell responses and viral evolution in women and infants. *J Immunol* 175:6976-6986.

Saper, M.A., P.J. Bjorkman, and D.C. Wiley. **1991**. Refined structure of the human histocompatibility antigen HLA-A2 at 2.6 A resolution. *J Mol Biol* 219:277-319.

Schmid, A., S. Gianella, V. von Wyl, K.J. Metzner, A.U. Scherrer, B. Niederost, C.F. Althaus, P. Rieder, C. Grube, B. Joos, R. Weber, M. Fischer, and H.F. Gunthard. **2010**. Profound depletion of HIV-1 transcription in patients initiating antiretroviral therapy during acute infection. *PLoS One* 5:e13310.

Schmitz, J.E., M.J. Kuroda, S. Santra, V.G. Sasseville, M.A. Simon, M.A. Lifton, P. Racz, K. Tenner-Racz, M. Dalesandro, B.J. Scallon, J. Ghrayeb, M.A. Forman, D.C. Montefiori, E.P. Rieber, N.L. Letvin, and K.A. Reimann. **1999**. Control of viremia in simian immunodeficiency virus infection by CD8+ lymphocytes. *Science* 283:857-860.

Schneidewind, A., M.A. Brockman, R. Yang, R.I. Adam, B. Li, S. Le Gall, C.R. Rinaldo, S.L. Craggs, R.L. Allgaier, K.A. Power, T. Kuntzen, C.S. Tung, M.X. LaBute, S.M. Mueller, T. Harrer, A.J. McMichael, P.J. Goulder, C. Aiken, C. Brander, A.D. Kelleher, and T.M. Allen. **2007**. Escape from the dominant HLA-B27-restricted cytotoxic T-lymphocyte response in Gag is associated with a dramatic reduction in human immunodeficiency virus type 1 replication. *J Virol* 81:12382-12393.

Schoeni-Affolter, F., B. Ledergerber, M. Rickenbach, C. Rudin, H.F. Gunthard, A. Telenti, H. Furrer, S. Yerly, and P. Francioli. **2010**. Cohort profile: the Swiss HIV Cohort study. *Int J Epidemiol* 39:1179-1189.

Schutz, C., M. Oelke, J.P. Schneck, A. Mackensen, and M. Fleck. **2010**. Killer artificial antigen-presenting cells: the synthetic embodiment of a 'guided missile'. *Immunotherapy* 2:539-550.

Scott, Z.A., E.G. Chadwick, L.L. Gibson, M.D. Catalina, M.M. McManus, R. Yogev, P. Palumbo, J.L. Sullivan, P. Britto, H. Gay, and K. Luzuriaga. **2001**. Infrequent detection of HIV-1-specific, but not cytomegalovirus-specific, CD8(+) T cell responses in young HIV-1-infected infants. *J Immunol* 167:7134-7140.

Seage, G.R., 3rd, E. Losina, S.J. Goldie, A.D. Paltiel, A.D. Kimmel, and K.A. Freedberg. **2002**. The relationship of preventable opportunistic infections, HIV-1 RNA, and CD4 Cell counts to chronic mortality. *J Acquir Immune Defic Syndr* 30:421-428.

Shalekoff, S., S. Meddows-Taylor, G.E. Gray, G.G. Sherman, A.H. Coovadia, L. Kuhn, and C.T. Tiemessen. **2009**. Identification of human immunodeficiency virus-1 specific CD8+ and CD4+ T cell responses in perinatally-infected infants and their mothers. *AIDS* 23:789-798.

Shan, L., K. Deng, N.S. Shroff, C.M. Durand, S.A. Rabi, H.C. Yang, H. Zhang, J.B. Margolick, J.N. Blankson, and R.F. Siliciano. **2012**. Stimulation of HIV-1-specific cytolytic T lymphocytes facilitates elimination of latent viral reservoir after virus reactivation. *Immunity* 36:491-501.

Shaw, K.T., A.M. Ho, A. Raghavan, J. Kim, J. Jain, J. Park, S. Sharma, A. Rao, and P.G. Hogan. **1995**. Immunosuppressive drugs prevent a rapid dephosphorylation of transcription factor NFAT1 in stimulated immune cells. *Proc Natl Acad Sci U S A* 92:11205-11209.

Shearer, W.T., H.M. Rosenblatt, R.S. Gelman, R. Oyomopito, S. Plaeger, E.R. Stiehm, D.W. Wara, S.D. Douglas, K. Luzuriaga, E.J. McFarland, R. Yogev, M.H. Rathore, W. Levy, B.L. Graham, and S.A. Spector. **2003**. Lymphocyte subsets in healthy children from birth through 18 years of age: the Pediatric AIDS Clinical Trials Group P1009 study. *J. Allergy Clin. Immunol.* 112:973-980.

Shepherd, B.E., P.B. Gilbert, Y. Jemiai, and A. Rotnitzky. **2006**. Sensitivity analyses comparing outcomes only existing in a subset selected post-randomization, conditional on covariates, with application to HIV vaccine trials. *Biometrics* 62:332-342.

Siliciano, J.D., J. Kajdas, D. Finzi, T.C. Quinn, K. Chadwick, J.B. Margolick, C. Kovacs, S.J. Gange, and R.F. Siliciano. **2003**. Long-term follow-up studies confirm the stability of the latent reservoir for HIV-1 in resting CD4+ T cells. *Nature Med.* 9:727-728.

Siliciano, R.F., and W.C. Greene. **2011**. HIV latency. *Cold Spring Harb Perspect Med* 1:a007096.

Silvestri, G., A. Fedanov, S. Germon, N. Kozyr, W.J. Kaiser, D.A. Garber, H. McClure, M.B. Feinberg, and S.I. Staprans. **2005**. Divergent host responses during primary simian immunodeficiency virus SIVsm infection of natural sooty mangabey and nonnatural rhesus macaque hosts. *J Virol* 79:4043-4054.

Silvestri, G., D.L. Sodora, R.A. Koup, M. Paiardini, S.P. O'Neil, H.M. McClure, S.I. Staprans, and M.B. Feinberg. **2003**. Nonpathogenic SIV infection of sooty mangabeys is characterized by limited bystander immunopathology despite chronic high-level viremia. *Immunity* 18:441-452.

Silvestri, S. 2015. Animal Models of HIV Prevention and Cure. In CROI. Seattle, WA, USA.

Sims, S., C. Willberg, and P. Klenerman. **2010**. MHC-peptide tetramers for the analysis of antigen-specific T cells. *Expert Rev Vaccines* 9:765-774.

Singh, K.K., P.K. Gray, Y. Wang, T. Fenton, R.N. Trout, and S.A. Spector. **2011**. HLA alleles are associated with altered risk for disease progression and central nervous system impairment of HIV-infected children. *J Acquir Immune Defic Syndr* 57:32-39.

Smith, M.W., M. Dean, M. Carrington, C. Winkler, G.A. Huttley, D.A. Lomb, J.J. Goedert, T.R. O'Brien, L.P. Jacobson, R. Kaslow, S. Buchbinder, E. Vittinghoff, D. Vlahov, K. Hoots, M.W. Hilgartner, and S.J. O'Brien. **1997**. Contrasting genetic influence of CCR2 and CCR5 variants on HIV-1 infection and disease progression. Hemophilia Growth and Development Study (HGDS), Multicenter AIDS Cohort Study (MACS), Multicenter Hemophilia Cohort Study (MHCS), San Francisco City Cohort (SFCC), ALIVE Study. *Science* 277:959-965.

Sperling, R.S., D.E. Shapiro, R.W. Coombs, J.A. Todd, S.A. Herman, G.D. McSherry, M.J. O'Sullivan, R.B. Van Dyke, E. Jimenez, C. Rouzioux, P.M. Flynn, and J.L. Sullivan. **1996**. Maternal viral load, zidovudine treatment, and the risk of transmission of human immunodeficiency virus type 1 from mother to infant. Pediatric AIDS Clinical Trials Group Protocol 076 Study Group. *N. Engl. J. Med.* 335:1621-1629.

Spivak, A.M., A. Bosque, A.H. Balch, D. Smyth, L. Martins, and V. Planelles. **2015**. Ex Vivo Bioactivity and HIV-1 Latency Reversal by Ingenol Dibenzoate and Panobinostat in Resting CD4+ T Cells from Aviremic Patients. *Antimicrob Agents Chemother* 59:5984-5991.

Streeck, H., M. Lichterfeld, G. Alter, A. Meier, N. Teigen, B. Yassine-Diab, H.K. Sidhu, S. Little, A. Kelleher, J.P. Routy, E.S. Rosenberg, R.P. Sekaly, B.D. Walker,

and M. Altfeld. **2007**. Recognition of a defined region within p24 gag by CD8+ T cells during primary human immunodeficiency virus type 1 infection in individuals expressing protective HLA class I alleles. *J Virol* 81:7725-7731.

Streeck, H., R. Lu, N. Beckwith, M. Milazzo, M. Liu, J.P. Routy, S. Little, H. Jessen, A.D. Kelleher, F. Hecht, R.P. Sekaly, G. Alter, D. Heckerman, M. Carrington, E.S. Rosenberg, and M. Altfeld. **2014**. Emergence of individual HIV-specific CD8 T cell responses during primary HIV-1 infection can determine long-term disease outcome. *J Virol* 88:12793-12801.

Surh, C.D., and J. Sprent. **2008**. Homeostasis of naive and memory T cells. *Immunity* 29:848-862.

Takahata, Y., A. Nomura, H. Takada, S. Ohga, K. Furuno, S. Hikino, H. Nakayama, S. Sakaguchi, and T. Hara. **2004**. CD25+CD4+ T cells in human cord blood: an immunoregulatory subset with naive phenotype and specific expression of forkhead box p3 (Foxp3) gene. *Exp. Hematol.* 32:622-629.

Tchakoute, C.T., A.C. Hesseling, E.B. Kidzeru, H. Gamieldien, J.A. Passmore, C.E. Jones, C.M. Gray, D.L. Sodora, and H.B. Jaspan. **2015**. Delaying BCG vaccination until 8 weeks of age results in robust BCG-specific T-cell responses in HIV-exposed infants. *J. Infect. Dis.* 211:338-346.

Tebas, P., D. Stein, W.W. Tang, I. Frank, S.Q. Wang, G. Lee, S.K. Spratt, R.T. Surosky, M.A. Giedlin, G. Nichol, M.C. Holmes, P.D. Gregory, D.G. Ando, M. Kalos, R.G. Collman, G. Binder-Scholl, G. Plesa, W.T. Hwang, B.L. Levine, and C.H. June. **2014**. Gene editing of CCR5 in autologous CD4 T cells of persons infected with HIV. *N. Engl. J. Med.* 370:901-910.

Thobakgale, C.F., A. Prendergast, H. Crawford, N. Mkhwanazi, D. Ramduth, S. Reddy, C. Molina, Z. Mncube, A. Leslie, J. Prado, F. Chonco, W. Mphatshwe, G. Tudor-Williams, P. Jeena, N. Blanckenberg, K. Dong, P. Kiepiela, H. Coovadia, T. Ndung'u, B.D. Walker, and P.J. Goulder. **2009**. Impact of HLA in mother and child on disease progression of pediatric human immunodeficiency virus type 1 infection. *J Virol* 83:10234-10244.

Thobakgale, C.F., D. Ramduth, S. Reddy, N. Mkhwanazi, C. de Pierres, E. Moodley, W. Mphatswe, N. Blanckenberg, A. Cengimbo, A. Prendergast, G. Tudor-Williams, K. Dong, P. Jeena, G. Kindra, R. Bobat, H. Coovadia, P. Kiepiela, B.D. Walker, and P.J. Goulder. **2007**. Human immunodeficiency virus-specific CD8+ T-cell activity is detectable from birth in the majority of in utero-infected infants. *J. Virol.* 81:12775-12784.

Topalian, S.L., F.S. Hodi, J.R. Brahmer, S.N. Gettinger, D.C. Smith, D.F. McDermott, J.D. Powderly, R.D. Carvajal, J.A. Sosman, M.B. Atkins, P.D. Leming, D.R. Spigel, S.J. Antonia, L. Horn, C.G. Drake, D.M. Pardoll, L. Chen, W.H. Sharfman, R.A. Anders, J.M. Taube, T.L. McMiller, H. Xu, A.J. Korman, M. Jure-Kunkel, S. Agrawal, D. McDonald, G.D. Kollia, A. Gupta, J.M. Wigginton, and M. Sznol. **2012**. Safety, activity, and immune correlates of anti-PD-1 antibody in cancer. *N Engl J Med* 366:2443-2454.

Troyer, R.M., J. McNevin, Y. Liu, S.C. Zhang, R.W. Krizan, A. Abraha, D.M. Tebit, H. Zhao, S. Avila, M.A. Lobritz, M.J. McElrath, S. Le Gall, J.I. Mullins, and E.J. Arts. **2009**. Variable fitness impact of HIV-1 escape mutations to cytotoxic T lymphocyte (CTL) response. *PLoS Pathog* 5:e1000365.

Tumeh, P.C., C.L. Harview, J.H. Yearley, I.P. Shintaku, E.J. Taylor, L. Robert, B. Chmielowski, M. Spasic, G. Henry, V. Ciobanu, A.N. West, M. Carmona, C. Kivork, E. Seja, G. Cherry, A.J. Gutierrez, T.R. Grogan, C. Mateus, G. Tomasic, J.A. Glaspy, R.O. Emerson, H. Robins, R.H. Pierce, D.A. Elashoff, C. Robert, and A. Ribas. **2014**. PD-1 blockade induces responses by inhibiting adaptive immune resistance. *Nature* 515:568-571.

Upham, J.W., P.T. Lee, B.J. Holt, T. Heaton, S.L. Prescott, M.J. Sharp, P.D. Sly, and P.G. Holt. **2002**. Development of interleukin-12-producing capacity throughout childhood. *Infect. Immun.* 70:6583-6588.

Valentine, L.E., J.T. Loffredo, A.T. Bean, E.J. Leon, C.E. MacNair, D.R. Beal, S.M. Piaskowski, Y.C. Klimentidis, S.M. Lank, R.W. Wiseman, J.T. Weinfurter, G.E. May, E.G. Rakasz, N.A. Wilson, T.C. Friedrich, D.H. O'Connor, D.B. Allison, and D.I. Watkins. **2009**. Infection with "escaped" virus variants impairs control of simian immunodeficiency virus SIVmac239 replication in Mamu-B*08-positive macaques. *J Virol* 83:11514-11527.

Vallari, A., V. Holzmayer, B. Harris, J. Yamaguchi, C. Ngansop, F. Makamche, D. Mbanya, L. Kaptue, N. Ndembi, L. Gurtler, S. Devare, and C.A. Brennan. **2011**. Confirmation of putative HIV-1 group P in Cameroon. *J Virol* 85:1403-1407.

van Bockel, D.J., D.A. Price, M.L. Munier, V. Venturi, T.E. Asher, K. Ladell, H.Y. Greenaway, J. Zaunders, D.C. Douek, D.A. Cooper, M.P. Davenport, and A.D. Kelleher. **2011**. Persistent survival of prevalent clonotypes within an immunodominant HIV gag-specific CD8+ T cell response. *J Immunol* 186:359-371.

van Lier, R.A., I.J. ten Berge, and L.E. Gamadia. **2003**. Human CD8(+) T-cell differentiation in response to viruses. *Nat Rev Immunol* 3:931-939.

van Zyl, G.U., M.A. Bedison, A.J. van Rensburg, B. Laughton, M.F. Cotton, and J.W. Mellors. **2015**. Early Antiretroviral Therapy in South African Children Reduces HIV-1-Infected Cells and Cell-Associated HIV-1 RNA in Blood Mononuclear Cells. *J. Infect. Dis.* 212:39-43.

Vigano, A., D. Trabattoni, L. Schneider, F. Ottaviani, A. Aliffi, E. Longhi, S. Rusconi, and M. Clerici. **2006**. Failure to eradicate HIV despite fully successful HAART initiated in the first days of life. *J. Pediatr.* 148:389-391.

Vince, N., A.A. Bashirova, A. Lied, X. Gao, L. Dorrell, P.J. McLaren, J. Fellay, and M. Carrington. **2014**. HLA class I and KIR genes do not protect against HIV type 1 infection in highly exposed uninfected individuals with hemophilia A. *J Infect Dis* 210:1047-1051.

Vincent, B.G., E.F. Young, A.S. Buntzman, R. Stevens, T.B. Kepler, R.M. Tisch, J.A. Frelinger, and P.R. Hess. **2010**. Toxin-coupled MHC class I tetramers can

specifically ablate autoreactive CD8+ T cells and delay diabetes in nonobese diabetic mice. *J Immunol* 184:4196-4204.

Wagner, R., B. Leschonsky, E. Harrer, C. Paulus, C. Weber, B.D. Walker, S. Buchbinder, H. Wolf, J.R. Kalden, and T. Harrer. **1999**. Molecular and functional analysis of a conserved CTL epitope in HIV-1 p24 recognized from a long-term nonprogressor: constraints on immune escape associated with targeting a sequence essential for viral replication. *J Immunol* 162:3727-3734.

Walker, B., C. Flexner, T.J. Paradis, T.C. Fuller, M.S. Hirsch, R.T. Schooley, and B. Moss. **1988**. HIV-1 reverse transcriptase is a target for cytotoxic T lymphocytes in infected individuals. *Science* 240:64-66.

Walker, B.D. 2016. T-cell control of HIV: Implications for vaccines and cure. Bernard Fields Lecture. In Conference on Retroviruses and Opportunistic Infections 2016. Boston, MA, USA.

Walker, B.D., S. Chakrabarti, B. Moss, T.J. Paradis, T. Flynn, A.G. Durno, R.S. Blumberg, J.C. Kaplan, M.S. Hirsch, and R.T. Schooley. **1987**. HIV-specific cytotoxic T lymphocytes in seropositive individuals. *Nature* 328:345-348.

Wallet, M.A., C.A. Rodriguez, L. Yin, S. Saporta, S. Chinratanapisit, W. Hou, J.W. Sleasman, and M.M. Goodenow. **2010**. Microbial translocation induces persistent macrophage activation unrelated to HIV-1 levels or T-cell activation following therapy. *AIDS* 24:1281-1290.

Weiss, S.H., D.L. Mann, C. Murray, and M. Popovic. **1985**. HLA-DR antibodies and HTLV-III antibody ELISA testing. *Lancet* 2:157.

Whelan, J.A., P.R. Dunbar, D.A. Price, M.A. Purbhoo, F. Lechner, G.S. Ogg, G. Griffiths, R.E. Phillips, V. Cerundolo, and A.K. Sewell. **1999**. Specificity of CTL interactions with peptide-MHC class I tetrameric complexes is temperature dependent. *J Immunol* 163:4342-4348.

Wherry, E.J., and M. Kurachi. **2015**. Molecular and cellular insights into T cell exhaustion. *Nat Rev Immunol* 15:486-499.

Whitney, J.B., A.L. Hill, S. Sanisetty, P. Penaloza-MacMaster, J. Liu, M. Shetty, L. Parenteau, C. Cabral, J. Shields, S. Blackmore, J.Y. Smith, A.L. Brinkman, L.E. Peter, S.I. Mathew, K.M. Smith, E.N. Borducchi, D.I. Rosenbloom, M.G. Lewis, J. Hattersley, B. Li, J. Hesselgesser, R. Geleziunas, M.L. Robb, J.H. Kim, N.L. Michael, and D.H. Barouch. **2014**. Rapid seeding of the viral reservoir prior to SIV viraemia in rhesus monkeys. *Nature* 512:74-77.

WHO. 2008. HIV/AIDS Programme. Antiretroviral therapy for HIV infection in adults and adolescents: recommendations for a public health approach. 2006 revision. In.

WHO. 2015a. Core Epidemiology Slides. July 2015. In http://www.who.int/hiv/data/en/. Accessed on 16 March 2016.

WHO. 2015b. Guideline on when to start antiretroviral therapy and on pre-exposure prophylaxis for HIV. September 2015 early release. Available at: http://apps.who.int/iris/bitstream/10665/186275/1/9789241509565_eng.pdf?ua=1. Accessed on 24 February, 2016. In.

Wong, J.T., and R.B. Colvin. **1987**. Bi-specific monoclonal antibodies: selective binding and complement fixation to cells that express two different surface antigens. *J Immunol* 139:1369-1374.

Wright, J.K., Z.L. Brumme, J.M. Carlson, D. Heckerman, C.M. Kadie, C.J. Brumme, B. Wang, E. Losina, T. Miura, F. Chonco, M. van der Stok, Z. Mncube, K. Bishop, P.J. Goulder, B.D. Walker, M.A. Brockman, and T. Ndung'u. **2010**. Gag-protease-mediated replication capacity in HIV-1 subtype C chronic infection: associations with HLA type and clinical parameters. *J Virol* 84:10820-10831.

Wright, J.K., V.L. Naidoo, Z.L. Brumme, J.L. Prince, D.T. Claiborne, P.J. Goulder, M.A. Brockman, E. Hunter, and T. Ndung'u. **2012**. Impact of HLA-B*81-associated mutations in HIV-1 Gag on viral replication capacity. *J Virol* 86:3193-3199.

Wright, J.K., V. Novitsky, M.A. Brockman, Z.L. Brumme, C.J. Brumme, J.M. Carlson, D. Heckerman, B. Wang, E. Losina, M. Leshwedi, M. van der Stok, L. Maphumulo, N. Mkhwanazi, F. Chonco, P.J. Goulder, M. Essex, B.D. Walker, and T. Ndung'u. **2011**. Influence of Gag-protease-mediated replication capacity on disease progression in individuals recently infected with HIV-1 subtype C. *J Virol* 85:3996-4006.

Yang, H., E. Yorke, G. Hancock, G. Clutton, N. Sande, B. Angus, R. Smyth, J. Mak, and L. Dorrell. **2013**. Improved quantification of HIV-1-infected CD4+ T cells using an optimised method of intracellular HIV-1 gag p24 antigen detection. *J Immunol Methods* 391:174-178.

Yang, O.O., S.A. Kalams, A. Trocha, H. Cao, A. Luster, R.P. Johnson, and B.D. Walker. **1997**. Suppression of human immunodeficiency virus type 1 replication by CD8+ cells: evidence for HLA class I-restricted triggering of cytolytic and noncytolytic mechanisms. *J Virol* 71:3120-3128.

Yang, O.O., P.T. Nguyen, S.A. Kalams, T. Dorfman, H.G. Gottlinger, S. Stewart, I.S. Chen, S. Threlkeld, and B.D. Walker. **2002**. Nef-mediated resistance of human immunodeficiency virus type 1 to antiviral cytotoxic T lymphocytes. *J Virol* 76:1626-1631.

Yuan, R.R., P. Wong, M.R. McDevitt, E. Doubrovina, I. Leiner, W. Bornmann, R. O'Reilly, E.G. Pamer, and D.A. Scheinberg. **2004**. Targeted deletion of T-cell clones using alpha-emitting suicide MHC tetramers. *Blood* 104:2397-2402.

Yukl, S.A., E. Boritz, M. Busch, C. Bentsen, T.W. Chun, D. Douek, E. Eisele, A. Haase, Y.C. Ho, G. Hutter, J.S. Justement, S. Keating, T.H. Lee, P. Li, D. Murray, S. Palmer, C. Pilcher, S. Pillai, R.W. Price, M. Rothenberger, T. Schacker, J. Siliciano, R. Siliciano, E. Sinclair, M. Strain, J. Wong, D. Richman, and S.G.

Deeks. **2013**. Challenges in detecting HIV persistence during potentially curative interventions: a study of the Berlin patient. *PLoS Pathog* 9:e1003347.

Zhang, L., B. Ramratnam, K. Tenner-Racz, Y. He, M. Vesanen, S. Lewin, A. Talal, P. Racz, A.S. Perelson, B.T. Korber, M. Markowitz, and D.D. Ho. **1999**. Quantifying residual HIV-1 replication in patients receiving combination antiretroviral therapy. *N. Engl. J. Med.* 340:1605-1613.

Zhang, N., and M.J. Bevan. **2011**. CD8(+) T cells: foot soldiers of the immune system. *Immunity* 35:161-168.

Zhao, G., J.R. Perilla, E.L. Yufenyuy, X. Meng, B. Chen, J. Ning, J. Ahn, A.M. Gronenborn, K. Schulten, C. Aiken, and P. Zhang. **2013**. Mature HIV-1 capsid structure by cryo-electron microscopy and all-atom molecular dynamics. *Nature* 497:643-646.

Zhu, P., E. Chertova, J. Bess, Jr., J.D. Lifson, L.O. Arthur, J. Liu, K.A. Taylor, and K.H. Roux. **2003**. Electron tomography analysis of envelope glycoprotein trimers on HIV and simian immunodeficiency virus virions. *Proc Natl Acad Sci U S A* 100:15812-15817.

Zhu, T., B.T. Korber, A.J. Nahmias, E. Hooper, P.M. Sharp, and D.D. Ho. **1998**. An African HIV-1 sequence from 1959 and implications for the origin of the epidemic. *Nature* 391:594-597.

Zinkernagel, R.M., and P.C. Doherty. **1974**. Restriction of in vitro T cell-mediated cytotoxicity in lymphocytic choriomeningitis within a syngeneic or semiallogeneic system. *Nature* 248:701-702.

Zuniga, R., A. Lucchetti, P. Galvan, S. Sanchez, C. Sanchez, A. Hernandez, H. Sanchez, N. Frahm, C.H. Linde, H.S. Hewitt, W. Hildebrand, M. Altfeld, T.M. Allen, B.D. Walker, B.T. Korber, T. Leitner, J. Sanchez, and C. Brander. **2006**. Relative dominance of Gag p24-specific cytotoxic T lymphocytes is associated with human immunodeficiency virus control. *J Virol* 80:3122-3125.